

**POLYMERIZATION
AND
POLYCONDENSATION
PROCESSES**

*ACS Library
Executive Secretary's Office*

A collection of papers based on the
Symposium on Polymerization and
Polycondensation Processes

Division of Industrial & Engineering Chemistry
140th Meeting of the American Chemical Society
Chicago, Ill., September 5-6, 1961

NORBERT A. J. PLATZER, *Symposium Chairman*



Number 34

ADVANCES IN CHEMISTRY SERIES

American Chemical Society

Washington, D. C.

1962

Copyright © 1962
AMERICAN CHEMICAL SOCIETY
All Rights Reserved

Library of Congress Catalog Card 62-15813
PRINTED IN THE UNITED STATES OF AMERICA

ADVANCES IN CHEMISTRY SERIES

Robert F. Gould, Editor

AMERICAN CHEMICAL SOCIETY APPLIED PUBLICATIONS

ADVISORY BOARD

Allen L. Alexander

John H. Fletcher

Wayne W. Hilty

Walter C. Saeman

William J. Sparks

Calvin L. Stevens

Glenn E. Ulllyot

Calvin A. VanderWerf

George W. Watt

Kinetics of Emulsion Polymerization

B. M. E. VAN DER HOFF

*Research and Development Division,
Polymer Corp., Ltd., Sarnia, Ontario, Canada*

Equations, which are also applicable to suspension, solution, and bulk polymerization, form an extension of the Smith-Ewart rate theory. They contain an auxiliary parameter which is determined by the rate of initiation, rate constant of termination, and volume of the particles. The influence of each variable on the kinetics of emulsion polymerization is illustrated. Two other variables are the number of particles formed and monomer concentration in the particles. Modifications of the treatment of emulsion polymerization are required by oil solubility of the initiator, water solubility of the monomer, and insolubility of the polymer in the monomer.

In few, if any, industrial chemical processes are more “ingredients” used to produce a single final product than in emulsion polymerization. Moreover, colloidal phenomena play a dominant role in these polymerization reactions. Both these features contribute to the complex nature of emulsion polymerization.

It is at present clearly impossible to understand all the aspects of these systems. Nevertheless the mechanism and kinetics of some emulsion systems are reasonably well understood—those in which the monomer is water-“insoluble” and in which the polymer is soluble in the monomer. An outline is given of this mechanism and the kinetics of polymerization are developed on the basis of this mechanism. This theoretical kinetic behavior is then compared with experimental data, both from the literature and from unpublished results. Whenever possible, the influence of monomer water solubility and monomer solubility of the polymer is commented on. These comments are mostly of a qualitative nature and sometimes even speculative. The present state of our knowledge does not permit going beyond such comments, although recently the literature has given a few attempts at quantitative interpretation of emulsion polymerization of water-soluble monomers.

Emulsion Polymerization Process

A brief description is given below of the emulsion polymerization process of a monomer which is slightly soluble in water. This picture, which is now gen-

erally accepted, is based on the work done by Harkins (29) and his collaborators during World War II, published in 1947. Independently, Yurzhenko and co-workers developed similar ideas on the mechanism of emulsion polymerization reactions (67, 70). German workers also had reached similar conclusions, but their results were not published in the open literature [cf. however (22)].

When an emulsifier or soap is dissolved in water, the solute molecules associate to form small clusters called micelles. The hydrocarbon parts of the emulsifier molecules constitute the interior of the micelles, the surface of which is formed by the ionic groups of the emulsifier. A small fraction of the soap is molecularly dissolved in the water and there is a dynamic equilibrium between the micelles and these single molecules in the aqueous phase. Micelles are of colloidal size, consisting of a relatively small number of soap molecules: of the order of 100 molecules. This corresponds to a diameter of about 50 A., if one assumes the cluster to be spherical. At the concentrations usually employed in emulsion polymerization, there are some 10^{18} micelles per milliliter of water.

On mixing this emulsifier solution with an only slightly water-soluble monomer, a small fraction of the monomer solubilizes in the micelles—i.e., some monomer dissolves in the hydrocarbon interior of the micelles, which swell to roughly double their original size. The remainder of the monomer is dispersed in small droplets, the size of which depends on the intensity of agitation. The diameter of these droplets is usually not smaller than about 1 micron (10,000 A.) and, hence, there are at most some 10^{11} droplets per milliliter of water at the normally employed ratio of monomer to water phase.

If now an initiator—potassium persulfate, for example—is added to the emulsion, it decomposes at sufficiently high temperatures into two radical ions: $\text{SO}_4^{\cdot-}$. At 50° C., some 10^{13} radicals are formed per milliliter of water per second at the usually applied concentration of initiator. The radical ions react with what little monomer is dissolved in the aqueous phase, forming organic sulfate ions. After reaction with a few monomer molecules, the product is a surface active radical ion which soon becomes incorporated in a micelle, because of the dynamic character of the equilibrium between micellar and molecularly dissolved emulsifier. In the interior of the micelle, the organic radical end of the newly formed chain encounters a high concentration of solubilized monomer and therefore chain growth proceeds rapidly. In the polymerization of styrene at 50° C., for example, a micelle being “stung” by a radical expands in 1 minute to about 250 times its original volume. All the monomer required for this almost explosive growth was not contained in the original micelle, but diffuses to it from the monomer droplets through the aqueous phase. The growth of a “stung” micelle is accompanied by the formation of new polymer-water interface onto which emulsifier molecules are adsorbed from the aqueous phase. Thus, the equilibrium between molecularly dissolved soap and micellar soap is disturbed and micelles disintegrate to restore the concentration of molecularly dissolved emulsifier to its equilibrium value. Thus, in the process of formation of one polymer particle many micelles disappear. Only a small fraction of the original micelles is transformed into polymer particles and the final latex contains some 10^{15} particles per milliliter of water. This process of particle formation results in adsorption of the emulsifier onto polymer particles early in the reaction; after about 10 to 20% conversion no micelles exist and hence no particles are formed. Polymerization inside a micelle or polymer particle does not deplete the particle of monomer. Because of osmotic forces, the amount of monomer diffusing from the droplets through the water to the particles is in excess of the amount consumed by polymerization.

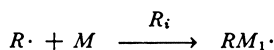
Provided that the monomer droplets are sufficiently small, which is usually the case, diffusion is rapid enough to replace monomer consumed in the reaction and to supply the additional amount required for equilibrium swelling of the polymer particles (24). Because of this swelling, monomer droplets disappear from the reaction mixture before polymerization is completed. From this moment on the reaction slows down. Final conversions of close to 100% can usually be obtained.

This picture of emulsion polymerization mechanisms, mainly due to Harkins (29, 30), is generally accepted as is borne out by its description in several recent textbooks on polymerization (4, 10, 13, 24, 68). An extensive review has been given by Gerrens (26).

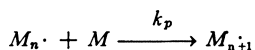
Emulsion Polymerization Kinetics

The process of polymerization consists in general of three steps: initiation, propagation, and termination. In radical polymerization, a catalyst is usually employed as a source of free radicals, the primary radicals. A fraction of these initiate a rapid sequence of reactions with monomer molecules, the primary radical thus growing into a polymer radical. Radical activity is destroyed by reaction of two radicals to form one or two molecules. This termination reaction is called mutual recombination, if only one molecule is formed. Termination by disproportionation results in two molecules. For many common monomers, recombination is the normal mode of termination and the kinetic treatment here is based on this termination reaction. Only slight modifications are required for polymerizations in which termination occurs by disproportionation. If both termination processes occur, another variable must be introduced to describe the kinetics of the system fully.

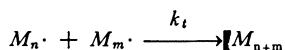
Let R_i designate the rate of initiation of polymer radicals—i.e., the number of gram radicals initiating chains per liter of reaction volume per second (R_i , mole liter⁻¹ sec.⁻¹).



R_p and k_p represent the rate and the rate constant of the propagation reaction (R_p , mole liter⁻¹ sec.⁻¹; k_p , liter mole⁻¹ sec.⁻¹):



The rate and rate constant of the termination process are indicated by R_t and k_t (R_t , gram radicals liter⁻¹ sec.⁻¹; k_t , liter mole⁻¹ sec.⁻¹):



Under certain conditions, which in emulsion polymerization are almost always fulfilled (56), the concentration of radicals in the reaction mixture $[R \cdot]$ is constant. Therefore, the rate of initiation must equal the rate of termination: $R_i = R_t$. Since

$$R_t = -d[R \cdot]/dt = 2 k_t [R \cdot]^2 \quad (1)$$

it follows that

$$[R \cdot] = (R_i/2 k_t)^{1/2} \quad (2)$$

The factor 2 in these two equations arises from the fact that two polymer radicals disappear on mutual termination. The rate of polymerization can now be expressed as:

$$R_p = k_p[M][R\cdot] = (R_i k_p^2 / 2k_t)^{1/2} [M] \quad (3)$$

where $[M]$ is the monomer concentration (mole per liter).

The degree of polymerization (DP)—i.e., the average number of monomer units per polymer molecule—is given by the number of chain propagation steps for each reaction between a pair of polymer radicals—i.e., for each formation of a “dead” polymer molecule. Therefore, DP is equal to the rate of chain growth divided by half the rate of chain termination:

$$DP = 2 R_p / R_t = (2k_p^2 / R_i k_t)^{1/2} [M] \quad (4)$$

These relations for rate and degree of polymerization, although based on a relatively simple chemical picture, agree well with experimental data obtained in solution and bulk polymerizations. In emulsion polymerization, however, a complication arises from the fact that the volume of the reaction mixture is subdivided into a very large number of very small volume elements, the particles, which are suspended in water. These particles are so small that they can accommodate only a limited number of polymer radicals at any one time. The peculiarities of emulsion polymerization stem from this limitation. Polymer radicals, being insoluble in water, are confined to the particle in which they are generated. Thus, a radical in one particle cannot be terminated by a radical in another particle. Therefore, the rate of termination in emulsion is much lower than that given by Equation 1.

To derive the kinetic relations which govern emulsion polymerization we reconsider Equation 1, while restricting ourselves for the time being to systems with water-soluble initiators where radicals enter the particle one by one. We rewrite this equation:

$$R_t = 2 k_t \frac{n/N_A}{v} \times \frac{n/N_A}{v}$$

in which n is the number of radicals in the reaction volume, v , and N_A is Avogadro's number. This formulation assumes that each radical can react not only with other radicals, but also with itself. As long as the number of radicals in volume v is large, this is a good approximation of the actual case—namely, that each radical can react with each other radical, but not with itself. In emulsion polymerization, however, the number of radicals in the volume elements is so small that we must use the exact expression:

$$R_t = 2 k_t \frac{n/N_A}{v} \times \frac{(n-1)/N_A}{v}$$

in which v is now the volume of a particle.

It is evident that the rate of termination and therefore the kinetic relations depend on the distribution of the radicals among the particles. To obtain these relations, one must seek information on this distribution. This can be done by the following considerations, first put forward by Smith and Ewart (58).

In emulsion polymerizations, the number of particles containing n radicals, N_n , normally assumes a steady-state value early in the reaction. Therefore the rate of formation of such particles equals their rate of disappearance. A particle containing n radicals is formed either from a particle with $n-1$ radicals which

gains a new radical or from a particle containing $n + 2$ radicals, losing two radicals by mutual termination. The rate of radical gain is given by:

$$\Delta n/\Delta t = R_i N_A/N = R_i N_{Av}$$

where N is the total number of particles per liter of organic phase. The rate of loss of pairs of radicals in a particle containing n radicals is given by:

$$-^{1/2}\Delta n/\Delta t = ^{1/2}R_i N_A/N = k_t n(n-1)/N_{Av}$$

Hence the rate of appearance of particles containing n radicals is:

$$\Delta N_n/\Delta t = \{R_i N_{Av}\} N_{n-1} + \{k_t(n+2)(n+1)/N_{Av}\} N_{n+2}$$

Similarly particles containing n radicals are lost by either gaining a radical or losing two radicals. The rate of loss is:

$$-\Delta N_n/\Delta t = \{R_i N_{Av}\} N_n + \{k_t n(n-1)/N_{Av}\} N_n$$

The steady-state condition requires:

$$\{R_i N_{Av}\} N_{n-1} + \{k_t(n+2)(n+1)/N_{Av}\} N_{n+2} = \{R_i N_{Av} + k_t n(n-1)/N_{Av}\} N_n$$

The general solution of this recursion relation has recently been given by Stockmayer (60). His result can be expressed by the following equations:

$$z \equiv \frac{\bar{n}}{a/4} = \frac{I_0(a)}{I_1(a)}$$

$$a = 4(R_i/2k_t)^{1/2} N_{Av} \quad (5)$$

in which \bar{n} is the average number of radicals per particle and I_0 and I_1 are the Bessel functions of the first kind of zero and first order, respectively. It follows from Equation 5 that the radical concentration is given by:

$$[R\cdot] = \bar{n} N/N_A = z(R_i/2k_t)^{1/2} \quad (6)$$

This relation is identical with Equation 2 except for the numerical factor z . Consequently Equations 3 and 4 become:

$$R_p = z(R_i k_p^2/2k_t)^{1/2} [M] \quad (7)$$

and

$$DP = z(2k_p^2/R_i k_t)^{1/2} [M] \quad (8)$$

These equations are perfectly general and therefore are applicable to solution, bulk, suspension, and emulsion polymerization systems. In the case of solution and bulk systems there is, in effect, only one "particle" with a volume of that of the whole reaction mixture. In emulsion and suspension polymerizations, the reaction mixture is subdivided into a large number of small particles and the influence of the state of subdivision is expressed by the factor z .

Figure 1 shows the value of this subdivision factor as a function of parameter a (upper curve), from which it can be seen that a polymerizing system follows solution polymerization kinetics ($z \sim 1$) as long as a is larger than about 10. In emulsion systems, a is usually smaller than 1 and both the rate of reaction and the molecular weight of the polymer increase with decreasing a . The influence of the three variables R_i , k_t , and v on parameter a are discussed later.

For values of a between 1 and 10, the character of the polymerization kinetics is intermediate between that of emulsion and that of solution polymerization. This is the region of suspension or pearl polymerization, where the rate and degree of polymerization are somewhat higher than for reaction in solution. The value

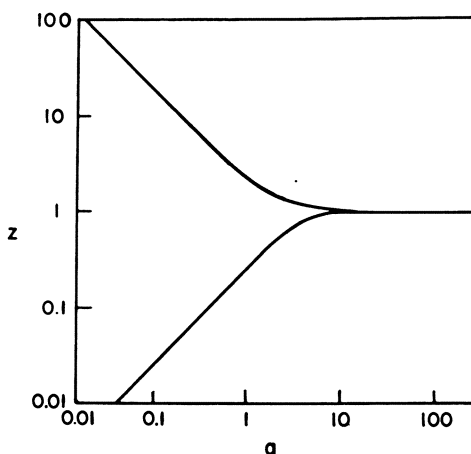


Figure 1. Subdivision factor z as a function of parameter a

From van der Hoff, B. M. E., *J. Polymer Sci.* 33, 487 (1958)

COURTESY *Journal of Polymer Science*

of the subdivision factor here is roughly between 3 and 1. It can readily be ascertained from series expansion of the Bessel functions in Equation 5 that when a approaches zero, $z \rightarrow 2/a$ and $\bar{n} \rightarrow 1/2$. The unreal case $a = 0$, $\bar{n} = 1/2$ will be called "ideal emulsion polymerization." If a is 1, 0.4, and 0.1, \bar{n} is, respectively, 0.558, 0.510, and 0.5002, which shows that for $a < 1$, the ideal case is rapidly approached.

That the average number of radicals per particle should be about 1/2 can also be seen by considering that, on entry of a new radical into a very small particle containing one polymer particle, termination between the two radicals occurs after a time lapse very small compared with the time interval between successive entries of new radicals under the conditions usually prevalent in emulsion polymerization. Hence, the particle contains either one or no radical and the average number of radicals per particle is 1/2. This simple description was first given by Smith and Ewart (58) and will be referred to as the Smith-Ewart rate theory. It follows from $\bar{n} = 1/2$ that $[R\cdot] = N/2N_A$.

Therefore

$$R_p = Nk_p[M]/2N_A \quad (9)$$

and hence, the rate of polymerization for a given number of particles is independent of initiator concentration. This unusual behavior is depicted in Figure 2.

It has been assumed in the above derivations that the primary radicals enter the particles one by one. This assumption is fulfilled for water-soluble initiators and probably for oil-soluble catalysts activated by water-soluble compounds. If, however, an unactivated oil-soluble initiator is employed, which decomposes into radical pairs within the particles, this assumption does not hold. A derivation similar to the one given, but based on the formation of radicals in pairs, leads to a different recursion relation. With the aid of the mathematical method employed by Stockmayer for the former recursion relation, this latter one can be simply solved to yield the same Equations 6, 7, and 8, where now $z = \tanh(a/4)$. This

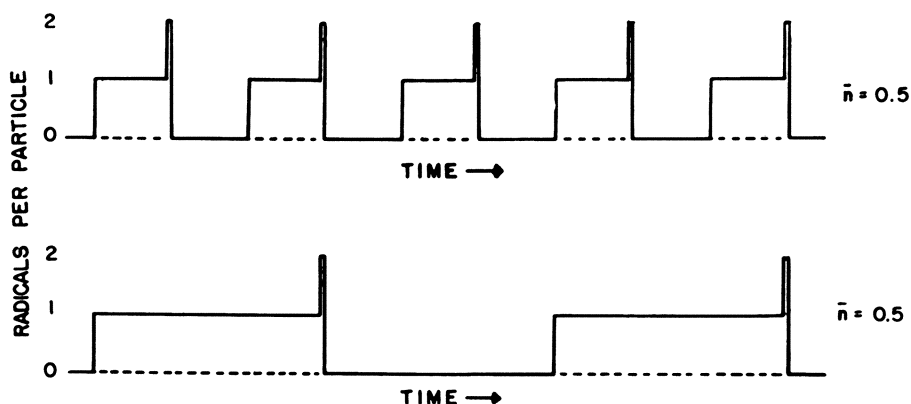


Figure 2. Schematic representation of number of radicals per particle at two different rates of entry of single radicals

result was first obtained by Haward (31) by a somewhat different mathematical route. Values of $\tanh(a/4)$ are also plotted in Figure 1 (lower curve), which shows that the subdivision factor and therefore rate and degree of polymerization decrease with a . For small values of a , z approaches $a/4$. Initiation with oil-soluble catalysts is discussed in more detail later.

The monomer concentration in the particles is nearly constant during part of the polymerization. The rate of polymerization in this region at a particular temperature, therefore, depends only on the number of particles present (Equation 9). This quantity, so important in emulsion polymerization, is discussed in the following section.

Number of Particles

Because of its overriding importance in determining the rate of emulsion polymerization, the factor discussed first is the number of particles formed. The mechanism of particle formation described above has been treated quantitatively by Smith and Ewart (58) on the basis of some simplifying assumptions. The most important of these is that a soap molecule occupies the same interfacial area whether it forms part of a micelle or is adsorbed on the polymer-water interface—i.e., during the period of particle formation, the total surface area of micelles plus polymer particles is constant.

Rigid application of diffusion laws leads unfortunately to as yet unsolved mathematical equations. An approximate solution is obtained by making either of two further assumptions and the number of particles formed is calculated on the basis of each of these. These computations are not given here; they have been amply described. Only the results of the calculations are briefly mentioned.

Assumption 1. The first additional assumption states that *only* micelles capture radicals. Since polymer particles undoubtedly can do the same, as is shown by continuing polymerization after the disappearance of the micelles, the number of particles calculated on this basis is too large. This number, N , is given by:

$$N = 0.53 (\rho/\mu)^{2/5} \times (a_0 S)^{3/5} \quad (10)$$

in which

- ρ = rate of radical production
 μ = rate of volume increase of a particle
 a_s = area occupied by one soap molecule
 S = amount of soap present

Assumption 2. The second additional assumption states that the radical diffusion flux—i.e., the number of radicals entering a particle per unit surface area per unit time—is independent of the radius of the particle. This will lead to too small a number of particles because it can be derived from Fick's law that, in symmetrical diffusion into a sphere, the current is proportional to the radius of the particle and therefore the diffusion flux is inversely proportional to that radius. In other words, the smaller the particles the more efficient they are in capturing radicals. N calculated on the basis of this assumption is given by:

$$N = 0.37(\rho/\mu)^{2/5} \times (aS_s)^{2/5} \quad (10a)$$

This relation differs from the one above only in the somewhat smaller numerical factor.

With these assumptions two different conversion-time curves are associated. It is easily derived that for the case of assumption 1, the number of particles and therefore the rate increase in proportion to the square of the reaction time, provided $[M]$ is constant (3). At the conversion, C_N , where the micelles have just disappeared, all particles contain a growing polymer radical and the rate is double the equilibrium rate given by Equation 9. The rate after C_N decays exponentially to the equilibrium value. If assumption 2 holds, the rate increases according to a complex function of reaction time. In Figure 3, examples are given of conversion-time curves which seem to correspond to the theoretical relations derived on the basis of either assumption. The usual course of the reaction is probably intermediate between the two types and may in addition be modified by changes in the monomer concentration in the particles during this period of transition from micelle to particle.

The conversion at the end of the period of particle formation has been reported by several authors who determined the disappearance of unabsorbed soap. Table I lists some of these results, which show that for the usual ratio soap-monomer C_N falls between 10 and 25% conversion, depending on the rate of initiation.

Table I. Values of Conversion at Which Micelles Disappear, C_N

Monomer	Soap	G. Soap/ 100 G. Monomer	C_N , %	Method	Ref.
Styrene	Laurate	5	23	Surface tension	(29)
Styrene	Myristate	5	24	Surface tension	(29)
Styrene	Myristate	8	20	Electrical conductivity	(3)
Styrene	Myristate	10	21	Electrical conductivity	(3)
Styrene/isoprene, 1/3	Oleate	5	12	Surface tension	(29)
Styrene/isoprene, 1/3	Myristate	4.5	14	Fluorescence	(35)
Vinyl chloride	Myristyl sulfate	—	<20	Surface tension	(33)

The theoretical predictions contained in Equations 10 and 10a have been tested by a number of authors, most extensively by Bartholomé *et al.* (6). It was found that the number of particles formed was accurately proportional to the 2/5 power of the amount of initiator (Figure 4).

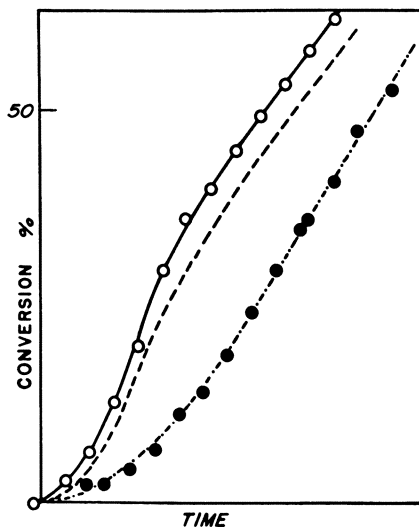


Figure 3. Theoretical and experimental relations between conversion and time

Reaction mixture 90 grams of styrene, 10 grams of butadiene, 3.65 grams of potassium palmitate, 175 grams of aqueous potassium hydroxide (0.001N), and 0.1 gram (O) and 0.2 gram (●), gram of potassium persulfate
Reaction temperature 65° C.

----- Calculated on assumption 1
- - - - - Calculated on assumption 2
Different time scales for O and ●

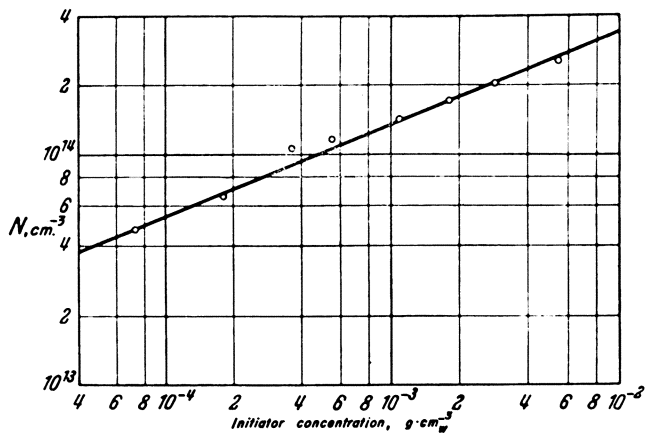


Figure 4. Number of particles as a function of initiator concentration in polymerization of styrene

Phase ratio constant

From Gerrens, H., Fortschr. Hochpolymeren-Forsch. 1, 234 (1959)

COURTESY Springer Verlag, Heidelberg

The dependence of the number of particles formed on the amount of soap (Figure 5) shows that the number is proportional to the $3/5$ power of the amount of soap (36, 69).

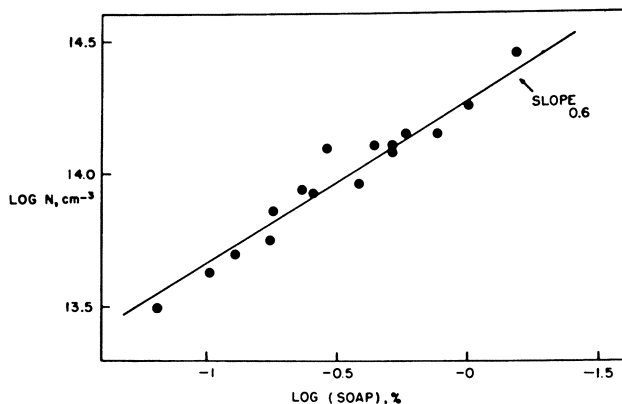


Figure 5. Number of particles as a function of soap concentration in polymerization of styrene

From Gerrens, H., *Fortschr. Hochpolymeren-Forsch.* 1, 234 (1959)

COURTESY Springer Verlag, Heidelberg

Other authors have reported that the number of particles increases with the square root of the amount of soap (3, 10, 12, 45). This discrepancy in the dependence of N on soap is not considered serious in view of the fact that several simplifying assumptions have been made in the derivation of the theoretical Equations 10 and 10a. N can be determined only with rather limited accuracy.

It is obvious that in the theoretical treatment sketched above, S , the amount of soap, refers to the amount of micellar soap. If in a polymerization mixture a soap is used with a relatively high critical micelle concentration (C.M.C.), it is necessary to correct for the amount of soap which is molecularly dissolved and does not contribute to particle formation, at least in the mechanism considered by Smith and Ewart. Consequently, the number of particles and hence the rate of polymerization decrease sharply with increasing C.M.C., as was observed by Staudinger (59), who reported initial polymerization rates of 0.041, 0.12, and 0.225% per minute for reactions in 3% solutions of potassium caprate, laurate, and stearate, where the C.M.C.'s are about 2.1, 0.60, and 0.17%, respectively.

Recently an attempt has been made to verify the Smith-Ewart number theory with respect to the absolute number of particles formed (63). In Figure 6, theoretical (dashed line) and experimental (solid line) numbers of particles are compared. There is fair agreement. The number actually generated is somewhat lower than the theoretically predicted value. This is for the most part due to loss of initiator radicals by side reactions—i.e., the efficiency of primary radicals in starting a polymer chain is less than unity. The difference between theoretical and experimental values corresponds to an efficiency of about 0.3 to 0.5 at phase ratios 2 to 5.

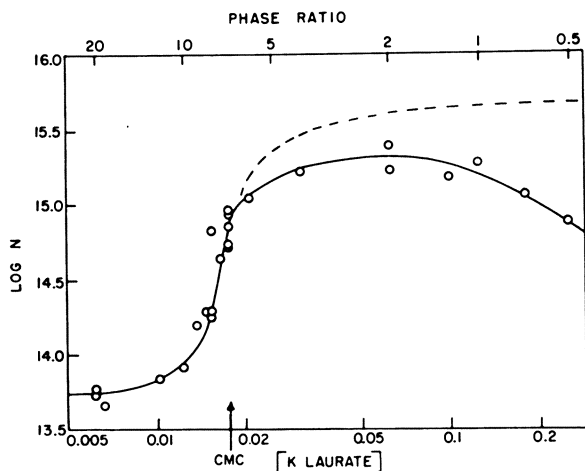


Figure 6. Number of particles formed as a function of emulsifier concentration in polymerization of styrene

Amount of emulsifier constant, amount of water varied

From van der Hoff, B. M. E., *J. Polymer Sci.* **33**, 487 (1958).

COURTESY *Journal of Polymer Science*

Other Mechanisms of Particle Formation

Particle Formation below Critical Micelle Concentration. Figure 6 shows furthermore that particle formation also occurs when the soap concentration is lower than the C.M.C. This phenomenon has been reported by a number of authors. Staudinger (59), for example, observed the initial reaction rate of butadiene styrene copolymerization in potassium caprylate solution at about half the C.M.C. He reported this rate to be about 1/10 of that of stearate at the same concentration, pointing to roughly 1/10 of the number of particles having been formed. It has been reported (25) that below the C.M.C. the number of particles generated is independent of the initiator concentration and that during the induction period, the surface tension of the aqueous phase decreases prior to the onset of cloudiness. These observations have led to the tentative suggestion that during the induction period surface active oligomers are being formed in the aqueous phase, which build up to a limiting surfactant concentration, followed by precipitous formation of micelles and/or particles not unlike particle formation in the precipitation of insoluble salts. This mechanism is characterized by coprecipitation of a relatively large number, n , of polymer molecules. The rate of this high-order reaction is proportional to the n th power of the polymer concentration in the water which gives rise to the occurrence of a critical concentration, a phenomenon not unlike that of micelle formation by soap molecules, but different in that polymer precipitation is irreversible while micelles are in dynamic equilibrium with molecular dissolved molecules.

Particle Formation with Water-Soluble Monomers. When the monomer is soluble in water, the mechanism of particle formation may be expected to deviate considerably from that given above. If the polymer also is soluble

in water, the system is homogeneous and surfactant will have no influence on the polymerization process other than that of a nonsurfactive additive. The rate will be independent of soap concentration. Often, however, the solubility of the polymer decreases with its molecular weight and the system becomes heterogeneous during polymerization. Particle formation can be envisaged as the precipitation of single polymer molecules with or without subsequent coalescence of these precipitate molecules to colloidal particles. Soap molecules are adsorbed by the molecules and/or particles. As the number of these particles increases, more and more of the precipitated polymer molecules will coalesce with them and will be absorbed by the particles particularly, since because of polymerization growth, their surface coverage with soap diminishes. This coverage decrease also affects the stability of the colloidal particles. Therefore the number of particles and hence the rate of reaction depend on the stabilizing properties of the emulsifier and the degree of agitation. This last effect has been clearly demonstrated in the aqueous polymerization of acrylonitrile (42). Coalescence of particles has recently been treated quantitatively for the emulsion polymerization of vinylidene chloride (21, 32, 39), where it is very pronounced.

In the mechanism of particle formation described above, soap micelles have not been mentioned. If only a little soap is present, the total surface of the precipitating polymer molecules and polymer particles is large enough to adsorb all micellar soap before the end of the period of particle formation. The rate of polymerization of vinyl acetate is constant from 0 to 2 times the C.M.C. of sodium dodecyl sulfate (49). One cannot expect this to be the general rule, since the amount and the nature of the soap influence particle stability. It is therefore not surprising that conflicting reports (18, 25, 48, 50, 52) have been given on the relation between soap concentration and the rate of polymerization of vinyl acetate. At higher soap concentrations, one can expect a competition between particle formation via micelles and via precipitating polymer molecules. The more water-soluble the monomer is, the more will the latter dominate and the lower will be the exponent n in the relation: Rate \propto [soap] ^{n} . This correlation between solubility and n has been mentioned by Cherdron (17, 18), whose data have been incorporated in Table II.

Table II. Comparison of Solubility of Monomer in Water and Dependence of Polymerization on Soap Concentration

Monomer	Water Soly. at 25° C., %	n	Ref.
Vinyl caproate	0.004	0.7	(50)
Styrene	0.03	0.6	(6)
Vinylidene chloride	0.01	0.6	(32)
Vinyl acetate	2.3	0-0.3	(49)
Styrene in 40% MeOH	2.8	0.31	(50)
Acrylonitrile	7.4	0.23-0.3	(17, 61)
Acrolein	2.1	0.17	(17, 18)

Period of Particle Formation. An important factor which influences the duration of the period of particle formation and hence the number of particles formed is the rate of growth of the particles. This rate in turn is strongly influenced by the solubility of the monomer in its polymer or rather the partition of monomer between polymer and aqueous phase. Table III lists approximate values of C_d , the conversion at which free monomer droplets disappear

from the emulsion system. These figures reflect the degree of swelling of the polymer particles by the monomer. Table III also gives the monomer concentrations in the particles, $[M]_p$, calculated from the values of C_d .

Table III. Approximate Values of Monomer Concentration in Polymerizing Particles, $[M]_p$, and Conversions at Which Monomer Droplets Disappear, C_d

Monomer	$[M]_p$, Moles Liter ⁻¹	C_d , %	Ref.
Vinyl acetate	9	15 ^a	(25)
Methyl methacrylate	7	30	(71)
Chloroprene	7	35	(43)
Styrene	5	45	(26, 63)
Butadiene	5	55	(70, p. 265; 45)
Isoprene	6	60	(46)
Vinyl chloride	4	75	(23)

^a From Equation 11 it is calculated with $\mu = 0.5$ (47) that C_d is 20% for 1000-Å. particles using a value of 3 dynes/cm. for interfacial tension.

Number of Particles after Period of Particle Formation. When the particles are formed from micelles only, no new particles are generated after the soap concentration decreases below the C.M.C. During further polymerization, the total particle surface increases and the surface coverage with soap diminishes accordingly. In spite of the resulting decreasing stability of the particles, there are many polymerization systems in which no appreciable coalescence of particles occurs; the number of particles remains constant after C_d . An example of such a system is the polymerization of styrene in solutions of fatty acid soaps. Figure 7 shows the number of particles, calculated from electromicrograph data, as a function of con-

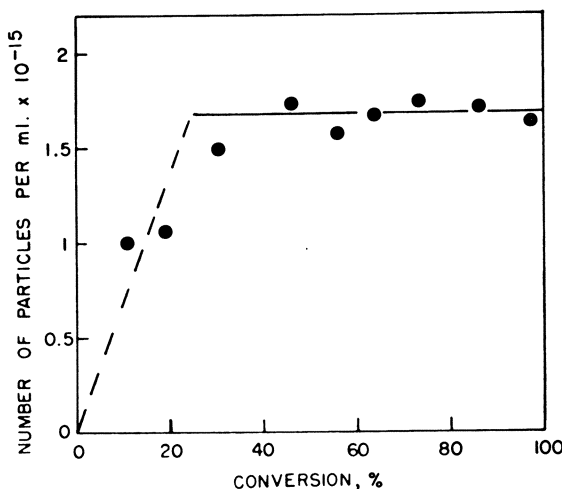


Figure 7. Number of particles as a function of conversion

Reaction mixture 0.100 grams of styrene, 3.1 grams of sodium myristate, 0.1 gram of potassium chloride, 200 grams of aqueous potassium hydroxide (0.001N), 0.3 gram of cumene hydroperoxide

Reaction temperature 40° C.

version. The results at low conversion are not very accurate, because of the lack of contrast on the micrographs for very small particles. It may nevertheless be concluded that in this case the number of particles is constant from about 30% conversion on.

For a water-soluble monomer, the above reasoning does not apply. Nevertheless the number of particles is constant after 20% conversion of vinyl acetate (25). This suggests that oligomers and/or polymers of this monomer are easily adsorbed by particles at less than full emulsifier coverage.

Coagulation of polymer particles, as of any colloidal dispersion, depends on a number of factors, among them the stabilizing action of the emulsifier, the compatibility of soap and polymer, and the consistency of the polymer-monomer interior of the particles. When vinyl chloride is polymerized above the softening point of the swollen polymer, particles coalesce to such an extent that the soap coverage remains about 100% (33)—i.e., the number of particles decreases with conversion. Extensive coalescence after the period of particle formation occurs in the polymerization of vinylidene chloride investigated by Sweeting and coworkers (21, 32, 39).

Initiation

Although it is possible to carry out thermal polymerization in emulsion (11, 20), it is usual to employ an additional source of free radicals to start chain growth. Gamma-rays and photolysis of photosensitive compounds are used occasionally to generate free radicals, but in most cases radicals are formed chemically. The compounds and the reactions which have been and are being employed as free radical sources are very numerous. The scope of this paper does not allow even listing the different types of reactions used. An extensive review of redox initiator systems has recently been given by Dolgoplosk and Tinyakova (19). A few simple systems are mentioned below. From the point of view of kinetics this omission is not serious. The chemistry and kinetics of many reactions which proceed via radical processes have been investigated, but in only a very limited number of cases can the information uncovered be applied to polymerizations, because monomers act in most cases as efficient radical traps, thus interfering with the chemical and kinetic scheme developed in the absence of monomers. Emulsion polymerization processes are now sufficiently well understood to allow deductions to be made from polymerization data on the chemistry and kinetics of radical-producing reactions rather than using the latter to derive information on the polymerization. Bartholomé and Gerrens (5) polymerized styrene, using the combination persulfate-triethanolamine as initiator system. They were able to derive the rate constant of the radical-producing reaction and showed that the bimolecular reaction between the redox partners produces only one radical capable of chain initiation per mole of reactants.

When polymerization is carried out at relatively high temperatures ($t > 40^\circ$ C.), thermally unstable compounds are frequently used as a source of free radicals. The persulfate ion, for example, decomposes with formation of two sulfate ion radicals: $\text{SO}_4^{\cdot-}$, a reaction which is strictly first-order at least in the absence of soap. In addition, another type of decomposition occurs at low pH where the H^+ ion reacts with persulfate (37). Also soap is known to influence the rate of decomposition of persulfate. These last reactions, however, do not produce radicals (2, 38, 63).

The radicals generated by decomposing persulfate are radical ions. Once a

pair of these ions is formed, they will separate because of their electrostatic repulsion. The anionic character of the radical will also prevent or at least impede diffusion into negatively charged micelles or particles present when anionic emulsifiers are used. Since, however, persulfate is an efficient initiator in emulsion polymerization, it is likely that initiation occurs in the aqueous phase even in the case of water-"insoluble" monomers. Hence, by very slow polymerization, oligomeric radicals are formed carrying a sulfate group. The presence of sulfate groups on polystyrene produced at 50° C. with persulfate catalyst was demonstrated by a dye partition method adopted from the procedure applied by Jones (34) to surfactants. After correction for transfer to monomer, at least 70% of the remaining polymer molecule ends carried sulfate groups. End group analysis has recently been developed by Palit (51).

Oligomeric sulfates are surfactive and will be incorporated in micelles or adsorbed by polymer particles, the ionic end group remaining in the aqueous phase. Thus, the radical activity at the other end of the molecule is transported into the hydrocarbon phase of micelles or particles where relatively high monomer concentrations prevail and polymerization proceeds rapidly.

In the derivation of the kinetic relations it was assumed that free radicals enter the particles one by one; the initiation process just described satisfies this condition. This is not the case when radicals are formed by thermal decomposition of an oil-soluble initiator. Such decomposition produces pairs of radicals in the hydrocarbon phase. One would expect a pair of radicals, confined to the extremely small volume of a latex particle, to recombine rapidly. The kinetics of this type of polymerization have been described above. It is recalled here that the subdivision factor, z , and hence rate and degree of polymerization are smaller than 1 and decrease with a . These predictions from kinetic theory are in contradiction to experimental observations. Although some oil-soluble initiators, which are good catalysts in solution systems, are poor initiators in emulsion polymerizations—e.g., benzoyl peroxide—other thermally decomposing peroxides and azo compounds produce polymer in emulsion at rates comparable to those observed in polymerization initiated by water-soluble catalysts, where the radicals enter the particles one by one. Such is the case for cumene hydroperoxide, which at low concentrations yields a rate of polymerization per particle equal to that of a persulfate-initiated reaction. It must therefore be concluded that, although oil-soluble initiators may decompose into radical pairs within the particles, polymer radicals are formed one by one. The following mechanisms are consistent with formation of polymer radicals singly.

One possibility is the entry of single radicals from the aqueous phase. The rate of entry of such radicals should depend on the concentration of the initiator in the water. This concentration is not so much determined by the solubility of the catalyst in water, as by its partition coefficient between hydrocarbon and aqueous phases. Although, for example, all the cumene hydroperoxide, in an amount usually employed in emulsion polymerization, easily dissolves in the aqueous phase, only a fraction of 1% of this amount is actually found in the water, the rest being dissolved in the monomer. The number of radicals formed in the water must therefore be very small indeed.

It is furthermore possible that small radicals like those formed on decomposition of the initiator or those formed by transfer reactions diffuse out of the polymer particle. A radical of molecular weight of a few hundred diffuses in 10^{-5} second over a distance of the order of 1000 Å, which is roughly the dimension of a polymer particle. This rate of diffusion is to be compared with the rate of chain initiation

by the catalyst fragment or by the transfer agent radical, which is probably of the same order of magnitude as the rate of propagation—i.e., 10^{-2} to 10^{-3} second per molecule. These figures seem to indicate that diffusion of a radical out of the particle is preferred over initiation. Transfer out of the particle of a hydrocarbon-type radical seems unlikely, however, because of the high interfacial energy associated with the formation of new hydrocarbon-water interface. For a polarizable radical, like $\cdot\text{OH}$, both the presence of an electrical double layer on the particle surface and solvation after transfer by the water favor the escape of the radical to the aqueous phase. In a recent publication Patsiga, Litt, and Stannett (52) have interpreted their experimental data to indicate that the small radical formed by transfer of a poly(vinyl acetate) radical to monomer does diffuse out of the particles.

The possibility of a radical leaving a particle has furthermore been mentioned by Edelhauser (20) and Breitenbach (12), who also point out that small monomeric radicals are being formed during polymerization by transfer reaction to monomer. Loss of radicals by diffusion out of the particles in a system which obeys the Smith-Ewart rate theory does not influence the kinetics, provided that there is no appreciable termination in the aqueous phase. For each particle losing one radical in a random process, another particle gains this radical in an equally random manner.

To account for the high rates of polymerization resulting from oil-soluble initiators which form pairs of radicals, another mechanism must be considered which allows single radicals to enter particles.

Several authors have pointed out that the rate of decomposition of peroxide compounds is greater in emulsion than in solution. Evidence has been presented that the decomposition rate of cumene hydroperoxide, for instance, in a polymerizing emulsion system is several times larger than in styrene solution (64). This suggests that the enhanced decomposition is an interfacial phenomenon and it is conceivable that, in the case of a hydroperoxide, pairs of radicals are produced in such a way that only the organic radical ($\text{RO}\cdot$) enters the particle while the inorganic fragment ($\text{HO}\cdot$) remains in the aqueous phase where it can undergo further reaction. Thus, radicals enter the particles one by one, as is the case for water-soluble initiators.

There is no direct evidence that any of these mechanisms in fact come into play, but they account for polymerization rates per particle equivalent to that of a particle containing a growing chain half the time, even if only a small fraction of initiating or terminating radicals transfers from one phase to the other. This is illustrated in Figure 8, which shows that periods of time during which the particle

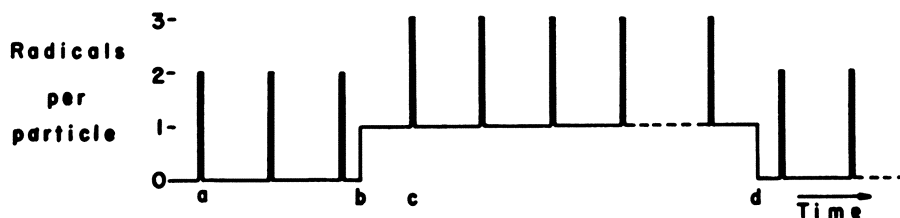


Figure 8. Schematic representation of number of radicals per particle
Radicals formed in pairs

From van der Hoff, B. M. E., *J. Polymer Sci.* **48**, 175 (1960)
COURTESY *Journal of Polymer Science*

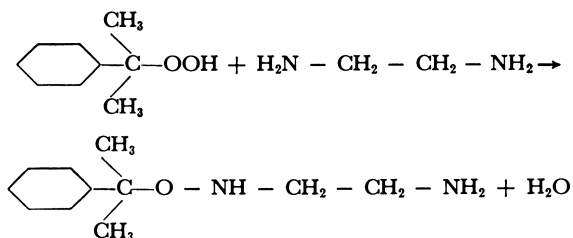
contains no growing chain alternate with periods during which there is one propagating polymer radical. The resulting rate equals that of a particle growing half the time.

On decomposition of hydroperoxides phase separation of the pair of primary radicals may occur. It is suggested that a similar process applies to the initiation systems in which radicals are produced by reaction of an oil-soluble initiator and a water-soluble activator. For example, the reaction between an organic hydroperoxide and complexed ferrous ions provides an effective source of free radicals in emulsion polymerization:

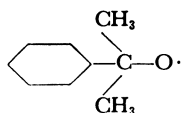


while the same peroxide in an organic solvent reacts instantaneously with an oil-soluble ferrous compound even at temperatures as low as -70°C . (19).

Another example of the importance of the particle-water interface is the redox system consisting of an organic peroxide and an oligomeric ethyleneamine. The reaction between cumene hydroperoxide and ethylenediamine:



produces a relatively unstable compound, which slowly decomposes with formation of



and $\text{H}_2\text{N} - \text{CH}_2 - \text{CH}_2 - \text{N}\cdot$ radicals (7).

The condensation reaction is very slow, unless the amine is complexed with ferric ions. In a polymerizing emulsion system, the peroxide is in the hydrocarbon phase; the amine-iron complex is in the water. The very large interface between these two phases now allows the rapid formation of the unstable condensation product and the chemical nature of this product points to the possibility of separation of the radicals formed on decomposition by diffusion into different phases.

Propagation

The rate of emulsion polymerization for water-"insoluble" monomers is determined by the product of four factors:

- The number of particles present
- The average number of radicals per particle
- The rate constant of the propagation reaction
- The monomer concentration in the particles

The first two factors have been dealt with above. As far as is known, the rate constant is not affected by the colloidal nature of the emulsion process. In fact, recent determinations of the propagation rate constant (k_p) of styrene in

emulsion systems show this constant to agree well with values obtained in bulk and solution polymerizations, as can be seen in Figure 9. Values for the propagation rate constant of several monomers have been critically examined and listed in recent publications (4, 13, 68).

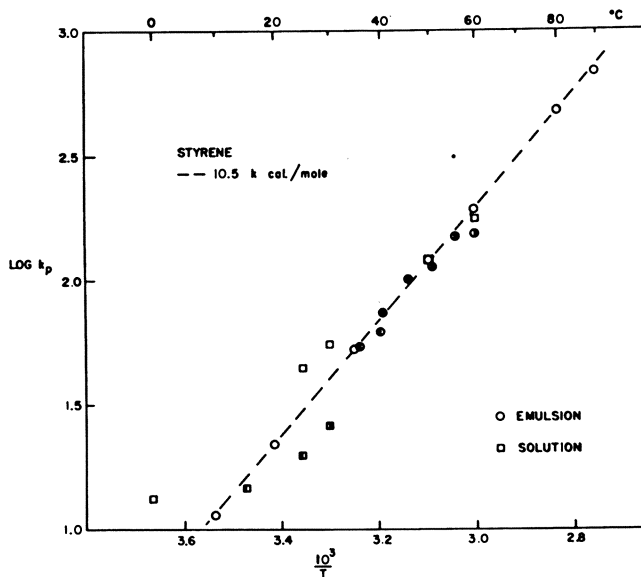


Figure 9. Arrhenius plot of the propagation rate constant of styrene

- ⊗ (28)
- (15, 16)
- (52)
- (65)
- (40)
- (14) assuming termination by recombination
- (41) assuming termination by recombination

The fourth factor determining polymerization rate is the monomer concentration in the particles. For some monomers the ratio of monomer to polymer in the particles is about constant during part of the polymerization. Smith (57) suggested that this results from "a balance between the effect on the monomer activity of the dissolved polymer and the effect of interfacial tension of the very small particles." This equilibrium was put in a quantitative form by Morton, Kaizerman, and Altier (44), who derived the following equation by combining an expression for the interfacial free energy of the particle with the Flory-Huggins equation for the activity of the solvent (monomer) in the monomer-polymer particle.

$$-\{\ln(1 - v_2) + v_2 + \mu v_2^2\} = \frac{2V_1\gamma}{rRT} \quad (11)$$

in which

- v_2 = volume fraction of the polymer in the particle
- μ = polymer-monomer interaction parameter
- V_1 = molar volume of the monomer
- γ = interfacial tension between particle and water
- r = radius of the particle

This relation has been tested by Morton, who determined values of μ and γ from equilibrium swelling measurements of polystyrene latices. The results obtained were in good agreement with values of μ and γ (54) determined by other methods. Allen (1) measured the swelling of natural rubber latex with methyl methacrylate and found the dependence of swelling on particle size to agree well with the above equation.

Equation 11 refers to equilibrium swelling conditions. Now, Flory (24) concludes from theoretical considerations that "monomer is easily supplied to the polymer particles at the required rate" even in the case of monomers which are little soluble in water, such as styrene. That equilibrium swelling is maintained during emulsion polymerization is supported by a comparison of values of the monomer concentrations determined in equilibrium swelling measurements with those found to prevail during polymerization and determined by analysis of reaction kinetics (see below). The results obtained by both methods are plotted in Figure 10.

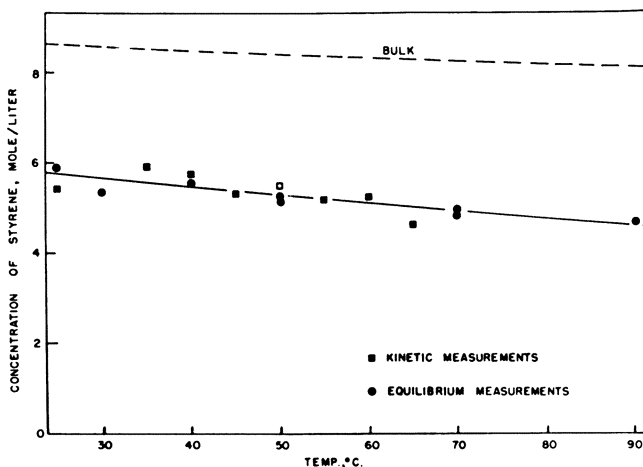


Figure 10. Concentration of styrene in polystyrene latex particles at different temperatures

Comparison of kinetic and equilibrium swelling measurements

- Average values (5, 6)
 - 25° (44), latex fraction 102E
 - 30°, 50°, 70°, Average values (66)
- - 50°, (57)
 - 40°, 50°, 70°, 90° (65)

All these values are not strictly comparable, because the diameters of the particles and the interfacial tension for the individual latices were not all equal. The agreement between the results obtained by both methods is nevertheless taken to support the assumption that during polymerization the particles are swollen to the equilibrium maximum. In the above it is assumed that stirring is sufficiently vigorous to prevent diffusion out of the monomer droplets from becoming the restrictive factor in the transport of monomer to the particles.

It follows from Equation 11 that during a particular emulsion polymerization, two factors, γ and τ , determine v_2 and hence the monomer concentration in the

particles. The fractional surface coverage of the particles with emulsifier decreases during polymerization and this coverage determines γ . The dependence of γ on the coverage is not known, but it seems reasonable to assume that γ is approximately a linear function of the surface coverage between the minimum value of about 4 dynes per cm. at surface saturation to about 35 dynes per cm. in the absence of emulsifier. Taking values of γ from $\gamma = 35 - 31\alpha$ dynes per cm. (α = fractional coverage), a value of 1000 Å. for the final diameter of a polystyrene latex particle and $\mu = 0.43$, the monomer concentration in that particle was calculated as a function of conversion. In Figure 11, the calculated monomer concentration is compared with experimental results. The calculated values show that the increases in γ and in r approximately compensate each other, the average monomer concentration in all the particles varying only by about 10%. It must therefore be concluded that the occurrence of a (nearly) zero-order reaction with respect to monomer is fortuitously due to compensating colloidal and thermodynamic effects.

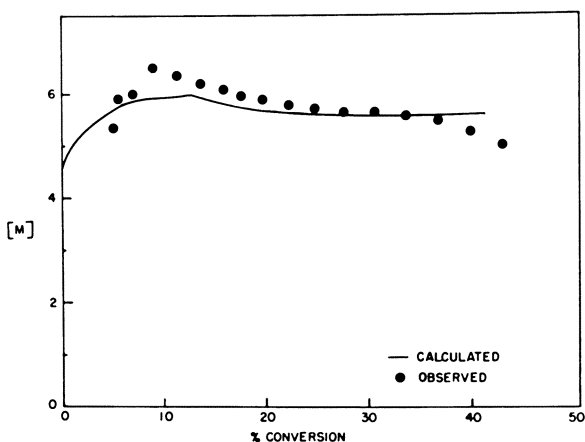


Figure 11. Dependence of concentration of styrene in particles during polymerization

When all the monomer has been imbibed by the particles, the monomer concentration decreases with conversion and the reaction becomes first-order, provided that the number of radicals per particle remains constant—i.e., at low initiation rate in small particles. Such a polymerization system is shown in Figure 12, where the logarithm of the reaction rate is plotted against time. From about 60 to 90% conversion, this plot gives a straight line, as is required by a first-order reaction.

From the conversion at which the order of the reaction changes from 0 to 1, the monomer concentration in the particles during the zero-order stretch can be calculated (6). The data of Figure 10 marked “kinetic measurements” result from such calculations.

Because of the scarcity of numerical values of the Flory-Huggins interaction parameter and the interfacial tension for different polymer-monomer systems, few calculations can be made of the expected emulsion polymerization behavior of different monomers.

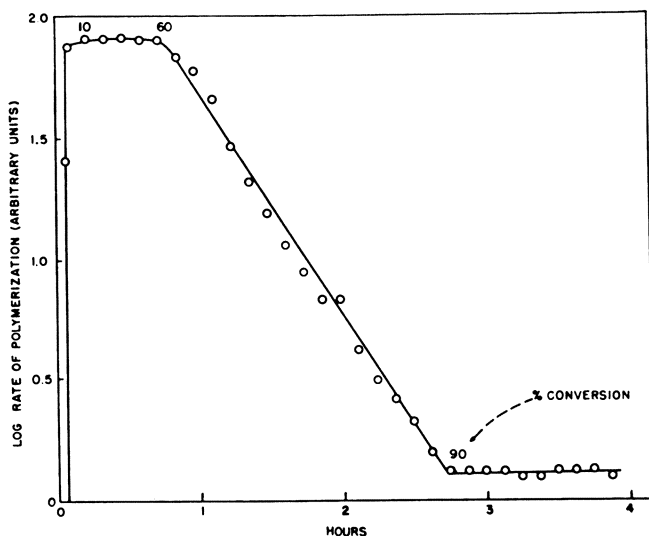


Figure 12. Rate of polymerization of styrene as a function of time in reaction mixture seeded with small particle size latex

Semilogarithmic plot

Termination

The termination reaction between radicals is a relatively fast process. The rate constant, k_t , for many polymers is of the order of 10^7 liters mole⁻¹ sec.⁻¹. It can be calculated that at this reaction rate two radicals can coexist in a particle of 1000-Å diameter, on the average, only 0.03 second, which is negligible with respect to the time of growth of a polymer radical.

Most reported values of k_t have been determined in solution polymerization or in bulk systems at low conversions. In bulk at higher conversions, or more generally in viscous media, the rate of termination is lower. The more viscous the reaction medium the more is the termination rate determined by the rate of diffusion of the macroradicals. The result of decreased termination is increased polymerization rate and increased molecular weight. This result is called the gel effect or Trommsdorff effect.

It has not always been realized that the gel effect is particularly important in emulsion systems, where the polymer concentration at the site of reaction is generally high. For styrene the local "conversion" in the particles is about 45% and this condition prevails from early in the polymerization.

It is possible to calculate k_t via the emulsion kinetics outlined previously. Some results are listed in Table IV.

Table IV. Values of k_t in Emulsion Polymerization of Styrene at 50° C.

k_t , Liter Mole ⁻¹ Sec. ⁻¹	Initiation	Ref.
$(3-30) \times 10^4$	$K_2S_2O_8$	(63)
$(1-50) \times 10^4$	Cumene hydroperoxide	(63)
$(1-10) \times 10^4$	γ radiation	(66)
0.2×10^4	$K_2S_2O_8$	(28)

These values for styrene at 50° C. are to be compared with those determined in solution or bulk, which are in the range $(0.5 \text{ to } 3) \times 10^7$ liters mole⁻¹ sec.⁻¹. In methyl methacrylate polymerizations, k_t is particularly strongly affected by conversion. The gel effect in bulk polymerization of this monomer has been determined by Robertson (53) and Benough and Melville (8). Robertson showed the decrease of k_t to start at conversions as low as 5% in certain systems. In emulsion polymerization of methyl methacrylate, the low value of k_t causes the gel effect to occur from very early in the reaction on, as demonstrated by Zimmt (71). The dependence of k_t on viscosity of the medium has been determined by Benson and North (9), who found that for methyl methacrylate, k_t decreases by a factor of about 100 when the viscosity is increased from a very low value to about 200 centipoises.

Nonideal Emulsion Polymerization

It has been pointed out that the degree of ideality of an emulsion polymerization is determined by the magnitude of parameter a , which in turn determines the value of the subdivision factor, z . Since

$$a = 4 (R_i/2k_t)^{1/2} N_A v$$

three variables govern the ideality of the system and deviations from ideal behavior arise when R_i or v is too large or k_t is too small.

When polymerization proceeds to high conversions, the viscosity at the site of reaction becomes high and k_t decreases rapidly with conversion. Parameter a increases and so does the average number of radicals per particle, \bar{n} . This is illustrated by data obtained by Gerrens (27), in the polymerization of styrene. Figure 13 shows the increase of \bar{n} with conversion.

Nonideal behavior is also brought about by too large a particle size. This effect can be seen in Figure 13 for the region of high conversions and in Figure 14 for conversions between 15 and 50%. In the latter figure, there is some variation in the rate of initiation in the different systems depicted, R_i varying by a factor of 18 between extreme cases. The effect of this variation on a is therefore by a factor of about 4, but this influence of R_i is small compared to the variation in v . The average volume of the largest particles shown is 100 times that of the smallest. The full line in Figure 14 is calculated from the empirical relation derived by Gerrens (27) from families of curves like the one in Figure 13 relating \bar{n} to R_i , DP, conversion, and temperature. It can be concluded that there is a fair agreement between nonideality caused by low values of k_t in small particles at high conversion and that caused by large volume of the particles at low conversions. The dashed line is calculated with a value of k_t derived from solution polymerization data ($k_t = 1.84 \times 10^7$) and shows the pronounced effect of the reduction in termination rate in emulsion systems due to the high viscosity in the particles.

The third factor governing the degree of ideality of an emulsion system is the rate of initiation. Its influence is shown in Figure 15. In a polymerization from which these data were obtained, a small particle latex was used as a seed under conditions such that no new particles were formed. Hence, the rate of polymerization in these reactions is proportional to \bar{n} . The dashed line indicates a polymerization rate corresponding to $\bar{n} = 1/2$. It can be seen from Figure 15 that in these experiments \bar{n} increases with R_i at constant v and k_t . Nonideality here is caused by initiation rates, which are too high for the given particle volume and termination rate of these systems. In seeded polymerizations v is larger than in polymeriza-

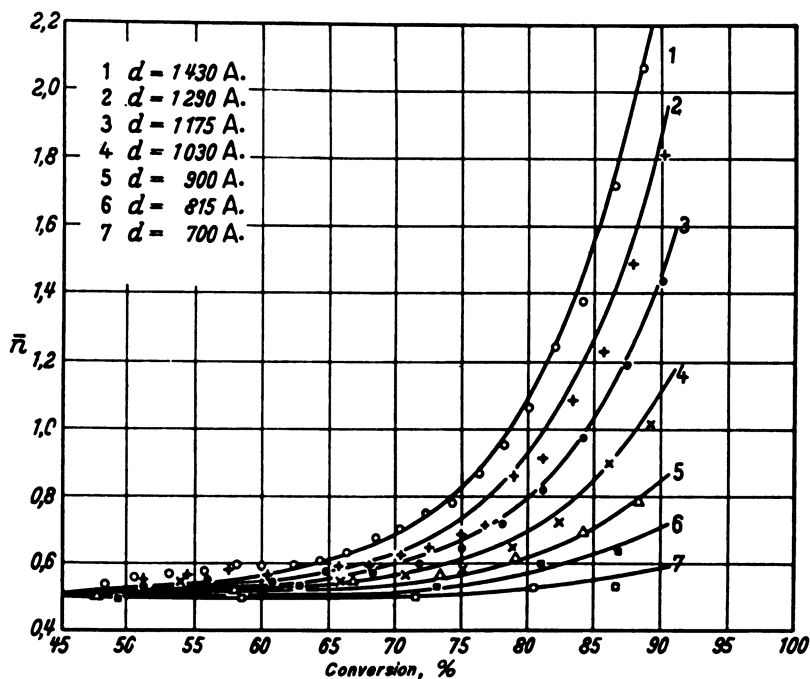


Figure 13. Average number of radicals per particle (\bar{n}) as a function of conversion during polymerization of styrene

From Gerrens, H., *Z. Elektrochem.* 60, 400 (1956)
 COURTESY *Zeitschrift für Elektrochemie*

tions initiated in soap micelles; hence even low initiation rates may cause deviations from ideal behavior. Seeded systems have, however, a great advantage in that the number of particles is fixed and easily reproducible. At very low rates of initiation \bar{n} is smaller than $1/2$. These low rates correspond to time periods of polymer radical growth of 1 to 2 minutes. It might be expected that during these very long time intervals other, very slow, termination processes come into play.

In the examples described above, the transition is shown from ideal ($\bar{n} = 1/2$) to nonideal ($\bar{n} > 1/2$) behavior. There are, however, systems for which ideal emulsion polymerization practically cannot be achieved. It is nevertheless possible to describe the kinetics of such systems quantitatively. Recently, Gerrens has obtained values of the propagation and termination rate constants at different temperatures for vinyltoluene and vinylxylene (28). The termination rate of polymer radicals of these monomers is so low that even at small rates of initiation in small particles, \bar{n} is larger than $1/2$. From measurements of the reaction rate before and after injection of additional initiator in the polymerizing system it was possible to calculate n both at the original and at the boosted initiation rate with the aid of Equation 5. Consistent results were obtained when the additional amount of initiator was varied. From these rate data, the termination rate constant was found to be 10^3 and $17 \text{ liters mole}^{-1} \text{ sec}^{-1}$ at 45° C . for vinyltoluene and vinylxylene, respectively. These values are to be compared with $\sim 10^4$ for styrene (Table IV).

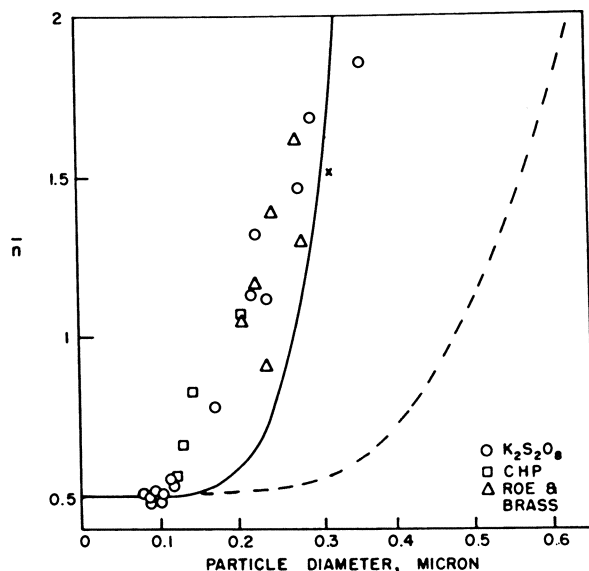


Figure 14. Average number of radicals per particle (\bar{n}) at low conversions as a function of particle size during polymerization of styrene

- Polymerization initiated by potassium persulfate
 - Polymerization initiated by cumene hydroperoxide
 - △ Calculated from (55)
- Experimental details given in Table VII (62)

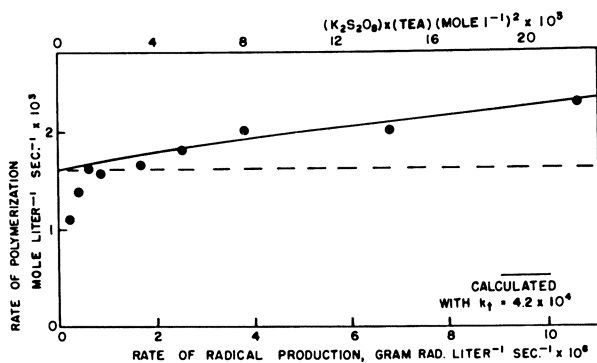


Figure 15. Rate of reaction in seeded polymerization of styrene as a function of rate of radical production

TEA = triethanolamine

Rate of radical production calculated with rate constants from (5)

----- Calculated rate of polymerization corresponding to $\bar{n} = 1/2$

————— Calculated with $k_1 = 4.2 \times 10^4$ liters mole⁻¹ sec.⁻¹

Conclusion

It seems justified to conclude that the theoretical aspects of emulsion polymerization kinetics have to a large extent been developed, at least for water-"in-

soluble" monomers. Experimental data satisfactorily support the theories. A recent mathematical advance has enlarged the scope of the original Smith-Ewart rate theory and made it possible not only to define accurately the conditions under which ideal emulsion polymerization behavior might be expected, but also to treat quantitatively nonideal emulsion reactions. It has now become possible to predict polymerization characteristics whether the system is, or is not, subdivided into particles of colloidal dimensions or of microscopic size.

Least understood is the mechanism of particle formation. Only in simple systems with water-"insoluble" monomers is this mechanism known and have its kinetic features been confirmed experimentally.

Much remains to be done with soluble monomers. Coalescence and coagulation of oligomeric and polymeric molecules and indeed of particles have prevented the quantitative treatment of such systems. It might be useful to use seeded polymerizations which provide a means of separating the processes of particle formation and particle growth.

Acknowledgment

The author thanks H. Gerrens for permission to use his data.

Literature Cited

- (1) Allen, P. W., *J. Colloid Sci.* **13**, 483 (1958).
- (2) Allen, P. W., *J. Polymer Sci.* **31**, 207 (1958).
- (3) Bakker, J., Ph.D. thesis, Utrecht University, Netherlands, 1952; *Philips Research Repts.* **7**, 344 (1952).
- (4) Bamford, C. H., Barb, W. G., Jenkins, A. D., Onyon, P. F., "Kinetics of Vinyl Polymerization by Radical Mechanisms," Academic Press, New York, 1958.
- (5) Bartholomé, E., Gerrens, H., *Z. Elektrochem.* **61**, 522 (1957).
- (6) Bartholomé, E., Gerrens, H., Herbeck, R., Weitz, H. M., *Ibid.*, **60**, 334 (1956).
- (7) Belonovskaia, G. B., Dolgoplosk, B. A., Vasiutina, Zh.D., Kulakova, M. N., *Izvest. Akad. Nauk S.S.S.R., Otdel. Khim.* **1958**, 24.
- (8) Benough, W. I., Melville, H. L., *Proc. Roy. Soc. (London)* **A249**, 455 (1959).
- (9) Benson, S. W., North, A. M., *J. Am. Chem. Soc.* **81**, 1339 (1959).
- (10) Bovey, F. A., Kolthoff, I. M., Medalia, A. J., Meehan, E. J., "Emulsion Polymerization," Interscience, New York, 1955.
- (11) Breitenbach, J. W., *Kolloid-Z.* **109**, 119 (1944).
- (12) Breitenbach, J. W., Edelhauser, H., *Makromol. Chem.* **44-46**, 196 (1961).
- (13) Burnett, G. M., "Mechanism of Polymer Reactions," Interscience, New York, 1954.
- (14) Burnett, G. M., *Trans. Faraday Soc.* **46**, 772 (1950).
- (15) Burnett, G. M., Lehrle, R. S., *Proc. Roy. Soc. (London)* **A253**, 331 (1959).
- (16) Burnett, G. M., Lehrle, R. S., Overall, D. W., Peaker, F. W., *J. Polymer Sci.* **29**, 417 (1958).
- (17) Cherdron, H., *Kunststoffe* **50**, 568 (1960).
- (18) Cherdron, H., Schulz, R. C., Kern, W., *Makromol. Chem.* **32**, 197 (1959).
- (19) Dolgoplosk, B. A., Tinyakova, E. I., *Khim. Nauka. i. Prom.* **2**, 280 (1957); *Gummi u. Asbest.* **12**, 438, 508, 582, 722 (1959).
- (20) Edelhauser, H., Breitenbach, J. W., *J. Polymer Sci.* **35**, 423 (1959).
- (21) Evans, C. P., Hay, P. M., Marker, L., Murray, R. W., Sweeting, O. J., *J. Appl. Polymer Sci.* **5**, 39 (1961).
- (22) Fikentscher, H., *Angew. Chem.* **51**, 433 (1938).
- (23) Fikentscher, H., Herrle, H., *Ibid.*, **A59**, 179 (1947).
- (24) Flory, P. J., "Principles of Polymer Chemistry," p. 210, Cornell Univ. Press, Ithaca, N. Y., 1953.
- (25) French, D. M., *J. Polymer Sci.* **32**, 395 (1958).
- (26) Gerrens, H., *Fortschr. Hochpolymeren-Forsch.* **1**, 234 (1959).
- (27) Gerrens, H., *Z. Elektrochem.* **60**, 400 (1956).
- (28) Gerrens, H., Köhnlein, E., *Ibid.*, **64**, 1199 (1960).
- (29) Harkins, W. D., *J. Am. Chem. Soc.* **69**, 1428 (1947).
- (30) Harkins, W. D., *J. Polymer Sci.* **5**, 217 (1950).
- (31) Haward, R. N., *Ibid.*, **4**, 273 (1949).

- (32) Hay, P. M., Light, J. C., Marker, L., Murray, R. W., Santonicola, A. T., Sweeting, O. J., Wepsic, J. G., *J. Appl. Polymer Sci.* **5**, 23 (1961).
- (33) Jacobi, B., *Angew. Chem.* **64**, 539 (1952).
- (34) Jones, J. H., *J. Assoc. Offic. Agr. Chemists* **28**, 398 (1945).
- (35) Klevens, H. B., *J. Colloid Sci.* **2**, 365 (1947).
- (36) Kolthoff, I. M., Medalia, A. I., *J. Polymer Sci.* **5**, 391 (1950).
- (37) Kolthoff, I. M., Miller, I. K., *J. Am. Chem. Soc.* **73**, 3055 (1951).
- (38) Kolthoff, I. M., O'Connor, P. R., Hansen, J. L., *J. Polymer Sci.* **15**, 459 (1955).
- (39) Light, J. C., Santonicola, A. T., Sweeting, O. J., *J. Appl. Polymer Sci.* **5**, 31 (1961).
- (40) Matheson, M. S., Auer, E. E., Bevilacqua, E. B., Hart, E. J., *J. Am. Chem. Soc.* **73**, 1700 (1951).
- (41) Melville, H. W., Valentine, L., *Trans. Faraday Soc.* **46**, 210 (1950).
- (42) Moore, D. E., Parts, A. G., *Makromol. Chem.* **37**, 108 (1960).
- (43) Morton, M., Cala, J. A., Altier, M. W., *J. Polymer Sci.* **19**, 547 (1956).
- (44) Morton, M., Kaizerman, S., Altier, M. W., *J. Colloid Sci.* **9**, 300 (1959).
- (45) Morton, M., Landfield, H., *J. Polymer Sci.* **8**, 111 (1952).
- (46) Morton, M., Salatiello, P. P., Landfield, H., *Ibid.*, **8**, 279 (1952).
- (47) Nakajima, A., Yamakawa, H., Sakurada, I., *Ibid.*, **35**, 489 (1959).
- (48) O'Donnell, J. T., Mesrobian, R. B., Woodward, A. E., *Ibid.*, **28**, 171 (1958).
- (49) Okamura, S., Motoyama, T., Intern. Symposium Macromolecular Chem., p. 82, Montreal, 1961.
- (50) Okamura, S., Motoyama, T., *J. Chem. Soc. (Japan), Ind. Chem. Sect.* **61**, 384 (1958).
- (51) Palit, S. R., *Kunststoffe* **50**, 513 (1960).
- (52) Patsiga, R., Litt, M., Stannett, V., *J. Phys. Chem.* **64**, 801 (1960).
- (53) Robertson, E. R., *Trans. Faraday Soc.* **52**, 426 (1956).
- (54) Roe, C. P., Brass, P. D., *J. Colloid Sci.* **9**, 602 (1954).
- (55) Roe, C. P., Brass, P. D., *J. Polymer Sci.* **24**, 401 (1957).
- (56) Schulz, G. V., Proc. Intern. Symposium Macromolecular Chem., p. 124, Prague, 1957.
- (57) Smith, W. V., *J. Am. Chem. Soc.* **70**, 3695 (1948).
- (58) Smith, W. V., Ewart, R. H., *J. Chem. Phys.* **16**, 592 (1948).
- (59) Staudinger, J. J. P., *Chem. & Ind. (London)* **1948**, 563.
- (60) Stockmayer, W. H., *J. Polymer Sci.* **24**, 314 (1957).
- (61) Thomas, W. M., Gleason, E. H., Mins, G., *Ibid.*, **24**, 43 (1957).
- (62) van der Hoff, B. M. E., *Ibid.*, **33**, 487 (1958).
- (63) *Ibid.*, **44**, 241 (1960).
- (64) *Ibid.*, **48**, 175 (1960).
- (65) van der Hoff, B. M. E., unpublished results, 1958.
- (66) Vanderhoff, J. W., Bradford, E. B., Tarkowski, H. L., Wilkinson, B. W., *J. Polymer Sci.* **50**, 265 (1961).
- (67) Voutzii, S. S., Zeizema, M. A., *Uspekhi Khim.* **16**, 69 (1947).
- (68) Walling, C., "Free Radicals in Solution," Wiley, New York, 1957.
- (69) Wiener, H., *J. Polymer Sci.* **7**, 1 (1951).
- (70) Yurzhenko, A. T., Kolechova, M., *Doklady Akad. Nauk S.S.S.R.* **47**, 354 (1945).
- (71) Zimmt, W. S., *J. Appl. Polymer Sci.* **1**, 323 (1959).

RECEIVED September 6, 1961.

Inverse Emulsion Polymerization

J. W. VANDERHOFF, E. B. BRADFORD, H. L. TARKOWSKI, J. B. SHAFFER, and R. M. WILEY

Physical Research Laboratory, The Dow Chemical Co., Midland, Mich.

In an inverse emulsion polymerization, a hydrophilic monomer, frequently in aqueous solution, is emulsified in a continuous oil phase using a water-in-oil emulsifier and polymerized using either an oil-soluble or water-soluble initiator; the products are viscous latices comprised of submicroscopic, water-swollen, hydrophilic polymer particles colloidally suspended in the continuous oil phase. The average particle sizes of these latices are as small as 0.05 microns. The technique is applicable to a wide variety of hydrophilic monomers and oil media. The inverse emulsion polymerization of sodium *p*-vinylbenzene sulfonate initiated by both benzoyl peroxide and potassium persulfate was compared to the persulfate-initiated polymerization in aqueous solution. Hypotheses for the mechanism and kinetics of polymerization were developed and used to calculate the various kinetic parameters of this monomer.

In a conventional emulsion polymerization, a hydrophobic monomer is emulsified in water using an oil-in-water emulsifier and polymerized using a water-soluble initiator. A schematic representation according to Harkins (19) is shown in Figure 1. The hydrophobic monomer exists in three loci—i.e., in the emulsion droplets, in the aqueous phase as solute molecules, and in the emulsifier micelles as solubilized molecules; most of the monomer is in the emulsion droplets. The emulsifier also exists in three loci—i.e., in the oil-water interface, in the aqueous phase as solute molecules, and in the micelles; most of the emulsifier is in the micelles. The primary free radicals are generated in the aqueous phase and migrate to the monomer-water interface. Since the total surface area of the micelles is large relative to that of the monomer droplets, the probability is great that the diffusing radical will enter a micelle rather than a droplet. The initiation of polymerization in a monomer-containing micelle transforms it into a monomer-swollen polymer particle before the initial polymer radical is terminated. The rapid chain propagation is sustained by monomer diffusing from reservoir droplets and neighboring micelles which have not captured a radical. This initiation process con-

Background Literature

Mechanism and Kinetics of Emulsion Polymerization

<i>Subject</i>	<i>Ref.</i>
General qualitative theory of the mechanism and kinetics of emulsion polymerization	(19)
General quantitative treatment (Smith-Ewart) of the foregoing theory	(35)
Experimental verification of the Smith-Ewart theory for the styrene-persulfate system	(33, 34)
Emulsion polymerization of butadiene in the "mutual recipe"	(30)
Emulsion polymerization of butadiene in the hydroperoxide-polyamine system	(31)
Emulsion polymerization of styrene in the persulfate and hydroperoxide-polyamine systems, and isoprene in the hydroperoxide-polyamine system	(32)
Emulsion polymerization of styrene in the persulfate-fatty acid soap system	(4)
Emulsion polymerization of styrene in the persulfate-Amphoseife system	(7)
Emulsion polymerization of styrene in the persulfate-triethanolamine-Amphoseife system	(6)
The gel effect at high conversions in styrene emulsion polymerization	(17)
Emulsion polymerization of styrene, vinyltoluene, and dimethylstyrene in the persulfate-Amphoseife system	(18)
Emulsion polymerization of styrene in the cumene hydroperoxide-fatty acid soap system	(22)
The gel effect at low conversions in styrene emulsion polymerization	(23)
Emulsion polymerization of styrene and styrene-acrylonitrile mixtures above and below the critical micelle concentration	(24)
Emulsion polymerization of styrene using oil-soluble initiators	(25)
Quantitative theoretical treatment of emulsion polymerization kinetics (more general than the Smith-Ewart theory)	(20, 36)
Emulsion polymerization of methyl methacrylate in the persulfate-Tergitol 7 system	(43)
The mechanism and kinetics of emulsion polymerization as inferred from particle size distributions determined by ultracentrifugation	(11-13)
Emulsion polymerization of vinylidene chloride in the persulfate-metabisulfite-sodium lauryl sulfate system	(16, 21, 27, 28)
Emulsion polymerization of styrene using the competitive growth technique	(10, 37-39)
Emulsion polymerization of styrene-divinylbenzene and styrene-acrylonitrile mixtures using the competitive growth technique	(40)
Emulsion polymerization of styrene initiated by γ -rays	(41)

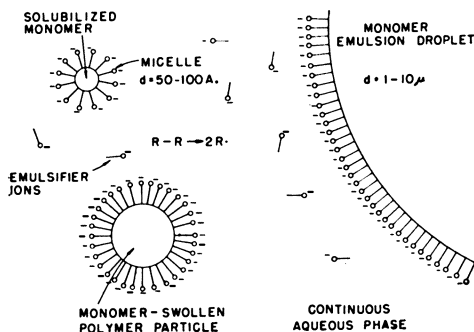


Figure 1. Schematic representation of a conventional emulsion polymerization

tinues until all of the micelles either become monomer-swollen polymer particles, or relinquish their monomer and emulsifier to a radical-containing neighbor. The disappearance of the micelles marks the end of stage 1, the particle initiation stage. In stage 2, the growth stage, no new particles are formed; those formed in stage 1 continue to grow until the supply of monomer or free radicals is exhausted. This hypothesis was treated quantitatively by Smith and Ewart (35) and applied successfully to the styrene system (33, 34). Since then, it has been extended by many investigators to other monomers and initiators over a wide range of conditions.

In an inverse emulsion polymerization, an aqueous solution of a hydrophilic monomer is emulsified in a continuous hydrophobic oil phase using a water-in-oil emulsifier. The polymerization is initiated with either oil-soluble or water-soluble initiators. Figure 2 shows a schematic representation of this system. The formation of micelles is uncertain, but is portrayed speculatively. The hydrophilic part of the emulsifier molecule is oriented toward the hydrophilic dispersed phase and the hydrophobic part toward the hydrophobic continuous phase. The initiation of polymerization proceeds by a mechanism analogous to that of the conventional system and submicroscopic particles of water-swollen hydrophilic polymer are generated in the continuous oil phase.

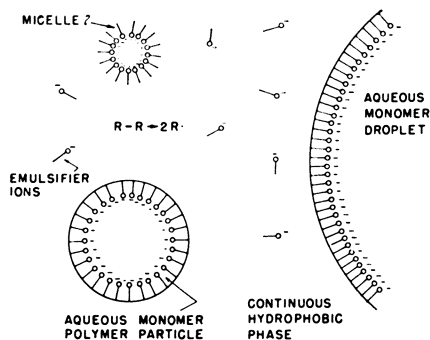


Figure 2. Schematic representation of an inverse emulsion polymerization

In conventional latices, the colloidal stability of the particles arises from the predominance of the electrostatic forces of repulsion over the London-van der Waal's forces of attraction. These electrostatic forces of repulsion result from the electric double layer formed by the emulsifier ions adsorbed on the hydrophobic polymer particle surface and the counterions from the aqueous phase. The London-van der Waal's forces of attraction are strongest when the particle-particle distance is very small. Therefore, in most particle-particle collisions, the particles repel one another until the particle-particle distance is decreased to the point where the London-van der Waal's forces of attraction are predominant over the electrostatic forces of repulsion. Thus, many conventional latices remain stable indefinitely without significant stratification or flocculation of the particles.

In an inverse latex, these electrostatic forces are quite different. For water-in-oil emulsions, Albers and Overbeek (1, 2, 3) found that, with ionic emulsifiers, flocculation was promoted by gravity because of the diffuse nature of the electric double layer relative to that of oil-in-water systems and, with nonionic emulsifiers,

flocculation was not prevented by adsorbed oleophilic chains up to 20A. in length. Thus it might be expected that inverse lattices will stratify or flocculate more readily than their conventional counterparts.

Experimental Methods, Results, and Discussion

General. Aqueous solutions of hydrophilic monomers were emulsified in xylene using water-in-oil emulsifiers, and polymerized using oil-soluble initiators. Typical hydrophilic monomers were sodium *p*-vinylbenzene sulfonate, sodium vinylbenzyl sulfonate, 2-sulfoethyl acrylate, acrylic acid, acrylamide, vinylbenzyltrimethylammonium chloride, and 2-aminoethyl methacrylate hydrochloride. Typical oil-soluble initiators were benzoyl and lauroyl peroxides. In some cases, water-soluble potassium persulfate was used, both separately and in mixtures with oil-soluble peroxides. Of the water-in-oil emulsifiers, one of the most effective was Span 60 (technical sorbitan monostearate, Atlas Chemical Industries, Inc.).

The emulsions were formed by dissolving the emulsifier in xylene and adding the aqueous monomer solution with stirring. Frequently the crude emulsions were homogenized (Cenco hand homogenizer) to decrease the average droplet size and increase the emulsion stability. The emulsions were heated with stirring at 40° to 70° C. to effect polymerization. The time required for essentially complete conversion varied from a few minutes to several hours. The viscosities of the final lattices were high—e.g., ca. 400 centipoises, as compared to ca. 10 centipoises for a conventional polystyrene latex of the same concentration.

These lattices consist of submicroscopic, water-swollen, hydrophilic polymer spheres colloiddally suspended in the continuous xylene phase. A typical electron micrograph of a diluted dispersion of a sodium poly (*p*-vinylbenzene sulfonate) latex which had been treated to remove water is shown in Figure 3. The inverse

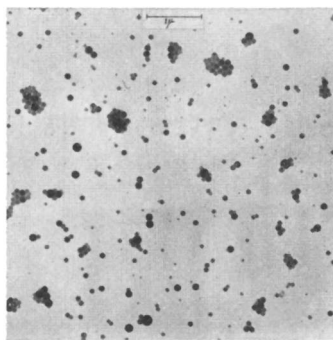


*Figure 3. Electron micrograph of sodium poly(*p*-vinylbenzene sulfonate) latex*

latex particles are spherical and as small as 300A. in diameter. Thus, the two criteria for an emulsion polymerization system—i.e., a segregated free radical system and a number of loci for polymerization within a few orders of magnitude of the number of free radicals existent at a given time, appear to be met by these systems.

These inverse lattices are less stable than conventional lattices; upon standing,

their particles will settle out in a few hours to a few days. In some cases, the stratified latices may be redispersed by gentle agitation. Continuous, gentle agitation will preserve the latex in its colloidal state indefinitely.

Purification of Sodium *p*-Vinylbenzene Sulfonate Monomer. The crude monomer was purified by recrystallization. A saturated solution of monomer was prepared in water containing sodium nitrite polymerization inhibitor at pH 11. This solution was cooled and the monomer crystals were filtered, washed with absolute alcohol, and dried under vacuum at 25° to 35° C. Three batches of purified monomer were prepared. Batch No. 1 was used for the benzoyl peroxide-initiated polymerizations, batch No. 2 for persulfate-initiated solution polymerizations, which will be described elsewhere, and batch No. 3 for persulfate-initiated emulsion and solution polymerizations. In batch No. 1, the monomer solution containing 20% monomer and 0.4% sodium nitrite was prepared at 25° C. and cooled to 0° C. to crystallize the monomer. The monomer crystals (one part) were treated twice by shaking with six parts of absolute alcohol, filtering in a fritted glass funnel, washing with five parts of absolute alcohol, and drying under vacuum at room temperature. For batch No. 2, the monomer was recrystallized three times. In the first crystallization, a saturated solution of monomer was prepared without sodium nitrite at 40° C. and cooled to 0° C. to effect crystallization. The product was dissolved in water under nitrogen and recrystallized in the same manner. This product was dissolved in water containing ca. 0.5% sodium nitrite at 55° C. and cooled to effect the crystallization. The crystals were filtered out at 32° and 22° C., squeezed dry, shaken in absolute alcohol for one hour, filtered, washed, dried under vacuum at 35° C. for three days, and stored under vacuum. Various analytical data are summarized in Table I. Batch No. 3 was recrystallized from batch No. 2; the saturated solution containing ca. 30% monomer and ca. 0.3% sodium nitrite at pH 11 was prepared at 50° C. The crystals were filtered out at ca. 35° and ca. 23° C. and were treated in the same manner at batch No. 2.

Table I. Analyses of Monomer

Compound	Batch No. 1		Batch No. 2	
	Original	Final	Original	Final
	Per Cent			
Monomer	93.62	98.48	71.49	98.32
NaBr	1.62	None	0.12	0.36
Na ₂ SO ₄	2.37	None	18.28	0.25
NaNO ₂	...	0.02	...	0.02
H ₂ O	2.82	0.23	...	0.16
Ethanol	...	0.87
Polymer	...	0.3	...	1.00
Sodium bromoethylbenzene sulfonate	1.40	0.89

The consistency of the three monomer batches is demonstrated by the rates of polymerization under equivalent conditions, 20% aqueous solution, 0.20% K₂S₂O₈ based on water (Figure 4, Table II). The polymerization rates were practically the same for batches Nos. 2 and 3, but were significantly lower for batch No. 1.

Table II. Polymerization Rates of Various Monomer Batches

Batch No.	Initial $R_p \times 10^4$, Moles/Liter Second		
	50° C.	60° C.	70° C.
1	1.34	3.28	9.13
2	1.87	5.16 ^a 3.96	11.9
3	1.98	4.21 ^a 4.44	11.3

^a Not shown in Figure 4.

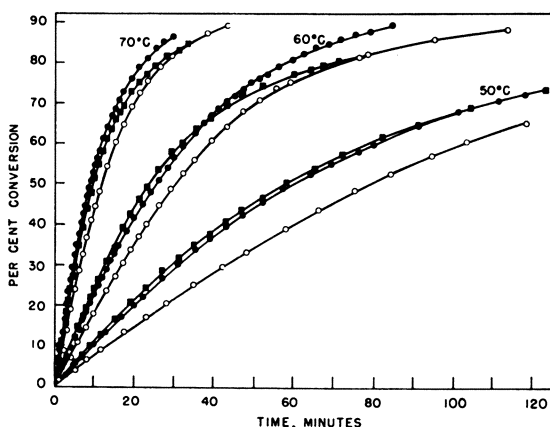


Figure 4. Variation of per cent conversion with time for various monomer batches polymerized in aqueous solution with persulfate initiator

○ Batch No. 1 ● Batch No. 2 ■ Batch No. 3

Benzoyl Peroxide-Initiated Polymerizations. A series of experiments were carried out using sodium *p*-vinylbenzene sulfonate as the hydrophilic monomer, benzoyl peroxide as the initiator, Span 60 as the emulsifier, and *o*-xylene as the continuous oil phase. In all polymerizations, the aqueous monomer solution contained 20% monomer, the xylene/monomer solution ratio was 70/30, and the nominal benzoyl peroxide concentration was 0.20% based on xylene. The polymerization rates were determined dilatometrically at 50°, 60°, and 70° C. The glass dilatometers were agitated by a magnetic stirring bar and held in a bath controlled within $\pm 0.05^\circ$ C. The emulsions were prepared without benzoyl peroxide initiator, homogenized, degassed by heating, and charged into the dilatometers. The benzoyl peroxide was added in xylene solution at the polymerization temperature and the rate of volume contraction with time was measured. After the polymerization had reached a high conversion, the latex was cooled, shortstopped, and analyzed for residual monomer by coulometric bromination. These analyses were used to determine the cubic centimeters of contraction per gram of polymerized monomer; the average of these values, 0.07639 ($\sigma = 0.00179$), was used to calculate the conversion-time curves. The values for the final per cent conversion are given in Table III.

Table III. Benzoyl Peroxide-

Temp., °C.	Emulsifier, G. Xylene, Cu. Cm.	Final Conversion, %	Av. Particle Diameter (σ), A.	Av. Particle Volume $\times 10^{18}$, Liters
50	0.033	93.5	1190(460)	1.27
	0.042	92.2	1100(440)	1.05
	0.050	92.7	930(260)	0.528
	0.067	93.2	770(250)	0.320
	0.083	94.7	710(210)	0.238
	0.125	91.9	660(180)	0.183
60	0.033	82.4	1480(370)	2.00
	0.042	95.6	1060(360)	0.842
	0.050	95.6	920(320)	0.560
	0.067	93.9	840(340)	0.484
	0.083	95.2	720(260)	0.278
	0.125	92.7	670(190)	0.198
70	0.033	76.1	1780(210)	3.07
	0.042	92.8	1460(370)	1.92
	0.050	96.9	1330(350)	1.49
	0.067	94.2	770(230)	0.309
	0.083	98.8	750(230)	0.287
	0.125	99.4	670(190)	0.200

To recover the polymer, latex samples were coagulated in absolute alcohol, filtered, washed with absolute alcohol, and dried under vacuum at 35° C. The polymer molecular weights were estimated from the reduced specific viscosities (0.400 gram of polymer per 100 cu. cm. of aqueous 0.5N NaCl solution, at 30° C.) according to the relationship of Vanderkooi, Schultz, and Sieglaff (42).

$$\eta_{sp}/C = 3.5 \times 10^{-6}[M]^{0.87}$$

Typical conversion-time curves are shown in Figure 5. These curves, for 0.125 gram of emulsifier per cu. cm. of xylene at 50°, 60°, and 70° C., were normalized to the origin to eliminate the induction period which was essentially non-existent at 70° C., but as great as 40 minutes at 50° C. After a short initial period, the per cent conversion increased almost linearly with time to 50 to 60% and then levelled off to approach complete conversion asymptotically. The shape of these curves is very similar to those of conventional emulsion polymerizations.

The values for the over-all rate of polymerization calculated from the linear portions of the conversion-time curves are listed in Table III. The variation of these over-all rates with emulsifier concentration is shown in Figure 6. At 50° C., the over-all rate was independent of emulsifier concentration; the least squares slope is -0.006 ($\sigma = 0.13$). At 60° and 70° C., the over-all rate increased with increasing emulsifier concentration; the least squares slopes of these lines are 0.58 ($\sigma = 0.11$) and 0.89 ($\sigma = 0.14$) respectively.

The final latices were prepared for electron microscopy by dilution with xylene to ca. 0.1% polymer followed by distillation to remove the water. The distilled latices were diluted further and dried on the specimen substrates. The electron microscope specimens could not be calibrated with monodisperse polystyrene particles because of the sensitivity of the sodium poly (*p*-vinylbenzene sulfonate) particles to water. Instead, the magnification was calibrated from one separate exposure of monodisperse spheres which was made on each photographic plate of five exposures.

Initiated Polymerizations

Number of Particles/Cu. Cm. Xylene $\times 10^{-15}$	$k_d [I] \times 10^8$, Moles/Liter Second	$R_p \times 10^4$, Moles/Liter Second	Rate/Particle $\times 10^{20}$, G./Particle/ Second	$\overline{DP} \times 10^{-3}$
0.253	1.91	1.94	5.13	4.03
0.304	1.85	1.53	3.34	3.72
0.597	1.87	2.24	2.46	4.61
0.970	1.87	1.74	1.16	4.85
1.28	1.87	1.99	0.985	4.80
1.46	1.98	2.03	0.771	4.54
0.160	7.42	3.45	14.4	2.94
0.377	7.48	3.91	6.84	3.10
0.563	7.51	5.86	6.82	4.85
0.637	7.52	5.66	5.70	3.66
1.09	7.45	6.36	3.86	4.46
1.34	7.92	8.57	3.53	5.21
0.104	29.5	7.60	48.5	1.99
0.164	29.3	9.08	36.3	2.13
0.210	29.8	10.3	31.9	2.36
0.996	29.6	19.0	12.2	3.68
1.05	29.6	19.0	11.4	4.54
1.32	31.5	25.6	10.7	3.88

The average particle volumes, $[(\pi/6) (\sum n_i D_i^3 / \sum n_i)]$, were calculated and corrected to compensate for the water removed by distillation. The correction factors based on a polymer density of 1.53 grams per cu. cm. were 7.12, 7.16, and 7.20 at 50°, 60°, and 70° C., respectively. The values for numbers of particles per cu. cm. of xylene (N) were calculated (Table III). The average particle diameters listed in this table are the number averages corrected for the water removed by distillation; the values of σ are given in parentheses following the average diameter. Since the particle size distributions were fairly broad, the statistical t- and F-tests were applied to determine possible variations with polymerization temperature; these results are given in Table IV. At the three highest

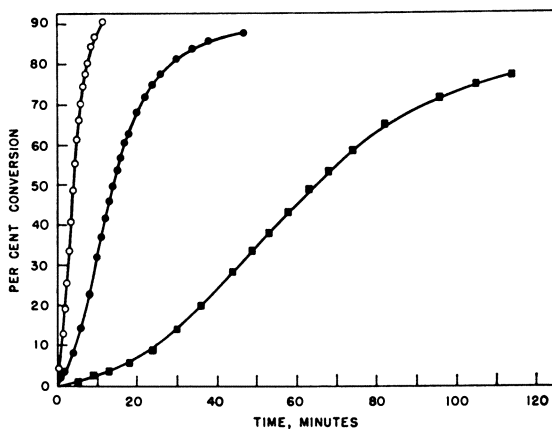


Figure 5. Variation of per cent conversion with time, benzoyl peroxide initiator, and 0.125 gram of emulsifier per cu. cm. of xylene

■ 50° C. ● 60° C. ○ 70° C.

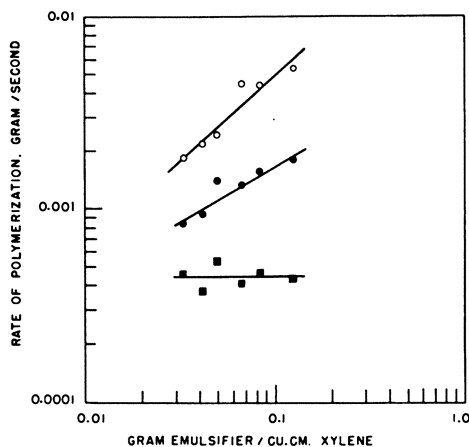


Figure 6. Variation of over-all rate of polymerization with emulsifier concentration

■ 50° C. ● 60° C. ○ 70° C.

emulsifier concentrations, 0.067, 0.083, and 0.125 gram per cu. cm. of xylene, N was independent of temperature and depended only upon the emulsifier concentration. At 0.042 and 0.050 gram of emulsifier per cu. cm. of xylene, the values of N at 50° and 60° C. were equivalent, but were smaller at 70° C. At the lowest concentration, 0.033 gram per cu. cm. of xylene, N decreased with increasing polymerization temperature. In conventional emulsion polymerization systems initiated by peroxide compounds, N usually increases with increasing temperature; however, in the γ -ray-initiated emulsion polymerization of styrene (41), N was observed to decrease with increasing temperature. Since the free radical concentration of γ -ray-initiated systems is independent of temperature, it was suggested that, with increasing temperature, the temperature-dependent propagation rate produces larger initial polymer molecules in the relatively few micelles which capture radicals. Therefore, a larger proportion of the micelles which have not captured radicals are forced to relinquish their emulsifier and monomer to support the growth of the radical-containing micelles. In systems initiated by peroxide compounds, the same competitive situation exists, but the activation energy for initiator decomposition is sufficiently greater than that of chain propagation to override this effect. However, this explanation is not applicable to the foregoing inverse emulsion polymerization data.

The variation of N with emulsifier concentration is shown on a log-log plot (Figure 7); N increased strongly with increasing emulsifier concentration (initial slope = 2.5 to 4.5) and levelled off at high concentrations. These results differ

Table IV. Variation of N With Polymerization Temperature

Emulsifier, G./Xylene, Cu. Cm.	Condition
0.033	Decreases with increasing temperature
0.042	Equivalent at 50° and 60° C.; decreases at 70° C.
0.050	Equivalent at 50° and 60° C.; decreases at 70° C.
0.067	Equivalent at 50°, 60°, and 70° C.
0.083	Equivalent at 50°, 60°, and 70° C.
0.125	Equivalent at 50°, 60°, and 70° C.

considerably from the Smith-Ewart case where a straight line with a slope of 0.6 was observed (33).

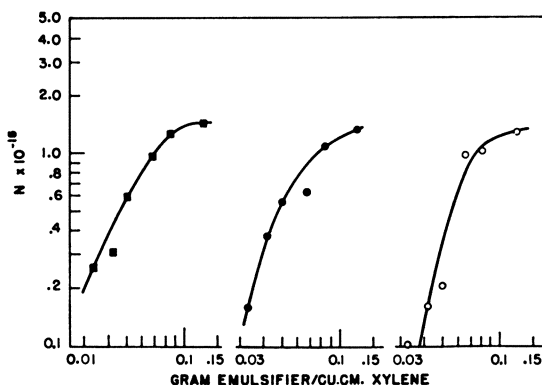


Figure 7. Variation of the number of particles per cubic centimeter of xylene with emulsifier concentration

■ 50° C. ● 60° C. ○ 70° C.

These unusual variations of N with emulsifier concentration and temperature suggest that the aqueous monomer droplets may furnish loci for polymerization initiation. In conventional emulsion polymerizations, the monomer droplets usually range in diameter from 1 to 10 microns; therefore their total surface area is small relative to that of the micelles, and they serve only as reservoirs in the particle initiation process. However, if these monomer droplets were smaller by one or two orders of magnitude, they would compete effectively with the monomer-swollen micelles for the available radicals and therefore would serve as loci for particle initiation.

In order to determine how small an emulsion droplet can be formed in this system, a 20% solution of sodium poly(*p*-vinylbenzene sulfonate) was prepared and emulsified in xylene containing 0.083 gram of emulsifier per cu. cm. in the same manner as the monomer solutions. The homogenized emulsion was then prepared for electron microscopy in the same manner as the final latex samples. Figure 8,B shows an electron micrograph of this dispersion, while Figure 8,A shows, for comparison, an electron micrograph of an inverse latex prepared using the same concentration of emulsifier. It is evident that this dispersion of polymer contained emulsion droplets as small as 200A. in diameter—i.e., in the same size range as the smallest particles of the analogous inverse latex.

This is supported by the values for the interfacial tension (du Nuöy ring method), 0 ± 0.01 dyne per cm., of a 20% aqueous monomer solution in contact with xylene solutions of emulsifier (0.033, 0.083, and 0.125 gram per cu. cm.). This very low interfacial tension is consistent with the formation of very fine emulsion droplets.

The critical micelle concentration of Span 60 in benzene has been determined as 0.0022 gram per cu. cm., the micellar molecular weight as 52,800, and the aggregation number as 94 (8, 9). Thus, the emulsifier concentrations of the foregoing polymerization experiments were considerably in excess of the critical micelle concentration. The shape and actual size of the micelles have not been

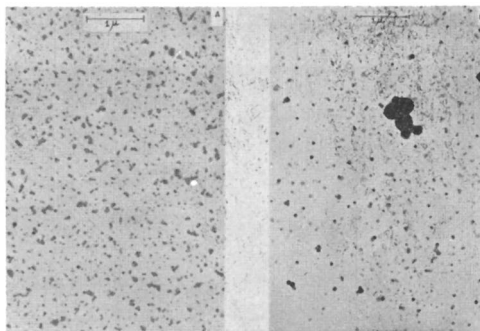


Figure 8. Electron micrographs

A. Sodium poly(*p*-vinylbenzene sulfonate) latex
 B. Emulsified sodium poly(*p*-vinylbenzene sulfonate) solution

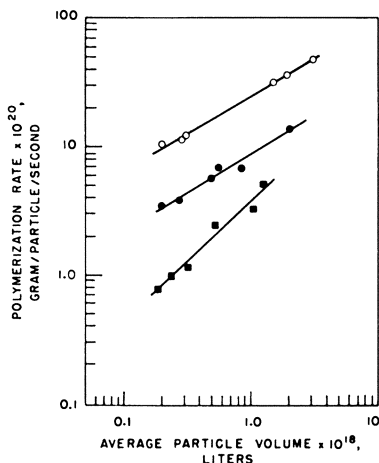


Figure 9. Variation of rate of polymerization per particle with average particle volume

■ 50° C. ● 60° C. ○ 70° C.

determined, but it is reasonable to assume a diameter of the order of 100A. for a spherical model.

Therefore, it is concluded that, although the monomer-swollen micelles furnish loci for particle initiation, many monomer droplets are small enough to serve also in this capacity and, as a result, particle initiation occurs in both the micellar and droplet phase. The reverse dependence of N on temperature at low emulsifier concentrations is still unexplained.

The variation of the rate of polymerization per particle with the average particle volume is shown in Figure 9. The increase of the polymerization rate is about the same for the 60° and 70° C. samples, but is greater for the 50° C. samples. The least squares slopes of these lines are 0.94 ($\sigma = 0.078$) for 50° C., 0.60 ($\sigma = 0.056$) for 60° C., and 0.58 ($\sigma = 0.022$) for 70° C. At 60° and

70° C., there is a subdivision effect typical of emulsion polymerization systems, while at 50° C., this effect is less marked and the kinetics resemble those of a solution polymerization.

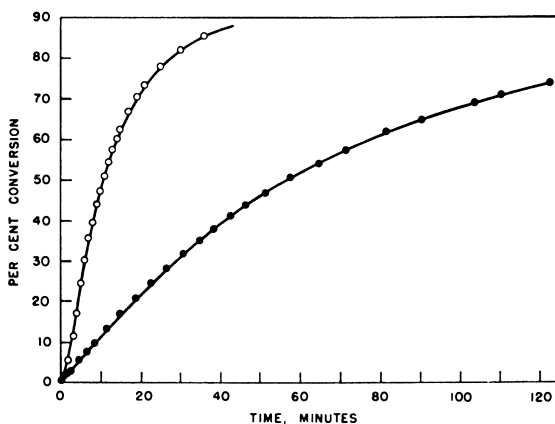


Figure 10. Variation of per cent conversion with time for persulfate-initiated polymerizations at 50° C.

● Solution ○ Emulsion

Potassium Persulfate-Initiated Polymerizations. A similar series of experiments was carried out using potassium persulfate as the initiator; the concentration was 0.20% based on water. A series of solution polymerizations was also carried out for comparison. For these polymerizations, an unstirred glass dilatometer in the shape of a cylindrical coil, 0.5 cm. in I.D. and 120 cm. in length, was used. Thus, portions of the same aqueous phase containing 20% monomer and 0.20 gram of initiator per 100 grams of water were polymerized in both emulsion and solution at 40°, 50°, 60°, and 70° C. Figure 10 shows the comparative conversion-time curves at 50° C. The polymerization rate was considerably more rapid in emulsion than in solution, but the shapes of the curves were similar. This disparity in rate decreased with increasing temperature (Figure 11); extrapolation of the polymerization rate-temperature curves indicated that the rates should be equivalent at about 90° C. Figure 12 shows the conversion-time curves of the emulsion polymerizations at various temperatures; the rates increased with increasing temperature as expected. The pertinent kinetic data from these experiments are listed in Table V.

Hypotheses Concerning Kinetic Parameters

The foregoing data were analyzed using the following equations suggested by van der Hoff (23) and taken from the theoretical analyses of Stockmayer (36) and Haward (20).

$$z = \bar{n}/(a/4) = I_0(a)/I_1(a) \quad (1a)$$

$$z = \bar{n}/(a/4) = \tanh (a/4) \quad (1b)$$

$$a/4 = (fk_d[I]/k_t)^{1/2}N_A V \quad (2)$$

Table V. Persulfate-Initiated Polymerizations

Temp., °C.	Type	Initial $R_p \times 10^4$, Moles/Liter Second	$k_d [I] \times 10^8$, Moles/Liter Second	Average Particle Diameter (σ), A.	Average Particle Volume $\times 10^{18}$, Liters
40	Inverse emulsion	6.24	0.116	1780(550)	4.35
40	Solution	0.935	0.116
50	Inverse emulsion	12.2	0.626	1490(550)	2.50
50	Solution	1.98	0.626
60	Inverse emulsion	14.4	3.11	1560(660)	3.16
60	Solution	4.44	3.11
70	Inverse emulsion	20.6	14.4	1590(780)	3.75
70	Solution	11.3	14.4

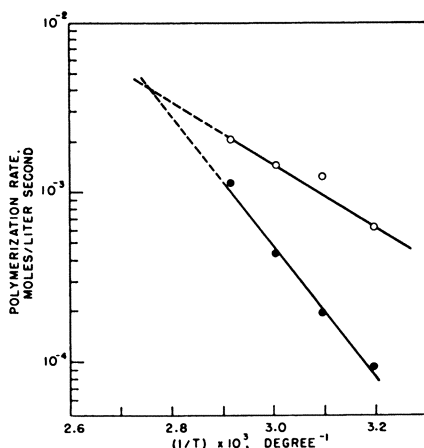


Figure 11. Variation of rate of polymerization with temperature

● Solution ○ Emulsion

$$R_p = z \{ (k_p^2/k_t) f k_d [I] \}^{1/2} [M] \quad (3)$$

$$1/\overline{DP} = (1/z) \{ (k_t/k_p^2) f k_d [I] \}^{1/2} (1/[M]) + (k_{tr}/k_p) \quad (4)$$

where \bar{n} is the average number of free radicals per particle, f is the average of efficiencies of both initiator fragments in initiating polymer chains, k_d is the rate constant for the decomposition of initiator, $[I]$ is the concentration of initiator based on the dispersed phase, $[M]$ is the monomer concentration in the particles, N_A is Avogadro's number, I_0 and I_1 are Bessel functions of the first kind of zero- and first-order respectively, and V is the average particle volume in liters. Equation 1a represents the case where the radicals are generated in, or enter, the particles singly, while Equation 1b represents the case where radicals are generated in, or enter, the particle in pairs. The variations of z and az with a are shown in Figure 13 [taken in part from reference (23)] where the upper curves correspond to Equation 1a and the lower curves to Equation 1b.

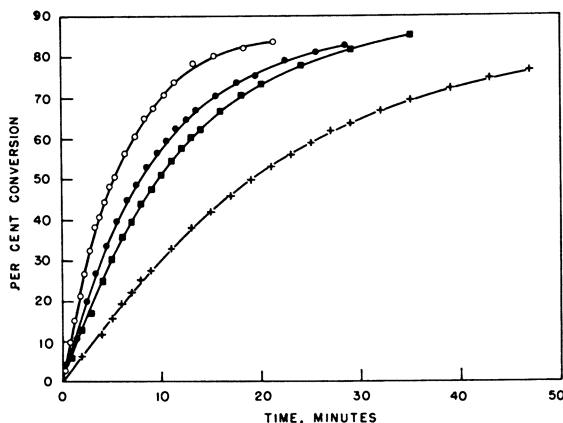


Figure 12. Variation of per cent conversion with time for persulfate-initiated emulsion polymerizations

+ 40° C. ■ 50° C. ● 60° C. ○ 70° C.

The values of k_d used for benzoyl peroxide decomposition at 50°, 60°, and 70° C. were 0.92, 3.7, and 15×10^{-6} per second, respectively (15). The values of k_d used for potassium persulfate decomposition at 40°, 50°, 60°, and 70° C. were 0.20, 1.0, 5.0, and 23×10^{-6} per second, respectively (26). The calculated values of $k_d [I]$ are listed in Tables III and V.

Except for the factor z , Equation 3 is a standard kinetic equation which should apply to the persulfate-initiated solution polymerization. Thus, if it is assumed that f, k_p , and k_t are equivalent for both solution and emulsion polymerizations at the same temperature, the ratio of the initial values for R_p for emulsion and

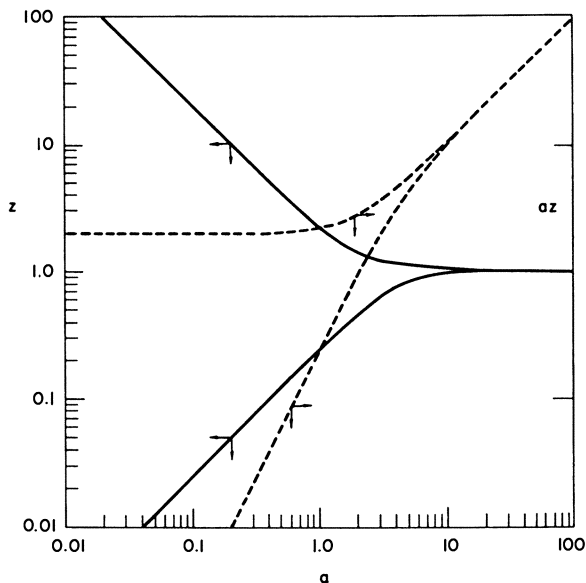


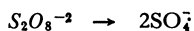
Figure 13. Variation of z and az with a

solution polymerizations should equal z . Once z is known, a and \bar{n} may be calculated from the appropriate form of Equation 1. The values used for R_p were the initial rates given (Table V). To determine z , the slopes of the conversion-time curves (Figure 10) were determined at every 5% of conversion. The values of z were found to vary only insignificantly up to 40 to 80% conversion. Therefore the values of z (Table VI) are these averages; the corresponding values of σ are indicative, at least in part, of the precision of measurement of the slopes. To determine k_p , Equations 2 and 3 may be combined to give

$$k_p = 4R_p N_A V / az[M] \quad (5)$$

Table VI shows the values for k_p as well as for k_t (calculated in terms of f from Equation 2).

All values of z are greater than 1. Since the initiation of radicals by persulfate ion has been proposed (26) as



it might be expected that the radicals would be generated in pairs in the particles and therefore the lower curve (Figure 13) would apply. However, the experimental values of z are all significantly greater than 1, and therefore it must be assumed that some mechanism for the generation of single radicals in an emulsion particle is operative. Possibly, as suggested for the styrene-cumene hydroperoxide system (25) even a very low rate of radical transfer in or out of the particle would explain the results. Thus, the values of a and \bar{n} (Table VI) correspond to those of the upper curve (Figure 13). The values of \bar{n} , ranging from 0.50 to 0.61, correspond to the Smith-Ewart case at 40° and 50° C., and increase with increasing concentration of free radicals. The values of k_p are approximately 30 times greater than those of styrene (23, 29). The Arrhenius plot of $\log k_p$ with reciprocal temperature is shown in Figure 14. The activation energy calculated from the least squares slope was 7.07 ($\sigma = 0.65$) kcal. per mole. This is in good agreement with previously published values for styrene (5, 14, 29, 32, 33).

Table VI. Persulfate-Initiated Polymerizations

Temp., °C.	z (σ)	a	\bar{n}	$k_p \times 10^{-3}$, Liters/Mole Second	$k_t \times 10^{-6}$, Liters/Mole Second
40	6.67(0.26)	0.302	0.50	2.77	1.10f
50	6.05(0.24)	0.332	0.50	3.54	2.05f
60	2.96(0.25)	0.715	0.53	5.04	3.53f
70	1.79(0.11)	1.36	0.61	7.47	6.37f

To estimate values for k_{tr}/k_p , Equations 3 and 4 were combined and rearranged to give

$$(1/\overline{DP}) = (fk_d[I]/R_p) + (k_{tr}/k_p) \quad (6)$$

If it is assumed that f is constant for a given series, a plot of $(1/\overline{DP})$ vs. $(k_d[I]/R_p)$ should have a slope of f and an intercept of k_{tr}/k_p at $(k_d[I]/R_p) = 0$. The benzoyl peroxide-initiated polymerization data were analyzed in this manner. There was considerable experimental scatter in these plots and therefore, the data are given (Table VII) as the least squares slopes and intercepts as well as their 95% confidence limits. The average values of k_{tr}/k_p , ranging from 0.8 to $1.1 \times$

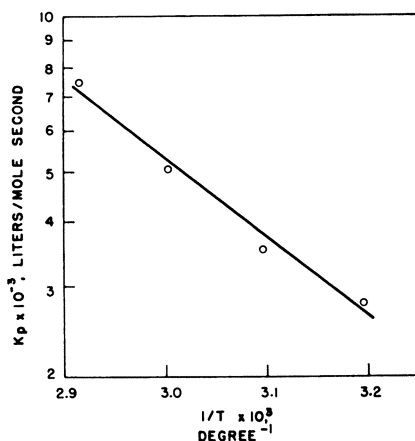


Figure 14. Variation of $\log k_p$ with reciprocal temperature

10^{-4} , are reasonable, and in the same range as the values for styrene, 0.35 and 0.65×10^{-4} at 50° and 70° C., respectively (25). However, the experimental scatter is such that these values can be regarded only as estimates. The values of f ranged from 1.1 to 1.3; these values are reasonable considering the experimental scatter and the possible errors.

Table VII. Estimated Values for k_{tr} and f

Temp., °C.	$k_{tr}/k_p \times 10^4$		k_{tr} , Liter/Mole Second		f	
	Av.	95% Confidence limits	Av.	95% Confidence limits	Av.	95% Confidence limits
50	1.1	0.17-1.9	0.37	0.060-0.69	1.2	0.34-2.1
60	0.76	0.40-1.1	0.38	0.20-0.57	1.3	1.0-1.5
70	0.98	0.60-1.4	0.73	0.45-1.0	1.1	0.94-1.2

The other parameters for the benzoyl peroxide-initiated polymerizations were calculated in the following manner. Using the subscripts B and P to denote the benzoyl peroxide- and persulfate-initiated polymerizations respectively, Equations 2 and 3 give

$$a_B = 4 \{ (f_B k_{d_B} [I]_B) / k_{i_B} \}^{1/2} N_A V_B \quad (7a)$$

$$a_P = 4 \{ (f_P k_{d_P} [I]_P) / k_{i_P} \}^{1/2} N_A V_P \quad (7b)$$

$$R_{PB} = z_B \{ (k_p^2 / k_{i_B}) f_B k_{d_B} [I]_B \}^{1/2} [M]_B \quad (8a)$$

$$R_{PP} = z_P \{ (k_p^2 / k_{i_P}) f_P k_{d_P} [I]_P \}^{1/2} [M]_P \quad (8b)$$

These equations are combined to give

$$a_B z_B = a_P z_P (V_B / V_P) (R_{PB} / R_{PP}) \quad (9)$$

Thus values of az can be calculated for the benzoyl peroxide-initiated polymerizations from the known values of az (persulfate-initiated polymerizations), and the ratios of average particle volumes and polymerization rates. These values of az may then be substituted in Equations 3 and 4 to give values for f/k_i and fk_i which may then be combined to give values for f and k_i . The results of these calculations are shown (Table VIII-A). The values of az are all considerably less than 2. From Figure 13, for the case where the radicals are generated in, or enter,

the particle singly, az should equal 2 at values of a up to 0.2 and then increase with increasing values of a . The benzoyl peroxide-initiated polymerizations would be expected to follow this case, if each initiator molecule decomposed in the continuous oil phase to form a pair of radicals which then enter the particles singly. However, the calculated values of az range from 0.02 to 0.7, all of them considerably smaller than 2. There are many possible experimental errors which might affect the value of az , but since this quantity is based on experimentally determined ratios of polymerization rates and average particle volumes, it is difficult to imagine a 100-fold error. Therefore, the case where the radicals are generated in, or enter, the particle in pairs must be considered. In order for this mechanism to be operative, the polymerization must be initiated only by those few peroxide molecules which enter the particles and decompose there, while most of the peroxide decomposes in the continuous oil phase to form radicals which are ineffective in initiating polymerization.

This hypothesis is admittedly tenuous, but at the present time, there is no other explanation which fits the observed results. Therefore the values for a , z ,

Table VIII. Benzoyl Peroxide-

A. Calculated from Equations

Temp., °C.	Emulsifier, G.		az	a	z
	Xylene, Cu. Cm.				
50	0.033		0.163	0.815	0.201
	0.042		0.106	0.655	0.163
	0.050		0.0781	0.561	0.140
	0.067		0.0367	0.383	0.0955
	0.083		0.0312	0.353	0.0880
	0.125		0.0244	0.312	0.0779
60	0.033		0.321	1.15	0.280
	0.042		0.153	0.788	0.195
	0.050		0.152	0.785	0.194
	0.067		0.127	0.717	0.177
	0.083		0.0822	0.576	0.143
	0.125		0.0788	0.563	0.140
70	0.033		0.736	1.77	0.415
	0.042		0.550	1.52	0.363
	0.050		0.484	1.41	0.339
	0.067		0.185	0.868	0.214
	0.083		0.172	0.836	0.206
	0.125		0.162	0.811	0.201

B. Recalculated using normalized

50	0.033	0.234	0.975	0.240
	0.042	0.152	0.785	0.194
	0.050	0.112	0.672	0.167
	0.067	0.0527	0.460	0.115
	0.083	0.0448	0.423	0.106
	0.125	0.0351	0.374	0.0933
60	0.033	0.435	1.35	0.325
	0.042	0.207	0.918	0.226
	0.050	0.206	0.915	0.225
	0.067	0.172	0.836	0.206
	0.083	0.111	0.670	0.166
	0.125	0.107	0.658	0.163
70	0.033	0.935	2.01	0.466
	0.042	0.699	1.72	0.405
	0.050	0.615	1.61	0.382
	0.067	0.235	0.979	0.241
	0.083	0.219	0.944	0.234
	0.125	0.206	0.915	0.226

and \bar{n} were determined from the lower curve (Figure 13). As expected for this mechanism, the values of \bar{n} , 0.006 to 0.2, are much lower than the values of 0.5 to 0.6 obtained for the persulfate-initiated system. The values of f and k_t are given as the average and the range, respectively. These designations refer to the average values and 95% confidence limits of k_{tr}/k_p listed (Table VII). The average values of f range from 0.8 to 1.5 and appear to be independent of temperature (in calculating k_{tr}/k_p , it was assumed that f was constant for the series at a given temperature). The values corresponding to the 95% confidence limits range from 0.1 to 2.4.

The average values of k_t range from 0.5 to 54×10^5 liters per mole second and increase with increasing temperature, increasing particle size, and decreasing polymer molecular weight. It is expected that k_t would increase with temperature. The variation of k_t with average particle volume is shown (Figure 15). The lines are almost parallel; the least squares slopes at 50°, 60°, and 70° C. are 1.20 ($\sigma = 0.071$), 1.34 ($\sigma = 0.11$), and 1.33 ($\sigma = 0.093$), respectively. The distance between these lines corresponds to an activation energy of about 15 kcal. per mole.

Initiated Polymerizations

3, 4, and 9

\bar{n}	f		$k_t \times 10^{-6}$, Liters/Mole Second	
	Av.	Range	Av.	Range
0.041	1.5	0.55-2.4	3.9	1.5-6.4
0.027	1.4	0.62-2.1	3.7	1.7-5.8
0.020	1.3	0.28-2.4	1.3	0.27-2.3
0.0092	0.93	0.11-1.8	0.70	0.084-1.3
0.0078	1.1	0.15-2.0	0.53	0.073-1.0
0.0061	1.2	0.27-2.1	0.46	0.10-0.82
0.080	1.2	1.1-1.4	16.	14.-18.
0.038	1.3	1.1-1.5	6.4	5.4-7.4
0.038	1.0	0.73-1.3	2.2	1.6-2.9
0.032	1.5	1.2-1.7	2.9	2.4-3.5
0.021	1.3	0.95-1.6	1.3	0.96-1.6
0.020	1.3	0.86-1.6	0.71	0.49-0.94
0.18	1.0	0.94-1.1	54.	49.-59.
0.14	1.2	1.0-1.3	31.	28.-35.
0.12	1.1	0.99-1.2	22.	19.-24.
0.046	1.1	0.88-1.4	2.4	1.9-3.0
0.043	0.79	0.55-1.0	1.6	1.1-2.1
0.041	1.3	1.0-1.6	1.5	1.1-1.8

values for R_p

0.059	2.1	0.79-3.4	3.9	1.5-6.4
0.038	1.9	0.89-3.0	3.7	1.7-5.8
0.028	1.9	0.40-3.5	1.3	0.27-2.3
0.013	1.3	0.16-2.5	0.70	0.084-1.3
0.011	1.6	0.21-2.9	0.54	0.073-1.0
0.0088	1.7	0.38-3.0	0.46	0.10-0.82
0.11	1.7	1.4-1.9	16.	14.-18.
0.052	1.7	1.5-2.0	6.4	5.4-7.3
0.052	1.4	0.98-1.8	2.2	1.6-2.9
0.043	2.0	1.6-2.4	2.9	2.4-3.5
0.028	1.7	1.3-2.1	1.3	0.96-1.6
0.027	1.7	1.2-2.2	0.71	0.48-0.93
0.23	1.3	1.2-1.4	53.	48.-58.
0.18	1.5	1.3-1.6	31.	28.-34.
0.15	1.4	1.3-1.6	21.	19.-24.
0.059	1.4	1.1-1.7	2.4	1.9-3.0
0.055	1.0	0.69-1.3	1.6	1.1-2.1
0.052	1.7	1.3-2.1	1.5	1.1-1.8

However, when the $\log k_t$ is plotted against \overline{DP} , (Figure 16), all of the points are fitted best by a single line. The vertical lines through each point correspond to the ranges of k_t calculated from the 95% confidence limits of k_{tr}/k_p (Table VIII-A). The single line shown was calculated by least squares using the average values of k_t . These data suggest that, even at a monomer concentration of only 20%, the termination process is diffusion-controlled and the effect of temperature is obscured.

It may be argued that the variation in polymerization rate (Table II, Figure 4) with the various monomer batches may introduce gross errors in the foregoing calculations. Therefore, the polymerization rates of batch No 1. were normalized to the average of the rates for batches Nos. 2 and 3; the factors used for 50°, 60°, and 70° C. were 1.44, 1.35, and 1.27, respectively. The recalculated values for k_{tr}/k_p were almost identical to those of Table VII. The values for f were somewhat larger, ranging from 1.4 to 1.8. The corrected values of az and the correspondingly higher values of a , z , and \bar{n} are listed (Table VIII-B). Although the values of f are somewhat larger, the calculated values of k_t are virtually identical of those of Table VIII-A.

Acknowledgment

The authors acknowledge gratefully the assistance of the East Main Analytical Laboratory, The Dow Chemical Co., which carried out the coulometric bromination and viscosity measurements.

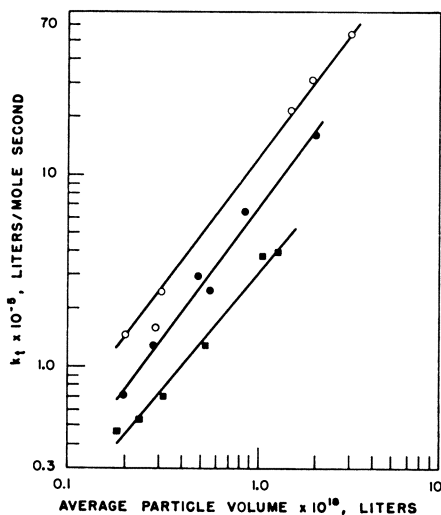


Figure 15. Variation of k_t with average particle volume

■ 50° C. ● 60° C. ○ 70° C.

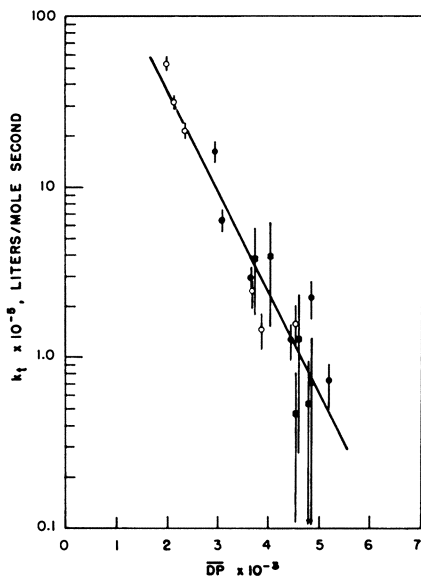


Figure 16. Variation of $\log k_t$ with \overline{DP}

Literature Cited

- (1) Albers, W., Overbeek, J. Th. G., *J. Colloid Sci.* **14**, 501 (1959).
- (2) *Ibid.*, p. 510.
- (3) *Ibid.*, **15**, 489 (1960).
- (4) Bakker, J., "Kinetics of the Emulsion Polymerization of Styrene," Ph.D. thesis, University of Utrecht, The Netherlands, 1952.
- (5) Bamford, C. H., Dewar, M. J. S., *Proc. Roy. Soc. London A***192**, 309 (1948).
- (6) Bartholomé, E., Gerrens, H., *Z. Elektrochem.* **61**, 522 (1957).
- (7) Bartholomé, E., Gerrens, H., Herbeck, R., Weitz, H. M., *Ibid.*, **60**, 334 (1956).
- (8) Becher, P., private communication, Atlas Chemical Industries, Inc., Wilmington, Del., September 1961.
- (9) Becher, P., Clifton, N. K., *J. Colloid Sci.* **14**, 519 (1959).
- (10) Bradford, E. B., Vanderhoff, J. W., Alfrey, T., Jr., *Ibid.*, **11**, 135 (1956).
- (11) Brodnyan, J. G., *Ibid.*, **15**, 563 (1960).
- (12) *Ibid.*, p. 573.
- (13) Brodnyan, J. G., Brown, G. L., *Ibid.*, **15**, 76 (1960).
- (14) Burnett, G. M., *Trans. Faraday Soc.* **46**, 772 (1950).
- (15) Doehnert, D. F., Mageli, O. L., 13th Annual Meeting, Reinforced Plastics Division, Soc. Plastics Ind., Inc., Feb. 4-6, 1958, Chicago, Ill.
- (16) Evans, C. P., Hay, P. M., Marker, L., Murray, R. W., Sweeting, O. J., *J. Appl. Polymer Sci.* **5**, 39 (1961).
- (17) Gerrens, H., *Z. Elektrochem.* **60**, 400 (1956).
- (18) Gerrens, H., Köhnlein, E., *Ibid.*, **64**, 1199 (1960).
- (19) Harkins, W. D., "The Physical Chemistry of Surface Films," chap. 5, Reinhold, New York, 1952.
- (20) Haward, R. N., *J. Polymer Sci.* **4**, 273 (1949).
- (21) Hay, P. M., Light, J. C., Marker, L., Murray, R. W., Santonicola, A. T., Sweeting, O. J., Wepsic, J. G., *J. Appl. Polymer Sci.* **5**, 23 (1961).
- (22) van der Hoff, B. M. E., *J. Phys. Chem.* **60**, 1250 (1956).
- (23) van der Hoff, B. M. E., *J. Polymer Sci.* **33**, 487 (1958).
- (24) *Ibid.*, **44**, 241 (1960).
- (25) *Ibid.*, **48**, 175 (1960).
- (26) Koltzoff, I. M., Miller, I. K., *J. Am. Chem. Soc.* **73**, 3055 (1951).
- (27) Light, J. C., Santonicola, A. T., *J. Polymer Sci.* **36**, 549 (1959).
- (28) Light, J. C., Marker, L., Santonicola, A. T., Sweeting, O. J., *J. Appl. Polymer Sci.* **5**, 31 (1961).
- (29) Matheson, M. S., Auer, E. E., Bevilacqua, E. B., Hart, E. J., *J. Am. Chem. Soc.* **73**, 1700 (1951).
- (30) Morton, M., Salatiello, P. P., Landfield, H., *J. Polymer Sci.* **8**, 111 (1952).
- (31) *Ibid.*, p. 215.
- (32) *Ibid.*, p. 279.
- (33) Smith, W. V., *J. Am. Chem. Soc.* **70**, 3695 (1948).
- (34) *Ibid.*, **71**, 4077 (1949).
- (35) Smith, W. V., Ewart, R. H., *J. Chem. Phys.* **16**, 592 (1948).
- (36) Stockmayer, W. H., *J. Polymer Sci.* **24**, 314 (1957).
- (37) Vanderhoff, J. W., Vitkuske, J. F., Bradford, E. B., Alfrey, T., Jr., *J. Polymer Sci.* **20**, 225 (1956).
- (38) Vanderhoff, J. W., Bradford, E. B., *Tappi* **39**, 650 (1956).
- (39) Vanderhoff, J. W., Bradford, E. B., Abstracts, p. 28S, 130th Meeting, ACS, Atlantic City, N. J., September 1956.
- (40) *Ibid.*, p. 20-I, 131st Meeting, ACS, Miami, Fla., April 1957.
- (41) Vanderhoff, J. W., Bradford, E. B., Tarkowski, H. L., Wilkinson, B. W., *J. Polymer Sci.* **50**, 265 (1961).
- (42) Vanderkooi, W. N., Schultz, J. A., Sieglaff, C. L., private communication, The Dow Chemical Co., Midland, Mich., November 1958.
- (43) Zimmt, W. S., *J. Appl. Polymer Sci.* **1**, 323 (1959).

RECEIVED September 6, 1961.

Polymer Synthesis at High Pressures

N. L. ZUTTY and R. D. BURKHART

*Research and Development Department,
Union Carbide Chemicals Co., South Charleston, W. Va.*

Experiments at high pressures are useful for gaining insight into polymerization mechanisms, and for preparing polymers that cannot be easily made in other manners. High pressure equipment can be obtained commercially for carrying out almost any type of addition polymerization and kinetic experiments under pressure can be designed to determine the pressure effect on the various steps of a free radical polymerization. The effect of pressure on comonomer reactivity ratios has revealed that radical selectivity is decreased with increasing pressure, resulting in more ideal copolymerizations at higher pressures. Finally, the high pressure copolymerization of ethylene with various comonomers allows the use of ethylene rather than styrene as a more logical base point for the Q-e scheme.

Polymer syntheses at high pressures present some unique problems not usually met under more normal polymerization conditions. These involve both the use of specialized high pressure equipment and pressure-induced changes in the physical and chemical properties of the substances being studied.

High pressure equipment is generally cumbersome to handle, and only in rare instances is it possible to make meaningful visual observations on a reacting system. It is almost always better to rely on indirect measurements. It is also unfortunate that *P-V-T* relations are known for only the most common monomers at high pressures, and in most cases it is necessary to estimate densities. Due largely to the work of Bridgman (4) some excellent *P-V-T* data are available for most common solvents.

In carrying out high pressure polymerizations one also should be constantly on the guard for both pressure-induced phase and solubility changes. An extreme example of the latter effect is found in the report that gases, widely different in polarity, may become partially immiscible at high pressures, even though they are above their critical temperature (14). This phenomenon is of course contrary to what is taught in the textbooks, where it is said that true gases are always completely miscible under any conditions. Therefore, in dealing with high pres-

tures it may be necessary to reorient thinking as to gas behavior. In the authors' experience, it is best to consider gases at high pressure as more nearly liquid in character. For example, ethylene above its critical temperature at 100° C. and 23,000 p.s.i. has a density of 0.526 gram per cc., while its critical density is only 0.22 gram per cc. Is it proper to consider such a substance a liquid or a gas?

The pressure-induced freezing of solvents may also lead to anomalous results. In this connection it is noteworthy that the freezing point of benzene is raised to about room temperature at 1000 atm. pressure (4).

Although the difficulties involved in carrying out high pressure polymerizations seem great, the possible yield in terms of new knowledge of polymerization mechanisms, and as an alternative route to new polymers, is commensurate. Walling (15) has pointed out the advantages of using high pressure as a means of studying free radical polymerizations and some further studies along these lines are discussed below. Parallel to these mechanism studies the opportunity arises for using high pressures to polymerize monomers which are unreactive to free radicals at atmospheric pressure. The use of high pressure also expands the number of monomer pairs which can be copolymerized. Finally, high pressures can also affect degrees of polymerization, chain transfer, and chain branching. Thus, in many cases, the polymerization pressure may have a profound effect on polymer structure and, hence, polymer properties.

High Pressure Equipment for Polymerization Work

The choice of a reactor for a high pressure polymerization is governed by the pressure required and the quantity and type of polymer desired. For reactions where efficient mixing is desired, both stirred autoclaves and rocking bombs are available commercially which are capable of maintaining at least 2000- to 3000-atm. pressure. Less efficient stirring is obtained in continuous tubular reactors, but the pressure limitations here are equal only to the pressure limitation of the tubing used and the pumps available. It is not unusual to find systems such as these capable of operating at 5000 atm. Static reactors providing no mixing may operate at much higher pressures (10,000 to 50,000 atm.), but the higher pressures inevitably result in a large decrease in reactor volume.

Pumps, gages, fittings, and valves for operation at these pressures are available from a number of manufacturers. Diaphragm pumps capable of pressurizing a fluid without contamination by pump oil have simplified the job of working with chemically pure systems.

Pressure Effects in Free Radical Polymerization

Most quantitative work on high pressure polymerizations has centered on reactions proceeding by a free radical mechanism and, among free radical polymerizations, ethylene has received the greatest attention, because high molecular weight polyethylene can be produced only by high pressure techniques when normal free radical catalysis is used. For a free radical reaction, where electrostriction forces may be neglected (9), the effect of pressure on the magnitude of the specific rate constant in any step of the reaction is given by Equation 1 (7)

$$\frac{\partial \log k}{\partial P} = \frac{-\Delta V^*}{RT} \quad (1)$$

where k is the specific rate constant; ΔV^* is the difference in volume between activated species and reactants in cubic centimeters per mole; P is the pressure;

and R and T have the usual meaning. Most experimental work has shown that Equation 1 is reliable only if the compressibilities of the activated species and the reactants are the same. In those cases where compressibilities are unequal, it is customary to take the value of ΔV^* extrapolated to atmospheric pressure.

As would be predicted from Equation 1, the rate of dissociation of free radical initiators is decreased by the application of pressure. Thus azobisisobutyronitrile dissociates with a rate constant equal to $4.47 \times 10^{-5} \text{ sec.}^{-1}$ at 1500 atm. but at 1 atm. the dissociation rate constant is $5.5 \times 10^{-5} \text{ sec.}^{-1}$ (8). Studies concerning the effect of pressure on the decomposition of benzoyl peroxide reveal that the rate of this reaction also decreases with increasing pressure (11, 18). The extent to which the radical-induced decomposition of this peroxide at high pressures affects the rate is not clear, but it appears that some complications arise from this cause.

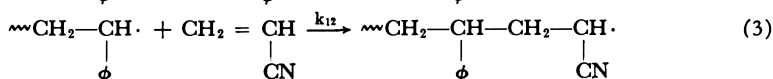
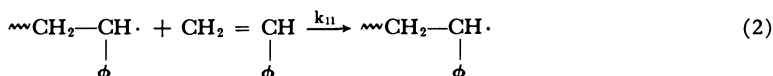
For practical purposes it is usually necessary to use a free radical initiator about 10° higher for each 1000-atm. pressure, in order to achieve the catalytic activity normally expected. On the basis of experience with a wide variety of initiators, the temperatures at which some of the more common initiators may be used at 1000 and 3000 atm. have been summarized in Table I.

Table I. Most Efficient Use Temperature Range for Some Common Initiators

Initiator	Temperature, °C.	
	1000 atm.	3000 atm.
Diisopropyl peroxydicarbonate	30-50	50-80
Diacetyl peroxide	40-60	60-70
Azobisisobutyronitrile	65-75	75-90
Dibenzoyl peroxide	70-90	110-130
Potassium persulfate	70-90	120-130
<i>tert</i> -Butyl hydroperoxide	120-140	160-180

The effect of pressure on the rate of free radical propagation reactions has been studied in homopolymerizations only for styrene. Since ΔV^* is negative for this reaction, the application of pressure increases the propagation rate. Nicholson and Norrish (12) list the propagation rate constant for styrene as 72.5 liters-mole⁻¹-sec.⁻¹ at atmospheric pressure and 30° C. This increases to 206 liters-mole⁻¹-sec.⁻¹ at 2000 atm. and 400 liters-mole⁻¹-sec.⁻¹ at 3000 atm. From these data it is possible to calculate the value of ΔV^* for the propagation step to be -13.3 cc. per mole. Walling and Pellon (16) report a value of -11.5 cc. per mole for the same reaction measured by a different technique.

By studying the effect of pressure on copolymerizations it is possible to obtain an activation volume difference for various homo- and cross-propagation reactions. For instance, in two of the propagation reactions occurring in the styrene-acrylonitrile polymerization:



The ratio k_{11}/k_{12} is found to vary with pressure, and $\Delta V^*_{11} - \Delta V^*_{12}$ has a value of -9.8 cc. per mole (5). Using the value of ΔV^*_{11} given by Norrish, ΔV^*_{12} is found to be -3.5 cc. per mole. It would be interesting to compare ΔV^* values for other cross-propagation reactions as a possible route to an understanding of the nature of the activated complex.

Although Equation 1 predicts that the rate of a radical termination reaction increases as pressure is applied, it appears that a point is reached where these reactions become diffusion-controlled, resulting in a positive rather than a negative ΔV^* . Recent work suggests that even at atmospheric pressure and at low conversions the termination step of many polymerizations may be diffusion-controlled (2, 3, 13). It is not surprising, therefore, that increasing pressure decreases the rate of radical termination reactions (12) rather than increasing the rate as might be expected.

The over-all rates for free radical polymerizations increase with increasing pressure. This means simply that the pressure-induced retardation of the initiator decomposition rate is more than offset by the increase in the rate of chain propagation and the decrease in the rate of chain termination. This is formally stated in terms of activation volumes in Equation 4 (15)

$$\Delta V_c^* = \Delta V_p^* + 1/2\Delta V_d^* - 1/2\Delta V_t^* \quad (4)$$

where a biradical reaction is assumed as the termination step. Subscripts *d*, *p*, and *t* refer to initiator decomposition, chain propagation, and chain termination, respectively.

It is also to be expected that pressure will affect the rate of chain transfer reactions to monomer, polymer, and solvent. In the polymerization of allyl acetate, where degradative chain transfer to monomer occurs, the rates of the propagation and transfer reactions increase by about the same amount for a given increase in pressure (17). The transfer reaction becomes less degradative—i.e., the allyl acetate radicals become more reactive—as pressure is increased.

Another aspect of free radical polymerizations under pressure which has been recently studied is the effect of pressure on comonomer reactivity ratios (5). In two copolymerization systems—styrene-acrylonitrile and methyl methacrylate-acrylonitrile—it was found that the product of the reactivity ratios, r_1r_2 , approaches unity as the pressure is increased. The monomer-polymer composition curves for these two copolymerizations at 1 and 1000 atm. are illustrated in Figures 1 and 2. The effect of pressure on the individual reactivity ratios and on the r_1r_2 product is given in Table II.

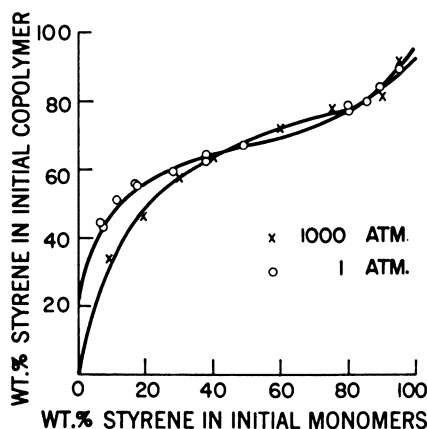


Figure 1. Monomer-polymer composition curve for the styrene acrylonitrile polymerization at 1 and 1000 atm. pressure

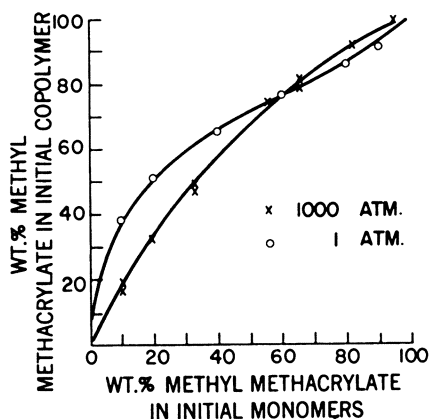


Figure 2. Monomer-polymer composition curve for the methyl methacrylate-acrylonitrile copolymerization at 1 and 1000 atm. pressure

Table II. Effect of Pressure on Monomer Reactivity Ratios

Pressure, Atm.	Monomer 1	Monomer 2	r_1	r_2	$r_1 r_2$
1	Styrene	Acrylonitrile	0.37	0.07	0.03
100	Styrene	Acrylonitrile	0.43	0.13	0.06
1000	Styrene	Acrylonitrile	0.55	0.14	0.08
1	MMA	Acrylonitrile	1.34	0.12	0.16
100	MMA	Acrylonitrile	1.46	0.37	0.54
1000	MMA	Acrylonitrile	2.01	0.45	0.91

The methyl methacrylate-acrylonitrile copolymerization is nearly ideal at 1000 atm. ($r_1 r_2$ approaches very close to unity)—i.e., the free radicals have almost completely lost their individual selectivity. In the case of styrene-acrylonitrile the free radicals are tending toward a loss in selectivity with increasing pressure, although the copolymerization is still far from ideal even at 1000-atm. pressure.

These results suggest that of the two copolymerization parameters, Q and e , only the e values are affected appreciably by an increase in pressure. Calculations have been made obtaining relative Q and e values which bear out this thesis. The decreasing radical selectivity found in these experiments implies an increased radical reactivity. This offers further support to Walling's suggestion that the allyl acetate radical increases in reactivity with increasing pressure.

These results, of course, mean that the use of high pressures allows one to carry out copolymerizations which do not occur readily at atmospheric pressure because of widely different monomer-radical reactivities. For example, at several thousand atmospheres styrene and vinyl acetate, which will not appreciably copolymerize at 1 atm. (10), may be made to give copolymers at a reasonable rate.

As well as increasing monomer-radical reactivity, increasing pressure will also increase monomer density, and if one or both of the monomers is normally gaseous, this will allow the preparation of polymers which cannot normally be made at atmospheric pressure. Chief among such monomers is ethylene which, mainly because of its low concentration, will not give high polymers nor copolymers rich in ethylene at low pressures with free radical initiators.

The fact that ethylene will copolymerize at high pressures is rather fortunate from not only a commercial but also a theoretical view, since it has long been believed that monomer reactivity ratios might be better correlated according to a scheme based on ethylene rather than the currently used Q - e correlation in which styrene is taken as the reference standard. However, until recently no quantitative data on ethylene copolymerizations have been available upon which to base such a scheme.

The advantages to be gained by utilizing an ethylene-based Q - e scheme are readily illustrated by reference to Equations 5 and 6.

$$r_1 = Q_1 \exp -(e_1)^2 \quad (5)$$

$$r_2 = \frac{1}{Q_1} \quad (6)$$

These are simply the equations of Alfrey and Price (1), which relate monomer reactivity ratios to Q and e values, and in which the reasonable values of $e_2 = 0$ and $Q_2 = 1$ are substituted, with the convention that the reference standard, ethylene, is monomer 2. In Equation 6 it is seen that the Q_1 value is simply a ratio of propagation rate constants unmodified by the presence of differences in e values, as is the case in the styrene-based scheme. This would seem to be a more desirable type of parameter to deal with, simply because its meaning is perfectly straightforward.

The reactivity ratio product is given by

$$r_1 r_2 = \exp -(e_1)^2 \quad (7)$$

Thus, the copolymerization ideality in ethylene copolymerizations—i.e., the proximity of $r_1 r_2$ to unity—is strictly dependent on the e value of the comonomer. Hence, we see that since ethylene, because of its lack of substituent groups, resides at the center of the e scale, relatively large positive or negative e values may be tolerated without seriously affecting the ideality of the copolymerization.

Table III. Reactivity Ratios and Q and e Values for Ethylene-Vinyl Chloride and Ethylene-Vinyl Acetate Copolymerizations

Copolymerization	r_1	r_2^*	Based on C_2H_4		Based on Styrene	
			Q_1	e_1	Q_1	e_1
Vinyl acetate-ethylene	1.08 ± 0.19	1.07 ± 0.06	0.93	0	0.03	-0.3
Vinyl chloride-ethylene	3.60 ± 0.3	0.24 ± 0.07	4.2	+0.37	0.04	-0.1

* Ethylene is monomer 2.

Some data recently obtained on high pressure ethylene copolymerizations illustrate the quantitative aspects of an ethylene-based Q - e scheme (6). In Figures 3 and 4 copolymer composition curves for the ethylene-vinyl chloride and the ethylene-vinyl acetate copolymerizations are given. The monomer reactivity ratios for these two systems are tabulated in Table III along with Q values and e values for vinyl chloride and vinyl acetate calculated using ethylene as the standard ($Q = 1.0$ and $e = 0$). These Q and e values may be compared with those obtained using styrene as the standard.

These ethylene-based Q and e values may be used to calculate the reactivity ratios for the copolymerization of vinyl acetate with vinyl chloride. Agreement is good when these values are compared with experimental values. In Table IV reactivity ratios calculated from ethylene- and styrene-based Q and e values are shown.

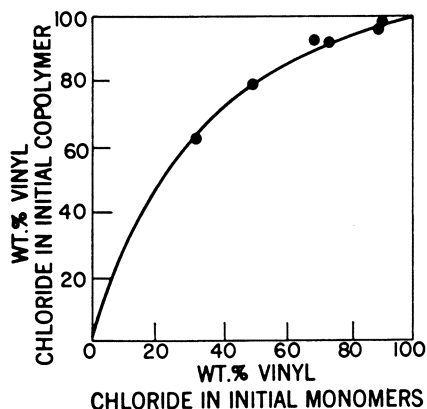


Figure 3. Monomer-polymer composition curve for ethylene-vinyl chloride copolymerization made at 90° C. and 15,000 p.s.i.

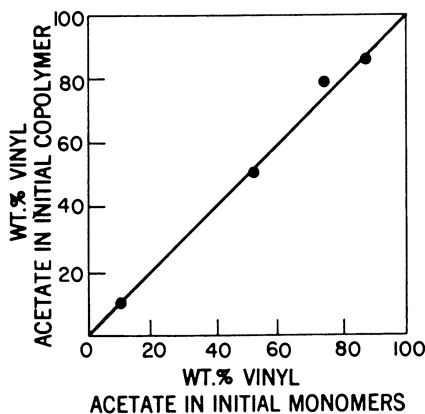


Figure 4. Monomer-polymer composition curve for ethylene-vinyl acetate copolymerization made at 90° C. and 15,000 p.s.i.

Table IV. Reactivity Ratios for Vinyl Chloride(M_1)-Vinyl Acetate(M_2) Copolymerization

	r_1	r_2
Ethylene $Q-e$ calculated	3.7	0.22
Styrene $Q-e$ calculated	1.36	0.67
Experimental	2.1	0.3

It appears that these ethylene-based Q and e values are capable of forming an internally consistent correlation scheme. It will be interesting to see whether this scheme is capable of yielding good results over the wide variety of monomers for which the styrene-based scheme has been so successful.

Literature Cited

- (1) Alfrey, T., Price, C. C., *J. Polymer Sci.* **2**, 101 (1947).
- (2) Allen, P. E. M., Patrick, C. R., *Makromol. Chem.* **47**, 154 (1961).
- (3) *Ibid.*, **48**, 89 (1961).
- (4) Bridgman, P. W., "The Physics of High Pressure," pp. 128-30, 198, G. Bell and Sons, London, 1958.
- (5) Burkhardt, R. D., Zutty, N. L., IUPAC Symposium on Macromolecular Chemistry, Montreal, July 1961; *J. Polymer Sci.*, in press.
- (6) *Ibid.*, in press.
- (7) Evans, M. G., Polanyi, M., *Trans. Faraday Soc.* **31**, 875 (1935).
- (8) Ewald, A. M., *Discussions Faraday Soc.* **22**, 138 (1956).
- (9) Hamann, S. D., "Physico-Chemical Effects of Pressure," pp. 163-6, Academic Press, New York, 1957.
- (10) Mayo, F. R., Lewis, F. M., Walling, C., *Discussions Faraday Soc.* **2**, 285 (1947).
- (11) Nicholson, A. E., Norrish, R. G. W., *Ibid.*, **22**, 97 (1956).
- (12) *Ibid.*, p. 104.
- (13) North, A. M., Reed, G. A., *Trans. Faraday Soc.* **57**, 859 (1961).
- (14) Tsiklis, D. S., *Doklady Akad. Nauk, S.S.S.R.* **86**, 1159 (1952).
- (15) Walling, C., *J. Polymer Sci.* **48**, 335 (1960).
- (16) Walling, C., Pellon, J., *J. Am. Chem. Soc.* **79**, 4776 (1957).
- (17) *Ibid.*, p. 4782.
- (18) *Ibid.*, p. 4786.

RECEIVED January 4, 1962.

Radiation Induced Polymerization of Some Vinyl Monomers in Emulsion Systems

DIETER HUMMEL, GREGOR LEY, and CHRISTEL SCHNEIDER

Institut für physikalische Chemie und Kolloidchemie an der Universität Köln, Germany

Aqueous emulsions of styrene, methyl methacrylate, methyl acrylate, and ethyl acrylate were polymerized with γ -radiation from a Co^{60} source in the presence of sodium dodecyl sulfate or sodium laurate. The continuous measurement of conversion and reaction rate was carried out dilatometrically. The acrylates polymerized fastest and the over-all polymerization rate increased as follows: styrene < methyl methacrylate < ethyl acrylate < methyl acrylate. The effects of radiation dose, temperature, and original monomer and emulsifier concentrations were studied with respect to the following factors: properties of polymer dispersions, number and size of polymer particles, viscometrically determined molecular weights, monomer-water ratio, and kinetic constants.

Organic compounds react under the influence of ionizing radiation mostly according to radical mechanisms. The radical-induced polymerization of vinyl compounds is started technically by peroxides, hydroperoxides, or other substances, which in decomposing produce radicals. The radiogenic radicals have similar effectiveness.

There are numerous publications about radiation-induced polymerization in homogeneous phases (2, 12, 14, 29, 36); but rather little is known about radiation-induced emulsion polymerization (EP).

Ballantine (4) observed that the γ -induced emulsion polymerization of styrene is about 100 times faster and yields higher molecular weights (up to 2×10^6) than the γ -induced bulk polymerization. He explains the large difference in reaction rates by the high radical yield (G_R value) of water, as compared with the G_R value of styrene. An over-all activation energy of 3.7 kcal. per mole was calculated from the temperature dependence of the reaction. Allen *et al.* (1) prepared and grafted polystyrene and poly(vinyl acetate) dispersions under the influence of γ -radiation. Mezhirova *et al.* (28) found a temperature-independent reaction rate of the γ -induced emulsion polymerization of styrene.

Okamura *et al.* (29) studied the γ -induced emulsion polymerization of styrene, methyl methacrylate (MMA), and vinyl acetate with anionic, nonionic, and cationic emulsifying agents and dose rates of 270 to 2×10^4 rad per hour. The over-all reaction rate increased with increasing emulsifier concentration, but depended highly on the kind of emulsifying agent. In the case of MMA, the over-all reaction rate increased with $I^{0.25}$ (I = intensity or dose rate).

In a recent publication, Vanderhoff *et al.* (39) reported on the mechanism and the kinetics of the γ -EP of styrene. In these investigations, the rate of formation of the radicals was found to be temperature-independent. The rate of growth of the particles was similar to that in persulfate-initiated systems. k_p had a mean value of about 120 liters mole⁻¹ sec.⁻¹ at 30° C. The values of k_t varied between 10^{-4} and 10^{-5} liter mole⁻¹ sec.⁻¹ at 50° C. The calculated activation energy was 7.2 kcal. per mole.

Chapiro and Maeda (13) polymerized styrene suspensions, which contained no emulsifier, but only poly(vinyl alcohol) as a protective colloid. The dose rates were 8340, 2124, and 930 rad per hour, respectively; 60% conversion was obtained with doses of about 58,000 rad.

On the emulsion polymerization of methyl acrylate (MA), which was studied by us in more detail, there are few publications. In an investigation of the influence of the chemical nature and concentration of emulsifiers on the emulsion polymerization of vinyl monomers, Okamura and Motoyama (30) found optimum concentrations of emulsifiers for a maximum reaction rate in the emulsion polymerization of MA.

Bulk and solution polymerization of MA was studied by many authors. They found high reaction rates and a strong gel effect. Furthermore, they observed that polymerization sometimes yields cross-linked, insoluble products. Walling (40) reported on bulk polymerization; as a result of the gel effect, the reaction rate increased steadily with increasing conversion. According to Bagdasaryan (2), the gel effect does not occur when solutions of MA in ethyl acetate of concentrations below 50% MA are polymerized. Matheson *et al.* (23, 24) and Melville *et al.* (25, 26) determined absolute reaction constants k_p and k_t for MA using the "rotating-sector technique." Matheson observed a steadily increasing over-all reaction rate from the beginning of polymerization. Melville *et al.* also determined k_p/k_t by other methods. Prevost-Bernas *et al.* (31) published G_R values for the radiation-induced polymerization of different monomers, the G_R value for MA being 23.4 (radical scavenger method). The statement of G_R values for polymerization reactions is problematic. When determined from results of a radical scavenger method, a definite reaction of the scavenger with all radicals is to be postulated. When determined from polymerization data, one has to assume identity of kinetic chain length and molecular weight, and this is never the case.

Scope of Work

Single values for reaction rates as determined from different experiments can be erroneous, because minute quantities of oxygen or other radical scavengers can introduce vast inhibition periods. Reaction rates and orders may be expected to vary strongly during radiation-induced polymerization. Knowledge of this differentiated (with respect to time) behavior of the polymerization reaction is decisive for a discussion of these processes.

The aim of this investigation was therefore the continuous measurement of conversion and reaction rate in polymerizing emulsion systems of different mono-

mers. In this connection the question to be studied was whether the theories of Harkins (18, 19) and Haward (20) and the quantitative theory of Smith and Ewart (32, 33) in its simple form are applicable for the γ -polymerization of our systems.

Experimental

Source of γ -radiation. We applied a cylinder of Co^{60} with an activity of about 6 to 7 curies. The dose rates in reaction vessel I were 1.1 to 1.3×10^4 rad per hour (Fricke dosimeter). The dose rates in the dilatometers were 200, 50, and 22.2 rad per hour, depending on the distance from the source. These values were determined by an electrostatic dosimeter, which was dipped in the dilatometers. The absolute error in this case may be $\pm 20\%$; the proportions between the three values are exact.

Purification of Substances. Water was demineralized on an ion exchanger column, then distilled from alkaline permanganate, and finally distilled with argon as an inert gas. Argon of technical grade was purified from traces of oxygen by pyrophoric copper on silica gel at 250°C ., following the specifications of Meyer and Ronge (27). Monomers were of analytical grade. Stabilizers were removed by fuller's earth. All monomers were distilled through a column under normal pressure, partly polymerized, and finally distilled several times under argon and in vacuo. The emulsifiers (sodium dodecyl sulfate and sodium laurate) were of analytical grade.

Equipment for Discontinuous Measurement of γ -Emulsion Polymerization. This assembly (Figure 1) consisted of a cylindrical glass vessel of about 350-ml. volume and a fingerlike intrusion at its bottom to receive the radiation source. The ground top of the vessel had a vibration stirrer with a gas-tight, silicone rubber

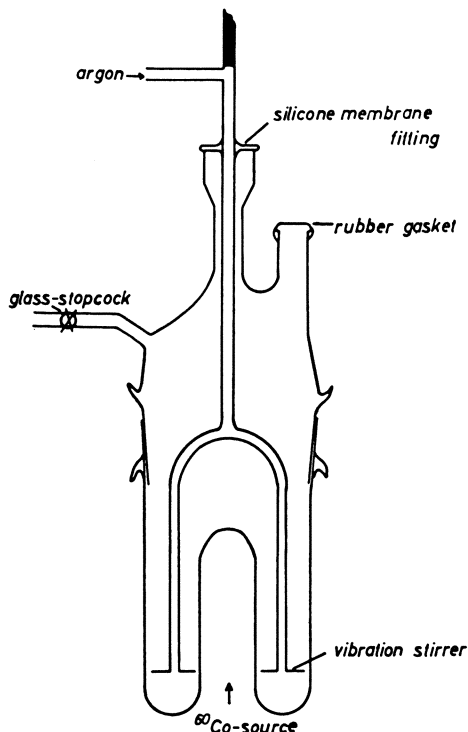


Figure 1. Equipment for discontinuous measuring of γ -induced emulsion polymerizations

membrane, a ground-in socket, and a stopcock. Argon passed the hollow shaft of the stirrer, bubbled through the emulsion, and left the assembly through the stopcock. The socket was closed with a cap of silicone rubber. The whole apparatus was surrounded with a thermostat mantle and reproducibly mounted in the irradiation chamber. An argon pressure of about 0.1 atm. in excess was maintained in the apparatus during irradiation. From time to time, the source was dropped, the cap pricked with the needle of a syringe, and 3 to 5 ml. of emulsion taken out for analysis. The sample was squirted in a known amount of hydroquinone solution and weighed. The polymer content of the sample was determined either by evaporating the volatile matter or by precipitating the polymer. The isolated polymer was dried for about 5 days at 50° C. in vacuo. The values according to both methods agreed well. The conversion was calculated from the weight of the sample, the weight of the polymer, and the original composition of the emulsion.

With this apparatus about 12 to 15 points of the conversion-time function could be determined from one experiment. Despite all precautions to prevent traces of oxygen from leaking in, the polymerization reaction was preceded by long inhibition periods. The end of these periods could be recognized only by sampling. This causes errors, since the dose rate is not equal in all parts of the vessel: Varying the geometry of the system in these cases means varying the initiation rate. We observed that sampling could retard polymerization or sometimes even produce another inhibition period (Figure 2). Therefore we constructed an assembly which allowed observation of the reaction without sampling.

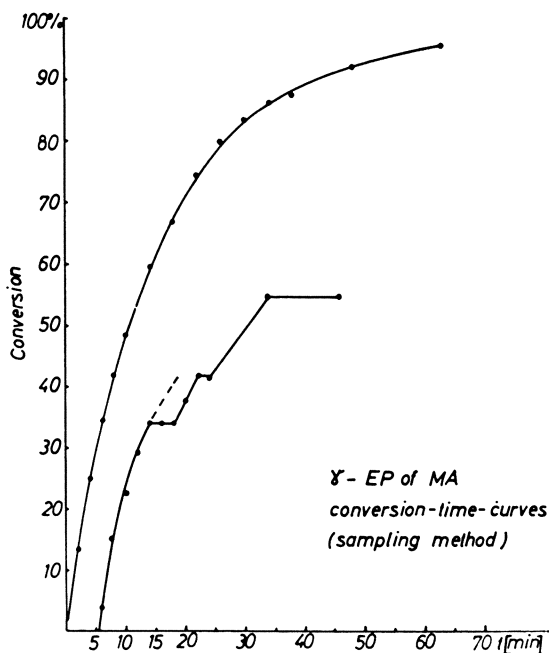


Figure 2. Conversion-time curves for MA, discontinuous method

Continuous Dilatometric Measurement of γ -Emulsion Polymerization. Polymerization of vinyl monomers causes a volume contraction up to 27% (vinyl acetate) of the volume of the monomer. This shrinkage is proportional to conversion and can be linearly interpolated, however consult Treloar (37). The dila-

tometric method was first applied by Starkweather and Taylor (34) for continuous measurement of the polymerization of vinyl acetate. Later on, many other authors accepted the method for studies on bulk and solution systems. There are only few dilatometric investigations on emulsion systems. An apparatus described by Bartholomé *et al.* (6) was somewhat modified by us (Figure 3).

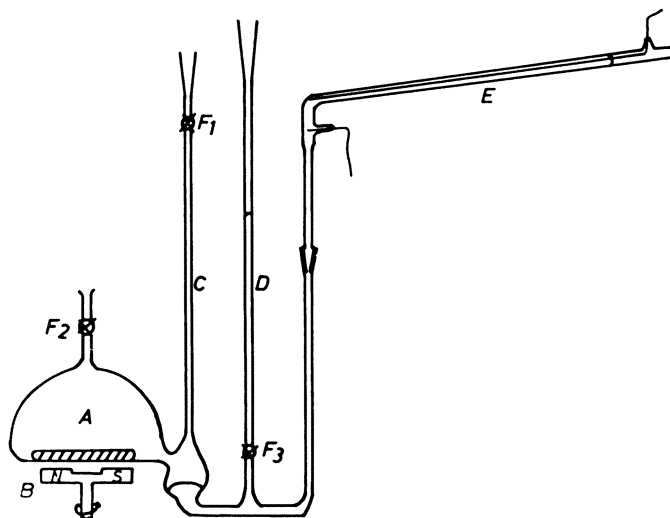


Figure 3. Dilatometer for continuous measurement of γ -induced emulsion polymerizations

- A. Dilatometer vessel
- B. Magnetic stirrer
- C. Filling capillary for emulsion
- D. Filling capillary for Hg
- E. Measuring capillary
- F₁. Teflon stopcock
- F₂. Teflon stopcock
- F₃. Glass stopcock

Measurement Principle. The essential part of our measuring device consists of a precision capillary with a lumen of 2 to 4 mm. and a set-in platinum wire 0.1 mm. ϕ . Mercury served as a connection liquid to the reaction vessel. During the reaction, the mercury column travels down the capillary and gradually releases the platinum wire in the capillary. Wire and capillary must be carefully cleaned of grease; otherwise the migrating mercury separates incompletely. The mercury itself was cleaned and distilled before use.

We scanned the electrical resistance of the measuring device with a Siemens Compensograph (5-mv. full deflection, 25-cm. scanning breadth). Finally we calibrated each capillary by plotting recorder deflection *vs.* meniscus level. A 10-mm. change of the meniscus corresponded to a recorder deflection of about 120 mm. The measuring capillary, which was surrounded by a thermostat, had a length of 400 mm. The bridge circuit was rebalanced whenever full deflection was reached.

Preparation of Emulsions. For this purpose we used the assembly described by Bartholomé *et al.* (6); all parts of the apparatus could be flushed with argon. Water, monomers, and emulsifier were vigorously agitated for 15 minutes. Ac-

ording to a recommendation of Gerrens, the temperature was maintained at 20° C. above the polymerization temperature.

After the emulsification of a monomer it is necessary to wait until the little argon bubbles collect on the surface. Subsequently the emulsion is pressed into the dilatometer.

Filling of a Dilatometer. First, the dilatometer was filled with mercury through the middle leg to such a height that the meniscus stood at the lower end of the little bulb beside the onionlike reaction vessel. The connection to the outer leg, and the middle capillary onto the stopcock, must be filled without bubbles. Thereupon, the inner capillary was connected by its ground top with the emulsification vessel. Teflon stopcock 2 was connected to the argon outlet valve (mercury tightened), and the assembly was flushed with argon. Now, the emulsion was pressed into the dilatometer, the first 20 ml. of the emulsion being rejected. When the dilatometer was filled, Teflon stopcocks 1 and 2 were closed. Then the measuring capillary was put in the ground-glass jacket of the outer capillary and fixed with steel springs. The assembly was next filled with mercury until the indicating meniscus stood at the upper end of the measuring capillary.

The dilatometer was so immersed in a thermostat, that the onionlike vessel with its stirring fish exactly matched an underwater stirrer magnet in the thermostat. The whole apparatus was reproducibly fixed in the irradiation chamber. To avoid creaming, the emulsion was stirred throughout the polymerization reaction.

Irradiation and Measurement. After the electrical circuits had been closed, the Compensograph was balanced and the scanning started. Finally, the source was driven out. In no case did polymerization start immediately. The inhibition periods lasted between 1 and 150 minutes, generally about 10 minutes. Compared with the very low dose rates, these inhibition periods were short.

To stop an experiment, the source was lowered. Immediately after this, the dispersion was mixed with a solution of hydroquinone and stored for analysis.

Evaluation of Results. At the beginning and end of a polymerization, the level of the mercury meniscus in the measuring capillary was read. The scannings of the Compensograph (conversion-time functions) were corrected using the calibration plot (pen deflection *vs.* meniscus level). The final conversion of the dispersions was determined. All values are based on the polymer content of the dispersions (milligrams of polymer per gram of dispersion) thus calculated, and by the assumption of a linear correlation between volume contraction and conversion.

The conversion-time functions were differentiated graphically; the values of the difference quotient, $\Delta U/\Delta t$, were plotted logarithmically *vs.* time. The conversion, U , is directly proportional to the concentration of the polymer, and ΔU is proportional to the decrease of the monomer concentration, $-\Delta[M]$. Reactions of zero order (with respect to monomer concentration) thus plotted produce a parallel to the time abscissa:

$$v_{Br} = - \frac{[d\bar{M}]}{dt} = k$$

Reactions of first order (with respect to monomer concentration) produce an inclined straight line:

$$\log \frac{[M]}{[M_0]} = -K_t \times t$$

Determination of Particle Number and Particle Sizes in Polymer Dispersions. Most of our dispersions were counted in the Zsigmondy ultramicroscope. Very fine dispersions give low counting values, since a fraction of the particles was small enough to be invisible in the ultramicroscope. Our institute does not have an

electron microscope; fortunately, Robert Bosch G.m.b.H. took a number of electron micrographs of our polystyrene and PMMA dispersions. PMA cannot be examined in the electron microscope by applying the normal preparation techniques, because the particles fuse either during drying or in the electron beam. Therefore, we can report particle sizes only for polystyrene and PMMA dispersions.

Determination of Viscosity Number and Average Molecular Weight of Polymers. The polymers were dissolved and coagulated several times in order to remove the emulsifier. The intrinsic viscosity was then determined with an Ubbelohde viscometer. Normally we measured values of η_{sp}/c at different concentrations; $[\eta]$ was then determined by graphical extrapolation at concentration zero.

Most values were determined with PMA. In this case, we established first of all an empirical relation between η_{sp}/c (at $c = 0.1$ gram per 10 ml.), and $[\eta]$. Then only values of η_{sp}/c at that concentration were measured directly.

For calculation of molecular weights from intrinsic viscosities we used the Staudinger equation (35). On account of the high molecular weights of emulsion polymers we exceeded the range for which the constants were determined to a considerable amount.

For polystyrene (benzene solution) we used a diagram of Marzolph and Schulz (22). The values for PMMA (solvent CHCl_3) were obtained with the formula (7)

$$\bar{P}_n = 1.81 \times 10^3 [\eta]^{1.22}$$

For PEA (acetone solution) Hachihama and Sumitomo (17) gave the following relation:

$$[\eta] = 5.33 \times 10^{-3} \bar{P}_n^{0.66}$$

The degree of polymerization for PMA can be calculated according to Staudinger

$$\bar{P}_n = 3.08 \times 10^3 [\eta]^{1.22}$$

$[\eta]$ in dl. per gram

or according to Fuhrmann and Mesrobian (15):

$$\bar{P}_n = 11.2 [\eta]^{1.22}$$

$[\eta]$ in cc. per gram of acetone solution

Determination of Solubility of Monomers in Dispersions of Polymer. We applied a method given by Smith for polystyrene dispersions (32). Known volumes of polymer dispersion and monomer were shaken together for 15 minutes in a graduated centrifuge glass tube, and then centrifuged. The excess monomer creams and can be determined by its volume. This method is not very accurate, but gives reproducible results sufficient for our studies (Table I).

Experimental Results and Discussion

Polymerizing Tendency of Different Monomers. Among the monomers studied by us the acrylates polymerized most rapidly by far. In sequence follow MMA, styrene, and far behind methyl isopropenyl ketone. Some monomers (methacrylonitrile and vinylidene chloride) showed no polymerization, even at rather high doses. As to methacrylonitrile, this may be due to the technical grade monomer. During the irradiation of the vinylidene chloride emulsion, the pH value of the water phase was not controlled; this is probably the reason for the complications.

Table I. γ -Initiated Emulsion Polymerization of Vinyl Monomers

(Dose rate 200 rad/hr. Temperature 25°C. Monomer concn. about 1.2 moles/kg. emulsion. Emulsifier about 0.046 mole sodium dodecyl sulfate/kg. solution)

Type	Monomer		$v_{Br_{max}}$ ^a	Reaction Characteristics		
	Solubility in H ₂ O, % (20°C.)	Soly. in polym. dispersions, polymer-monomer ratio		k_p (25°C.) ^b liters/mole/sec.	Conversion, %	Dose, r
Vinyl acetate	2.4 (20°C.)	—	0.2	1100 (other authors 1954, 2024)	64	2167
Styrene	0.0126 (20°C.)	Min. 1:1 Max. 1:1.7	0.4	18.7	70-80	765
Methyl methacrylate	1.59 (20°C.)	Min. 1:2.5 Max. 1:3.1	1.25	512 (other authors 310, 128)	70	450
Ethyl acrylate	1.82 (30°C.)	—	4.1	—	70-80	530
Methyl acrylate	5.2 (30°C.)	Min. 1:6 Max. 1:7.5	4.4	1500	80-90	200

^a Mg. polymer/min. g. emulsion.^b Values from published literature.

Table I shows some values of the maximum over-all reaction rate ($v_{Br_{max}}$; milligrams of polymer per minute per gram of emulsion) of some monomers, and literature values for absolute propagation constants (k_p). Both entities increase in the same sense. Vinyl acetate is an exception, which we cannot yet explain. $v_{Br_{max}}$ is dependent not only on k_p ; this is discussed below.

Properties of Dispersions and Polymers. All polymer dispersions with SDS (sodium dodecyl sulfate) as an emulsifier were stable for at least 8 months. Dispersions with Na laurate as emulsifier flocculated after a short time. Polyacrylates on drying yielded clear and coherent films; polystyrene and PMMA dispersions gave opaque and brittle layers. The doses needed for polymerization were well below a dose which causes cross linking or degradation.

Number and Size of Particles. The monomer-water ratio in our experiments varied between 1:2.2 and 1:33.2, respectively; the most frequent value was about 1:8 (grams of monomer per gram of H₂O). The particle numbers were determined ultramicroscopically on polystyrene and PMA dispersions. The order of magnitude was always 10¹⁴ per ml. of dispersion (Table II). The same order of magnitude was observed for the catalytic emulsion polymerization of styrene by several authors. The number of particles per milliliter increased with the dose rate. The geometry of the particles varied somewhat depending on the electron microscope preparation technique. We took one reliable micrograph out of each series for polystyrene and PMMA (Figures 4 and 5, undiluted dispersion, film cautiously washed). The figures calculated from these micrographs are given in Table II.

Table II. Properties of Latices and Polymers

(Temperature 25°C. Emulsifier 0.045 to 0.0465 mole SDS/kg. solution)

Type	Monomer		Latex			Polymer		Dose Rate, rad/hr.
	Concn. g./g. H ₂ O	No. of particles/ml. $\times 10^{14}$	Particle Diameter, A. Least Largest Medium			$[\eta]$, Dl./g.	Mol. wt. $\times 10^6$	
Styrene	1:8.7	5	—	—	—	7.7	2.7	200
	1:7.3	1.12	—	—	—	—	—	200
	1:7.8	4.75	880	1440	1136	9.2	3.5	50
MMA	1:8.0	—	320	1100	495	4.5	1.13	200
EA	1:7.4	—	—	—	—	3.2	1.6	50
MA	1:7.9	1.85	—	—	—	3.85	1.38	200

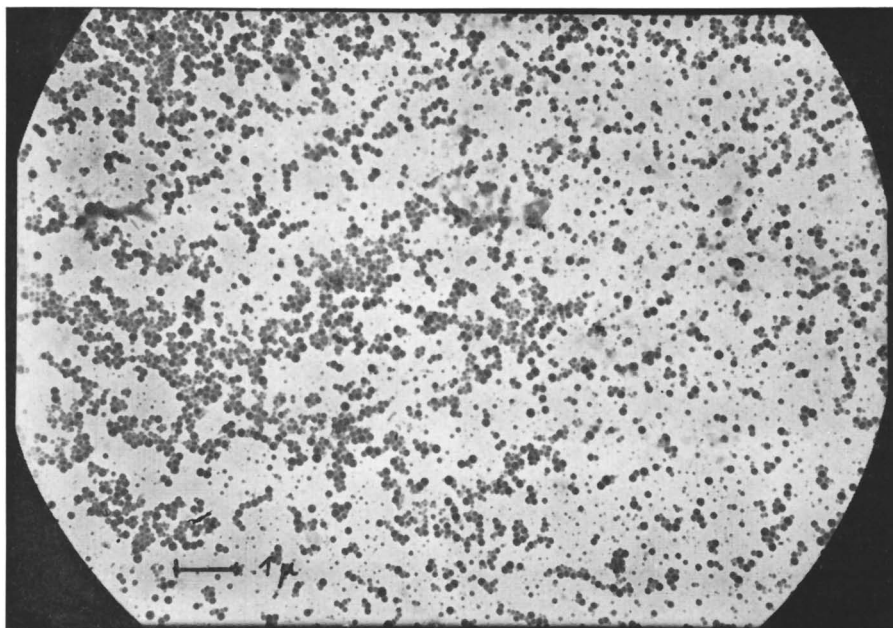


Figure 4. Electron micrograph of a polystyrene dispersion

Magnification $\sim 8000\times$

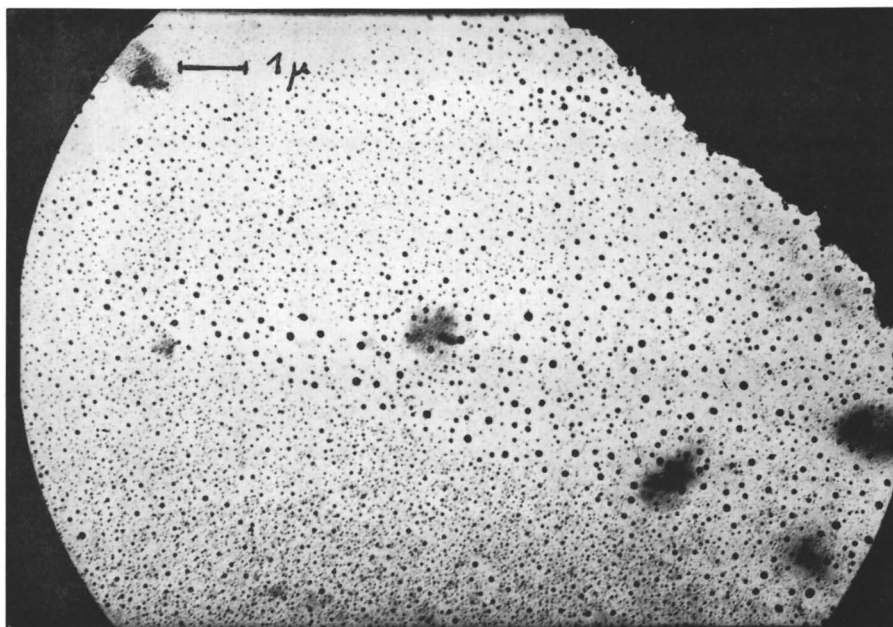


Figure 5. Electron micrograph of a PMMA dispersion

Magnification $\sim 8000\times$

The particles in the polystyrene dispersions had an average diameter of about 1150 A. The particles in the PMMA dispersions showed an average diameter of about 500 A.

Molecular Weights. The viscometrically determined molecular weights of the polymers were of the order of 10^6 . They decreased (polystyrene and PMA) with increasing dose rate. The absolute figures given are uncertain, because the Staudinger constants used (literature values) were determined at considerably lower molecular weights.

PMA showed special difficulties. Several samples did not fully dissolve, and probably contained cross-linked fractions. It is remarkable that these samples originated from experiments in which the polymerization was stopped at low conversions. We did not investigate the change of molecular weight, or the fraction of cross-linked polymer, in the course of a polymerization; therefore we cannot explain this effect. We observed further that η_{sp}/c plotted vs. concentration produced no straight lines, but more or less curved functions. This rendered the extrapolation for zero concentration more difficult. We therefore applied a double extrapolation method following Heller (21). This method is based upon the fact that the mathematical expressions

$$\frac{\eta - \eta_0}{\eta_0 c}$$

and

$$\frac{\ln(\eta/\eta_0)}{c}$$

become equal when $c \rightarrow 0$. All molecular weights were calculated from the arithmetic mean of the values for $[\eta]$, obtained by the two extrapolation methods.

Some irregularities in the behavior of our MA polymers may be explained with structure viscosity, and they might have their origin in branched structures. Emulsion polymers show higher degrees of branching than bulk or solution polymers of the same monomer. This is generally explained by the fact that in emulsion polymerization systems the concentration of the polymer in the monomer-polymer particles is already rather high in the early stages of reaction; for this reason, radical transfer from the growing chain to the dead polymer is favored. PMA due to its α -H atoms is particularly capable of undergoing transfer reactions. The assumption of branched structure for our MA polymers is therefore reasonable.

To show this structure viscosity we measured the intrinsic viscosity of the same polymer solutions in viscometers with different capillary lumen (Table III). The lumen had a strong influence on the measured values: the greater it was, the smaller were the figures for the intrinsic viscosity.

Table III. η_{sp}/c Values of Different Samples of PMA

(Capillaries of different width. Solvent Acetone)

Vis- cometer (De- creasing Width)	t_0 , Sec. in Ace- tone	Concentration, G./Dl.								
		Sample 1			Sample 2			Sample 3		
		0.125	0.1	0.05	0.5	0.4	0.25	0.5	0.4	
I	7.5	—	—	—	12.2	9.7	6.3	9.2	7.4	
II	44.4	—	7.3	6.0	—	20.9	—	—	16.2	
III	46.6	8.25	—	—	28.1	—	14.0	20.8	—	
IV	86.5	9.1	8.6	7.3	—	—	—	—	—	

In trying to fractionate samples of PMA by a gradient column according to Baker and Williams (3), we found small quantities (some parts per thousand) of an acetone-insoluble polymer at the top of the column. The viscosity numbers of the eluted PMA were between 4.2 (first fraction) and 4.55 (last fraction). Before fractionation, the polymer mixture showed a reproducible viscosity number of 5.3.

Styrene. Figure 6 shows the over-all reaction rate (logarithmic) plotted vs. time in the case of the γ -EP of styrene. v_{Br} in the beginning goes up steeply; after about 40 minutes (at a dose rate of 200 rad per hour) it becomes constant for some time: a period of zero order with respect to monomer concentration. After about 140 minutes and 40 to 50% conversion, v_{Br} decreases linearly: a period of first order with respect to monomer concentration.

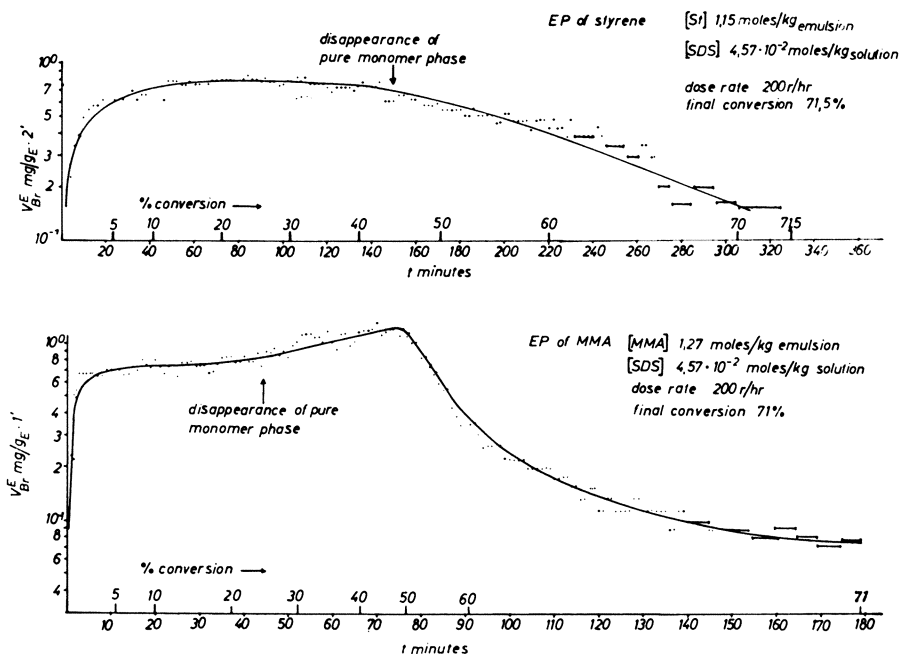


Figure 6. Over-all reaction rate vs. time

In two experiments, the polymerization was started with a dose rate of 50 rad per hour, and continued with a dose rate of 200 rad per hour. In the first experiment, the dose rate was raised before and in the second experiment after the reaction rate had become constant. In the first case, $v_{Br,max}$ (period of zero order) rose to twice the original value. In the second case, it increased only about 30%.

The course of the reaction rate/time function, measured by us, is exactly like the course of the same function in the case of the catalyzed emulsion polymerization of styrene. The small dependence of v_{Br} on the initiation rate in the period of zero order, which was observed by us, agrees well with classical conceptions: The period of particle formation is over and the radicals formed now affect initiation and termination likewise. Therefore the initiation rate can not influence the reaction rate. (Actually the reaction rate increases somewhat, on strongly increasing the dose rate. This shows that the mean radical concentration, \bar{n} , in the particles is slightly higher than 0.5. The termination reaction is already retarded.)

Finally, we polymerized four standard charges, two each with dose rates of 50 and 200 rad per hour respectively. The maximum over-all reaction rate rose by a factor of 2 with quadruple dose rate, from about 0.2 to about 0.4 mg. of polymer per minute per gram of emulsion. This corresponds to the "square root law" (termination with two radicals):

$$v_{Br} \sim I^{0.5}$$

where I = radiation intensity or dose rate (4). It cannot be decided from our experimental results, whether the exponent amounts to 0.5 or 0.4 according to Smith and Ewart (33).

MMA. Figure 6 shows the over-all reaction rate plotted logarithmically vs. time in case of the γ -emulsion polymerization of MMA. After the sharp rise of v_{Br} , a period of zero order of v_{Br} seems to follow. But then v_{Br} increases further and reaches a maximum at about 50% conversion. Soon afterwards, the curve drops sharply, and v_{Br} decreases almost as fast as if the radiation source were removed at this point. This decrease does not follow, or follows for only a short time, a first-order law with respect to monomer concentration. There also is no reaction of the second order with respect to $[M]$.

The first part of the $\log v_{Br}/t$ function up to the maximum may be interpreted as follows. At the beginning, the reaction proceeds according to the conception of Harkins. Dispersed PMMA takes up 3 to 4 times its monomer (by weight); contrary to PMMA, dispersed polystyrene dissolves only 1 to 1.5 times its own weight of monomer (Table I). In the case of the emulsion polymerization of MMA, the pure monomer phase therefore disappears at about 30% conversion. From here on, the Trommsdorff (38) or gel effect acts to increase the over-all reaction rate until the maximum is reached. During this period, the bulk of the monomer in monomer-polymer particles is consumed.

The following sharp drop of v_{Br} may probably be explained by the assumption that because of high concentration of polymers of high molecular weight in monomer-polymer particles, diffusion of not only polymer molecules but also monomer molecules is retarded. Therefore further polymerization takes place more slowly, despite the high mean radical concentration (gel effect)!

Trommsdorff *et al.* (38) and Baxendale *et al.* (7, 8) observed a similar behavior in the catalytic emulsion polymerization of MMA; the reaction was not studied dilatometrically, however. The conversion-time functions of Baxendale and coworkers do not show the acceleration effect as obviously as the curves of Trommsdorff or ours, probably because of long intervals between sampling.

Ethyl Acrylate (EA). Figure 7 shows the over-all reaction rate plotted logarithmically vs. time in case of the γ -emulsion polymerization of EA. The function shows a very simple form: from the beginning v_{Br} increases rather fast (in 6.5 minutes at 200 rad per hour) up to a maximum, and then decreases slowly without a period of zero order, following with considerable accuracy the first-order law with respect to $[M]$. At high conversions and very low reaction rates (about 0.05 mg. per minute per gram of emulsion), the curve falls less steeply.

Other authors observed that acrylic esters showed smaller gel effects, the larger the alkyl groups linked. According to Melville (25, 26), butyl acrylate polymerized in bulk shows no gel effect. If one assumes that EA shows no gel effect (at least under our conditions of γ -emulsion polymerization), and that the pure monomer phase disappears at the maximum of v_{Br} , then the behavior of our system harmonizes well with theory: after the maximum, the over-all reaction rate must decrease following first order with respect to $[M]$.

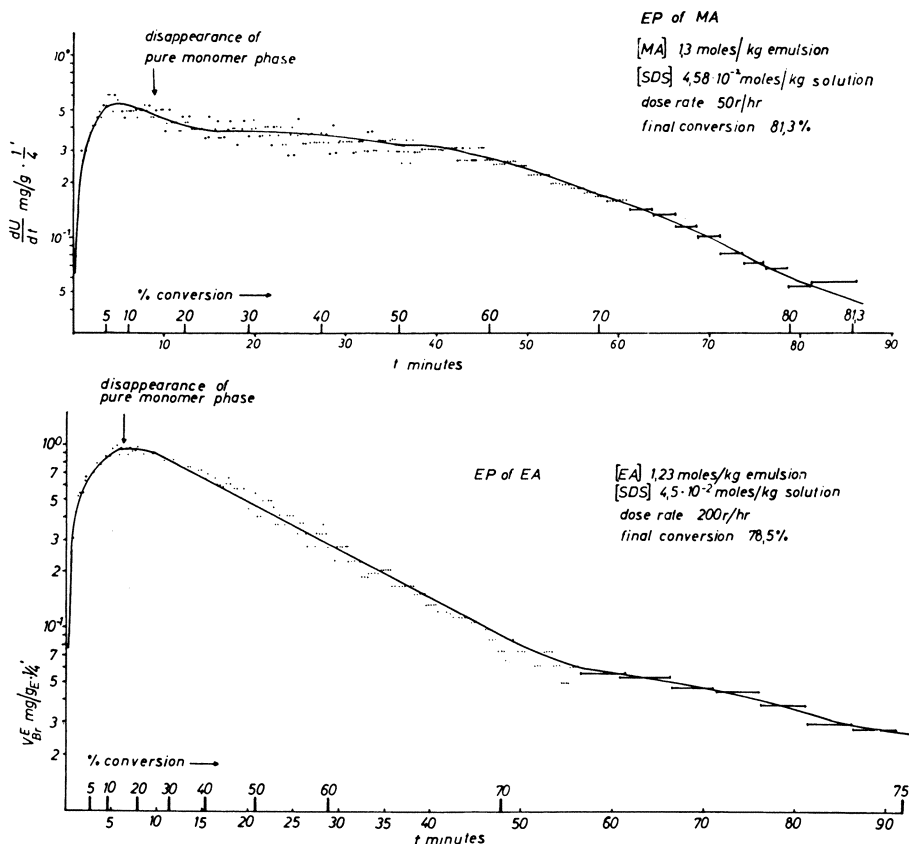


Figure 7. Over-all reaction rate vs. time

Methyl Acrylate (MA). The γ -emulsion polymerization of MA was studied most intensively in our investigations. The dependence of the reaction rate/time function, and the maximum reaction rate, on composition of the mixture, dose rate, and temperature was studied.

INFLUENCE OF DOSE RATE. Figure 8 shows the reaction rate/time functions for the γ -emulsion polymerization of MA at three different dose rates. The "standard function" at 200 rad per hour very rapidly passes up to a maximum (period I); this is reached after 5 to 7 minutes. The reaction rate then falls off in two periods (II and III), first slowly, and then faster. Both periods are linear in the first approximation. At high conversions, the reaction rate decreases somewhat more slowly (similar to EA, period IV). At lower dose rates period II becomes longer, and the maximum value of v_{Br} decreases.

$v_{Br_{max}}$ plotted vs. dose rate in double logarithmic presentation (Figure 9) produces a straight line with the slope 0.55. The same diagram shows the slope of periods II and III, plotted vs. dose rate. The resulting straight lines show similar slopes. Table IV shows the measured values.

INFLUENCE OF TEMPERATURE. We determined reaction rate/time functions for reaction temperatures of 15°, 25°, and 50°C. (Table IV). None of the parameters showed a remarkable temperature influence.

Table IV. Influence of Dose Rate and Temperature on γ -Emulsion Polymerization

Dose Rate, rad/Hour	$\frac{v_{Brmax}}{G \cdot Emulsion} \times Min.$	Slope ^a		N, Particles/ML. $\times 10^{14}$	$[\eta]$, Dl./G.	Mol. Wt. $\times 10^6$
		Per. II	Per. III			
DOSE RATE ^b						
200	4.4	1.16	3.16	1.85	3.85	1.38
			3.36	1.85	—	—
50	2.2	0.51	1.54	1.55	—	—
			1.84	1.55	4.4	1.62
22.2	1.2	0.25	0.77	1.27	5.0	1.88
			0.90	1.27	—	—
TEMPERATURE ^c						
Temp., °C.						
15	2.1	0.45	1.46	1.95	4.4	1.62
	2.2	0.45	1.55	—	—	—
25	2.2	0.51	1.54	1.55	—	—
	2.2	0.51	1.84	—	4.4	1.62
50	2.0	0.46	1.24	1.55	4.3	1.58
	1.8	0.46	1.28	—	—	—

^a Arbitrary units.

^b Temp. 25°C. Emulsifier 0.045 to 0.046 mole sodium dodecyl sulfate/kg. soln. 1.29 to 1.32 moles MA/kg. emulsion.

^c Dose rate 50 r/hour. Monomer 1.30 to 1.34 moles MA/kg. emulsion. Emulsifier 0.0451 to 0.046 mole sodium dodecyl sulfate/kg. soln.

INFLUENCE OF MONOMER CONCENTRATION IN ORIGINAL MIXTURE. v_{Brmax} increases with $[M]^{0.8}$ (Figure 10); at the same time, the maximum values are reached earlier. At the highest monomer concentrations investigated by us, v_{Brmax} seems to become independent of monomer concentration. This is shown in Figure

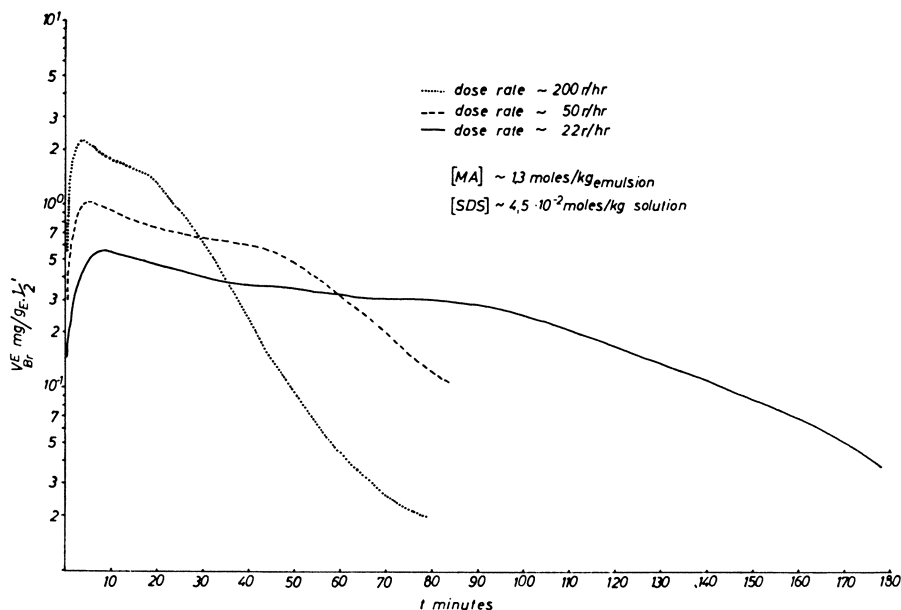


**Figure 8. Influence of dose rate on v_{Br}/t curve
25°C.**

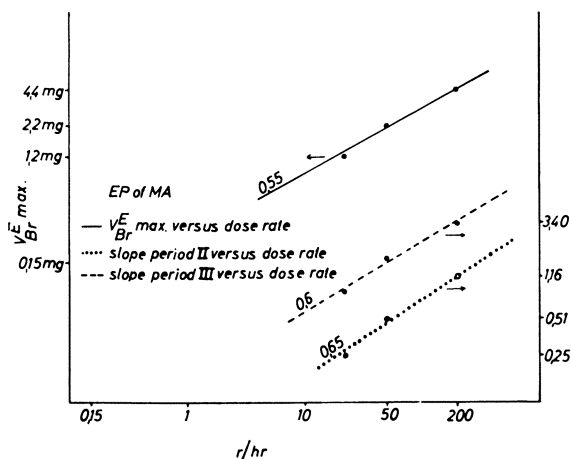


Figure 9. Effect of dose rate on maximum reaction rate and slope of periods II and III

10, where v_{Br}^E is plotted vs. monomer concentration in a double logarithmic scale. Period II becomes shorter with decreasing monomer concentrations, and finally it cannot be distinguished from period III (Figure 11). Period III becomes steeper with decreasing monomer concentration. The number of particles per milliliter of dispersion seems to increase with monomer concentration; the values from the highest monomer concentrations studied by us are not uniform, however.

The viscosity number of the polymers increases with monomer concentration, but seems to fall again at the highest monomer concentrations. In this case also the values were not uniform. Table V shows the measured values.

INFLUENCE OF EMULSIFIER CONCENTRATION. Most experiments on the influence of emulsifier concentration were carried out at a dose rate of 50 rad per hour, with a monomer concentration of 1.2 to 1.4 moles per kg. of emulsion

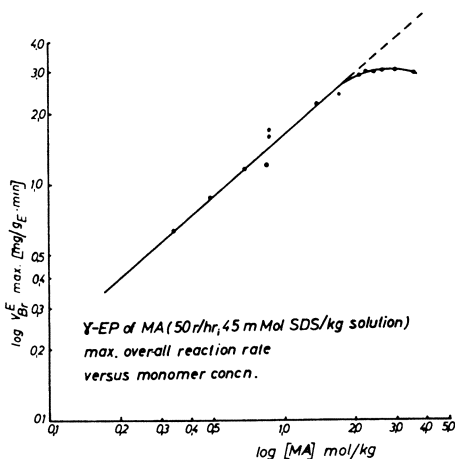


Figure 10. Effect of monomer concentration on maximum over-all rate
25° C.

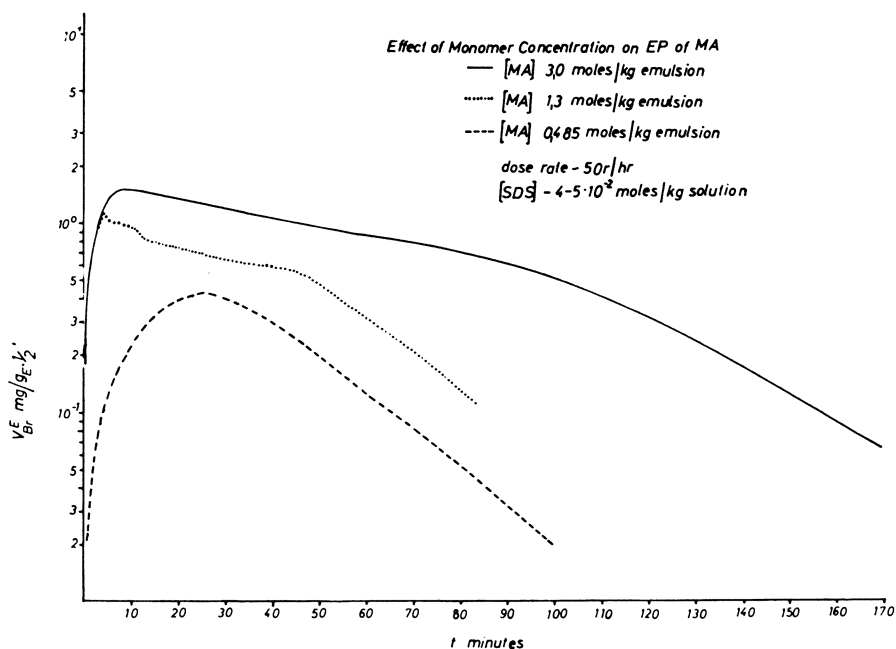


Figure 11. Effect of monomer concentration on v_{Br}/t curve
25° C.

(volume ratio 1 to 7), and at a temperature of 25°C. The concentrations of sodium dodecyl sulfate were varied between 0.77×10^{-2} and 11.9×10^{-2} mole per kg. of solution.

Table V shows the results of our measurements. The reaction rate/time functions of three emulsions with lowest, medium, and highest emulsifier concentration are shown in Figure 12. Periods II and III become indistinguishable at the lowest emulsifier concentrations (about 2 grams of SDS per kg. of solution) studied by us: After rapidly rising to a maximum, $\log v_{Br}$ decreases linearly with time. At higher emulsifier concentrations, a break appears between periods II and III. Simultaneously, period II becomes longer, until a long period of constant reaction rate has formed at the highest emulsifier concentrations.

Maximum over-all reaction rate is always reached after about 5 to 7 minutes. It is highest at the lowest emulsifier concentrations, and decreases continuously with rising emulsifier concentrations (Figure 13).

The number of particles per milliliter of dispersion increases with increasing emulsifier concentration; the diameter of the particles decreases simultaneously. At the highest emulsifier concentrations used, the particle sizes fell below the resolving power of the ultramicroscope, and we could not count them.

Intrinsic viscosity and molecular weight of the polymers increase with increasing emulsifier concentrations.

EFFECT OF INTERMITTENT RADIATION. If during the γ -emulsion polymerization of MA, the irradiation is stopped once or repeatedly, the reaction rate/time function always rises again to the value which would have been reached with continuous irradiation and at the same conversion (Figure 14). Neither $v_{Br, \max}$ nor other figures measured by us change with intermittent irradiation, except the falling and rising of the $\log v_{Br}/t$ function at stopping and starting of irradiation.

Table V. Influence of Original Monomer and Emulsifier Concentrations on γ -Emulsion Polymerization of Methyl Acrylate

(Dose rate: 50 rad/Hour. Temp. 25 °C.)

[MA], Moles/Kg. Emulsion	[SDS], Mmoles/ Kg. Soln.	$v_{Brmax.}$ Mg. Polymer/ G. Emulsion \times Min.	Slope ^a		N_s , Particles/ Ml. $\times 10^{14}$	[η], Dl/G.	Mol. Wt. $\times 10^6$
			Per. II	Per. III			
ORIGINAL MONOMER CONCN.							
0.485	41.2	0.88	1.58	—	—	4.1	1.49
		0.88	1.58	—	—	—	—
0.680	42.8	1.16	1.73	1.05	—	4.65	1.73
		1.16	1.73	—	—	—	—
0.836	44.3	1.1	1.6	—	—	5.0	1.88
		1.2	1.7	—	—	—	—
0.870	45.5	1.6	1.75	—	—	5.1	1.92
		1.7	1.75	—	—	—	—
1.30	45.8	2.2	0.51	1.54	1.55	—	—
		2.2	0.51	1.84	—	4.4	1.62
1.72	45.5	2.4	0.52	1.04	2.6	6.0	2.36
		2.72	0.52	1.46	—	—	—
2.10	51.4	2.8	0.44	—	3.2	3.6	1.28
		3.0	0.44	1.7	—	—	—
2.24	51.3	2.9	0.48	1.38	—	3.7	1.32
		3.0	0.48	1.38	—	—	—
2.64	52.0	3.0	0.395	1.19	—	3.5	1.24
		3.0	0.395	1.25	—	—	—
3.0	55.4	3.0	0.29	0.92	3.1	4.3 ^b	1.58 ^b
		3.1	0.365	0.92	—	—	—
3.57	58.5	2.8	0.2	—	—	2.55	0.83
		2.9	0.2	—	—	—	0.83
EMULSIFIER CONCENTRATION							
1.25	22.9	2.88	0.68	1.68	2.0	4.4	1.62
		—	—	—	—	—	—
1.20	23.0	2.6	0.62	1.76	2.0	5.3	2.0
		2.8	0.62	1.76	—	—	—
1.33	23.0	3.2	0.91	1.76	2.1	3.6	1.36
		3.2	0.91	1.76	—	—	—
1.30	45.8	2.2	0.51	1.54	1.55	4.4	1.62
		2.2	0.51	1.64	—	—	—
1.49	60.0	2.2	0.45	1.28	2.25	4.8	1.8
		2.2	0.45	1.32	—	—	—
1.37	74.3	1.6	0.3	1.08	2.8	5.6	2.15
		1.8	0.3	1.4	—	—	—
1.42	90.2	1.26	0.1	1.12	3.3	5.8	2.25
1.32	90.2	1.2	0	1.04	c	5.3	2.02
		1.2	0	1.25	—	—	—
1.39	119	1.0	0	1.07	c	6.0	2.36
		1.5	0	1.34	—	—	—

^a Arbitrary units.^b Soluble fraction.^c Invisible with Zsigmondy microscope.

The pre- and after-effects are characteristic; they are discussed below.

EFFECT OF INTENSITY CHANGES DURING POLYMERIZATION. In three experiments, the irradiation was stopped after having reached different stages of polymerization. Hereafter, the reaction was continued with fourfold dose rate. In all cases v_{Br} increased to twice the value which would have been obtained with the lower dose rate.

Discussion of γ -Emulsion Polymerization of MA. Period I of increased reaction rate is caused by the growing of the stationary radical concentration in the system. The interpretation of this part of the curve is like the interpretation of the same period in the emulsion polymerization of styrene.

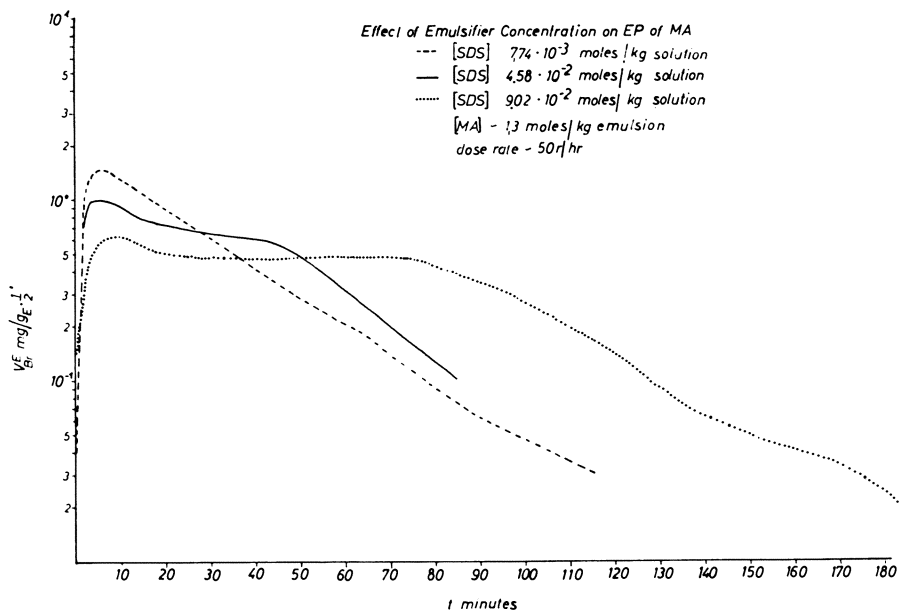


Figure 12. Effect of emulsifier concentration on v_{Br}^E/t curve
25° C.

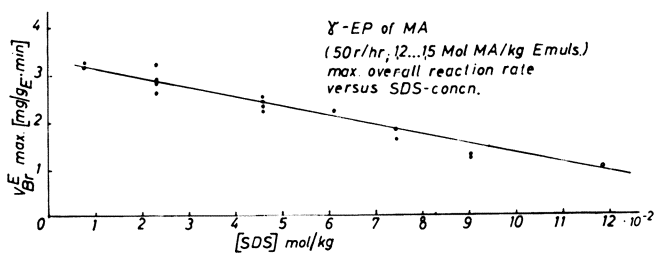


Figure 13. Effect of emulsifier concentration on maximum over-all reaction rate
25° C.

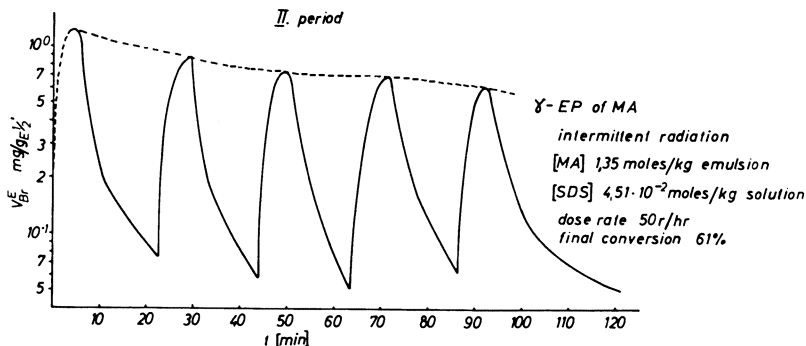


Figure 14. Effect of intermittent irradiation on v_{Br}^E/t time curve
25° C.

Having passed the maximum, v_{Br} falls without forming a real period of zero order (see styrene) with respect to $[M]$. This is probably due to the high capacity of the dispersed polymer for its monomer: PMA particles take up monomer up to six to seven times their weight (Table I). Therefore, the pure monomer phase disappears at about 15% conversion. In the course of polymerization, MA differs from EA with respect to the kinetics: v_{Br} normally does not drop according to the first order with respect to $[M]$. As we have seen, two periods (II and III) are formed with different slopes. With increasing $[M]$ in the original mixture, the decrease of v_{Br} becomes slower, and $v_{Br_{max}}$ increases. Finally, increasing values of $[E]$ cause steady falling of $v_{Br_{max}}$.

These observations can be explained by the assumption of a strong gel effect during the emulsion polymerization of MA. In emulsion polymerization systems, this gel effect probably occurs still earlier than in bulk systems, because the P/M ratio in the monomer-polymer particles is already high in the early stages of polymerization. This ratio determines the viscosity in the particles, and the speed of diffusion toward each other of two living polymer chains, as well. Especially in the case of MA, the volume of the monomer-polymer particles is probably already high in early stages of polymerization; this is due to the high capacity of PMA particles for monomer. The larger the monomer-polymer particle, the longer is the mean diffusion path of two radicals on their way toward each other. Both factors—high P/M ratio and large particle size—cause the strong and early gell effect. Our experimental results lead to the conclusion that the gel effect controls also the magnitude of $v_{Br_{max}}$. Enlargement of the particles by increasing $[M]$ enhances the gel effect and $v_{Br_{max}}$ as well. Reduction of particle size by increasing $[E]$ lowers the gel effect and $v_{Br_{max}}$ as well. Finally, the course of v_{Br} after the maximum is ruled by the same mechanism. The stronger the gel effect, the more the v_{Br}/t function deviates from the first-order law (with respect to $[M]$) to higher values of v_{Br} .

This assumption is supported by other observations. The most important of these observations are the increase of v_{Br} , when the dose rate was enhanced at different stages of polymerization. In all these cases, the increase of v_{Br} followed rather exactly the square root law ($v_{Br} \sim I^{0.5}$). According to the theory of emulsion polymerization, extended by Gerrens (16), this behavior must be expected for the case of the gel effect. The high molecular weight of PMA is another support for our assumption.

The following experimental result seems to contradict our interpretation. The slope of period II after the maximum v_{Br} becomes flatter with increasing $[E]$. At the largest emulsifier concentrations used by us, v_{Br} remains constant even during a longer period. However, enhancement of $[E]$ should produce the opposite behavior, because the gel effect decreases with reduced particle size.

We cannot give a proved interpretation for this behavior. However, the following assumption of continued particle formation is not unlikely. In the case of emulsion polymerization of styrene with normal emulsifier concentrations (1 to 3%), the phase of particle formation is probably over at a conversion of about 20%. This is due to the fact that the emulsifier concentration at this point falls off below the critical value for micelle formation (c.m.c.); therefore no micelles are further available. At higher emulsifier concentrations (5 to 6% with respect to water), this does not happen during the whole polymerization process (9). Particle formation therefore should be possible throughout the reaction. According to Bovey (9) this is not the case, because disappearance of the pure styrene phase at about 30% conversion stops particle formation. As far as we know, this

was not proved by measuring the number of particles during the emulsion polymerization of those mixtures.

The statement of Bovey probably is based upon the assumption that, after the disappearance of the pure monomer phase, the concentration of the monomer in the micellar phase is so low that the micelles can be disregarded as a place of reaction (as the pure aqueous phase). The following considerations show that Bovey's assumption may not hold true in all cases.

Considering a polymerizing emulsion system at its distribution balance, the three phases must show the same monomer activity: the monomer-polymer particles, the micellar phase, and the water phase. Both monomer-polymer particles and the organic part of the micelles are lipophilic, and, therefore, compete for monomer. It does not seem plausible to assume that equal monomer activities in these two phases belong to monomer concentrations which differ by several orders of magnitude. Therefore it is likely that new particles are formed also after the disappearance of the pure monomer phase, provided there is a micellar phase, and enough monomer in the monomer-polymer particles as well.

In the case of monomers with a high solubility in water there is another possibility to be considered—that of formation of new particles. A fairly concentrated aqueous solution of MA is about 0.57M, 1 ml. of this solution contains about 3.5×10^{20} molecules of MA probably in molecular dispersion. An initiating radical has a better chance to react with MA in the water phase than in the case of styrene, which has a solubility about 500 times lower than MA. If there is sufficient free emulsifier, the growing chain will be soon surrounded by emulsifier, and a new particle is formed.

Our assumption of prolonged particle formation during the emulsion polymerization of MA can explain the course of v_{Br} in mixtures with high emulsifier concentration. For proving this assumption it would be necessary to measure the change in particle number during the course of the emulsion polymerization of MA; this has not yet been done. The results of our work on the γ -induced emulsion polymerization of MA cannot be interpreted in terms of the Smith-Ewart theory in its simple form (33). Therefore one cannot expect that v_{Br} is independent of the monomer-water ratio or proportional to $[E]^{0.6}$ or to $[\text{initiator}]^{0.4}$ (dose rate and initiator concentration can be substituted). A quantitative interpretation of the γ -induced emulsion polymerization of MA cannot yet be formulated, because of the complexity of the phenomena involved. To make this possible, considerable further work on this subject has to be done. The dependence of $v_{Br, \max}$ on $[M]^{0.8}$ for rather low monomer-water ratios and its independence of $[M]$ for the highest monomer to water ratios studied are remarkable, but cannot yet be explained. If the gel effect would control the maximum over-all reaction rate solely, then the values of $v_{Br, \max}$ would increase proportionally to $[M]$.

In experiments with "normal" recipes, $v_{Br, \max}$ increases with $I^{0.55}$ ($I =$ dose rate). The exponent is in accord (within experimental error) with the square root law, postulated for the dependence of the stationary radical concentration on light intensity with incomplete absorption of the quanta, and a termination reaction involving two radicals.

INITIATION RATE IN γ -INDUCED EMULSION POLYMERIZATION. In all our foregoing discussions on the kinetics of the γ -initiated emulsion polymerization with constant dose rate we have assumed that the initiation rate or the rate of formation of radicals in the system remains constant throughout the reaction.

The fact that the γ -induced emulsion polymerization of styrene (probably also

of MMA) resembles the course of the catalytic emulsion polymerization with considerable accuracy is not evident theoretically. One of the basic assumptions of the Harkins view and the Smith-Ewart theory is that the initiating radicals are generated in the true aqueous phase with a constant velocity, the radicals entering the particles singly.

Considering the efficiency of initiators in catalytic emulsion polymerization, Vanderhoff had to define a factor, f

$$f = \frac{\text{total number of initiating radicals}}{\text{total number of generated radicals}}$$

The numerical value of the factor was found to be always smaller than 1. According to Chapiro (12, 13) in γ -induced polymerization all substances in the system (water, emulsifier, monomer, and polymer) are able to produce radicals under the influence of radiation. The different sensibilities of substances to radiation impact are described by the factors in his equation. In addition, we have to consider the differing reactivity, r , of the radicals generated. Hence the initiation rate in our system should be described by an equation of the form

$$I = \frac{dP}{dt} = \varphi(r_1 \Phi_{H_2O}[H_2O] + r_2 \Phi_E[E] + r_3 \Phi_M[M] + r_4 \Phi P[P])$$

The concentrations of monomer and polymer are (during the reaction) functions of time. The equation does not take into account that each substance in the irradiated system may form several different types of radicals with (probably) different reactivities. Also radicals of different reactivities generated by transfer reactions are neglected.

Considering these facts we must realize that the initiation rate in γ -induced emulsion polymerization is a matter of great complexity. To estimate only their constancy or inconstancy during polymerization, we have to neglect many possible reactions, assuming that they occur to an insignificant extent only. Two extreme cases of such an estimation are as follows.

The assumption that in the emulsion polymerization system (containing 80 to 90% water) all ingredients have G_R values equal to or lower than that of water, and that all radicals produced have similar reactivities, to initiate polymerization, leads to the conclusion that the rate of radical formation, and initiation of polymerization (to a first approximation), will be constant throughout the reaction.

If the molecules of monomer show a sensitivity to radiation impact higher by far than all other substances in the system, we shall have a system with a preponderant effect of radiation on the monomer. This situation gives rise to a rate of initiation strongly dependent on monomer concentration; hence the initiation rate must decrease during the polymerization.

The total number of radicals produced in 1 gram of emulsion per hour by a dose rate of 200 rad per hour is about 3×10^{14} (G_R value of water is 3). Really under these conditions, in the case of styrene, the period of particle formation lasts about 1 hour (formation of about 10^{14} particles per milliliter). During the period of maximum reaction rate, in 1 gram of emulsion about 10^{14} molecules of polystyrene are formed in 1 minute ($v_{Br \max}$ 0.4 mg. of polystyrene per minute per gram of emulsion; molecular weight 1.25×10^6). However, during the same time only about 10^{13} radicals are formed in 1 ml. of emulsion ($G_{R_{H_2O}} = 3$).

This discrepancy is still larger in the case of MA. Maximum reaction rate is reached in a few minutes after the start of the polymerization, and during this interval only some 10^{13} radicals are produced by radiolysis. During the period of maximum reaction rate (4.4 mg. of PMA per minute per ml. of emulsion) about

1.75×10^{15} molecules of PMA are formed in 1 minute and in 1 ml. of emulsion, compared with a maximum of about 10^{13} radicals produced in the same time.

These discrepancies are very strange and difficult to explain. In our opinion the following mechanisms could contribute to the effect:

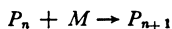
The mean distance of the monomer swollen micelles is of the order of the diameter of the "spurs" (elementary reaction regions of secondary electrons, produced by the γ -radiation). Therefore, possibly, a certain fraction of the radiolytical radicals does not recombine in the Frank-Rabinovitch cage, but breaks into the micelles or particles and is trapped therein.

Furthermore, part of the excitation energy of the spur may be transferred directly to the micelles or particles without producing radicals in the water phase. Exciton transfer occurs, especially in the case of crystalline matter. Because of strong intermolecular forces, and the quasicrystalline character of liquid water, exciton transfer may occur also in aqueous media, at least between short distances.

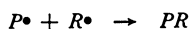
Both effects would be able to enhance considerably the efficiency of radiation.

Transfer reactions can cause formation of a number of polymer molecules by only one primary radical. However, the extent of such transfer reactions, necessary to balance the lack of radicals, seems to be high.

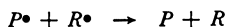
DETERMINATION OF QUOTIENT k_p/k_t . Theory of Pre- and Aftereffect (3). k_p is the "absolute" propagation constant of the chain propagation reaction in free radical polymerization corresponding to



It is assumed that k_p is independent of the size of the growing radical (given above by the index n in terms of monomer units). k_t is the "absolute" termination rate constant. Termination may occur by combination or disproportionation:



or



The rate of a polymerization reaction with a long kinetic chain length in the stationary state is given by:

$$-\frac{d[M]}{dt} = k_p[M][R^\bullet]$$

The stationary state condition is:

$$\frac{d[R^\bullet]}{dt} = 0$$

In the nonstationary state ($\frac{dR^\bullet}{dt} \neq 0$), the variation of radical concentration is given by

$$-\frac{[dR^\bullet]}{dt} = J - k_t[R^\bullet]^2$$

J describing the production, the second term the disappearance of radicals. Because there is an unknown amount of thermal initiation, and a certain remanent γ -intensity caused by incomplete shielding of the source, we have to assume two initiation rates: $J_1 + J_2$ for the source at the upper position and J_1 for the source shielded. Addition or subtraction of J_2 causes the nonstationary state.

The total pre-effect is the difference between the conversion actually observed during the nonstationary state and the conversion which would have been obtained, if the reaction rate of the new stationary state had been set up immediately. The value of the total pre-effect is given by

$$\Delta M_{\text{pre}} = \frac{k_p[M]}{k_t} \log \frac{2\theta}{\theta + 1}$$

$$\text{with } \theta = \left(\frac{J_1 + J_2}{J_1} \right)^{1/2} \quad (5)$$

The only measured quantities in this equation are the ratio of the initiation rates and the monomer concentration. By measuring these values and the total pre-effect as well, it is possible to evaluate the ratio k_p/k_t . The aftereffect can be treated analogously. In the beginning there is a stationary state corresponding to $J_1 + J_2$; at time $t = 0$, the initiation rate is lowered to J_1 . The total aftereffect is given by:

$$\Delta M_{\text{after}} = \frac{k_p[M]}{k_t} \log \frac{\theta + 1}{2}$$

$$\theta = \left(\frac{J_1 + J_2}{J_1} \right)^{1/2}$$

The equation shows that the total aftereffect depends only on the values of k_p/k_t , $[M]$, and the ratio of the initiation rates.

These equations were originally set up for homogeneous kinetics. Nevertheless, we applied them to our heterogeneous system because—as far as we can see—the heterogeneity of the system does not interfere with the basic assumptions of the deduction of the equations used by us. Naturally the numerical value of the quotient k_p/k_t determined by us includes all the specific properties of the system.

DETERMINATION OF THE TOTAL PRE- AND AFTEREFFECT. Measurement in the nonstationary state requires a method of altering the initiation rate of the system instantaneously, and a precise determination of the small amount of conversion involved. The first condition in most cases is met by photochemical initiation methods. This was, to our knowledge, never done on emulsion systems, because the vast and varying dispersion of visible and ultraviolet light by the system during the reaction prevents the homogeneous illumination of the reaction vessel. These difficulties can be successfully met by applying γ -radiation.

To determine the total aftereffect, we measured the total conversion, obtained after the interruption of the irradiation, and the monomer concentration at about half of this conversion.

To determine the total pre-effect, the sample in the dilatometer was polymerized to a considerable extent. After this, the irradiation was interrupted, and later on started once more. In our calculation, we used only the pre-effect appearing upon repeating the irradiation. This was done to prevent changes in the value of ΔM_{pre} by effects of incomplete consumption of inhibitors (causing the inhibition period at the beginning of irradiation) or the formation of monomer-polymer particles (during the first period of the emulsion polymerization). For the determination of the numerical value of ΔM_{pre} , we used an extrapolation method given by Burnett *et al.* (10, 11). If v is the "stationary" reaction rate reached at time t , which is great with respect to the duration of the pre-effect, the amount of monomer converted at time t is given by:

$$\Delta M_t = vt - \Delta M_{\text{pre}}$$

Plotting M_t vs. t produces a function with a linear part. Extrapolation of this line gives a negative intercept on the M_t axis, which is the numerical value of ΔM_{pre} (Figure 15).

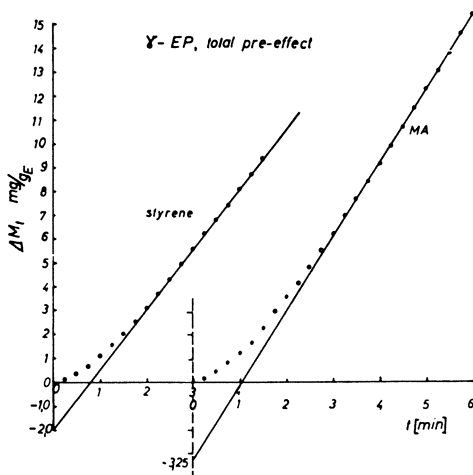


Figure 15. Determination of total pre-effect by extrapolation

Results and Discussion

The results of our measurements on the emulsion polymerization of styrene and MA systems are listed in Table VI. The dose rates were 200 and 50 rad per

Table VI. Pre- and Aftereffect in the γ -Emulsion Polymerization

($I_1 + I_2 = 200$ r/hour or 50 r/hour for last six values. $I_1 = 0.15$ r/hour. Temp. 25°C.)

Styrene, Mg./G.	ΔM_{PRE} , Mg./G. Emulsion	ΔM_{AFTER} , Mg./G. Emulsion	k_p/k_t	k_t , Liter/Mole Second
80.0	2.3	—	0.0991	294
60.0	1.25	—	0.0719	405
71.9	2.0	—	0.096	303
				Av. 334
98.2	—	6.34	0.0549	530
73.2	—	7.95	0.0815	342
81.9	—	11.54	0.11	264
89.0	—	11.85	0.105	279
69.0	—	8.11	0.0922	316
				Av. 346
[MA]				Liter/Mole Second $\times 10^4$
113.3	2.7	—	0.082	2.6
91.3	1.5	—	0.0567	3.77
67.1	1.6	—	0.0822	2.6
35.0	0.7	—	0.069	3.1
83.0	3.25	—	0.135	1.56
				Av. 2.73
120.5	—	6.237	0.0526	4.06
164.5	—	8.58	0.053	4.03
143.0	—	11.46	0.0815	2.62
143.0	—	8.59	0.061	3.5
125.6	—	7.73	0.0625	3.42
77.1	—	8.87	0.117	1.83
77.1	—	7.48	0.0985	2.16
40.1	—	8.41	0.164	1.3
102.3	—	9.73	0.0745	2.87
90.3	—	8.38	0.0727	2.93
				Av. 2.82

hour, respectively ($J_1 + J_2$), and 0.15 rad per hour for a shielded source (J_1). k_p/k_t was calculated from

$$\frac{k_p}{k_t} = \frac{\Delta M_{\text{pre}}}{f'[\bar{M}]}$$

$$f' = \log \frac{\theta \times 2}{\theta + 1}$$

or

$$\frac{k_p}{k_t} = \frac{\Delta M_{\text{after}}}{f[\bar{M}]}$$

$$f = \log \frac{\theta + 1}{2}$$

f and f' are nondimensional coefficients and $\Delta[M]$ and $[M]$ are both given in milligrams per gram of emulsion.

The numerical values of k_p/k_t thus calculated agree well; the errors in the single values of ΔM_{pre} and ΔM_{after} are rather high. These errors appeared because the irradiation device did not allow the setting of time marks with great precision. Some time is needed to lower the source into the shielding, and to raise it again.

The values of k_p/k_t , determined by measuring the pre- or the aftereffect, were in good agreement. This shows that the aftereffect really is caused by varying the radiation intensity, and not by decomposition of initiators like H_2O_2 or other peroxides formed under the influence of the ionizing radiation.

If one assumes the absolute propagation rate constant, k_p (measured by means of the rotating-sector technique or other "absolute" methods in block or solution polymerization systems), to be independent of the physical properties of the system (temperature excepted), it is possible to use these values for emulsion polymerization systems too.

The average of some k_p values at 25° C. (10, 11) is 29.1 liters mole⁻¹ sec.⁻¹ for styrene, and 2135 liters mole⁻¹ sec.⁻¹ for MA. Table VI shows k_t values calculated with our values of k_p/k_t , and the average values of k_p as well.

The numerical values $c^f k$, thus calculated are some decimal powers lower than those determined by different methods in homogeneous systems. This fact demonstrates—if our interpretation is right—the effective hindrance of the termination reaction in the emulsion polymerization system. It must be caused by the heterogeneity of the system, which is divided into numerous isolated reaction phases. The retardation of the termination reaction, postulated by all workers on the subject, is thus demonstrated experimentally by the values of k_t .

Conclusion

Styrene, methyl methacrylate, ethyl acrylate, and methyl acrylate are easily polymerized in aqueous emulsion under the action of Co^{60} γ -radiation. The maximum over-all reaction rate increases in the sequence given above. Using a dose rate of 200 rad per hour, the doses required to obtain a conversion of 80 to 90% amount to about 10³ rad. This dose is far lower than the doses required for a measurable degradation or cross linking of the polymers formed. The G value of formation of polymer molecules was found to be orders of magnitude higher than the G_R (H_2O) values referred to in the literature.

The course of the γ -induced emulsion polymerization was followed with a highly sensitive self-recording dilatometer. The variation of the over-all reaction rate with time in the emulsion polymerization of MMA, EA, and MA deviated

from the classical behavior of styrene. During the γ -emulsion polymerization of MA, the Trommsdorff or gel effect controls v_{Br} from the very beginning of the reaction. Variation of the temperature between 15° and 50° C. had no detectable effect on the polymerization.

During the γ -emulsion polymerization of MMA a strong gel effect seems to occur.

By γ -ray initiation of the emulsion polymerization, the initiation rate can be altered instantaneously without interfering with the system. The termination constants of the emulsion polymerization systems are orders of magnitude lower than the corresponding values of k_t , determined in homogeneous systems. Thus the hindrance of the termination reaction in the emulsion polymerization system is demonstrated by the values of k_t .

Polymers obtained at small dose rates had rather high molecular weights ($> 10^6$). The number of particles of polymer dispersions were in the magnitude range of 10^{14} particles per ml.

Acknowledgment

The authors thank G. Schmid, director of the Institut für physikalische Chemie und Kolloidchemie, University of Cologne, E. Trommsdorff, Röhm & Haas G.m.b.H., for many helpful discussions, and E. Zehender, Robert Bosch G.m.b.H., for the electron micrographs. This work was supported by the Bundesminister für Atomkernenergie und Wasserwirtschaft. One of us (G. Ley) thanks the American Research Foundation for a stipendium.

Literature Cited

- (1) Allen, P. E. M., Downer, J. M., Hastings, G. W., Melville, H. W., Molyneux, H. P., Urwin, J. R., *Nature* **177**, 910 (1956).
- (2) Bagdasaryan, K. S., *J. Phys. Chem. (Moscow)* **22**, 1181 (1948).
- (3) Baker, C. A., Williams, R. J. P., *J. Chem. Soc.* 1956, 2352.
- (4) Ballantine, D. S., *Rept. Brookhaven Natl. Lab.* T-50 No. **294**, p. 18; T-53 No.317, 7 (1954).
- (5) Bamford, C. H., "Kinetics of Vinyl Polymerization," Butterworths, London, England, 1958.
- (6) Bartholomé, E., Gerrens, H., Herbeck, R., Weitz, H. M., *Z. Elektrochem.* **60**, 334 (1956).
- (7) Baxendale, J. H., Bywater, S., Evans, M. G., *J. Polymer Sci.* **1**, 237, 466 (1946).
- (8) Baxendale, J. H., Evans, M. G., Kilham, J. K., *Trans. Faraday Soc.* **42**, 668-75 (1946).
- (9) Bovey, F. A., Kolthoff, I. M., Medalia, A. I., Meehan, E. J., "Emulsion Polymerization," Interscience, New York, 1955.
- (10) Burnett, G. M., "Mechanism of Polymer Reactions," Interscience, New York, 1954.
- (11) Burnett, G. M., *Trans. Faraday Soc.* **46**, 772-82 (1950).
- (12) Chapiro, A., *Ind. plastiques mod. (Paris)* **8** (9) 67 (1956); **9** (1), 41; **9** (2) 34 (1957).
- (13) Chapiro, A., Maeda, N., *J. chim. phys.* **56** (2), 230 (1957).
- (14) Charlesby, A., "Atomic Radiation and Polymers," Pergamon Press, New York, 1960.
- (15) Fuhrmann, N., Mesrobian, R. B., *J. Am. Chem. Soc.* **76**, 3281 (1954).
- (16) Gerrens, H., "Fortschritte der Hochpolymeren-Forschung," Vol. I, No. 2, Springer Verlag, Berlin, 1959.
- (17) Hachihama, Y., Sumitomo, H., *Tech. Repts., Osaka Ind. Tech Research Inst.* **3**, 91, 385 (1953).
- (18) Harkins, W. D., *J. Am. Chem. Soc.* **69**, 1428 (1947).
- (19) Harkins, W. D., *J. Polymer Sci.* **5**, 217 (1950).
- (20) Haward, R. N., *Ibid.*, **4**, 273 (1949).
- (21) Heller, W., *J. Colloid Sci.* **9**, 547 (1954).
- (22) Marzolph, H., Schulz, G. V., *Makromol. Chem.* **13**, 120 (1954).
- (23) Matheson, M. S., *J. Am. Chem. Soc.* **73**, 5395 (1951).

- (24) Matheson, M. S., Auer, E. E., Bevilacqua, E. B., Hart, E. J., *Ibid.*, **73**, 1700 (1951).
- (25) Melville, H. W., *Trans. Faraday Soc.* **45**, 1049 (1949).
- (26) Melville, H. W., *et al.*, *Proc. Roy Soc.* **207 A**, 285 (1951).
- (27) Meyer, F. W., Ronge, G., *Angew. Chem.* **52**, 637 (1939).
- (28) Mezhirova, A. P., *et al.*, *Vysokomolekulyarnye Soedineniya* (Moscow) **1**, 68 (1959).
- (29) Okamura, S., *et al.*, Intern. Conf. on "Application of Large Radiation Sources in Industry and Especially to Chemical Processes," Warsaw Poland, Sept. 8 to 12, 1959.
- (30) Okamura, S., Motoyama, T., *Chem. High Polymers (Tokyo)* **12**, 102 (1955).
- (31) Prevost-Bernas, A., *et al.*, *Discussions Faraday Soc.* **12**, 98 (1952).
- (32) Smith, W. V., *J. Am. Chem. Soc.* **70**, 3695 (1948).
- (33) Smith, W. V., Ewart, R. H., *J. Chem. Phys.* **16**, 592 (1948).
- (34) Starkweather, H. W., Taylor, R. H., *J. Am. Chem. Soc.* **52**, 4708 (1930).
- (35) Staudinger, H., *J. prakt. Chem.* **155**, 261 (1940).
- (36) Swallow, A. J., "Radiation Chemistry of Organic Compounds," Pergamon Press, New York, 1960.
- (37) Treloar, F. E., *Polymer* **1** (4) 513 (1960).
- (38) Trommsdorff, E., Kohle, H., Lagally, P., *Makromol. Chem.* **1**, 169 (1947).
- (39) Vanderhoff, J. W., *et al.*, *J. Polymer Sci.* **50**, 265 (1961).
- (40) Walling, C., *J. Am. Chem. Soc.* **70**, 2561 (1948).

RECEIVED September 5, 1961.

Graft Copolymers of Wheat Starch

ROBERT L. WALRATH and ZOILA REYES

Stanford Research Institute, Menlo Park, Calif.

C. R. RUSSELL

Northern Regional Research Laboratory, Peoria, Ill.

Preparation of graft copolymers of wheat starch and vinyl monomers was studied, using gamma irradiation to initiate the grafting process. Wheat starch, heat-treated, azeotropically dried, "as is," swollen, or gelatinized, was used. Graft copolymers were obtained by irradiation of starch in the presence of monomers, or by reaction of the monomers with preirradiated starch. Acrylonitrile, vinyl acetate, and vinyl chloride were used as monomers. The rate of diffusion of the monomer into the starch appears to be the most important factor affecting the degree of grafting, and is dependent on the polarity of the monomer, the state of the starch, the temperature of reaction, and the presence of solvents or diluents. Electron spin resonance studies on irradiated starch showed formation of a relatively large amount of trapped free radicals, which decay slowly and are stable to moderate changes in temperature.

As part of a utilization program sponsored by the United States Department of Agriculture, we are investigating the preparation of graft copolymers of wheat starch for industrial applications. Various methods of grafting have been studied, with a wide variety of vinyl monomers. This paper presents the results of a study on the preparation of graft copolymers of wheat starch with acrylonitrile, vinyl acetate, and vinyl chloride, using gamma irradiation to initiate copolymerization.

Experimental Procedures

Vinyl Monomer Preparation. The vinyl monomers (Matheson, Coleman, and Bell) were treated as follows: Acrylonitrile was dried over calcium chloride and distilled twice; vinyl acetate was purified by distillation, and both monomers were stored under refrigeration and redistilled before use. Vinyl chloride was used directly from the lecture bottle in which it was obtained.

Wheat Starch Preparation. Edible wheat starch (Hercules No. 120) obtained through the Northern Utilization Research and Development Division, U. S. Department of Agriculture, Peoria, Ill., was used throughout these experiments. The dry starch was prepared by dispersing it in benzene, distilling off the azeotrope, and drying in a vacuum oven at 100° C.

Swollen starch was prepared by heating a 15% aqueous dispersion with agitation for 1 hour at 65° C. Excess water was removed by filtration. The gelatinized starch was prepared in a like manner at 85° C. Where the inclusion method of adding the monomer was used, it was incorporated by the solvent displacement method originated by Hermans and De Leeuw (3). The water in the gelatinized starch was displaced with methanol and the methanol displaced with the monomer to be used.

The British gum was made by stripping off water at 140° C. and then heating for 1 hour at 200° C. under nitrogen with strong agitation.

Irradiation. Irradiation was conducted in a Co⁶⁰ source at a dose rate of about 4×10^5 rep per hour. Preirradiated starch was prepared by irradiation of starch under vacuum in a tube fitted with a break-off tip. The monomer was added to the tube after irradiation and freed from air, using the freeze-thaw technique. Then the tube was sealed and the tip broken, thus allowing the monomer to saturate the starch. For starch irradiated in the presence of monomer, the materials were thoroughly mixed, charged to a tube, evacuated using the freeze-thaw method, and immediately irradiated.

Electron Spin Resonance. Trapped free radicals in irradiated starch were studied utilizing an electron paramagnetic resonance instrument (Varian Associates Type 4500) fitted with a 100-kc. field modulation, Hi-lo power microwave bridge, and a multipurpose specimen cavity. The instrument is stated to have an accuracy of $\pm 10\%$ and a minimum resolution of about 10^{12} spins per cc. Varian's 0.1% pitch mixed with potassium chloride calibration standard containing 10^{15} spins per cm. of length was used as the reference curve. Samples and standard were contained in quartz tubes, 4 mm. in i.d., in sufficient depth to fill the cavity.

The starch was irradiated under vacuum in borosilicate glass tubes, transferred to quartz tubes, and sealed under vacuum for scanning. Initial scanning was performed immediately after preparation and decay rate studies were made on these samples, allowing them to age at room temperature.

Isolation Methods. All reactions were terminated by pouring the mixture into warm water containing 0.1% hydroquinone. The solid products were collected on a filter, washed with water, and fractionated by extraction with suitable solvents. The aqueous filtrate was examined and any water-soluble product isolated.

Proof of Grafting. Grafting was proved by infrared and elementary analyses of the isolated products and of the fractions obtained by acid hydrolysis of the grafts. The general procedure was to determine the infrared spectra of the purified products, and if these spectra indicated grafting, elementary analyses were conducted on the grafts containing nitrogen and chlorine. The acetyl group content of the vinyl acetate grafted products was determined by saponification of the products with 0.5N NaOH, followed by neutralization with 0.5N HCl, using phenolphthalein as indicator, and back-titration with 0.05N NaOH.

Grafting was confirmed by analysis of the products of acid hydrolysis of the grafts. Hydrolysis was carried out by using 1% product in 0.5N HCl and refluxing for 2.5 hours. The resulting mixtures were then neutralized with 1N NaOH, and the soluble and insoluble fractions isolated for analysis. When the product was a graft, the infrared spectrum of the water-insoluble fraction showed the typical bands of glucose and those of the grafted monomer. In the case of physical mixtures, the insoluble fraction showed the spectrum of the corresponding homopolymer, since starch was completely removed by hydrolysis.

Graft Copolymers Obtained by Irradiation of Wheat Starch in Presence of Monomers. Because it is the most obvious approach, the initial studies were made on irradiation of mixtures of starch and vinyl monomers with and without additional components or treatment.

Table I shows the results of experiments with acrylonitrile. A ratio of 3 parts

of starch to 1 part of monomer by weight was used in all but the last experiment, where a one-to-one ratio was used.

Table I. Irradiation of Starch-Acrylonitrile and Starch-Vinyl Acetate Mixtures

Monomer	State of Starch	Diluent	Grafted Polymer, %	Homopolymer, %	Conversion, %
Acrylonitrile	As is ^a	None	31.2	0	93.5 ^b
	As is	None	33.1	0	99.5
	Swollen	None	16.9	14.5	95.5
	Gelatinized	None	23.6	0	68.5
	As is	H ₂ O	12.1	12.4	74.3
	As is	DMF	0	33	97
	As is	Acrylonitrile	0	96	96
Vinyl acetate	As is ^a	None	2.01	91.5	93.5 ^b
	As is	None	2.60	91.4	94.0
	Swollen	None	9.3	89.2	98.5
	Gelatinized	None	3.5	80.5	84.0
	As is	Dioxane	0	67.2	67.2

^a Reaction stopped immediately after irradiation.

^b Conversion is fraction of monomer converted to polymer.

In the first experiment, the reaction was stopped immediately after irradiation, while the rest of the reactions were allowed to stand for 24 hours at ambient temperature before termination. The total dose in all reactions was 8 Mrep.

It can be seen by comparing the first two reactions (Table I) that the reaction was about 95% complete at the end of the irradiation period. Essentially complete conversion was also obtained using this radiation dose. The per cent grafting represents the per cent weight increase observed in the starch samples.

Swelling the starch granules prior to irradiation increases the amount of water present and the viscosity of the medium. This caused undesirable formation of homopolymer and a consequent reduction in the degree of grafting. This result closely resembles that in which water is simply added before irradiation (fifth experiment, Table I). In these two reactions, about one half of the polymer formed was recovered as homopolymer, whereas, in the first two reactions, homopolymer could not be isolated.

Grafting could not be proved simply by extraction, because cross-linked or intertangled high molecular weight homopolymer remained in the starch. This made hydrolysis necessary to remove ungrafted starch. The infrared spectrum of the purified water-insoluble fraction was determined, and if the characteristic bands of both glucose and acrylonitrile were present, the product was considered to be a graft.

In the gelatinized starch experiment, the inclusion method of adding monomer was used. This reaction, conducted in the absence of water, led to the lowest conversion of monomer in this series. However, no homopolymer was isolated.

Adding a homopolymer solvent—*N,N'*-dimethylformamide—to the reaction, or increasing the concentration of acrylonitrile to equal that of starch, led to homopolymerization (sixth and seventh experiments, Table I).

Generally, the graft products of these reactions were infusible and insoluble in all the solvents tested. They did, however, make a clear, viscous, stable dispersion in dimethyl sulfoxide.

Table I presents the results of irradiation of mixtures of wheat starch and vinyl acetate. In this series, as in the previous one, a dose of 8 Mrep was used and the grafted products were hydrolyzed in order to obtain proof of grafting. It was

found that starch could be completely removed from intimate mixtures with poly(vinyl acetate) by acid hydrolysis. Consequently, the presence of the characteristic bands of glucose and vinyl acetate in the infrared spectrum of the purified, water-insoluble fraction of a hydrolyzed product was considered proof of grafting. The degree of grafting is low in comparison to acrylonitrile. Again it can be seen by comparing the first two experiments that the reaction is essentially complete at the end of the irradiation period. Also, the presence of homopolymer solvent-dioxane—lowers conversion and leads to homopolymer.

The reaction with swollen starch produced the greatest amount of grafted polymer and the largest conversion of monomer. This was probably due to the high viscosity of the medium, which caused reduction in the termination rate by immobilization of the polymeric free radicals produced by irradiation.

Although conversion is high in this vinyl acetate series, the degree of grafting achieved was low. This can be explained by the low solubility and lower polarity of the vinyl acetate in comparison to starch. Acrylonitrile, having much higher polarity, readily entered the starch structure and resulted in a high yield of grafted product. Comparable but opposite results were obtained by Cooper, Sewell, and Vaughan (2) in grafting vinyl monomers to natural rubber under similar conditions. Styrene and methyl methacrylate could be grafted easily to rubber, whereas grafting with acrylonitrile was difficult. As vinyl acetate produces highly reactive free radicals when irradiated, it will not graft to natural rubber (2). In this work the authors were able to achieve some degree of grafting of vinyl acetate to starch. No suitable solvent was found for these grafted products.

Electron Spin Resonance Studies of Free Radicals Produced by Gamma Irradiation of Wheat Starch. Because irradiation of the starch-monomer mixtures leads to cross linking and consequent insolubility, the effect of irradiation of the starch was investigated with the view of grafting vinyl monomers to the active sites created in starch by gamma irradiation. Starch is very sensitive to irradiation, and general degradative changes, including chain scission which leads to increased solubility in water, have been reported by Samec (5). The authors conducted electron spin resonance studies to determine the trapped, free radical concentration produced in starch by gamma irradiation and the rate of decay of such radicals. In these studies, starch was irradiated in the "as is" hydrated form, the azeotropically dried form, and as a type of British gum obtained by heat treatment.

Figure 1 presents the concentration of free radicals *vs.* the total dose. Removal of the bound water increases the total concentration of trapped, free radicals in the starch. The rates of formation of the trapped, free radicals are approximately equivalent, but the total dose necessary for equilibrium between the rate of formation and the rate of dissipation is greater for the drier starches. The equilibrium dosage is approximately 8 to 18 Mrep.

Figure 2 shows the decay rates of these trapped, free radicals. The rates are comparable for the samples aged under vacuum and are rather slow. The sample exposed to air has a considerably faster rate of decay, but still had a significant free radical concentration after 3 days of exposure, which indicates that the rate of the reaction of radicals with oxygen is slow. This agrees with results obtained by Kuri and Ueda (4), who made electron spin resonance studies of starch irradiated under vacuum and in the presence of NO, H₂S, and SO₂. The spectra obtained were the same, indicating the extreme nonreactivity of the starch free radicals toward these gases. In general, they found high polymers containing

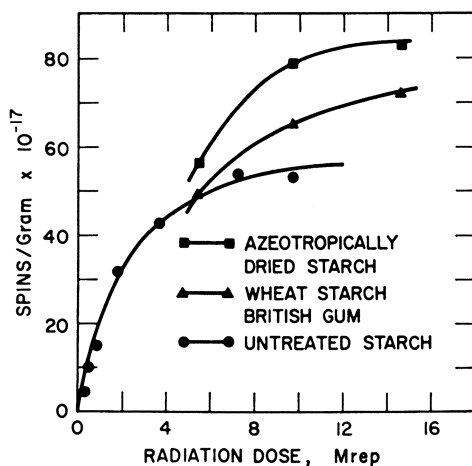


Figure 1. Trapped free radical concentration

hydroxyl groups to have this characteristic nonreactivity and ascribed it to inter- or intramolecular hydrogen bonds.

The net result is that the concentration of trapped, free radicals produced in starch by irradiation is high, and they are very stable. Consequently, there should be a sufficient supply to initiate a significant degree of vinyl grafting.

Graft Copolymers Prepared by Reaction of Monomers with Preirradiated Starch. Grafting initiated by preirradiated starch was studied with acrylonitrile vinyl acetate, and vinyl chloride. Reactions with liquid monomers were carried out by adding degassed monomer to the irradiated starch. Figure 3 shows the equipment used for this process. Grafting at two dose levels and at two temperatures was studied. A large excess of monomer was used in these experiments to ensure its availability for grafting.

Figure 4 shows results of grafting acrylonitrile to preirradiated "as is" starch. Increasing the total dose from 8 to 16 Mrep slightly increases the amount of grafting, and increasing the reaction temperature from 25° to 60° C. approxi-

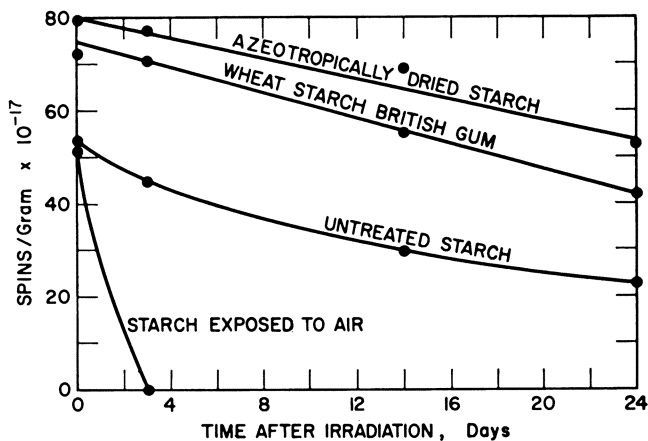


Figure 2. Trapped free radical decay

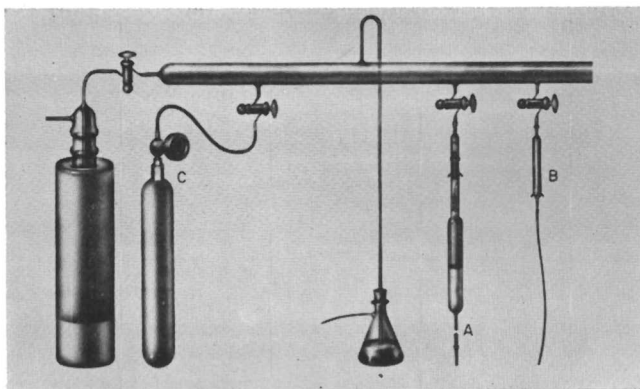


Figure 3. Apparatus for addition of monomers to pre-irradiated starch

- A. Starch addition port, sealed off
 B. Nitrogen sweep
 C. Vinyl chloride lecture bottle

mately doubles the amount of grafted acrylonitrile. Similar results were obtained by Ballantine and others (1) in grafting styrene to high density polyethylene (PE). The free radicals produced by irradiation of PE are trapped and immobilized within the crystalline regions of the polymer; consequently, they are practically inaccessible for reaction. However, raising the grafting temperature markedly increased the degree of grafting, and this they attributed to an increase in the rate of diffusion of the monomer into the radical-containing crystalline regions caused by the higher temperature. In the case of low density PE, because of its lower degree of crystallinity and greater chain mobility, increasing the temperature increased the rate of mutual destruction of the free radicals and thereby decreased the degree of grafting. The molecular mobility in starch is less affected by moderate temperature changes, because of hydrogen bonding. Unlike low density polyethylene, the rate of mutual destruction of free radicals in irradiated starch is not a serious deterrent to grafting in the temperature range employed. In grafting to starch, increasing the temperature increases the solubility and rate of diffusion of the acrylonitrile into the starch and, therefore, increases the degree of grafting. The optimum temperature for the greatest amount of grafting was not determined.

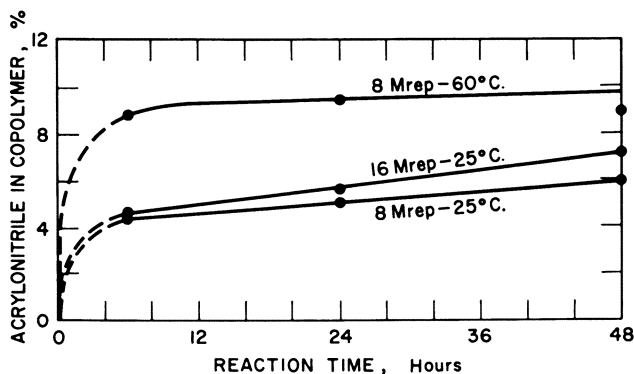


Figure 4. Grafting acrylonitrile to preirradiated starch

In these experiments the number of initiating sites is a set value and cannot be increased. The rate of mutual destruction, the rate of diffusion of the monomer into the starch polymer, and the propagation rate are the controlling factors in the degree of grafting. The diffusion rate would be the critical factor governing the number of starch to acrylonitrile bonds achieved. These factors determine whether a block or a graft copolymer will be obtained.

Figure 5 shows results of grafting vinyl acetate to preirradiated starch. The largest amount of grafting occurs in the first 6 hours, regardless of temperature or total dose. Also, the reactions did not appear complete at the end of 48 hours, when they were terminated. This is similar to the results just shown in grafting acrylonitrile to preirradiated starch. Again, increasing the temperature from 25° to 60° C. approximately doubles the degree of grafting. In this case, however, increasing the total dose from 8 to 16 Mrep made a significant difference in the degree of grafting. Since there is not a comparable increase in active sites nor were conditions changed so as to alter the rates of propagation, the structure of the starch must have been so altered as to increase the rate of diffusion of vinyl acetate into the starch.

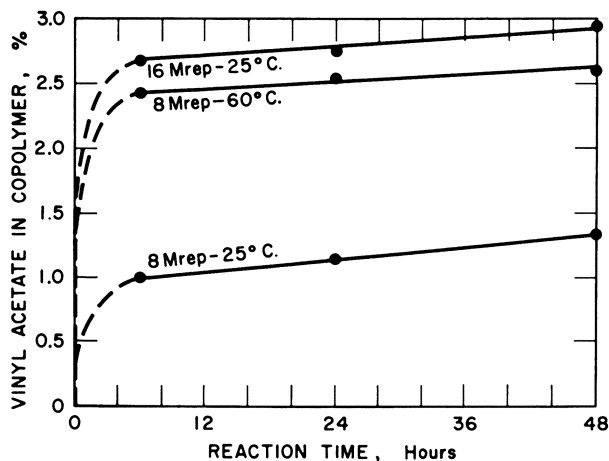


Figure 5. Grafting vinyl acetate to preirradiated starch

Table II presents the results of further work in grafting vinyl acetate to preirradiated starch. Again, excess monomer was used, and azeotropically dried, swollen, and gelatinized starches were irradiated, as well as starch "as is." In this case, the monomer was allowed to penetrate the starch for 48 hours before the temperature was raised. The starch received a total dose of 8 Mrep prior to treatment with monomer.

Comparison of the first two reactions shows that using a reflux cycle increased the degree of grafting by about seven times. The presence of additional water as in swollen and gelatinized starch greatly reduced the degree of grafting, because water prevents diffusion of vinyl acetate into the starch crystallites. The dry starch is tightly bonded, which reduces the diffusion rate of monomer, and results in a low yield of graft. The reaction products of vinyl acetate with preirradiated starch were extracted with acetone, but no homopolymer was extracted.

In a comparable series of reactions with acrylonitrile (Table II) the results

Table II. Grafting Vinyl Acetate or Acrylonitrile to Preirradiated Starch

<i>Monomer</i>	<i>State of Starch</i>	<i>Reflux, Hours^a</i>	<i>Extractable Starch, %</i>	<i>Grafted Polymer, %</i>
Vinyl acetate	As is	0	2.9	1.30
	As is	1	0	9.4
	Dry	1	0	1.03
	Swollen	1	0	0.05
	Gelatinized	1	0	1.03
Acrylonitrile	As	0	4.0	6.05
	As is	1	0.8	7.80
	Dry	1	14.4	2.5
	Swollen	1	32.2	28.5
	Gelatinized	1	62.5	24.3

^a Starch-monomer slurry allowed to stand at room temperature for 48 hours prior to refluxing.

are almost the opposite of those obtained with vinyl acetate. Reaction with irradiated swollen or gelatinized starch greatly increased the degree of grafting, whereas a reflux cycle made little difference. Dried starch again yielded a low degree of grafting because of the difficulty of monomer diffusion into the active sites. In using the method described earlier of presenting per cent graft, the results with gelatinized starch appear comparable to those with swollen starch. However, with gelatinized starch a large amount of ungrafted starch could be removed from the product by extraction with water; consequently, the concentration of acrylonitrile in the grafted product is well over 50%, the greatest amount achieved in these systems. The extracted material, after drying, was determined by infrared analysis to be ungrafted starch. The reaction product of preirradiated starch with acrylonitrile was extracted with dimethylformamide, but homopolymer was not obtained.

Attempts were also made to graft vinyl chloride to preirradiated starch. Figure 3 shows the apparatus used for these experiments. These reactions were performed by simply exposing the irradiated starch to an atmosphere of vinyl chloride. Grafting was proved by elementary and infrared analysis, as well as by hydrolysis of the isolated products. Table III shows the results of these experiments. Negligible grafting occurs, unless formamide is present. An equal weight of formamide was added and, in another experiment, 80% dioxane was added. The increased degree of grafting cannot be simply due to the solution of vinyl

Table III. Grafting Vinyl Chloride to Preirradiated Starch

<i>State of Starch</i>	<i>Diluent</i>	<i>Grafted Polymer, %</i>
As is	None	0.2
Swollen	None	0.1
As is	Dioxane	0.1
As is	Formamide	2.45

chloride. Dioxane appeared to dissolve a much larger amount than did the formamide, yet practically no grafting occurred in the reaction involving dioxane. Formamide causes a decrease in hydrogen bonding between starch chains, thus permitting more rapid diffusion of monomer to the reactive sites. Also, formamide, being slightly basic, may accelerate the propagation rate. This would account for the increased amount of grafted monomer.

Conclusions

The work presented in this article was of an exploratory nature, designed to study the factors involved in grafting vinyl monomers to wheat starch by gamma irradiation. Diffusion of monomer into the starch is the most important factor governing the degree of grafting, and this factor is dependent upon polarity of the monomer, the state of the starch, the temperature of reaction, and the presence of solvents or diluents. Polar monomers such as acrylonitrile, acrylamide, and acrylic acid can be grafted to starch rather easily. As the polarity decreases—vinyl acetate, styrene—it becomes more difficult to achieve grafting. Reaction with pre-irradiated starch is the preferred method of grafting, because it yields no homopolymer. The free radicals in irradiated starch are stable to moderate changes in temperature; consequently heat may be used to increase the degree of grafting. However, with monomers of low polarity, selective additives are needed to increase the solubility and rate of diffusion of the monomers to the active sites without destroying them. Although proof of grafting was obtained, systematic characterization of the copolymers was not carried out. Further studies are needed to determine the kind and extent of grafting required to obtain a product with significant commercial potential. This and grafting to the individual components of starch—amylose and amylopectin—will be the subject of future publications.

Literature Cited

- (1) Ballantine, D., Glives, A., Adler, G., Metz, D. J., *J. Polymer Sci.* **34**, 419–38 (1959).
- (2) Cooper, W., Sewell, P. R., Vaughan, G., *Ibid.*, **41**, 167–76 (1959).
- (3) Hermans, P. H., De Leeuw, A. J., *Kolloid Z.* **82**, 63 (1938).
- (4) Kuri, Z., Ueda, H., *J. Polymer Sci.* **50**, 349–59 (1961).
- (5) Samec, M., *J. Appl. Polymer Sci.* **3**, No. 8, 224–6 (1960).

RECEIVED October 6, 1961. Work done under contract with the U. S. Department of Agriculture and authorized by the Research and Marketing Act of 1946.

New Vistas in Anionic Polymerization

MICHAEL SZWARC

*Department of Chemistry, State University College of Forestry
at Syracuse University, Syracuse 10, N. Y.*

Anionic polymerization carried out under suitable conditions results in the formation of living polymers—i.e. species which may grow further, if a suitable monomer is present in the system. This characteristic feature of living polymers, which arises from the elimination of all the termination steps, permits the following: preparation of block polymers, polymers possessing two terminal functional groups, monodispersed polymers, etc.; studies of the thermodynamics of the propagation step—i.e. determination of ΔF , ΔH , and ΔS of the propagation for a high molecular weight polymer and for oligomers; determination of the absolute rate constants of homopropagation and of copolymerization. A review of methods and results is given.

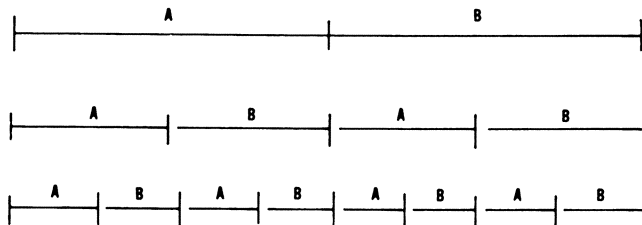
Anionic polymerization may be carried out under conditions preventing termination and the resulting polymers retain their ability to grow. We shall refer to such species as “living” polymers in contradistinction to those which are terminated and are known as “dead” polymers. The lack of termination has many important ramifications: it provides interesting syntheses, permits investigation of the thermodynamics of polymerization processes, and greatly simplifies studies of polymerization kinetics.

The synthetic opportunities arising from the existence of living polymers have been discussed in previous publications (19, 20, 21), hence in this article only a brief summary of the subject is given. Three important facets may be explored: preparation of block and graft polymers; preparation of polymers with the desirable functional end groups; and preparation of narrow molecular weight polymers.

The living ends of a suitable polymer may initiate polymerization of another monomer, and thus lead to the synthesis of block polymers free of homopolymers. For example, one prepares living polystyrene then adds pure methyl methacrylate to its solution and produces in this way a block polymer of styrene and methyl methacrylate (22). Actually, it is possible to produce living polymers with two active ends which can form a block polymer containing three segments—ABA.

If the living end of A initiates polymerization of B, and vice versa, one can

produce a whole spectrum of polymer molecules all having the same composition and molecular weight, but differing in the distribution of monomers along the chain, e.g.



Levy and Schlick (9) applied this technique to the system polystyrene-polyisoprene and produced polymers containing 3, 5, 7, and 9 blocks respectively.

The reactive end of a living polymer P_A attacks a suitable group on a dead polymer P_B and grafts P_A on P_B as shown by Schreiber (15), who grafted living polystyrene on dead poly(methyl methacrylate). Such a procedure may lead to cross linking or to the formation of a loop, if both ends of the living polymer are active. Other block polymers prepared by this technique are: polymers of styrene and ethylene oxide (14), polymers of styrene and dimethylsiloxanes (13), and polymers of styrene and vinylpyridine (16).

The presence of living ends permits the addition of desirable functional end groups to the polymer molecule; carboxylation introduces carboxyl groups; addition of ethylene oxide produces hydroxyl groups, etc. Polymers possessing two living ends are transformed in this way into bifunctional macromolecules which may be used for further synthetic work. Polystyrene terminated by carboxyl groups may be condensed with nylon terminated by amino groups to form a block polymer of polystyrene and nylon.

Whenever the initiation of polymerization is fast and termination is eliminated, monodispersed polymers may be formed by slow addition of monomer to a well-stirred solution of low molecular weight living polymers. This technique, suggested by the author, was developed by McCormick and Brewer (12), Bywater and Worsfold (17), Wenger (27), and others. Polymers of the narrowest molecular weight distribution were actually produced by this method.

Other synthetic possibilities provided by the living polymer technique may permit syntheses of star-shaped polymers, uniform networks of cross-linked polymers, regular branched polymers, etc.

Thermodynamic Studies

The thermodynamic studies of living polymers stem from the fact that these species retain their ability to grow by adding further monomer molecules and, therefore, in accordance with the principle of microscopic reversibility, they should also degrade into lower polymers and monomer. It follows that a solution of living polymer must come to equilibrium with its own monomer. If k_p denotes the rate constant of propagation and k_d the rate constant of depropagation, then the following equation describes the state of equilibrium:

$$k_p \sum_{n_0}^{\infty} P_n^* \cdot [M]_e = k_d \sum_{n_0+1}^{\infty} P_n^*$$

Here P_n^* denotes a living n -mer, $[M]_e$ the equilibrium concentration of the monomer, and n_0 the minimum size of a living polymer. $P_{n_0}^*$ represents therefore, the living n -mer which may grow, but which cannot degrade spontaneously.

For high molecular weight polymers, $\sum_{n_0}^{\infty} P_n^* \approx \sum_{n_0+1}^{\infty} P_n^*$ and, hence in such a system $[M]_e \approx k_d/k_p = K_e^{-1}$, where K_e denotes the equilibrium constant of the propagation step. This equilibrium constant, like any thermodynamic entity, is independent of the reaction mechanism. The polymerization of living polymers proceeds by an anionic mechanism and the equilibrium constant, K_e , determined from the equilibrium concentration of the monomer, is derived from studies of an anionic system. Nevertheless, this value of K_e applies equally well to radical or carbonium ion polymerizations and more generally to any polymerization of a monomer, provided the structure of the polymer does not change with the type of reaction involved. Since $-RT \ln K_e$ gives the free energy change of the propagation step, and $d \ln K_e / dT$ leads to the respective ΔH of propagation, all the thermodynamic functions pertaining to the propagation step are determined by this simple technique. The studies of McCormick (11) and of Worsfold and Bywater (31, 32) illustrate applications of this method to such systems as α -methylstyrene-poly-(α -methylstyrene) and styrene-polystyrene. The results obtained for the system α -methylstyrene-poly(α -methylstyrene) are shown in Figure 1.

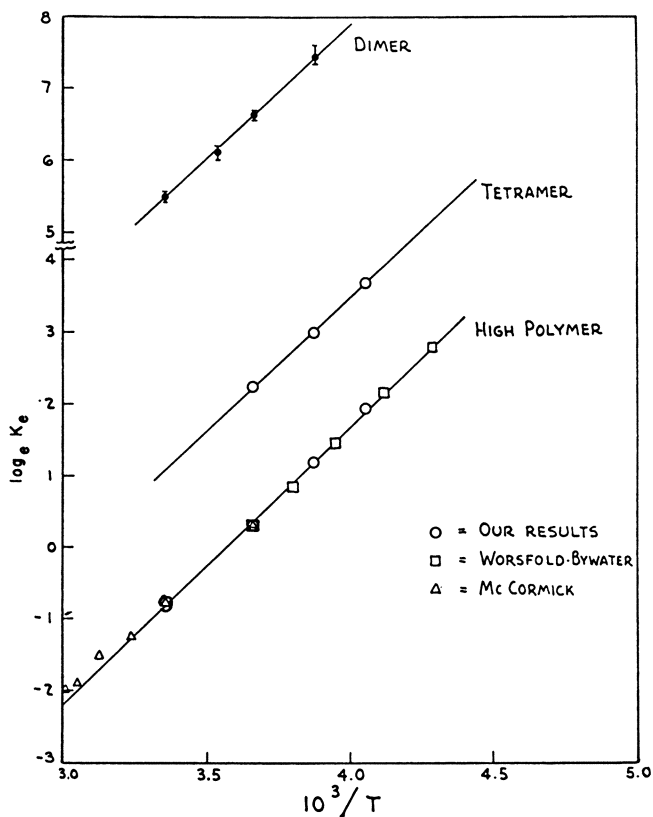
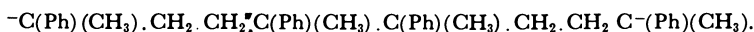


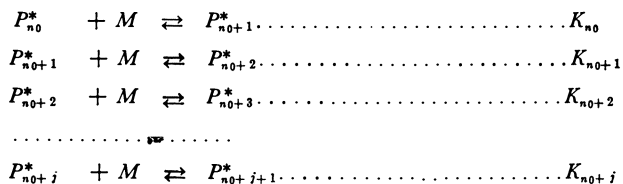
Figure 1. Equilibria between α -methylstyrene polymers and oligomers and monomeric α -methylstyrene

Equilibrium between a high molecular weight living polymer and its monomer exhibits some features which do not apply to a similar equilibrium pertaining to a low molecular weight living polymer. As stated above, any thermodynamic conclusion remains valid whatever path is chosen to perform the investigated change. In the reaction $P_n + M \longrightarrow P_{n+1}$, we may break the chain of the n -mer somewhere in the middle, insert the monomer unit and link it to the fragments, thus rebuilding the polymer molecule which would now contain $n + 1$ units instead of n . If the chain is sufficiently long, this process should not be affected by any changes taking place at its ends. Hence, the increase in free energy, ΔF , due to chain enlargement is the same whether radicals, ions, complexes or stable and unreactive moieties form the chain ends. However, if the chain is short, this argument no longer applies and the respective ΔF may depend on the size of the polymer molecule as well as on the nature of its end.

The equilibria between short, living polymers and their monomer were recently investigated in our laboratory (25, 26). The starting material was a solution of a well-defined living oligomer $P_{n_0}^*$, which could further add monomer units, but did not degrade. Increasing amounts of monomer were added to this solution, the system brought to equilibrium at the desired temperature, and the growing ends terminated by adding a drop of water. The equilibrium concentration of the monomer $[M]_e$ was then determined as a function of the variable $[M]_0$ (concentration of the initially added monomer) for a constant $[P_{n_0}^*]$. A plot of $[M]_e$ vs. $[M]_0$, (Figure 2) illustrates the results (25, 26) obtained for the system living α -methylstyrene "tetramer"— α -methylstyrene monomer at 0° C. The experimental curve passes through the origin, proving that the α -methylstyrene tetramer grows, but does not degrade—i.e. it is not a mixture of dimers, trimers, tetramers, etc. with a $P_n = 4$ —but a well-defined chemical species. Evidence, which is presented later, indicates the structure of this tetramer to be



The system resulting from addition of monomer to living oligomer, $P_{n_0}^*$, is represented by the following set of equations:



Such a system must fulfill the conditions given below:

$$\sum_0^{\infty} [P_{n_0+j}^*] = [P_{n_0}^*]_{\text{initial}}$$

$$[P_{n_0+1}^*] + 2[P_{n_0+2}^*] + 3[P_{n_0+3}^*] + \dots = [M]_0 - [M]_e$$

Let us now assume that $K_{n_0} = K_{n_0+1} = K_{n_0+2} = \dots$. Then, the investigated system is uniquely determined by K_{n_0} , $[P_{n_0}^*]_{\text{initial}}$, $[M]_0$, and $[M]_e$. In fact, as shown by Tobolsky (23), the following equation relates the variables listed above:

$$([M]_0 - [M]_e) / [P_{n_0}^*]_{\text{initial}} = K_{n_0} \cdot [M]_e \cdot (1 - K_{n_0} \cdot [M]_e)^{-1}$$

Hence, each point of the curve shown in Figure 2 determines K_{n_0} , since each one refers to a particular set of values for $[M]_0$, $[M]_e$, and $[P_{n_0}^*]_{\text{initial}}$ (the latter being, of course, a

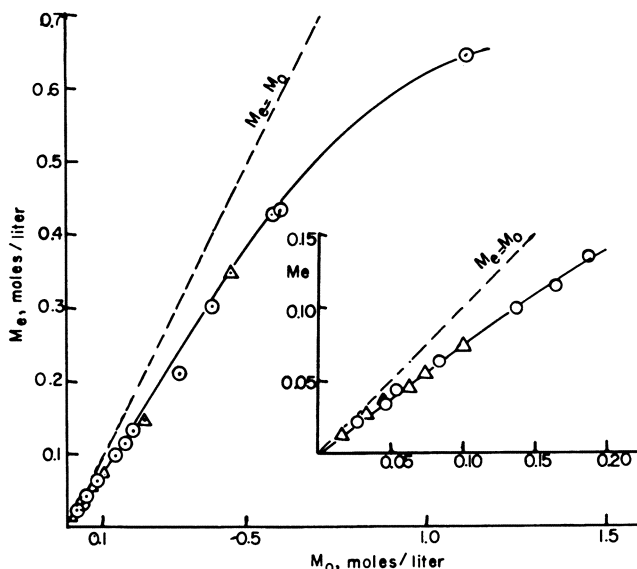
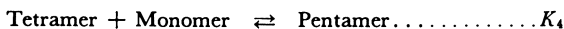
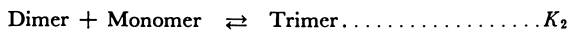


Figure 2. Equilibrium between living α -methylstyrene tetramer and α -methylstyrene monomer

constant). If our assumption about the constancy of K_{n_0+j} were correct, then the calculated K_{n_0} should be independent of $[M]_0$. The plot of K_{n_0} as a function of $[M]_0$, for the α MS-tetramer- α MS monomer system at 0° C. is shown in Figure 3. (MS is used for methylstyrene, S for styrene.) It shows that K_{n_0+j} 's are not constant; however, extrapolating the curve to zero concentration of M_0 gives the true value of K_{n_0} . Having determined K_{n_0} , we assume in turn that all the remaining K_{n_0+j} ($j \neq 0$) are constant and equal to K_{n_0+1} which, of course, must be different from K_{n_0} . Now, the relation between $[M]_0$, $[M]_e$, $[P_{n_0}^*]_{\text{initial}}$, K_{n_0} , and K_{n_0+1} can be derived, (25) and from it, K_{n_0+1} is calculated for each pair of values of $[M]_0$ and $[M]_e$, inserting for $[P_{n_0}^*]_{\text{initial}}$ and K_{n_0} their constant values. Thus, K_{n_0+1} is found to be a function of $[M]_0$ and, if its value is not constant, the correct K_{n_0+1} may again be derived by extrapolation to $[M]_0 = 0$. The procedure is repeated, and by inserting the values of K_{n_0} and K_{n_0+1} we find the value of K_{n_0+2} , and so on.

We investigated two systems by this method, namely, the living α -methylstyrene tetramer + monomer and the living α -methylstyrene dimer + monomer. Both the tetramer and dimer represent those oligomers which may grow, but not degrade. This means that the present tetramer is different from a tetramer obtained from the dimer. (Further discussion of this point is given below.)

The results lead to the equilibrium constants for the systems:



The values reported in our preliminary publication (25) are too low, since some corrections, introduced in the final calculations (26), were not taken into account in earlier work.

Extrapolating the apparent K_{n_0} to $[M]_0 \rightarrow \infty$ gives K_∞ —i.e. the equilibrium constant of propagation for a high-molecular weight polymer. The results obtained by this method agree excellently with those reported by other investigators

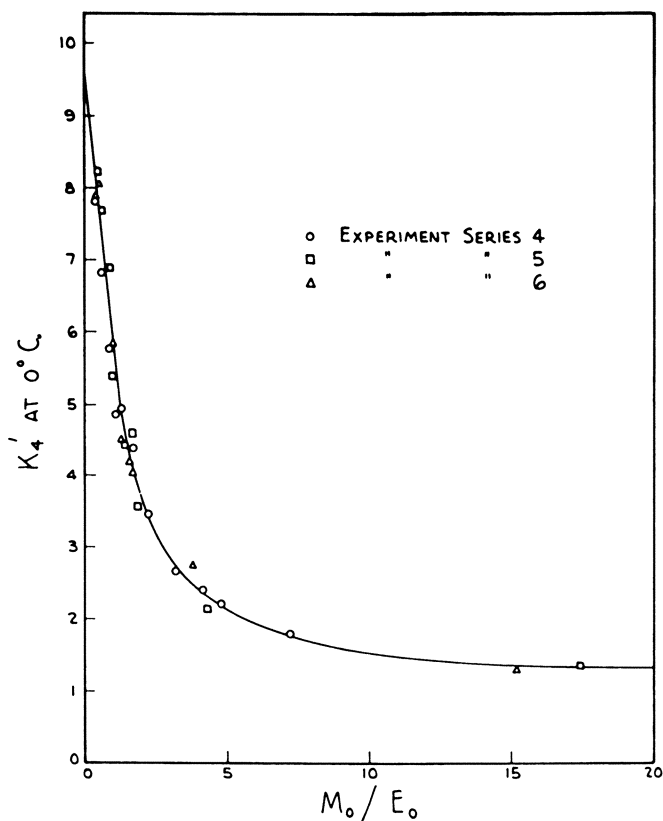


Figure 3. Equilibrium between the disodium salt of α -methylstyrene, tetramer, and monomer

(Figure 1). This value may also be obtained from an $[M]_e$ vs. $[M]_0$ plot by extrapolating to $[M]_0 \rightarrow \infty$. Such an asymptotic value of $[M]_e$ is equal to the reclusion. It should be emphasized that the same values were obtained for K_∞ from studies of both dimer and tetramer systems. It seems that the equilibrium constant for the system



is indistinguishable from K_∞ .

The temperature dependence of these equilibrium constants shows that all these processes correspond to the same ΔH , but differ in ΔS . This is a rather unexpected result.

I will not discuss here the significance of the numerical values of these equilibrium constants, or the nature of the factors which cause their change with molecular weight since this problem requires still further studies. I wish to emphasize, however, that the method described here for determining K_∞ , as well as the procedure leading to the evaluation of K_{n_0} , K_{n_0+1} , etc. become feasible because we are dealing with living polymers—i.e. the elimination of the termination process is essential in this treatment.

Before we leave this subject, I would like to discuss and compare the systems

living α -methylstyrene tetramer and living α -methylstyrene dimer. The tetramer is formed (8) when a diluted solution of α -methylstyrene (0.05 to 0.5M) reacts with sodium at room temperature. Figure 3 shows the progress of such a reaction and one notices that the conversion of the monomer to polymer is very rapid. In spite of this, the \overline{DP} of the initially formed polymer is only 4, and if the polymer is left for a longer time in contact with sodium, or still better with potassium or sodium-potassium alloy, a slow degradation to the dimer is observed (Figure 4).

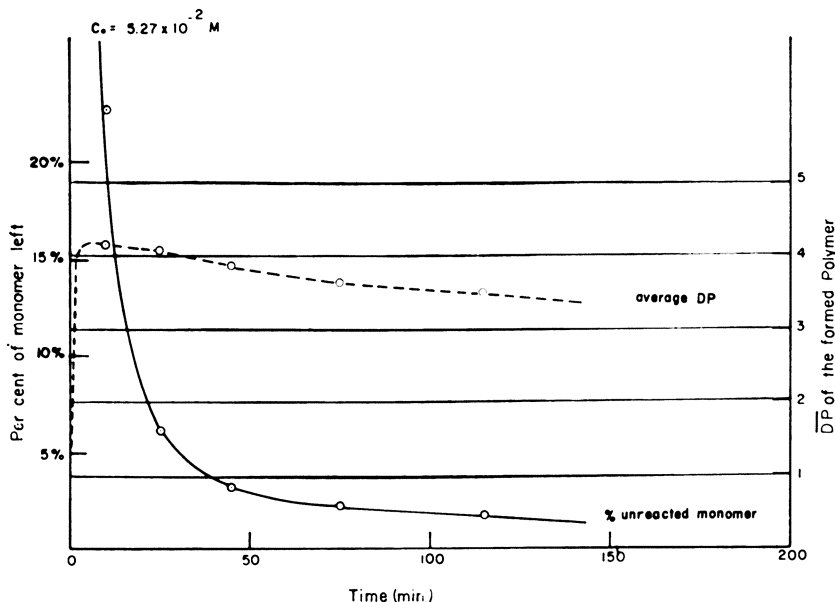
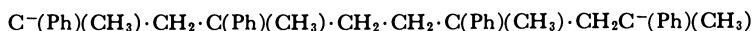
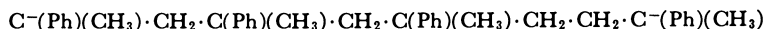


Figure 4. Reaction of α -methylstyrene with a sodium mirror

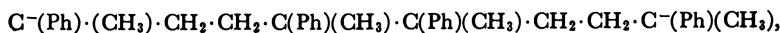
It is also possible to form the dimer directly by adding α -methylstyrene to a sodium emulsion in tetrahydrofuran (5). Its structure was examined and as predicted (19, 20, 21), it was shown (5) to be $C-(Ph)(CH_3)\cdot CH_2\cdot CH_2\cdot C-(Ph)(CH_3)$. Now, the addition of two equivalents of α -methylstyrene to this living dimer produces a living tetramer. However, the equilibrium concentration of the monomer in contact with such a tetramer is at least 10 times greater than that observed in the system containing the directly formed tetramer (26). It is obvious, therefore, that the living tetramer formed from the living dimer must have a different structure from that of the directly formed tetramer. The mode of preparation of the former implies that this is



or



The presence of head-to-tail linkages in such tetramers is responsible for the relatively high value of $[M]_e$, while the low value for $[M]_e$ (approximately zero) observed in the solution of the directly formed tetramer shows that its molecule does not contain the terminal head-to-tail linkages. This leaves the formula

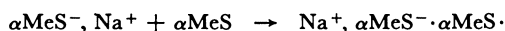


as the only possible structure for the directly formed tetramer. Here, therefore, is an example of structure determination of an oligomer by a thermodynamic argument.

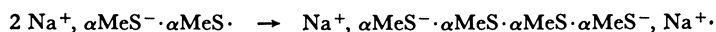
The mechanism of tetramer formation which is reported (8, 19) involves the following steps. The reaction of α -methylstyrene with sodium produces radical-ions,



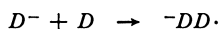
which rapidly add monomer-forming dimeric radical-ions,



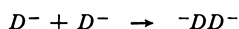
These dimeric radical-ions dimerize in turn, thus forming the tetramer



A more thorough study (10, 18) of the 1,1-diphenylethylene (*D*) system and its radical-ion (*D*⁻) proved that under these experimental conditions the reaction



is faster than the reaction



Apparently, a similar situation is encountered in the α -methylstyrene system.

Kinetic Studies

The lack of termination greatly simplifies studies of the kinetics of anionic polymerization. The living polymer may be prepared at the desired concentration, then mixed with monomer. A reaction then ensues and its progress can be followed by any suitable technique. Since termination is eliminated, the polymerization is first order with respect to monomer, and hence its concentration C_t is given by the usual equation:

$$C_t = C_0 \exp(-k_p[LE] \cdot t)$$

where k_p is the absolute rate constant of propagation and $[LE]$ the concentration of growing (living) ends. The method therefore permits direct determination of the absolute propagation rate constant.

Studies of such systems are reported in the literature. Worsfold and Bywater (28) determined k_p for the anionic homopolymerization of α -methylstyrene in tetrahydrofuran solution and Allen, Gee, and Stretch (1, 2) studied the polymerization of styrene in dioxane. Both groups utilized the dilatometric technique to follow the reaction and show the absence of termination.

In our laboratory, a flow technique was developed (6) which follows a very fast polymerization during as short a time as 0.1 second. The basic principle is very simple, although its successful application requires consideration of many technical details which are of the utmost importance to a reliable operation. The apparatus is shown in Figure 5. The solution of living polymers, of a known concentration of living ends, is introduced into a reservoir and the monomer solution into the other. Both solutions are forced into a T-shaped, three-way capillary stopcock which serves as a mixing chamber, then the reacting mixture flows through the vertical capillary into a beaker containing wet tetrahydrofuran. There termination takes place instantly, and the time of polymerization is given by the ratio of capillary volume to the rate of flow.

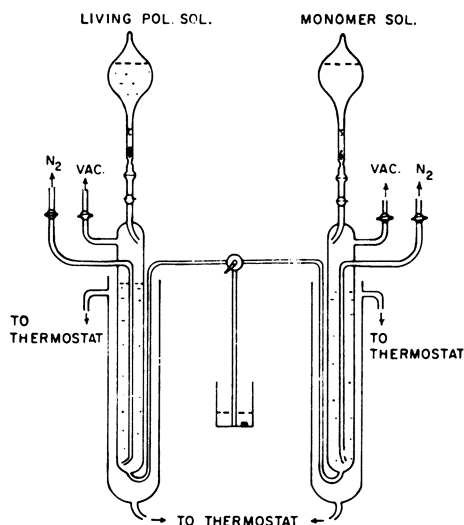
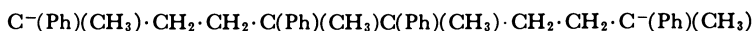


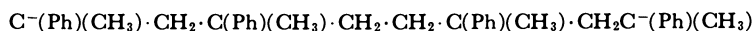
Figure 5. Flow apparatus for measuring rates of fast reactions

The method described here has many advantages. It allows measurement of the rates of very fast reactions at the very initial stage. In fact, most of our work is done with times of reaction between 0.05 to 1 second. A low ratio $[M]/[\text{living ends}]$ may be maintained in such experiments, which means that only a fraction of the growing ends adds one monomer unit, and a negligible fraction adds more than one. This is an important feature of our technique. In a conventional polymerization process, each growing end adds many monomer units, and hence one determines only an average propagation rate constant. In our system, however, the rate of addition of one unit is measured by extrapolating the observed rate to zero time. Moreover, since the technique of living polymers yields monodispersed polymers, or low molecular weight polymers of a definite and unique structure and molecular weight, we can investigate the problem of how the length of polymer molecules affects the propagation rate constant. Of course, one does not expect any detectable change between say a ten-mer and a hundred-mer, but it is plausible to expect significant changes in k_p at a low DP (2,3 or 4).

We are also in a position to change the structure of the starting material and to investigate how this affects k_p . For example, the α -methylstyrene tetramer



differs from the tetramer

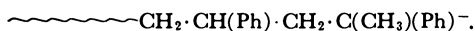


and one might expect different k_p 's for these isomers.

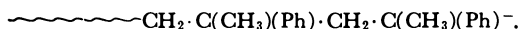
The most important advantage of our technique is the possibility of a direct determination of the absolute rate constants of copolymerization (7). If the living polymer is a poly-A, and a monomer B is the second component of the reacting mixture, then the initial rate determined in our system gives the absolute rate constant $k_{A,B}$ —the rate constant of the addition of monomer B to the polymer possessing unit A at its end. The rate constants for addition of α -methylstyrene to living polystyrene and styrene to living poly(α -methylstyrene) were determined

(1). Further examples of such reactions will be given and the results will be discussed.

Finally, we may produce a living polymer with a desirable end unit and a chosen penultimate unit; by adding one equivalent of α -methylstyrene to living polystyrene we get:



A similar addition to living poly(α -methylstyrene) yields



Different rate constants were found for the addition of styrene to these polymers (Table I), showing that the penultimate group affects the propagation rate constant.

Table I. Effect of Penultimate Unit Upon the Rate of Addition of Styrene to $\sim\sim\sim\alpha\text{MeS}^-$

T = 25° C., Solvent Tetrahydrofuran

System	k_{12} , Liter/Mole Second
$\sim\sim\sim\text{CH}_2\cdot\text{CH}(\text{Ph})\cdot\text{CH}_2\cdot\text{C}(\text{CH}_3)(\text{Ph})^- + \text{S}$	1500
$\sim\sim\sim\text{CH}_2\cdot\text{C}(\text{CH}_3)(\text{Ph})\cdot\text{CH}_2\cdot\text{C}(\text{CH}_3)(\text{Ph})^- + \text{S}$	1200

Let us consider some of the results obtained by the flow method. Figure 6 illustrates the homopolymerization of styrene (6). It is obvious that the reaction is first order with respect to monomer, even at 90% conversion, but the apparent first order rate constant seems to depend on the concentration of living ends. Figure 7 shows that the apparent k_p increases with decreasing concentration of living ends. A similar effect was observed in all the systems investigated in our laboratory. Its significance, however, is still obscure, although there are several explanations which might be suggested. One may argue, e.g. that the high rate, at low concentration of living ends, is due to the relatively high concentration of isolated ions, while the rate observed at higher concentration of living ends characterizes the growth of ion pairs. Studies of the conductivity of living polystyrene solution, carried out by Bywater and Worsfold (30) show however that the concentration of free ions is negligible even in a $10^{-3}M$ solution, and this forces us to abandon this approach. Indeed, any explanation based on the idea that the system involves two species remaining in equilibrium as described by the equation $X_2 \rightleftharpoons 2X$ or $X \rightleftharpoons Y + Z$, each growing with a different rate, must lead to a much less sharp curve than the one shown in Figure 7. An alternative explanation invokes an equilibrium between associated and nonassociated ends. This again demands a flatter curve than the one shown in Figure 7. In addition, it suggests an abnormal increase in the viscosity of the living polystyrene solution with concentration which is not observed. The association of polymers was observed (3) when end groups such as $-\text{COO}^-$, Na^+ or $-\text{CH}_2\text{O}^-$, Na^+ were present, and it is also of importance in hydrocarbon solutions of living polymers (29). [Similar observations were reported by M. Morton at various meetings.] However, the bulkiness of benzyl $^-$ ions and the diffuse character of their charge probably hinders the association of living polystyrene in tetrahydrofuran solution.

A few experiments were carried out with living polystyrene solutions containing sodium perchlorate or sodium tetraphenylboron (6). These salts had no effect on the rate of polymerization, although their concentration exceeded by

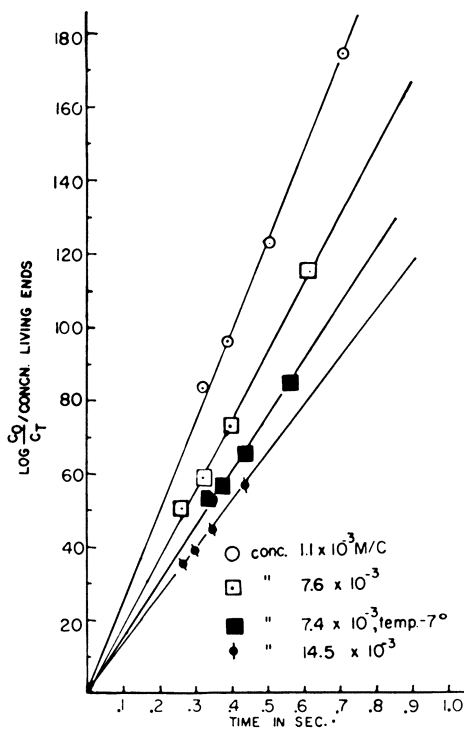


Figure 6. Rate of polymerization of living polystyrene at 25°C.

Effect of varying the concentration of living ends

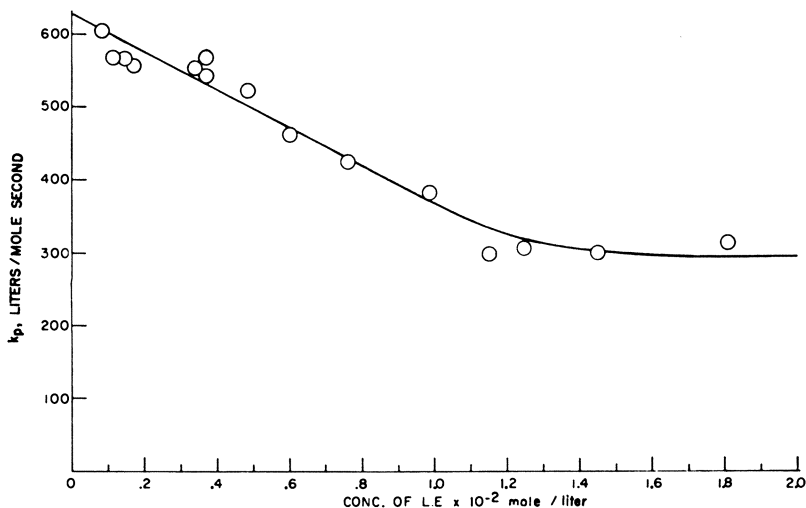


Figure 7. Dependence of k_p on the concentration of the living end in the anionic polymerization of styrene in tetrahydrofuran

a factor of 10 that of the living ends. We feel, therefore, that more work is needed to clarify the cause of the effect of concentration of living ends upon the rate of polymerization.

The activation energy of anionic propagation in the homopolymerization of styrene was determined to be about 1 kcal. per mole. This value refers to the reaction proceeding in tetrahydrofuran solution. The activation energy for the same reaction in dioxane was reported (1, 2) to be 9 ± 3 kcal. per mole. This is one of many examples which stresses the importance of a solvent in ionic polymerization.

Since k_p for the anionic homopolymerization of styrene in tetrahydrofuran solution is ~ 600 liters per mole second and the respective activation energy is only 1 to 2 kcal. per mole, the entropy of activation is substantially more negative (by about 14 eu.) than ΔS for a radical polymerization of styrene. It is likely that the additional decrease in the entropy of activation is due to immobilization of the counterion in the transition state in the middle between the last unit of the growing end and the new unit being added, i.e.



An even greater decrease in the entropy of activation (~ 18 to 20 eu.) is observed in the anionic polymerization of α -methylstyrene in tetrahydrofuran (28).

The nature of the counterion affects the rate of growth. The results obtained in tetrahydrofuran solution indicate that k_p decreases along the series Li^+ , Na^+ , K^+ , and Cs^+ (Table II). This was an unexpected result. Actually, work carried out in another laboratory (4) shows a reverse trend in dioxane. Obviously, the nature of the solvation shell must be of great importance. The discussion of this topic should be postponed, however, until more information is gathered.

Table II. Effect of Counterion on the Rate of Anionic Homopolymerization of Styrene in Tetrahydrofuran at 25° C.

$$[\text{LE}] = 5 \times 10^{-3}M$$

Counterion	k_p , Liter/Mole Second
Li^+	~ 600
Na^+	500
K^+	325
Cs^+	115

Figure 8 gives results of some copolymerization studies, namely, the addition of styrene to living α -methylstyrene tetramer and the addition of styrene to living poly(p -methylstyrene). Table III gives the propagation rate constants of some homopolymerizations and copolymerizations and the discussion of these values is interesting.

The $k_{A,B}$ values for addition of styrene, p -methylstyrene, and 2-vinylpyridine to living polystyrene demonstrate the importance of the polar character of the monomer. The addition of vinylpyridine is much faster than the addition of styrene, whereas addition of p -methylstyrene is slower. Hence, a decrease in the negativity of the $\text{C}=\text{C}$ bond enhances the addition (vinylpyridine as compared with styrene), its increase having the opposite effect (p -methylstyrene as compared with styrene). On the other hand, the change in the polarity of the ion has a less pronounced effect as shown by the $k_{A,B}$'s for the addition of styrene monomer to

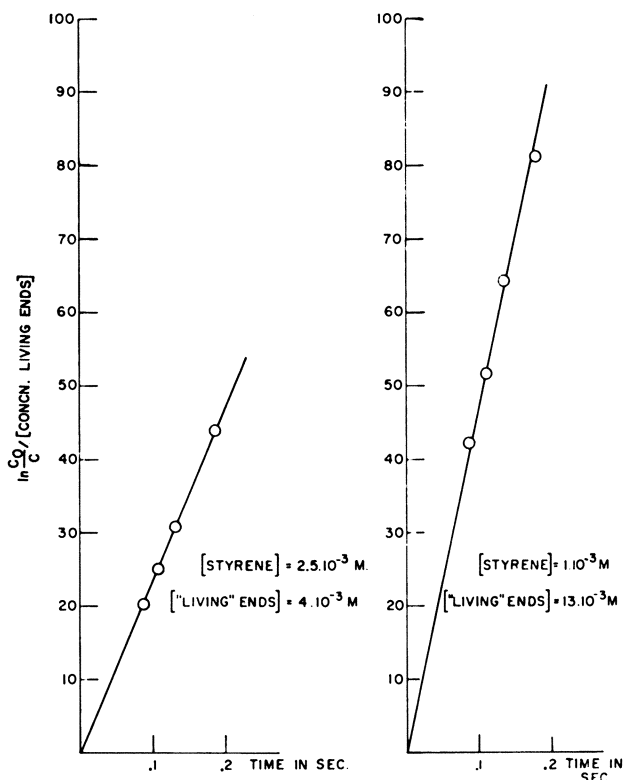


Figure 8. Copolymerization results
Addition of styrene to living poly(α -methylstyrene)

Table III. Anionic Homo- and Copolymerization in Tetrahydrofuran at 25° C.

Counterion Na⁺; extrapolated to 0 concentration of living ends

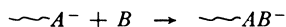
Growing anion, A ⁻	Monomer, B	k _{AB} , Liter/Mole Second
Styrene ⁻	Styrene	625
Styrene ⁻	α -Methylstyrene	27
Styrene ⁻	β -Methylstyrene	~200
Styrene ⁻	o -Methylstyrene	~400
Styrene ⁻	2,4-Dimethylstyrene	200
Styrene ⁻	2-Vinylpyridine	> 30,000
α -Methylstyrene ⁻	Styrene	1200
α -Methylstyrene ⁻	α -Methylstyrene	2.5
β -Methylstyrene ⁻	Styrene	1000
β -Methylstyrene ⁻	β -Methylstyrene	300
2-Vinylpyridine ⁻	Styrene	very low
2-Vinylpyridine ⁻	2-Vinylpyridine	4500

living poly(p -methylstyrene) and polystyrene but an enormous change is observed for 2-vinylpyridine⁻.

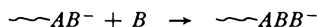
The lower value of k_{AB} in the addition of α -methylstyrene to living polystyrene reflects the effect of polarity and also the steric strain which is greater in this reaction than in the addition of styrene to living polystyrene. This steric strain is still greater in the addition of α -methylstyrene to living poly(α -methylstyrene) (compare $k_{\alpha\text{MeS, MeS}}$ with $k_{\text{S,S}}$). However, it is interesting to notice

that for this pair of monomers the decrease in the propagation rate constant amounts to a factor of 25; whereas a factor of about a million is found for the respective propagation equilibrium constants. This shows that the strain in the final state—i.e. in poly(α -methylstyrene) is much greater than the strain in the transition state describing the addition of α -methylstyrene to poly(α -methylstyrene). This point was emphasized earlier by Alfrey.

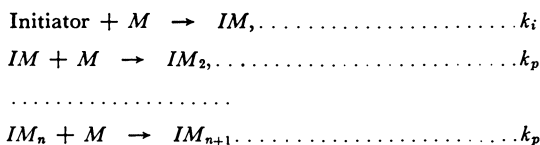
The described technique for determining $k_{A,B}$ in anionic copolymerization is limited to those reactions for which $k_{A,B}$ is not much smaller than $k_{B,B}$ —i.e. if the reaction



is not much slower than the reaction



If this condition is not fulfilled, another technique has to be applied. Such a technique was developed in our laboratory, and is useful in determining k_p/k_i , where k_p is the propagation rate constant and k_i that of initiation by an anion. It was pointed out (19) that if a polymerization is described by the equations



and termination is eliminated in such a process, then the initiator is never quantitatively used in the reaction. Denoting by f the fraction of consumed initiator, and by M_{total} and I_{total} the total amounts of monomer and initiator introduced in the system, one finds that the following equation relates them:

$$M_{\text{total}}/I_{\text{total}} = (k_p/k_i)[\ln(1-f)^{-1} - f] + f$$

In a copolymerization involving a slow step, one considers $k_{A,B}$ as k_i and $k_{B,B}$ as k_p , the concentration of $\sim\sim A^-$ as $[I]_{\text{total}}$, and the added monomer B corresponds to $[M]_{\text{total}}$. In this way, $k_{B,B}/k_{A,B}$ was determined for systems such as



to be (24) ~ 850 . Since $k_{B,B}$ for styrene homopolymerization is 600 liters per mole second, $k_{A,B}$ is calculated to be ~ 1.5 liters per mole second.

Acknowledgment

The author acknowledges the help given by his colleagues and students, and in particular he thanks M. Levy and J. Smid whose enthusiasm and hard work made these investigations a success. This work was supported by the National Science Foundation (Grant No. G14393) and the Quartermaster Corps (Grant No. DA-19-129-QM-1297).

Literature Cited

- (1) Allen, G., Gee, G., Stretch, C., *J. Polymer Sci.* **48**, 189 (1960).
- (2) Allen, G., Gee, G., Stretch, C., *Polymer* **2**, 151 (1961).
- (3) Brody, H., Richards, D., Szwarc, M., *Chem. & Ind. (London)* **45**, 1473 (1958).
- (4) Dainton, F., private communication.
- (5) Frank, C. F., *et al*, *J. Org. Chem.* **26**, 307 (1961).

- (6) Geacintov, C., Smid, J., Szwarc, M., *J. Am. Chem. Soc.* **83**, 1253 (1961); **84**, in press.
- (7) Lee, C. L., Smid, J., Szwarc, M., *Ibid.*, **83**, 2961 (1961).
- (8) Lee, C. L., Smid, J., Szwarc, M., *J. Phys. Chem.* in press.
- (9) Levy, Schlick, S., *Ibid.*, **64**, 883 (1960).
- (10) Levy, M., Feld, M., Szwarc, M., *Trans. Faraday Soc.* in press.
- (11) McCormick, H. W., *J. Polymer Sci.* **25**, 488 (1957).
- (12) *Ibid.*, **36**, 341 (1959); **41**, 329 (1959).
- (13) Morton, M., Rembaum, A., Bostick, E. E., *Ibid.*, **32**, 530 (1958).
- (14) Richards, D. H., Szwarc, M., *Trans. Faraday Soc.* **55**, 1644 (1959).
- (15) Schreiber, H., *Makromol. Chem.* **36**, 86 (1959).
- (16) Sigwalt, P., Fontanille, M., *Compt. rend.* **251**, 2947 (1960).
- (17) Siriani, R. F., Worsfold, D. J., Bywater, S., *Trans. Faraday Soc.* **55**, 2124 (1959).
- (18) Spach, G., Levy, M., Szwarc, M., *Ibid.*, in press.
- (19) Szwarc, M., *Makromol. Chem.* **35**, 132 (1960).
- (20) Szwarc, M., *Nature* **178**, 1168 (1956).
- (21) Szwarc, M., Levy, M., Milkovitch, R., *J. Am. Chem. Soc.* **78**, 2656 (1956).
- (22) Szwarc, M., Rembaum, A., *J. Polymer Sci.*, **22**, 189 (1956).
- (23) Tobolsky, A. V., *Ibid.*, **25**, 220 (1957); **31**, 126 (1958).
- (24) Ureta, E., Levy, M., Szwarc, M., unpublished results.
- (25) Vrancken, A., Smid, J., Szwarc, M., *J. Am. Chem. Soc.* **83**, 2772 (1961).
- (26) Vrancken, A., Smid, J., Szwarc, M., *Trans. Faraday Soc.* in press.
- (27) Wenger, F., *Makromol. Chem.* **34**, 143 (1960).
- (28) Worsfold, D. J., Bywater, S., *Can. J. Chem.* **36**, 1141 (1958).
- (29) *Ibid.*, **38**, 1891 (1960).
- (30) Worsfold, D. J., Bywater, S., *J. Chem. Soc.* **1960**, 5234.
- (31) Worsfold, D. J., Bywater, S., *J. Polymer Sci.* **26**, 299 (1957).
- (32) Worsfold, D. J., Bywater, S., in press.

RECEIVED December 4, 1961.

Cationic Polymerizations at Ultralow Temperatures

J. P. KENNEDY and R. M. THOMAS

Chemicals Research Division, Esso Research and Engineering Co., Linden, N. J.

The cationic polymerization of isobutene was studied at very low temperatures. Equipment was constructed, convenient for liquid phase experiments at temperatures as low as -190°C ., and a technique to lower the freezing points of the reactants was developed. Liquid isobutene polymerizes instantaneously under the influence of dissolved AlCl_3 even at -185°C . The relationship $\log DP$ vs. $1/T$ is linear in the region of -30° to -100°C . Below -100°C ., the Arrhenius-type plot starts to deviate from linearity and assumes a lesser slope. This effect is explained by differences in the activation energies of the various chain-breaking processes. The degree of polymerization of polyisobutene was found to vary with monomer concentration at -180°C ., showing a maximum at a monomer solvent mole ratio of 0.135. The bearing of low temperature experiments on the problem of water as cocatalyst in cationic polymerization is discussed.

The study, and also the technique, of the low temperature cationic polymerization of isobutene is relatively far advanced (4, 26, 29, 33-37). Significantly, liquid-phase polymerization of this monomer at a temperature as low as -180°C . has been reported (14) from this laboratory.

The study of cationic polymerization reactions at extremely low temperatures, which was undertaken and is described in this article, has great scientific significance. The dependence of polymer molecular weight on reaction temperature has long been recognized (8, 33) and has been at least qualitatively explained (28). For many systems, the plot of \log molecular weight vs. $1/T$ is a straight line which can be represented formally by an equation of the Arrhenius type. Such plots can be used to estimate the apparent activation energy of polymerization E_{DP} . However, if an Arrhenius plot is linear, it is so, generally, only in a certain temperature range (2) which must be determined experimentally. It was of interest to find out to what extent the linear Arrhenius relation holds for the isobutene- AlCl_3 system and to see how the slope of the plot of \log molecular weight vs. $1/T$ changes at very low temperatures.

The polymerization of isobutene initiated by aluminum chloride has been found to be too rapid for systematic kinetic investigation (14, 15). One usually effective means of slowing down fast reactions is to cool the reagents to very low temperatures. It was hoped that experiments at ultralow temperatures might slow down the polymerization reaction and thus open the door for systematic kinetic studies.

In addition, it was thought that low temperature experiments could shed some light on the problem of cocatalysis in carbonium ion-initiated polymerizations. Plesch and his school maintain that polymerization cannot be initiated, except in the presence of a suitable cocatalyst (24, 25, 29, 31). Water could act as such an agent. Other investigators (27), especially Russian workers (9-12, 22), claim that if the temperature is high enough and/or the dielectric constant of the medium is sufficiently large, no cocatalyst is required for polymerization. There is, however, some controversy about the reliability of these results. In a related area, Kern and Jaacks (20) have shown that for the cationic polymerization of trioxane the presence of a cocatalyst was not necessary. Thus, it appears that there is no general answer to the question whether a cocatalyst is necessary, and that every system must be scrutinized individually. The isobutene- AlCl_3 system has yet to be studied under conditions of extreme dryness.

It seemed possible that the cumbersome high-vacuum experimentation could be avoided and extremely anhydrous conditions achieved by conducting polymerizations at ultralow temperatures. The vapor pressure of water is 5×10^{-4} Torr. at -78°C . and 1.6×10^{-23} Torr. at -194°C . (13). It is difficult to conceive of moisture (liquid water) acting as cocatalyst at increasingly low working temperatures.

Experimental

Materials. The purity and analysis of isobutene, methyl chloride, and aluminum chloride have been described (16). Ethyl chloride gas (U.S.P. grade, 99.99% minimum purity, Matheson Co.) was further purified by scrubbing through Molecular Sieves (5A, Linde Co.) and BaO , and distillation into the dry box. Vinyl chloride (99.9% minimum purity, Matheson Co.) was distilled into the box, cooled to -78°C ., and filtered cold until free from solid matter. Propane gas (instrument grade and natural grade, Matheson Co.) was passed over Molecular Sieves and then condensed into the box.

Equipment. One objective of these investigations at ultralow temperatures was to develop an experimental technique convenient for a widened temperature range. This was necessary for fundamental kinetic studies.

The equipment used to establish and maintain convenient working conditions (Figure 1) consists of a stainless steel box equipped with a continuous electrolytic water analyzer and a temperature controller and recorder. Through a three-way valve (energized by a temperature controller connected to a thermocouple) liquid nitrogen can be injected into the cooling coils of an insulated vessel. The vessel holds a propane-isopentane mixture used as bath fluid. The amount of cooling liquid injected can be controlled so that any desired temperature can be maintained, down to as low as -190°C . Before an experiment was started, the moisture level in the box was reduced to a minimum by placing within the box a Dewar vessel filled with liquid N_2 . The water content of the N_2 gas used for sweeping the box was 1 to 3 p.p.m. However, the humidity in the box was around 100 p.p.m., apparently due to leakage through the rubber gloves, back-diffusion

from the vent, and adventitious organic matter (such as gaskets, paper, even fingerprints) which acts as a reservoir for water and slowly releases adsorbed moisture.

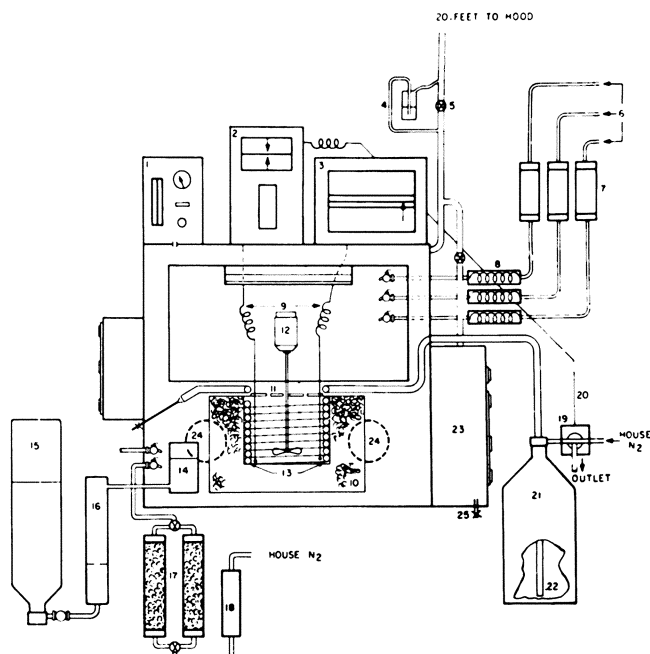


Figure 1. *Equipment used for polymerization experiments*

1. Electrolytic water analyzer (MEECO Instrument)
2. Temperature controller (West Instrument Co.)
3. Low temperature recorder
4. Mercury-filled safety valve
5. Main valve to hood
6. Copper tubing for gas inlet
7. Driers filled with BaO and Molecular Sieves
8. Condensers cooled to -78°C .
9. Thermocouples
10. Insulated container
11. Cover
12. Stirring motor
13. Cooling coils
14. Dry ice machine (Snow Man)
15. Extra dry CO_2
16. Activated charcoal drier
17. Driers filled with Molecular Sieves
18. Dry ice trap
19. Three-way valve
20. Connection between temperature controller and three-way valve
21. Dewar filled with liquid nitrogen
22. Copper tube for liquid nitrogen inlet
23. Air lock
24. Portholes for heavy-duty gloves
25. Multipurpose opening

Methods. Details of the catalyst solution preparation, catalyst concentration determination, general polymerization technique, product purification, and polymer molecular weight determination have been given (16).

Results and Discussion

Lowering the Freezing Points. A number of problems had to be solved before systematic experimentation could begin. Heretofore, the polymerization of isobutene had generally been carried out in methyl chloride diluent, which is also the vehicle for the AlCl_3 catalyst (14, 16, 33-37). Because of its comparatively high dielectric constant of 17.7 at -78°C . (18), methyl chloride provides the milieu necessary for the ionic species involved in the polymerization. Unfortunately, the freezing point of methyl chloride is relatively high (-98°C .), and this sets a lower limit on the polymerization temperature.

To carry out investigations at ultralow temperatures, a suitable low-freezing substitute for methyl chloride had to be found. Ethyl chloride, having a rather low freezing point (-138.7°C .) and a sufficiently high dielectric constant of 16.75 at -78°C . (23), seemed the logical first choice. Semiquantitative experiments showed that complicated chemical reactions occur when AlCl_3 is refluxed with ethyl chloride under dry nitrogen and massive amounts of HCl are evolved. Simultaneously, the liquid phase darkens from yellow to dark red and the viscosity increases, the liquid gradually becoming oily. The reactions between alkyl chlorides and AlCl_3 have been investigated and reported on extensively (1, 5, 32); however, discussion of the published information is outside the scope of this article.

To avoid complications, AlCl_3 catalyst solution was prepared under mild conditions. The salt was dissolved in ethyl chloride overnight at -78°C . A faintly yellow solution was obtained. Preliminary experiments showed that such a solution readily polymerizes isobutene. It was also observed that these solutions can be supercooled to about -150°C . without precipitation or freezing-out of AlCl_3 . At lower temperatures, however, the solution solidifies.

In the search for a solvent or solvent mixture for the catalyst to permit liquid phase polymerization below -150°C ., a number of low-freezing alkyl chlorides were tested. Some of the compounds evaluated showed low freezing points (*n*-butyl chloride, -122.8°C .; ethylhexyl chloride, -135°C .) but could not be used because they became too viscous, when cooled. Mixtures of AlCl_3 in ethyl chloride with hydrocarbons could not be used because the AlCl_3 was precipitated immediately on mixing. However, when $\text{AlCl}_3\text{-C}_2\text{H}_5\text{Cl}$ solutions were mixed with increasing amounts of liquid vinyl chloride, no precipitation occurred. Significantly, such mixtures could be cooled down to liquid nitrogen temperature without freezing, although they did become more viscous.

Incidentally, pure vinyl chloride is a poor solvent for AlCl_3 . When 1.50 grams of AlCl_3 was placed in contact for 2 hours with 160.5 grams of boiling vinyl chloride under dry nitrogen and then filtered, only 0.012 weight % of AlCl_3 went into solution. When the slightly yellow solution was quickly added to 100 ml. of isobutene stirred at -78°C ., only a few per cent of low molecular weight (oily) products were formed.

Experiments were conducted in the hope of lowering the freezing point of isobutene (-140.7°C .) by admixing inert "antifreezes." It was found that with increasing amounts of liquid propane (natural grade) the freezing point of isobutene can be depressed to the vicinity of -190°C .

The development of a suitable deactivator or quenching agent for the catalyst was also mandatory. Meaningful data can be obtained only if the polymerization is stopped at the preselected temperature. It was found that dilute solutions of 1-propanol in propane possess good viscosity properties even below -160°C .

Accordingly, these mixtures were used for deactivating the catalyst.

Polymerization at -145°C . Experiments were run to determine the temperature range where the $\log DP$ (degree of polymerization) vs. $1/T$ relation begins to become nonlinear. Cooled catalyst solutions were added to the monomer at various temperatures and the molecular weight of the polymer produced was determined.

The catalyst solution was prepared by dissolving AlCl_3 (1.85×10^{-2} mole per liter or 0.245 weight %) in ethyl chloride at -78°C . With a cooled, automatic pipet, 0.5 ml. of this solution was added dropwise to a duplicate series of isobutene-propane mixtures at -50° , -78° , -100° , -125° , and -145°C . The monomer concentration was 0.088 mole fraction (1.267 moles per liter) of isobutene. (Although the volume concentration is strictly valid only for -78°C ., it can be used over the whole temperature range without significant error.) Polymerization occurred instantaneously upon introduction of the catalyst at every temperature. The polymer was precipitated as a mushy white conglomerate. After deactivation of the catalyst and evaporation of unreacted gases, the molecular weight of the unfractionated polymer in each instance was determined.

Figure 2 shows the dependence of $\log DP$ of polyisobutene on the reciprocal temperature. The plot starts to deviate from linearity around -100°C ., then bends over to assume a lesser slope. The corresponding over-all activation energies are -3.54 and -0.22 kcal. per mole, respectively. Substantially identical trends

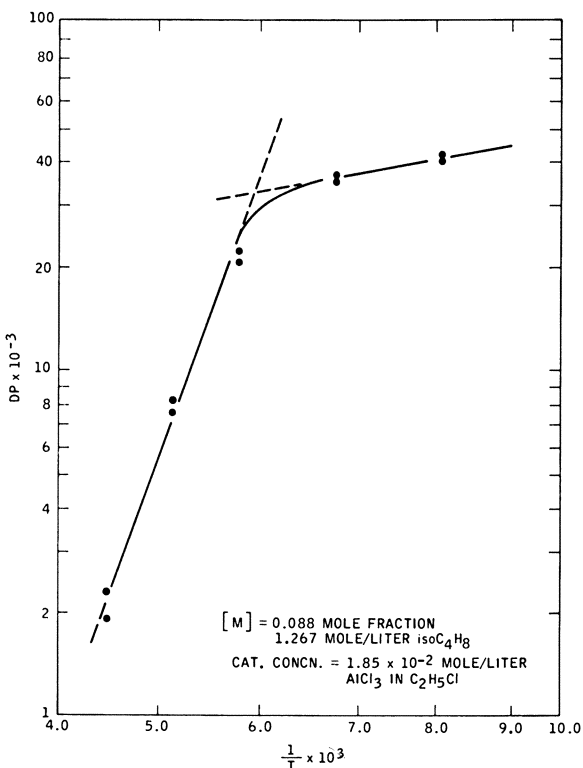


Figure 2. Temperature dependence of DP of polyisobutene in propane solvent

in DP dependence on temperature have been demonstrated in these laboratories in a great number of related experiments (18).

A possible explanation of this phenomenon is that the viscosity of the system at low temperatures increases to such an extent that the supply of monomer units to the active carbonium ion becomes rate-determining. At higher temperatures, the amount of monomer furnished by diffusion which has been calculated (17), is probably more than enough to supply the propagating center. However, at very low temperature the viscosity of the medium can increase to such an extent that diffusion—i.e., monomer depletion—becomes a rate-determining (and DP -determining) factor.

This explanation could be expanded on the basis of changes in the individual activation energies at low temperatures. The apparent activation energy E_{DP} which determines the slope of the $\log DP$ vs. $1/T$ plot is a combination of a set of different E 's. A number of elementary steps, such as propagation, transfers, termination, and their relation to each other, influence the magnitude of E_{DP} . The linear plot over the range -30° to about -100° C. suggests that the contribution of the activation energies of different chain-breaking processes to the apparent activation energy remains the same in this region. It can be expected, however, that the relative contributions will change with temperature. The other alternative, that only one type of chain-breaking process occurs, is unlikely.

Plesch (30) has suggested that at these very low temperatures, the DP -determining function is the ratio of rate of propagation to rate of monomer transfer (or k_p/k_m). Thus, the over-all or apparent activation energy would be given by the difference in respective activation energies—i.e., $E_p - E_m \cong 0.2$ kcal. per mole.

Polymerization below -150° C. Experiments conducted at -145° C. brought to light no appreciable effect of temperature on the velocity of polymerization. Subsequently, an attempt was made to lower the reaction temperature further. It was hoped that, at some temperature, the rate of reaction would become such as to be more amenable to systematic kinetic investigation. By use of special techniques it was possible to depress the liquid phase reaction temperature to -185° C. Even at this low temperature, the reaction rate did not decrease to an observable degree.

A representative experiment was carried out as follows.

Catalyst was prepared by dissolving 0.566 gram of $AlCl_3$ in a mixture of 20.6 grams of ethyl chloride and 42.8 grams of vinyl chloride (7.1×10^{-2} mole of $AlCl_3$ per liter at -78° C.). This solution was frozen with liquid nitrogen and then added in one lump to a stirred mixture of 17.7 grams of isobutene in 268.0 grams of propane at -185° C. (isobutene, 0.702 mole per liter at -78° C.). Shortly after its introduction, the frozen catalyst was broken up by a Teflon stirrer, and a sharp temperature increase ($\Delta T = \sim 17^\circ$ C.) resulted. This indicated the onset of exothermic polymerization. Simultaneously, the content of the reactor became milky. About 1 minute after catalyst introduction, a considerable amount of polymer had formed. This was deposited over the vessel, thermowell, and stirrer shaft. About 10 minutes later, a precooled 1-propanol-propane solution was added to the reactor and stirred until the slightly yellow color of the active catalyst disappeared (about 5 to 7 minutes). The unreacted gases were evaporated and the amount of polymer formed and its molecular weight determined. The yield was 85% of a polymer of DP 21,400.

The catalyst concentrations used in these ultralow temperature experiments are comparatively high. This might be the reason why the molecular weights are rather low. Relatively concentrated solutions of catalyst are required, because the "threshold" concentration appears to increase with decrease in temperature.

Reaction rates at these very low temperatures are remarkably high. Visual observation did not reveal any reduction in rate of polymer formation, and polymerization was too rapid for measurement, even at -185°C . These observations are not too surprising in the light of the theoretical considerations proposed by Evans (6). According to this theory, propagation consists of a reaction between electrostatically satisfied molecules and positive ions. Such a reaction requires no, or only very little, activation energy; it is a process with a substantially monotonically decreasing potential energy curve. Of course, in view of the experimental evidence, the activation energy of initiation must be very low also. The isobutene molecule, carrying two electron-releasing groups on one double-bonded C atom, is polar. The congregation and alignment of polarized units, especially in a solvent of fairly high dielectric constant and at low temperatures, are conceivable. Under the attack of a suitable initiator, charge rearrangement occurs and thousands of molecules combine within a fraction of a second. The theoretical exothermicity of the polymerization has been calculated as 20 kcal. per mole, while that found experimentally is 12.8 kcal. per mole (3). Presumably, the difference is due to the energy required to overcome steric hindrance presented by the two methyl groups on the quaternary C atom.

In another series of experiments, changes in polymer molecular weight with initial monomer concentration were investigated at -180°C . The concentration of monomer was varied by dilution with propane, and the ethyl chloride-vinyl chloride mixture was used as polar solvent for the AlCl_3 catalyst.

A typical experiment consisted of the following.

A series of liquid isobutene-propane mixtures was prepared by condensing the gases at -78°C . and cooling them down to -180°C . Monomer concentrations at -78°C . were 4.45, 3.55, 2.55, 1.90, 1.25, and 0.60 mole per liter or 0.324, 0.262, 0.182, 0.135, 0.088, and 0.042 mole fraction, respectively. The AlCl_3 catalyst concentration was 1.77×10^{-2} mole per liter in ethyl chloride-vinyl chloride at -78°C . (0.373 gram of AlCl_3 in a mixture of 5.15 grams of $\text{C}_2\text{H}_5\text{Cl}$ and 10.7 grams of CH_2CHCl). After thermal equilibration, 2.0 ml. of the pre-cooled catalyst solution was introduced into each vigorously agitated monomer mixture. Polymerization occurred instantly, and the conversions were in the vicinity of 10%. After deactivation of the catalyst at -180°C ., evaporation of unreacted gases, and drying, the molecular weights of the products were determined. Table I shows the results.

Table I. Influence of Monomer Concentration on Polymerization of Isobutene at -180°C .

$[M]$ Isobutene/Solvent, Mole Fraction	$DP \times 10^{-5}$	$\ln \eta_{rel}/c$
0.324	1.36	8.590
0.262	1.75	10.12
0.182	2.10	11.38
0.135	2.17	11.65
0.088	1.80	10.38
0.042	1.75	10.12

The DP values are far below those anticipated from an extrapolation of linear data obtained between -35° and -100°C . Also, the DP is greatest at $[M] = 0.135$, which is similar to the situation found at -78°C . (16, 17). The DP values were calculated by means of Flory's empirical viscosity equation (7). Since the validity of Flory's equation in this region of high molecular weights has not been established, the molecular weights could be in error. For this reason, inherent viscosities are shown in the third column of the table.

These investigations might help to clarify the role of water as cocatalyst in cationic polymerizations. Obviously, liquid water cannot be considered as cocatalyst at these extreme temperatures. Uncertainty is introduced by the fact that traces of moisture in the catalyst solution might have been incorporated before or during cooling to very low temperatures. In other words, the "active" catalyst might have been formed before cooling. There is also a remote possibility that water from the dry box atmosphere could condense in so fine a state—in particles of down to molecular dimensions—that reaction with the $AlCl_3$ might result. Somewhat similar theories have been proposed by Plesch, Polanyi, and Skinner to explain peculiarities in their experiments (21).

There is no drastic reduction in the amount of polymer formed at these very low temperatures as would be expected if liquid water were needed as cocatalyst and consumed. Independent experiments show that water deliberately added to the monomer mixture does not either depress the degree of polymerization or augment the yield (19). Only a direct experiment executed under extreme dryness can furnish the final answer.

Literature Cited

- (1) Baddeley, G., *Quart. Revs. (London)* **8**, 355 (1954).
- (2) Benson, S. W., "Foundations of Chemical Kinetics," McGraw-Hill, New York, 1960.
- (3) Biddulph, R. H., Longworth, W. R., Penfold, J., Plesch, P. H., Rutherford, P. P., *Polymer* **1**, 521 (1960).
- (4) Biddulph, R. H., Plesch, P. H., *J. Chem. Soc.* **1960**, 3913.
- (5) Brown, H. C., Pearsall, H. W., Eddy, L. P., Wallace, J. J., Grayson, M., Nelson, K. L., *Ind. Eng. Chem.* **45**, 1962 (1953).
- (6) Evans, A. G., Polanyi, M., *J. Chem. Soc.* **1947**, 252.
- (7) Flory, P. J., *J. Am. Chem. Soc.* **65**, 372 (1943).
- (8) Flory, P. J., "Principles of Polymer Chemistry," Cornell Univ. Press, Ithaca, N. Y., 1953.
- (9) Gantmakher, A. R., Medvedev, S. S., *Doklady Akad. Nauk S.S.S.R.* **106**, 1031 (1956).
- (10) Gantmakher, A. R., Medvedev, S. S., *Zhur. Fiz. Khim.* **23**, 516 (1949).
- (11) *Ibid.*, **26**, 175 (1952).
- (12) Gantmakher, A. R., Medvedev, S. S., Lyudvig, E. B., *Doklady Akad. Nauk S.S.S.R.* **127**, 100 (1959).
- (13) International Critical Tables, Vol. III, p. 385, McGraw-Hill, New York, 1928.
- (14) Kennedy, J. P., Thomas, R. M., *J. Polymer Sci.* **45**, 229 (1960).
- (15) *Ibid.*, **46**, 233 (1960).
- (16) *Ibid.*, p. 481.
- (17) *Ibid.*, **49**, 189 (1961).
- (18) Kennedy, J. P., Thomas, R. M., International Symposium on Macromolecular Chemistry, Montreal, Canada, 1961.
- (19) Kennedy, J. P., Thomas, R. M., Linden, N. J., unpublished data, 1961.
- (20) Kern, W., Jaacks, V., *J. Polymer Sci.* **48**, 399 (1960).
- (21) Landolt-Börnstein, Eucken, E. A., "Physikalisch-Chemischen Tabellen," 5th ed., E.g. III, p. 1961, Springer, Berlin, Germany, 1936.
- (22) Lipatova, T. E., Gantmakher, A. R., Medvedev, S. S., *Doklady Akad. Nauk S.S.S.R.* **100**, 925 (1955).
- (23) Longworth, W. R., Plesch, P. H., *J. Chem. Soc.* **1959**, 1618.
- (24) Longworth, W. R., Plesch, P. H., Rutherford, P. P., *Doklady Akad. Nauk S.S.S.R.* **127**, 97 (1959).
- (25) Longworth, W. R., Plesch, P. H., Rutherford, P. P., *Proc. Chem. Soc.* **1960**, 68.
- (26) Norrish, R. G. W., Russel, K. E., *Trans. Faraday Soc.* **48**, 91 (1952).
- (27) Okamura, S., Higashimura, T., *J. Polymer Sci.* **21**, 289 (1956).
- (28) Pepper, D. C., *Quart. Revs. (London)* **8**, 88 (1954).
- (29) Plesch, P. H., *J. Chem. Soc.* **1950**, 543.
- (30) Plesch, P. H., Linden, N. J., private communication, 1961.
- (31) Plesch, P. H., Polanyi, M., Skinner, H. A., *J. Chem. Soc.* **1947**, 257.
- (32) Thomas, C. A., Moshier, M. B., Morris, H. E., Moshier, R. W., "Anhydrous Aluminum Chloride in Organic Chemistry," Reinhold, New York, 1941.
- (33) Thomas, R. M., Sparks, W. J., Frolich, P. K., Otto, M., Müller-Cunradi, M., *J. Am. Chem. Soc.* **62**, 276 (1940).
- (34) Zlamal, Z., Section III, Symposium on Macromolecular Chemistry, Wiesbaden, Germany, 1959.

- (35) Zlamal, Z., Ambroz, J., Ambroz, L., *Chem. listy* **49**, 1506 (1955).
- (36) Zlamal, Z., Ambroz, L., *J. Polymer Sci.* **29**, 595 (1958).
- (37) Zlamal, Z., Kazda, A., Section II, International Symposium on Macromolecular Chemistry, Moscow, U.S.S.R., 1960.

RECEIVED September 6, 1961.

Stereospecific Polymerization with Alkali Metal Organic Compounds

D. BRAUN, M. HERNER, and W. KERN

Organisch-Chemisches Institut der Universität Mainz, Germany, and Deutsches Kunststoff-Institut, Darmstadt, Germany.

Styrene and methyl methacrylate can be polymerized stereospecifically with alkylsodium, Alfin catalysts, and triphenylpotassium. These initiators are effective in heterogeneous systems while alkyl lithium derivatives are effective in a homogeneous medium. The various alkali organometallic derivatives and polar and nonpolar solvents used required different lower temperatures to give stereospecific polymers. The decrease in stereospecificity runs parallel to the increase in polymerization rate with rise in temperature. The surface of the catalyst plays an important part in determining the amount of crystalline polymer formed. The nature of the cation present and inorganic compounds like sodium chloride do not affect the stereospecificity of the polymerization reaction. Organolithium derivatives as associated ions promote the stereospecific polymerization of styrene. The degree of tacticity of crystalline polymers is determined by melting points, x-ray diffraction, and nuclear magnetic resonance spectra.

Since the discovery of stereospecific polymerization (17), numerous initiators and methods have been found which are suitable in influencing steric conditions during the polymerization of unsaturated and cyclic compounds.

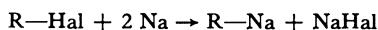
During the last few years, we have been seeking alkali organometallic compounds as initiators for the polymerization of styrene and methyl methacrylate (3, 4, 5, 13). Morton and Grovenstein (15) have already reported the suitability of organosodium compounds for the polymerization of styrene. By means of similar experiments, we have established that under appropriate conditions isotactic polystyrene is obtained with amylsodium, and its properties agree with those of the product obtained with Ziegler-Natta catalysts (13). Other alkali organometallic compounds such as the Alfin catalysts (16, 22) or triphenylpotassium (23) also

promote the stereospecific polymerization of styrene. Being insoluble, all these initiators were effective in heterogenous systems, and under definite reaction conditions, isotactic polystyrene is obtained also with lithium organometallic compounds in a homogeneous medium (3, 12). Hence, we have here a very interesting class of initiators for stereospecific polymerization which has been little investigated.

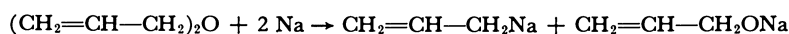
Polymerization of Styrene with Sodium and Potassium Compounds

The alkylsodium compounds can be prepared by various methods:

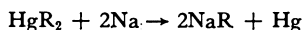
1. From alkyl halides and metallic sodium



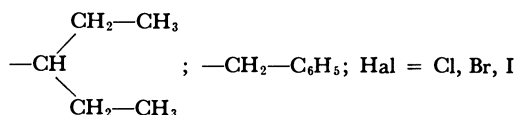
2. By cleavage of suitable aliphatic ethers—e.g., diallyl ether with sodium



3. From mercury dialkyls and sodium



R = $-CH_2-(CH_2)_n-CH_3$ ($n = 1$ to 14); $[-CH_2-\underset{\substack{| \\ CH_3}}{CH}-CH_2-CH_3]$;



The sodium used was in a very finely divided form, the diameter of the particles being about 5 to 25 microns. The organopotassium compounds are obtained in an analogous manner.

It is known from the work of Morton, on polymerization with Alfin catalysts, that the inorganic constituent of the catalysts (NaCl) plays an important part in the special effectiveness of these initiators. Hence, the question had to be examined if, likewise, the presence of inorganic substances is necessary for stereospecific polymerization with organosodium and -potassium compounds. As a result, it has been established that all the organometallic compounds derived as indicated in the above preparative methods facilitate the stereospecific polymerization of styrene in *n*-heptane. In addition, the nature and chain length of the residue R have no significant influence on the initiators. In fact, R can be linear or branched or aryl-aliphatic. Also, phenyl or triphenylmethylsodium yields isotactic polystyrene.

Crystallizable tactic polymers of styrene are obtained by treatment of the first formed amorphous polymers with boiling *n*-heptane. The evaluation of the degree of tacticity of the crystalline products is possible by melting points and x-ray diagrams. The polymerization temperature has a significant bearing upon the stereospecificity of the reaction. Using organosodium compounds only poorly crystallizable polystyrene was obtained at temperatures of 0° C. and above, whereas, at temperatures of -20° to -30° C. polymers were produced, which in their crystallinity were hardly differentiable from those products so obtained with trialkylaluminum-titanium halide mixed catalysts. Again, at sufficiently low temperatures practically no atactic portion can be extracted with boiling *n*-heptane, the extractable part increasing with a rise in polymerization temperature. The crystallinity and softening point of the nonextractable polymers decrease simultaneously (Table I, Figure 1,A).

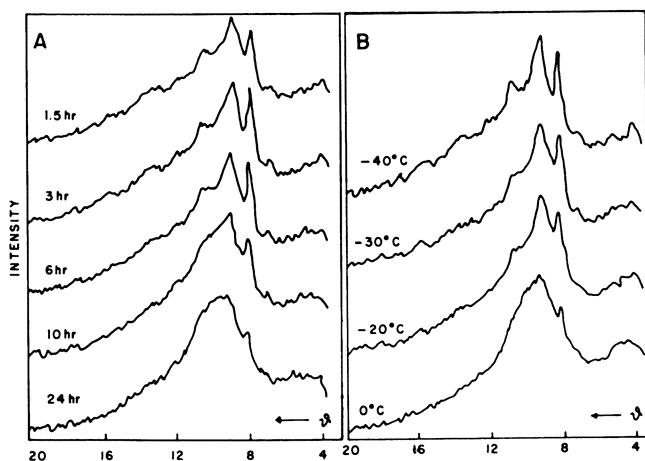


Figure 1. X-ray diagram of crystalline polystyrene obtained from reaction using *n*-amylsodium-NaCl

A. At different polymerization times
B. At different temperatures

Table I. Polymerization of Styrene with *n*-Amylsodium-NaCl at Different Temperatures

[Styrene, 10.0 grams (0.09 mole); initiator 0.01 mole in 100 ml. of *n*-hexane; polymerization time, 4 hours]

Temperature, °C.	Yield, %	Crystalline Portion, % ^a		Softening Pt. after Cryst.	[η], ^b Cc./Gram	Crystallinity
		Monomer	Total poly- merizate			
-30	8.1	5.4	67.0	211	24.3	Very good
-20	12.5	8.1	65.3	209-210	22.7	Good
0	63.1	18.5	29.3	200-203	8.2	Poor
+10	86.5	1.3	1.5	200-202	7.0	Very poor
+20	94.0	1.1	1.2	198-203	6.4	Very poor

^a Crystallization by immersion of 1 gram of polymer in 50 ml. of boiling *n*-heptane for 4 hours.

^b Measured in toluene at 20.0° C.

Aliphatic hydrocarbons such as hexane or heptane were preferred as solvents for the stereospecific polymerization of styrene using the already mentioned initiators. Toluene can also be used as solvent, but in this case a lower polymerization temperature, about -40° C., is necessary to achieve good tacticity. Under similar conditions, considerably poorer crystallizable polymers were produced using Alfin-type catalysts; this fact was also confirmed by Williams (23) and Morton (16).

If conditions are held constant, the polymer yield increases with reaction time as expected, but the tacticity decreases with progressive conversion, as indicated by the decrease in crystallinity as shown in Figure 1, B. This effect can be explained from the covering on the catalytic surface during polymerization. A sterically uniform arrangement of monomeric units, which doubtless is conditioned by this surface, is not possible to the same extent as at the start of the polymerization, when the free surface is exposed. After being kept for four weeks at -10° C. with exclusion of air, the alkali metal organic initiators did not lose their properties or catalytic powers. Therefore, a change in the catalyst cannot be the cause of

lower stereospecificity. Likewise, a subsequent action of the catalyst upon the already formed isotactic polystyrene does not occur, as revealed by control tests. In general, the steric configuration of the isotactic polystyrene is very stable and is resistant to many reagents, which normally racemize low molecular weight optically active compounds (6).

Potassium and rubidium alkyls behave alike when used as polymerization initiators (5); *n*-amylpotassium, *n*-octylpotassium, *n*-hexadecylpotassium, and benzylpotassium all produce tactic polystyrene. However, an astonishing fact is that to achieve the same stereospecificity, the polymerization in *n*-hexane must be conducted at a temperature of -60° to -70° C. with potassium initiators; in the case of dodecylrubidium, a lower temperature of -80° C. is necessary, whereas with *n*-amylsodium a temperature of only -20° C. is required. The decrease in stereospecificity runs parallel with the increase in polymerization rate as temperature rises.

Mechanism of Stereospecific Polymerization of Styrene with Sodium and Potassium Alkyls

Doubtless, the surface of the initiators plays an important part in polymerization with alkyl metal alkyls. With progressive conversion, the crystallinity of the produced polystyrene decreases without significantly altering the molecular weight. On the other hand, if the amount of catalysts—the effective surface area—is increased and the reaction conditions are kept the same, the crystallinity of the polymerize remains constant up to a considerably higher conversion (Figure 2).

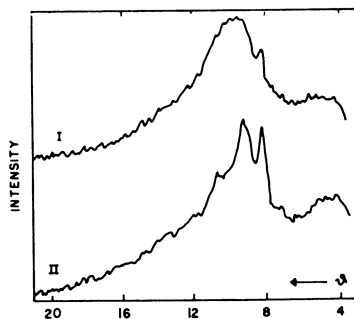


Figure 2. X-ray diagram of polystyrene obtained by polymerization with *n*-amylsodium-NaCl at -20° in *n*-hexane

I. Styrene, 0.1 mole; initiator, 0.01 mole; 25.75% yield
II. Styrene, 0.1 mole; initiator, 0.02 mole; 26.2% yield

This effect can be explained as due to the deposit of the stereoregulated polymer on the surface of the catalyst, which after a definite conversion is covered by the resulting polymer. It can be assumed, that the polymerization with alkali metal alkyls is of an anionic nature, whereby the steric regulation depends upon the orientation of the adding monomer on the solid surface of the catalyst. This agrees with the fact that neither the nature of the cation (Na^+ or K^+) nor the presence of inorganic materials like NaCl has any significant bearing on the stereo-

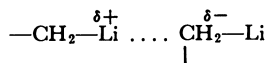
specificity of the reaction. Certainly, the quantitative differences between the various catalysts are based upon the different surface areas of the individual compounds.

The influence of the polymerization rate is important. Generally, tacticity decreases with an increase in reaction rate as shown by a lowering of stereospecificity with rise in polymerization temperature, and further by transition from a pure nonpolar solvent, hexane, to polar systems, perhaps by addition of toluene or ether. Hereby, polarization of the alkyl-metal bond as well as the rate of polymerization increases. At the same temperature, polymerization in toluene proceeds more rapidly than in *n*-hexane, with the tacticity of polystyrene decreasing with a rise in the polymerization rate. By decreasing the polymerization rate—that is, by lowering the temperature—good crystallizable polystyrene is obtained, even when toluene is used. In this case, the resulting polymer is dissolved and the catalyst is the only heterogeneous part, whereas in hexane, the polystyrene is insoluble throughout polymerization.

In contrast to the pure aliphatic alkylmetal derivatives, compounds like triphenylmethylpotassium also function stereospecifically at high polymerization temperatures (23), although the released anion due to possible resonance stability is less active as shown by the slower polymerization rate.

Polymerization with Lithium Compounds

In contrast to sodium and potassium alkyls, the organolithium compounds are soluble in hydrocarbons. The first conception of the mechanism of stereospecific polymerization was in connection with the presence of heterogeneous catalysts (9). Patat and Sinn (18) were the first to announce that stereospecific polymerization should also be possible in homogeneous media. However, their experiments did not demonstrate this as the temperatures employed were much too high (21). On the other hand, we ascertained (3) independently of Kern (12), that it was possible to conduct the stereospecific polymerization of styrene with *n*-butyllithium at about -30° C. in hydrocarbons. It is very important that the polymerization temperature not be too high. The appropriate temperature range for *n*-heptane is between -10° and -30° C. and for toluene about -30° C. Addition of ethers to the polymerization run greatly increases the rate of polymerization and decreases the amount of tactic polymer in favor of the atactic constituent. Presumably, in the case of stereospecific polymerization, organolithium compounds of the following association type are the initiators



The existence of such associated organolithium compounds has been established in various cases (19, 20, 24). In addition to isotactic polystyrene, a considerable amount of atactic material is always present; it is formed by starting the polymerization on the nonassociated part of the organolithium compounds which probably promote a nonstereospecific anionic polymerization. The stereoregulation of the polymerization of styrene by heterogeneous alkali metal alkyl initiators is limited by the forces on the surface of the catalyst while the dissolved organolithium initiators in their associated form cause the stereospecific polymerization.

Polymerization of Methyl Methacrylate

Numerous initiator systems have been used for the tactic polymerization of methyl methacrylate (7, 8, 14). Reaction conditions determine the structure of each polymer, and each structure might vary considerably from one polymer to another. Nearly pure isotactic and syndiotactic polymers are known, in addition to all transitions between these limits and also stereoblock copolymers. In the amorphous state, the differences in the individual structures are clearly shown by their ultrared (1) and nuclear resonance spectra (2, 11).

The polymerization of methyl methacrylate by alkali metal organic compounds yields different types of polymerizates depending upon the conditions. With alkyllithium, -sodium, and -potassium, polymerization proceeds faster than with styrene. The influence of polymerization temperature upon the tacticity of the resulting polymers is very slight; however, the type of reaction medium plays an important part. In polar solvents, like dimethoxyethane or pyridine, the polymers have chiefly a syndiotactic linkage of the fundamental units, whereas, in nonpolar media such as toluene or petroleum ether, isotactic structures are favored. This can be confirmed by means of nuclear magnetic resonance (Figure 3). In nonpolar solvents and at a constant polymerization temperature, the number of isotactic linkages depends upon whether polymers are produced by alkyllithium, -sodium, or -potassium and follows the sequence $\text{Li} > \text{Na} > \text{K}$. In polar media, the number of syndiotactic linkages increases in a similar manner.

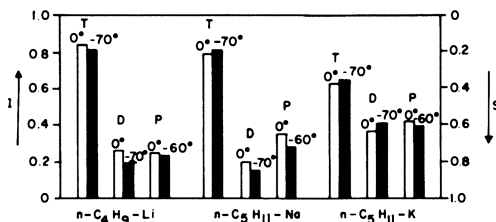


Figure 3. Effect of catalyst, solvent, and temperature on the tacticity of poly(methyl methacrylate)

I. Probability that an isotactic step follows on an isotactic placement
 S. Probability that a syndiotactic step follows on a syndiotactic placement
 Solvents. T = toluene; D = dimethoxyethane; P = pyridine

By means of nuclear resonance spectra, the average length of the isotactic and syndiotactic blocks can be determined—in general, between four and seven units—from which the very poor crystallinity of tactic poly(methyl methacrylate) can be explained. From the energy point of view, for the formation of stable crystalline structures, a definite minimum number of chain members of the same tacticity is necessary. It is very rare to have chain segments of the same tacticity containing more than 10 to 20 monomer units (10). Therefore, the possibility for formation of stable crystalline structures is very limited. Table II summarizes data regarding tacticity and average block lengths. Hence, according to reaction conditions, it is possible to produce with alkylalkali initiators poly(methyl methacrylate) of any desired degree of tacticity.

Table II. Polymerization of Methyl Methacrylate with Alkali Organometal Initiators in Different Solvents

[Methyl methacrylate, 0.05 mole; solvent, 50 ml.; initiator, 0.003 mole; polymerization time, 30 minutes]

Run	Initiator	Solvent ^a	Polymerization Temp., °C.	Tacticity, % Placements			Average Length Segments	
				Iso- tactic	Syndio- tactic	Hetero- tactic	Iso- tactic	Syndio- tactic
M-A 60/1	<i>n</i> -C ₄ H ₉ Li	T	0	72.0	10.7	17.3	9.6	3.3
M-A 60/4		T	-70	67.0	12.5	20.5	8.6	3.2
M-P 60/1	D	D	0	16.6	57.3	26.1	3.3	6.4
M-P 60/5		D	-70	7.0	68.6	24.4	2.6	7.6
M-A 61/1	<i>n</i> -C ₅ H ₁₁ Na	T	0	56.7	12.4	30.9	5.7	2.8
M-A 61/4		T	-70	66.7	8.8	24.5	7.5	2.7
M-P 61/2	D	D	0	6.5	65.3	28.2	2.5	6.6
M-P 61/5		D	-70	4.0	73.0	23.0	2.4	9.2
M-P 24	E	E	-70	55.5	14.3	30.2	5.7	3.0
M-A 62/1		<i>n</i> -C ₅ H ₁₁ K	T	0	34.6	23.3	42.1	3.7
M-A 62/4	T		-70	37.3	22.6	40.2	3.9	3.1
M-P 62/2	D	D	0	13.8	40.4	45.8	2.6	3.8
M-P 62/5		D	-70	12.0	39.0	49.0	2.5	3.6

^a T = toluene; D = dimethoxyethane; E = diethyl ether.

Acknowledgment

The authors thank U. Johnsen, Darmstadt, for the nuclear resonance spectra and their evaluation.

Literature Cited

- (1) Baumann, U., Schreiber, H., Tessmar, K., *Makromol. Chem.* **36**, 81 (1959).
- (2) Bovey, F. A., Tiers, G. V. D., *J. Polymer Sci.* **44**, 173 (1960).
- (3) Braun, D., Betz, W., Kern, W., *Makromol. Chem.* **42**, 89 (1960).
- (4) Braun, D., Herner, M., Kern, W., *Ibid.*, **36**, 232 (1960).
- (5) Braun, D., Herner, M., Kern, W., *J. Polymer Sci.*, **51**, S2 (1961).
- (6) Braun, D., Hintz, H., Kern, W., unpublished work.
- (7) Fox, T. G., *et al.*, *J. Am. Chem. Soc.* **80**, 1768 (1959).
- (8) Fox, T. G., *et al.*, *J. Polymer Sci.* **31**, 173, (1958).
- (9) Gaylord, N., Mark, H., *Makromol. Chem.* **44/46**, 448 (1961).
- (10) Johnsen, U., *Kolloid-Z.* **178**, 161 (1961).
- (11) Johnsen, U., Tessmar, K., *Kolloid-Z.* **168**, 160 (1960).
- (12) Kern, R. F., *Nature (London)* **187**, 410 (1960).
- (13) Kern, W., Braun, D., Herner, M., *Makromol. Chem.* **28**, 66 (1958).
- (14) Miller, R. G. J., *et al.*, *Chem. & Ind. (London)* 1958, 1323.
- (15) Morton, A. A., Grovenstein, E., *J. Am. Chem. Soc.* **74**, 5435 (1952).
- (16) Morton, A. A., Taylor, L. D., *J. Polymer Sci.* **38**, 7 (1959).
- (17) Natta, G., *Angew. Chem.* **68**, 393 (1956).
- (18) Patat, F., Sinn, H., *Ibid.* **70**, 496 (1958).
- (19) Piotrovskii, K. B., Ronina, M. P., *Doklady Akad. Nauk S.S.S.R.* **115**, 737 (1957).
- (20) Rodionow, A. N., Schigorin, D. N., Talalajewa, T. W., Kotscheschkow, K. A., *Ibid.*, **123**, 113 (1958).
- (21) Sinn, H., Lundborg, C., Kirchner, K., *Angew. Chem.* **70**, 744 (1958).
- (22) Williams, J. L. R., *et al.*, *J. Am. Chem. Soc.* **78**, 1260 (1956); **79**, 1716 (1957).
- (23) Williams, J. L. R., *et al.*, *J. Org. Chem.* **23**, 638, 1206 (1958).
- (24) Wittig, G., Meyer, F. J., Lange, G., *Liebigs Ann. Chem.* **571**, 167 (1951).

RECEIVED December 26, 1961.

Polymerization of Conjugated Dienes with Heterogeneous Ziegler-Natta Catalysts

NORMAN G. GAYLORD

Gaylord Associates Inc., 20 Mt. Pleasant Ave., Newark 4, N. J.

HERMAN F. MARK

Polytechnic Institute of Brooklyn, Brooklyn 1, N. Y.

The structure of the polymer obtained in the polymerization of butadiene and isoprene with heterogeneous Ziegler-Natta catalysts depends on the nature of the monomer, catalyst system, and reaction conditions. Previously reported results are reviewed and a mechanism is proposed for the stereoregulated polymerization of conjugated dienes. The polymerization of cyclopentadiene with $\text{LiAlH}_4\text{-TiCl}_4$ or $\text{LiAlR}_4\text{-TiCl}_4$ catalyst system yields a readily oxidized polymer for which a 1,2-structure is proposed.

The structure of the polymer obtained by the polymerization of butadiene, isoprene, and other dienes with organometallic catalysts depends on the nature of the monomer, the catalyst system, and reaction conditions. In this article, the authors review and propose a mechanism for some of the previously reported results on the polymerization of butadiene and isoprene and present some new data on the polymerization of cyclopentadiene.

Butadiene and Isoprene Polymerization

The polymerization of butadiene and isoprene with an organometallic compound-transition metal compound Ziegler-Natta type catalyst can lead to polymers with a microstructure which is all *cis*-1,4-, *trans*-1,4-, isotactic 1,2- (or 3,4-), syndiotactic 1,2- (or 3,4-), or a combination of two or more of these structural units. The polymer microstructure may be dependent upon the ratio of the catalyst components, the temperature, and the reaction medium.

Table I indicates the microstructure of polybutadienes prepared by means of the indicated catalyst systems. It shows that at some given ratio of components, not necessarily at all ratios, a particular catalyst system is capable of yielding polymer with the indicated structural composition. The patent literature, in some cases, contains conflicting data, indicating the influence of unspecified, and possibly unknown, factors.

Table I. Butadiene Polymerization with Ziegler-Natta Catalysts

Catalyst Composition	Nature of Unsaturation			Ref.
	<i>trans</i> -1,4-	<i>cis</i> -1,4-	1,2-	
AlR ₃ + TiCl ₃	+			(10)
AlR ₃ + TiCl ₄	+			(7)
AlR ₃ + TiI ₄		+		(19)
AlR ₃ + VCl ₃	+			(10)
AlR ₃ + VCl ₄	+			(7)
AlR ₃ + Ti(OR) ₄			+	(11)
AlR ₃ + TiAc ₃ ^a			+	(11)
LiAlH ₄ + TiCl ₄			+	(19)
LiAlH ₄ + TiI ₄	+			(19)
CdR ₂ + TiCl ₄	+			(3)

^a Titanium acetylacetonate.

The dependence of the polymer microstructure on the ratio of catalyst components is related to the nature of these components. The structure of polybutadiene obtained with an aluminum triisobutyl (AlBu₃)-titanium tetrachloride catalyst system is a function of the Al/Ti molar ratio (Table II). Polybutadiene prepared at Al/Ti ratios of 0.5 to 8 in benzene or heptane and at 3° or 25° C. contain at least 90% 1,4- units. Polymerizations carried out at ratios of 1.0 and less at 25° C. in heptane and at ratios of 1.25 or less at 3° C. in heptane or benzene give crystalline polymers containing more than 96% *trans*-1,4- structure (6). A similar temperature dependence of polymer structure has been reported in the polymerization of butadiene with a diethylcadmium-titanium tetrachloride catalyst system (3). Polybutadiene obtained with a triethylaluminum-titanium tetrachloride catalyst system at a 0.9 Al/Ti ratio at 30° C. in benzene is reported to contain 67% *cis*-1,4- units (19).

Table II. Polymerization of Butadiene with Al(iso-C₄H₉)₃-TiCl₄ Catalyst (6)

Solvent	Temp., °C.	Al/Ti Mole Ratio	Unsaturation, %			Solubil- ity ^a
			<i>trans</i> -1,4-	<i>cis</i> -1,4-	1,2-	
Heptane	25	0.5-1.0	96-99	0	1-4	I
		1.25-1.6	56-61	32-40	3-7	B
		2.0-8.3	50-79	13-46	2-10	B
	3	1.0-1.25	97-98	0	2-3	I
		1.5	40	56	4	B
Benzene	25	0.5-1.0	79-82	11-16	5-8	I
		1.25	61	35	4	B
	3	0.6-1.25	95-99	0-2	1-3	I
		1.50	50	45	5	B
Heptane-Et ₂ O ^b	3	1.0	86	8	6	I

^a I = insoluble in hot xylene. B = soluble in cold benzene.

^b Reaction mixture contained 2% by weight of diethyl ether based on TiCl₄.

Although polymers containing as much as 98% *trans*-1,4- structure are obtained under the indicated conditions with the AlBu₃-TiCl₄ catalyst system, no polymer with greater than 60% *cis*-1,4- structure is obtained. Natta (12, 16) has indicated that polybutadiene is actually a mixture of high *cis* and high *trans* polymer rather than a polymer containing significant amounts of both *cis*-1,4- and *trans*-1,4- units. However, fractionation of the polybutadiene obtained with the AlBu₃-TiCl₄ catalyst system has yielded only approximately 10% of polymer with 80% *cis*-1,4- content (4).

The influence of the reaction medium is shown in the different behaviors in

benzene and heptane. This is further illustrated by the experiment in which the addition of 2% by weight of diethyl ether (based on TiCl_4) to a 1 to 1 mixture of AlBu_3 and TiCl_4 in heptane yields a rubbery, xylene-insoluble polymer containing only 86% *trans*-1,4- structure in contrast to the crystalline 98% *trans*-1,4-polymer obtained in the absence of ether. The influence of ether is more than a solvent effect and apparently affects the catalyst-monomer-polymer relationship.

In contrast to the structure-catalyst ratio dependence shown in the AlBu_3 - TiCl_4 system, the polymerization of butadiene with a catalyst prepared by reaction of aluminum triethyl or diethylaluminum chloride with vanadium tetrachloride or oxychloride reportedly yields a polymer whose structure is relatively unaffected by the Al/V ratio—i.e., the polybutadiene obtained in heptane at 15° C. contains 95 to 99% *trans*-1,4-, 0 to 1% *cis*-1,4-, and 1 to 5% 1,2- structures at Al/V ratios ranging from 0.5 to 10. After extraction with diethyl ether, diisopropyl ether, and benzene, the residual polymer, constituting 55 to 75% of the total polymer, has 99 to 100% *trans*-1,4- structure (15).

The polymerization of butadiene with an aluminum trialkyl-titanium tetraiodide catalyst system apparently yields a polybutadiene containing more than 85% *cis*-1,4- structure (19). The limited amount of data available does not cover a sufficiently wide range of Al/Ti ratios to permit the drawing of conclusions analogous to those drawn in the case of the *trans*-1,4-polybutadienes. However, as shown in Table III, over the range of Al/Ti ratios from 1.5 to 5.0, the polybutadiene prepared in benzene at 30° C. contains 85 to 93% *cis*-1,4-, 3 to 11% *trans*-1,4-, and 3 to 5% 1,2- structures.

Table III. Polymerization of Butadiene with $\text{AlR}_3\text{-TiI}_4$ Catalyst (19)^a

Al Compound	Al/Ti Mole Ratio	Unsaturation, %		
		<i>cis</i> -1,4-	<i>trans</i> -1,4-	1,2-
$\text{Al}(\text{C}_2\text{H}_5)_3$	1.5-4.0	85-89	7-10.5	4-4.5
	5.0	92.5	3.0	4.5
$\text{Al}(\text{i-C}_4\text{H}_9)_3$	5.0	92-93	4-5	3.0

^a Polymerization in benzene at 30°C.

Table IV indicates the microstructure of polyisoprene obtained by the use of various catalyst systems.

Table IV. Isoprene Polymerization with Ziegler-Natta Catalysts

Catalyst Composition	Nature of Unsaturation			Ref.
	<i>trans</i> -1,4-	<i>cis</i> -1,4-	3,4-	
$\text{AlR}_3 + \text{TiCl}_3$	+			(10)
$\text{AlR}_3 + \text{TiCl}_4$		+		(7)
$\text{AlR}_3 + \text{VCl}_3$	+			(10)
$\text{AlR}_3 + \text{VCl}_4$	+			(7)
$\text{AlR}_3 + \text{Ti}(\text{OR})_4$			+	(11)
$\text{AlR}_3 + \text{TiAc}_3$			+	(11)
$\text{LiAlH}_4 + \text{TiI}_4$	+			(19)
$\text{CdR}_2 + \text{TiCl}_4$		+		(3)

Comparison of Tables I and IV reveals several interesting aspects. Thus, the $\text{AlR}_3\text{-TiCl}_4$ and $\text{CdR}_2\text{-TiCl}_4$ catalyst systems yield a *trans*-1,4-polybutadiene and a *cis*-1,4-polyisoprene. The $\text{LiAlH}_4\text{-TiI}_4$ and $\text{AlR}_3\text{-VCl}_3$ or -VCl_4 catalyst systems yield *trans*-1,4-polybutadiene and *trans*-1,4-polyisoprene. The $\text{AlR}_3\text{-TiI}_4$ catalyst system which yields a *cis*-1,4-polybutadiene is not an active catalyst in the attempted polymerization of isoprene (19).

IN POLYMERIZATION AND POLYCONDENSATION PROCESSES; PLATZER, N.;

Advances in Chemistry; American Chemical Society: Washington, DC, 1962.

As in the case of butadiene polymerization, the microstructure of polyisoprene is dependent upon the ratio of catalyst components, the reaction temperature, and the reaction medium. As shown in Table V, using an aluminum triethyl-titanium tetrachloride catalyst system, an Al/Ti ratio of 1.0 or higher yields a polyisoprene containing 96% *cis*-1,4-, 4% 3,4-, and essentially no *trans*-1,4- or 1,2- units. Below this ratio, the *trans*-1,4- structure is produced apparently at the expense of the *cis*-1,4- structure (1). An AlBu₃-TiCl₄ catalyst system is reported (7) to yield an essentially all-*trans*-1,4-polyisoprene at an Al/Ti ratio of 0.67 and below.

Table V. Polymerization of Isoprene with Al(C₂H₅)₃-TiCl₄ Catalyst (1)

Al/Ti Mole Ratio	Unsaturation, %		
	<i>cis</i> -1,4-	<i>trans</i> -1,4-	3,4-
0.2-0.4	42-50	44-52	3-4
0.8	90	6	4
1.0-2.0	95-96	0-1	3-5

The microstructure of the polyisoprene is affected by temperature, a higher Al/Ti ratio being required at -30° C. to produce a structure comparable to that obtained with lower ratios at room temperature. Thus, a 1 to 1 ratio yields a polymer with 40% *trans*-1,4- structure at -30° C. and 0% at room temperature. A 0% *trans*-1,4- structure is obtained at -30° C. with a 1.2 to 1.4:1 Al/Ti mole ratio.

As in the polymerization of butadiene, the presence of polar solvents affects the microstructure of polyisoprene obtained with a Ziegler-Natta catalyst in a hydrocarbon reaction medium (1, 21).

Comparison of results from the polymerizations of butadiene and isoprene with an AlR₃-TiCl₄ catalyst system reveals some interesting features. The 1 to 1 Al/Ti ratio yields a *cis*-1,4-polyisoprene and a *trans*-1,4-polybutadiene. Kinetic studies have, in fact, indicated that in both cases, the rate of polymerization at this ratio is proportional to the first power of the monomer pressure (6, 21). At lower Al/Ti ratios, higher *trans*-1,4- content is observed in both polyisoprene and polybutadiene. At comparable Al/Ti ratios, lower temperatures increase the *trans*-1,4- structure in both polymers. Although essentially all-*cis*-1,4-polyisoprene and all-*trans*-1,4-polybutadiene can be prepared, variations in the ratio of catalyst components yield a polyisoprene containing no more than 60% *trans*-1,4- structure and a polybutadiene containing no more than 60% *cis*-1,4- structure.

The heterogeneous polymerization of a conjugated diene or any other monomer can be visualized as involving two distinct steps. In the first step, the monomer is adsorbed on the catalyst surface and/or forms an active monomer-catalyst complex. The second step involves addition of the adsorbed and/or complexed monomer unit to the polymer chain.

The configuration which a given monomer molecule assumes upon adsorption on the catalyst surface or on being complexed with the catalyst is related to the structure and/or nature of the effective sites. The influence of structure is seen in the differing catalytic activity of α -TiCl₃ (layer structure) and β -TiCl₃ (fibrous structure). The nature of the effective site is also apparently determined by the ratio of the catalyst components and the resultant valence state of the transition metal. The nature of these catalytic sites is the same regardless of the monomer being polymerized.

It has been previously considered that a major factor in the tendency to form *cis*- or *trans*- polymers was the geometric configuration of the diene. Mono-

meric isoprene was reported to contain 85% of the *cis*- isomer at 50° C. (17), while monomeric butadiene contained 96% of the *trans*- isomer at room temperature (20, 22). The polymerization of isoprene to a *cis*-1,4-polyisoprene and of butadiene to a *trans*-1,4-polybutadiene by means of the same 1 to 1 AlR₃/TiCl₄ catalyst system apparently involved adsorption of the monomer molecules on the catalyst surface, in the same configuration in which they were present in the reaction medium, without rearrangement. In the second step of the polymerization reaction, these adsorbed monomer molecules were added to the polymer chain in whatever configuration they presented to the active chain "end," again without rearrangement.

It has recently been proposed (8), however, that both isoprene and butadiene possess the same *trans* configuration. The preparation of *cis*-1,4-polyisoprene at a 1 to 1 Al/Ti ratio, therefore, represents a situation in which monomer inversion occurs. The degree of inversion is apparently a function of the Al/Ti ratio in the AlR₃/TiCl₄ system.

At the present time, the most likely concept of the mechanism of a heterogeneous polymerization catalyzed by a Ziegler-Natta catalyst involves a complex in which the organometallic component and the transition metal component—i.e., the Al and Ti atoms—are joined by electron-deficient bonds. Natta, Corradini, and Bassi (13) have reported such a structure for the active catalyst prepared from bis(cyclopentadienyl)titanium dichloride and aluminum triethyl. Natta and Pasquon (14), Patat and Sinn (18), and Furukawa and Tsuruta (2) have proposed mechanisms for the stereospecific polymerization of α -olefins in terms of such electron-deficient complexes.

In addition to having a specific orientation of the monomer adsorbed on the catalyst surface or complexed with a catalytic site, a stereoregular polymerization requires orientation of the monomer molecule with respect to the growing polymer "end" and restricted rotation around the C₁-C₂ axis in the metal-C₁-C₂ sequence. Furukawa and Tsuruta (2) have proposed that rotation is restricted by the formation of a bond between a hydrogen atom attached to C₂ and a metal atom on the surface.

If one assigns to the titanium atom the functions of complexing with new monomer molecules as well as participating with aluminum in the formation of a rotation-restricting hydrogen bridge, the mechanism of stereoregular diene polymerization can be schematically represented in terms of electron-deficient coordination complexes, as shown in Figure 1 for the polymerization of isoprene to *cis*-1,4-polyisoprene.

As shown in Figure 1, A, the isoprene monomer is bound to the catalyst surface as a result of an attraction of π electrons by the titanium atom. At the same time, the titanium atom and the aluminum atom are part of a halide-bridged electron-deficient complex in which a hydrogen atom on C₃ of the monomer coordinated with the polymer "end" is momentarily joined to the two metal atoms by hydrogen bonding. In Figure 1, B, the π electrons of the diene become associated with 3*d* electrons of the titanium, the ti-H_a bond becomes weakened, and a new ti . . . C₁ electron-deficient bond is formed. At the same time, a new ti-H_b bond is formed, the al-H bond is strengthened, and the al . . . C₄-deficient bond is weakened. As a result, C₂ and C₄ acquire slight residual valences (represented by °). Although free rotation around the ti . . . C₁ bond is restricted, the ti . . . C₁-C=C-C₂° bond system rotates freely and swings into the complex. The C₂° atom and the C₄° atom, both possessing slight residual valences, are brought into juxtaposition and, as shown in Figure 1, C, overlapping of the 2*p* electrons occurs

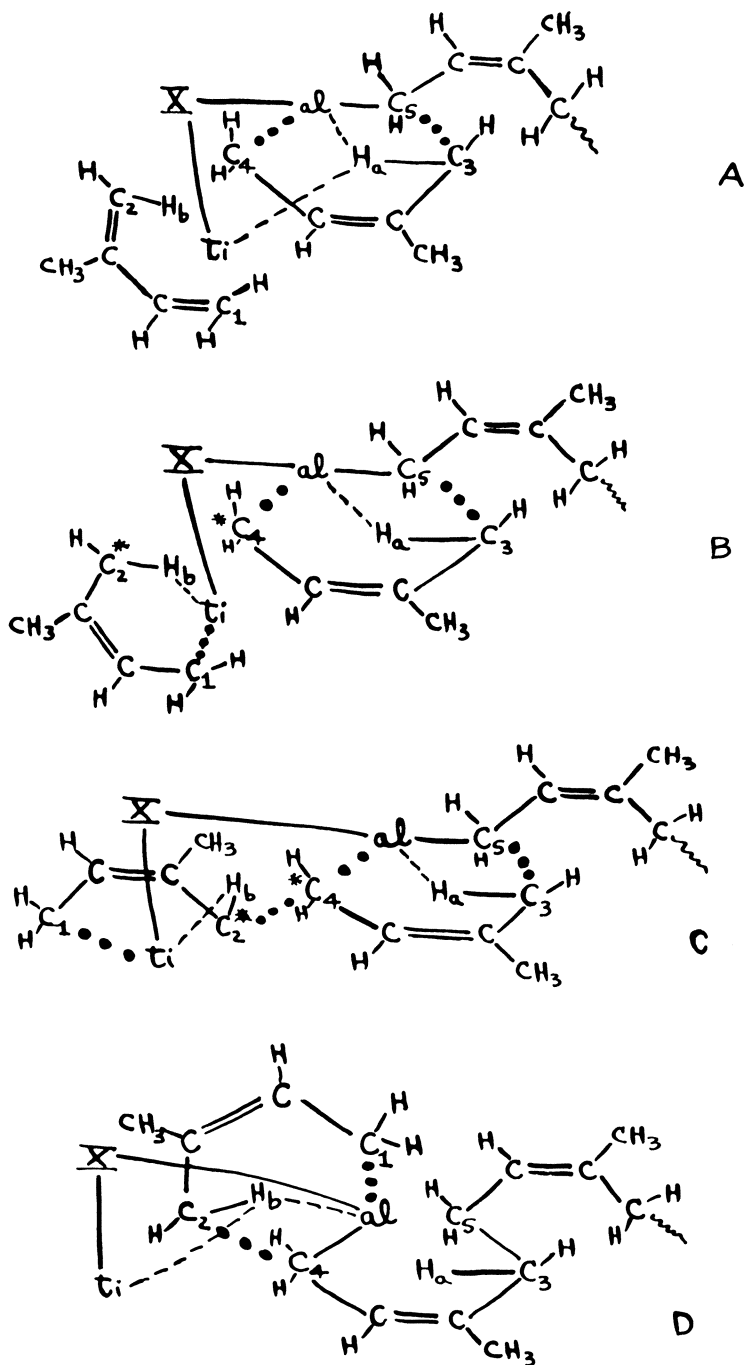


Figure 1. Scheme for polymerization of isoprene to *cis*-1,4-polyisoprene with Ziegler-Natta type catalyst

al and *ti* (lower case) imply only one valence of metal represented in formula, corresponding to form adopted by Ziegler

and results in hybridization. The rotation of the $ti \dots C_1-C=C-C_2^\circ$ bond system brings H_b into the range of the al atom and, as shown in Figure 1, *D*, the $al-H_a$ bond is broken and a new $al-H_b$ bond is formed. Simultaneously, the $al-C_5$ and the weakened $ti \dots C_1$ bonds are cleaved. As a result the $al-C_4$ bond is strengthened and a new $al \dots C_1$ -deficient bond is formed. The over-all result is a return to the condition shown in Figure 1, *A*, and the process can resume again.

The representation of H_a in Figure 1, *A*, as well as H_b in Figure 1, *D*, with an apparent coordination number of 3 and of the titanium atom in Figure 1, *B* and *C*, with an apparent coordination number of 5, is not intended to imply the existence of structures with finite life times, but rather the momentary formation of a transition state which is immediately superseded by the suggested next step.

The same representation can be applied to the polymerization of butadiene to 1,4-*trans*-polybutadiene with the structure of the complex shown in Figure 2.

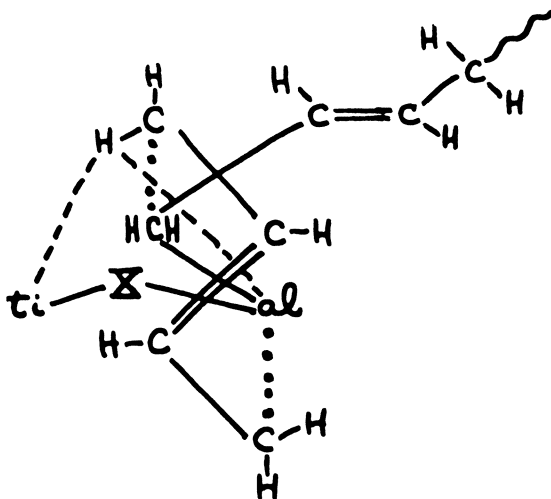


Figure 2. Transition state in polymerization of butadiene to *trans*-1,4-polybutadiene with Ziegler-Natta type catalyst

The occurrence of stereoregular polymerization at a specific molar ratio of catalyst components is indicative of the ability of the catalyst complex formed at that ratio to fulfill the geometric requirements of the proposed mechanism. At another ratio of catalyst components—e.g., at higher Al/Ti ratios—the transition metal may be present at a different valence state and the crystalline complex has a different structure. The latter structure may permit the accommodation of two monomer molecules, or an overlapping of two molecules, in different configurations, as implied by kinetic data (6). If the titanium atom at this valence state is not capable of forming a sufficiently strong $ti-H_b$ bond (Figure 1, *B*), free rotation around the $\sim C=C-C_2^\circ$ axis may bring this bond system in juxtaposition to the C_4° atom in an inverted configuration.

A further factor in configuration inversion involves the nature of the haloaluminum alkyl and other products of the reaction of the catalyst components which are adsorbed on the catalyst surface or are present in solution. Association of these materials with the aluminum atom may interfere with the formation of the $al-C_4$ or, of even greater significance, the $al-H_b$ bond (Figure 1, *D*). The

influence of ethers or other polar materials in the reaction mixture may result in coordination with the aluminum atom, which readily forms etherates which may interfere with complex formation. Alternatively, the extraneous materials present in solution may actually cause inversion of the monomer in solution and affect the equilibrium concentration of the *cis*- and *trans*- configurations. This might account for the fact that while a given catalyst system is stereoregulating for one configuration of a monomer, a change in the Al/Ti ratio does not make it stereoregulating for the other configuration and would imply that there is not preferential adsorption or entering into the complex of one configuration over the other, as discussed earlier.

The ability to proceed from a *trans*-1,4-polybutadiene to a *cis*-1,4-polybutadiene by changing the nature of the catalyst components implies, in accord with the proposed mechanism, either the production of more soluble catalyst compositions—e.g., as would be expected from TiI_4 as compared with $TiCl_4$ —inversion of the monomer in solution, ease of adsorption of the *cis*- monomer on the surface of the insoluble catalyst complex, or ease of hydrogen bond formation between the *cis*- monomer and the aluminum atom present in the complex. Alternatively, the inversion can occur in the formation of the monomer-catalyst complex without recourse to inversion in solution.

In those cases where the stereoregularity is insensitive to changes in the ratio of catalyst components—e.g., the polymerization of butadiene with AlR_3-VCl_4 and $-VOCl_3$ catalyst systems—it is probable that an active stereoregulating complex is formed at all ratios, although the structure of the complex may vary with the ratio, and that the other products of the reaction of catalyst components, either adsorbed or in solution, do not invert the monomer in solution or during the various stages of complex formation.

Cyclopentadiene Polymerization

The polymerization of cyclopentadiene (5) was investigated in bulk and in solution with lithium aluminum hydride–titanium tetrachloride and lithium aluminum tetraoctyl–titanium tetrachloride catalyst systems. The polymerizations were carried out in nitrogen atmosphere using highly purified—i.e., freshly distilled—reactants.

In the absence of solvents or at temperatures from 25° to 50° C. polymerizations carried out with a $LiAl(C_8H_{17})_4-TiCl_4$ catalyst system at Al/Ti ratios of 0.28 to 2.8 gave 32 to 62% yields of black gel-like polymeric masses.

At temperatures below 10° C., polymerization in toluene or cyclohexane with a $LiAl(C_8H_{17})_4-TiCl_4$ catalyst at Al/Ti ratios of 0.55 to 8.3 gave light brown polymer, with optimum yields of 78 to 94% at an Al/Ti ratio of 0.55. $LiAlH_4-TiCl_4$ was an effective catalyst system, resulting in quantitative yields of polymer at an Al/Ti ratio of 0.55 (Table VI).

Polymer samples either isolated by precipitation with 2-propanol or permitted to stand in toluene solution rapidly became insoluble in toluene on standing in air. Brittle films cast directly from toluene solution were rapidly insolubilized, unless antioxidants were present.

The ash content of the polymer was less than 0.1%. X-ray diffraction powder diagrams indicated that the polymer was amorphous. Infrared spectra prepared by means of the potassium bromide disk technique indicated the presence of unsaturation and hydroxyl groups.

Table VI. Polymerization of Cyclopentadiene

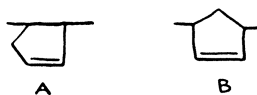
Catalyst Composition, Mole			Al/Ti, Mole Ratio	Mono- mer, Grams	Solvent, ^a Ml.	Temp., °C.	Yield, %
LiAlH ₄	TiCl ₄	<i>l</i> -Octene					
0.025	0.045	0.11	0.55	80	—	40–45	42
0.025	0.009	0.11	2.78	64	—	25	32
0.025	0.090	0.11	0.28	64	—	25	62
0.025	0.009	0.11	2.78	64	C, 200	<10	3
0.025	0.045	0.11	0.55	64	C, 200	<10–25	78
0.075	0.009	0.33	8.3	64	C, 160	<10	9
0.075	0.009	0.33	8.3	64	C, 160	<10	2
0.025	0.045	0.11	0.55	64	T, 200	<10	94
0.025	0.045	—	0.55	80	T, 300	<10	100
0.025	0.045	—	0.55	80	T, 300 ^b	<10	106

^a C = Cyclohexane, T = toluene.

^b Oxygen bubbled into reaction mixture.

Polymer prepared in the strict absence of air by distilling the cyclopentadiene into a heterogeneous reaction mixture consisting of solvent and catalyst, but without special precautions in the isolation procedure, had an elemental analysis corresponding to an empirical formula of C₅H₆O, indicating one oxygen atom per ring. The polymer decolorized bromine in carbon tetrachloride and liberated HBr. Treatment of the polymer with bromine liberated HBr and gave a material containing one bromine atom and one oxygen atom per ring. Treatment of the polymer with benzoyl chloride gave a benzoylated product which showed on analysis one benzoyl group per five carbon atoms, C₅H₅OCOC₆H₅, and chlorine to the extent of one chlorine atom per 40 ring carbon atoms. The brominated and benzoylated polymers were insoluble in toluene.

Polycyclopentadiene would be expected to have either a 1,2- (A) or a 1,4 (B) structure.



1,3-Cyclohexadiene has been reported to polymerize by 1,4- addition by means of aluminum triisobutyl-titanium tetrachloride catalyst (9).

The evolution of HBr in the bromination reactions and the uptake of one bromine atom per ring indicate substitution at a secondary allylic carbon atom. The ease of oxidation and cross linking of the polymers and the presence of hydroxyl groups imply the intermediate formation of hydroperoxides on allylic carbon atoms. Treatment of the hydroxyl-containing polymer with benzoyl chloride indicates that the bulk of the hydroxyl groups are on secondary carbon atoms, since tertiary hydroxyl groups would tend to be replaced by chlorine. Although these results do not permit the elimination of structure B, it appears that the bulk of the structural units in the polycyclopentadiene corresponds to 1,2- addition (A).

The polymerization of cyclopentadiene with triisobutyl aluminum-titanium tetrachloride catalyst system is reported (7) to yield polycyclopentadiene with 1,4- structure. Apparently the polymerization of cyclopentadiene is analogous to that of butadiene, wherein, as shown in Table I, in a TiCl₄ catalyst system, AlR₃ yields a 1,4- structure and LiAlH₄ yields a 1,2- structure.

The addition of phenyl-2-naphthylamine to a reaction mixture immediately upon completion of the polymerization reaction resulted in the isolation of a polymer which contained less oxygen—i.e., one oxygen atom per 15 carbon atoms

—than polymer obtained in the absence of the antioxidant. When a large amount of antioxidant was added to the reaction mixture in toluene, precipitation with 2-propanol and vacuum drying gave a nearly white powder which was sufficiently soluble (approximately 25%) in toluene at room temperature to permit determination of the intrinsic viscosity. The $[\eta]$ value of 0.14 is in the same range as the inherent viscosities of 0.11 to 0.16 found for poly-1,3-cyclohexadiene (9) and considered as corresponding to a molecular weight of 5000 to 10,000.

In an attempt to prepare polycyclopentadiene which would be stable in toluene solution, the polymer was hydrogenated over a platinum oxide catalyst in a Parr bomb immediately after the completion of the polymerization reaction. Infrared analysis indicated the presence of residual unsaturation and the polymer became insolubilized on standing. An attempted copolymerization of cyclopentadiene with propylene gave a product whose infrared spectrum indicated the presence of C-methyl groups but which was still insoluble in toluene. No attempt was made to determine whether copolymerization had occurred.

Attempts to polymerize dicyclopentadiene with a $\text{LiAl}(\text{C}_8\text{H}_{17})_4\text{-TiCl}_4$ catalyst at a 2.8 Al/Ti ratio in toluene, under the same conditions which yielded polycyclopentadiene, failed to yield any polymer.

Literature Cited

- (1) Adams, H. E., Stearns, R. S., Smith, W. A., Binder, J. L., *Ind. Eng. Chem.* **50**, 1507 (1958).
- (2) Furukawa, J., Tsuruta, T., *J. Polymer Sci.* **36**, 275 (1959).
- (3) Furukawa, J., Tsuruta, T., Saegusa, T., Onishi, A., Kawasaki, A., Fueno, T., *Ibid.*, **28**, 450 (1958).
- (4) Gaylord, N. G., Chandrasekaran, S., Polytechnic Institute of Brooklyn, unpublished results.
- (5) Gaylord, N. G., Indictor, N., unpublished results.
- (6) Gaylord, N. G., Kwei, T. K., Mark, H. F., *J. Polymer Sci.* **42**, 417 (1961).
- (7) Goodrich-Gulf Chemicals Inc., Belg. Patent **543,292** (Dec. 2, 1955).
- (8) Gresser, J., Rajbenbach, A., Szwarc, M., *J. Am. Chem. Soc.* **82**, 5820 (1960).
- (9) Marvel, C. S., Hartzell, G. E., *Ibid.*, **81**, 448 (1959).
- (10) Montecatini (Società generale industria mineraria e chimica), Belg. Patent **545,952** (March 10, 1956).
- (11) *Ibid.*, **549,554** (July 14, 1956).
- (12) Natta, G., *Chim. e ind. (Milan)* **42**, 1207 (1960).
- (13) Natta, G., Corradini, P., Bassi, I. W., *J. Am. Chem. Soc.* **80**, 756 (1958).
- (14) Natta, G., Pasquon, I., *Advances in Catalysis* **11**, 1 (1959).
- (15) Natta, G., Porri, L., Mazzei, A., *Chim. e ind. (Milan)* **41**, 116 (1959).
- (16) Natta, G., Porri, L., Mazzei, A., Moreno, D., *Ibid.*, **41**, 398 (1959).
- (17) Nikitin, V. N., Yakovleva, T. V., *Zhur. Fiz. Khim.* **28**, 697 (1954).
- (18) Patat, F., Sinn, H., *Angew. Chem.* **70**, 496 (1958).
- (19) Phillips Petroleum Co., Belg. Patent **551,851** (Oct. 17, 1956).
- (20) Richards, C. M., Nielsen, J. R., *J. Opt. Soc. Am.* **40**, 438 (1950).
- (21) Saltman, W. M., Gibbs, W. E., Lal, J., *J. Am. Chem. Soc.* **80**, 5615 (1958).
- (22) Vol'kenshtein, M. V., Nikitin, V. N., Yakovleva, T. V., *Izvest. Akad. Nauk S.S.S.R., Ser. Fiz.* **14**, 471 (1950).

RECEIVED August 22, 1961. Division of Petroleum Chemistry, Symposium on Monomers and Polymers from Petroleum, 139th Meeting ACS, St. Louis, Mo., March 1961.

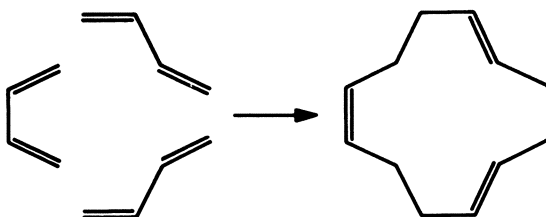
Reactions of New Pi-Complex Catalysts

GÜNTHER WILKE, BORISLAV BOGDANOVIČ, PAUL HEIMBACH,
MICHAEL KRÖNER, and ERNST WILLI MÜLLER

Max-Planck-Institut für Kohlenforschung, Mülheim-Ruhr, Germany

Three molecules of butadiene can be combined into 1,5,9-cyclododecatriene, using typical Ziegler-type catalysts. New π -complex catalysts have been developed by which it is possible to direct the synthesis at will in direction of a trimerization or dimerization. 1,5-Cyclo-octadiene or 1,5,9-cyclododecatriene can be obtained in 95% yields. The catalysts can be isolated and are mostly crystalline—for instance, $\text{Ni}(\text{O})\text{-}[\text{P}(\text{C}_6\text{H}_5)_3]_4$. It has been possible to isolate a definite intermediate of the trimerization, the structure of which has been determined. Some reactions of this intermediate elucidate the mechanism of the trimerization. The cyclic olefins obtained from butadiene are valuable starting materials for the production of $\alpha\text{-}\omega$ difunctional compounds.

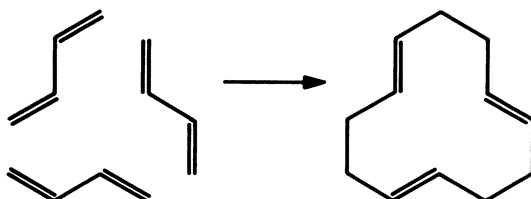
As reported in 1959 at the Symposium on Stereoregulated Polymers in Boston (1), it is possible to combine three molecules of butadiene into *trans,trans,cis*-1,5,9-cyclododecatriene, using a typical Ziegler-type catalyst which can be prepared by reaction of TiCl_4 with $\text{Al}(\text{C}_2\text{H}_5)_2\text{Cl}$.



One can polymerize ethylene, using the same catalysts, into high molecular weight polyethylene (9).

With special catalyst combinations, yields of over 90% can be obtained at normal pressure and at about 40° C. By using a catalyst prepared on the basis of

chromium compounds, *trans,trans,trans*-1,5,9-cyclododecatriene has been synthesized (1):



This article presents investigations on the elucidation of the reaction mechanism of this remarkable cyclo-oligomerization, as well as improvements in the cyclotrimerization and cyclodimerization of butadiene.

In this latter connection two well-known processes should be mentioned:

About 10 years ago Ziegler and coworkers (10, 11) investigated the thermal dimerization of butadiene. They obtained, under extreme conditions, vinylcyclohexene as a main product and 15% of 1,5-cyclo-octadiene.

In 1954, Reed (5) reported that it is possible to synthesize 1,5-cyclo-octadiene from butadiene with Reppe catalysts obtained from nickel carbonyl. The yields were in the range of 30 to 40%. Recently, some patents granted to the Cities Service Co. (1, 6) show that great improvements have been made in this process also.

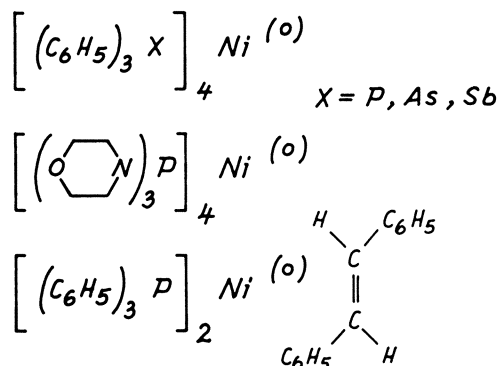
Soon after discovery of cyclotrimerization, we tried to find a way to change this reaction into a cyclodimerization which would lead to 1,5-cyclo-octadiene. However, all our efforts to alter the typical Ziegler-type catalysts to effect cyclodimerization were fruitless as long as catalysts based on titanium compounds were used. Later on we tried to prepare a catalyst based on nickel compounds, because the Reppe-Reed catalysts have shown that nickel is effective in some way in such a reaction; but on treating nickel compounds with organometallic compounds, a precipitate of metallic nickel which had very little activity as a catalyst was always obtained. Then a simple way was found to stabilize the reduced nickel by π -complex formation. This method finally originated from investigations on the dimerization of ethylene by $\text{Al}(\text{C}_2\text{H}_5)_3$ in the presence of a nickel co-catalyst (8).

The first active catalyst system found was prepared by reaction of nickel acetylacetonate with organoaluminum compounds in the presence of phenylacetylene. A dark red solution was obtained which reacted at 80° C. under pressure with butadiene to about 24% cyclo-octadiene, 8% vinylcyclohexene, and 63% all-*trans*-cyclododecatriene. The component which stabilizes the reduced nickel was then changed systematically to discover the possibility of directing the synthesis at will in the direction of a trimerization or dimerization. Today we can synthesize cyclo-octadiene in yields of 95% or cyclododecatriene in similarly good yields only by altering the electron-donor molecules used in preparing the catalyst.

What compounds are the active catalysts in this process? By this method of catalyst preparation we do not obtain a mixture of indefinite composition, but π -complexes which can be isolated and are mostly crystalline. If, for instance, nickel acetylacetonate is reduced in the presence of $\text{P}(\text{C}_6\text{H}_5)_3$ we obtain a new compound, $\text{Ni}(\text{O})\text{-}[\text{P}(\text{C}_6\text{H}_5)_3]_4$. This compound is itself an active catalyst for the cyclo-oligomerization of butadiene, producing about 65 to 70% cyclo-octadiene, 20% vinylcyclohexene, and 10% cyclododecatriene. Instead of $\text{P}(\text{C}_6\text{H}_5)_3$ we can introduce $\text{As}(\text{C}_6\text{H}_5)_3$ and isolate $\text{Ni}(\text{O})\text{-}[\text{As}(\text{C}_6\text{H}_5)_3]_4$ as an active cata-

lyst, by which we obtain yields of 11% cyclo-octadiene, 5% vinylcyclohexene, and 81% cyclododecatriene.

These examples explain the general principle. By this method we have synthesized a great number of different compounds, a selection of which is shown below.



For studying the cyclotrimerization reaction mechanism these new catalyst systems seemed to be much more convenient than the above-mentioned Ziegler-type catalysts. The authors assumed the following reaction sequence:

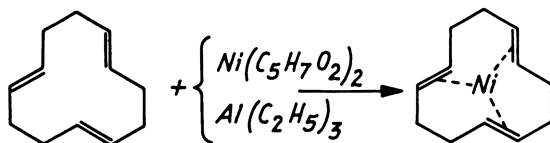
π -Complex formation between butadiene molecules and the transition metal of the catalysts, preformation of the ring and activation of the butadiene molecules in this complex.

C-C linking with formation of, for instance, cyclododecatriene which still remains on the transition metal in the form of a new π -complex.

Displacement of cyclododecatriene by further butadiene molecules which again form an intermediate complex, starting a new cycle.

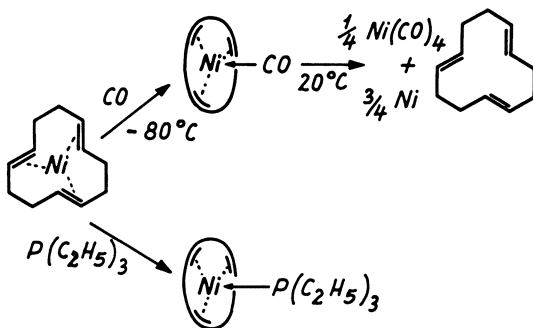
To prove this idea we tried to isolate a reaction intermediate. Below is described the synthesis of a compound which seems to be very important in this connection.

By reaction of nickel acetylacetonate with organometallic compounds in ether in the presence of all-*trans*-cyclododecatriene, we obtained an intensely red solution from which dark red crystals could be isolated. These are volatile under high vacuum and have the composition $NiC_{12}H_{18}$. The mass spectrum shows the molecule to have peaks at 220 and 222. This is in agreement with $NiC_{12}H_{18}$, if we consider that nickel consists of the isotopes Ni^{58} and Ni^{60} . The infrared spectrum shows that all double bonds are shared with nickel, because there is no absorption corresponding to normal *trans* double bonds.



If a solution of this compound is shaken with hydrogen, three equivalents of gas are absorbed immediately. We obtain as reaction products cyclododecane and metallic nickel. By heating to $140^\circ C.$, the compound can be decomposed into cyclododecatriene and nickel. Reaction of the compound with carbon monoxide at normal pressure and $20^\circ C.$ yields cyclododecatriene and nickel carbonyl.

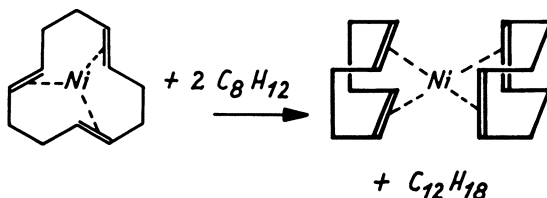
The authors assumed that this compound might have a planar structure with a trigonal nickel atom in the center of the ring. If we take into consideration that all π -electrons of the three double bonds are shared with the nickel atom, we find that nickel can only reach a 16-electron shell. This electron configuration is very unusual for zero-valent nickel. To date we cannot exactly decide whether the compound has a planar structure or not. An x-ray investigation which might clear up this problem is under way. Nevertheless, the authors feel that they also have some chemical indication for a possible structure. The centro-nickel compound was treated with carbon monoxide at -80°C . In a short reaction period, the red color disappeared and precisely one equivalent of CO was absorbed, forming white crystals. Apparently the CO now occupies the fourth coordination position of the nickel atom which thereby can fill its electron shell to a closed noble gas shell. But this compound is stable only below 0°C . Above that temperature, it decomposes, forming one-fourth $\text{Ni}(\text{CO})_4$, three-fourths Ni, and cyclododecatriene. At first, we interpreted this reaction by assuming that starting from a trigonal planar structure the addition of one CO led to a strongly distorted tetrahedral structure, stable at low temperature. At higher temperatures, however, this structure was converted into a perfect tetrahedron, a transformation apparently impossible for the ring, so that the compound decomposed. Latest results, however, indicate that this explanation cannot be correct, because the authors were able to synthesize a comparable compound, which is completely stable at room temperature, by addition of $\text{P}(\text{C}_2\text{H}_5)_3$ instead of CO:



Therefore, the instability of the former and the stability of the latter compound must have another reason than a geometrical one. Today, it is assumed that the type of bonding between the nickel and the ligand is different in both cases.

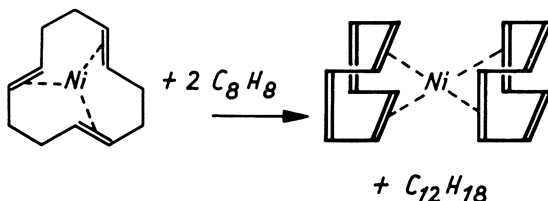
If it is now assumed that cyclododecatriene-nickel could be an intermediate in the cyclododecatriene synthesis, this compound should undergo displacement reactions with other electron donors and especially with butadiene.

To test this hypothesis the centro-nickel compound was treated with cyclo-octadiene and a new, nicely crystalline, yellow compound was obtained which was found to be bis(1,5-cyclo-octadiene) nickel:

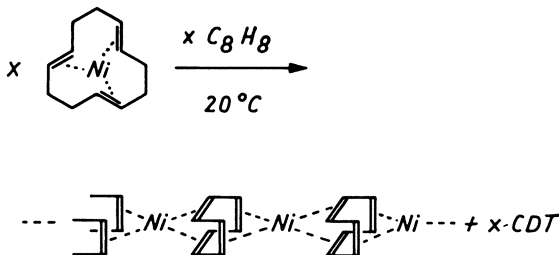


By this reaction, the nickel atom can reach an 18-electron shell, and this might be the reason why the cyclododecatriene molecule can be displaced so easily by cyclo-octadiene.

In the same way, cyclo-octatetraene displaces a cyclododecatriene molecule, but there are two different possibilities. If this reaction is conducted at -40°C ., an orange-colored crystalline compound is obtained, which has a similar structure. Two cyclo-octatetraene molecules are bound to one nickel atom to yield bis(cyclo-octatetraene) nickel:



The same reaction when carried out at 20°C ., leads to black crystals with a metallic luster, of composition $(\text{NiC}_8\text{H}_8)_x$, which may be polymeric because the solubility is very low. On each side of the folded cyclo-octatetraene ring, one nickel atom shares the π -electrons of two double bonds.

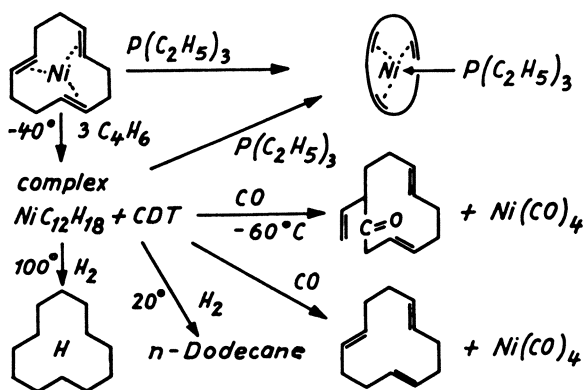


The two compounds, bis(cyclo-octadiene)nickel and (cyclo-octatetraene) nickel, can also be synthesized directly by reduction of nickel acetylacetonate in the presence of olefins. But bis(cyclo-octatetraene)nickel is obtained only by a displacement reaction on the centro-nickel compound.

The next step was to investigate the reaction of the centro-nickel compound with butadiene. When a solution of this compound is saturated with butadiene at room temperature, we observe that after a certain period the excess of butadiene has reacted with formation of cyclododecatriene and a new complex which can be isolated by removing the cyclododecatriene under high vacuum. The same catalytic reaction can be carried out by using bis(1,5-cyclo-octadiene)nickel as a catalyst. Cyclododecatriene synthesized in this way consists of three isomers. The main product is *trans,trans,trans*-cyclododecatriene and the isolated by-products are *trans,trans,cis*- and *cis,cis,trans*-cyclododecatriene. The latter compound is a new isomer, previously unknown (b.p.₁₄ 110°C ., n_D^{20} 1.5129). The synthesis of this isomer furnished very good proof of the correctness of the configuration assumed for *trans-trans,cis*-cyclododecatriene, which, however, had been contested by Greenwood (3).

The intermediate complex mentioned above can be prepared in a very pure state if the centro-nickel compound is treated at -40°C . with an excess of butadiene. Also in this case the cyclododecatriene will be displaced, but no catalytic reaction takes place, and if the excess butadiene is removed at low temperature,

the residue contains cyclododecatriene, nickel, and butadiene in a mole ratio of 1:1:3. The cyclododecatriene again can be removed under high vacuum, and the complex can be recrystallized from liquid butadiene. With this complex, different reactions were carried out:



Reaction with CO yielded cyclododecatriene and nickel carbonyl.

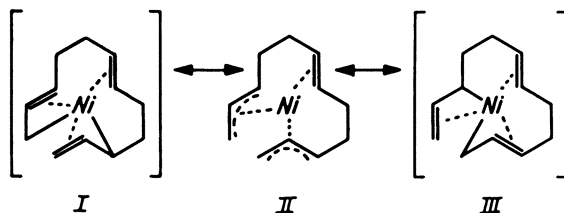
Shaking with hydrogen gave metallic nickel and *n*-dodecane.

Heating the complex to 100° C. and then shaking with hydrogen formed metallic nickel and cyclododecane.

Reaction with CO at -60° C. yielded nickel carbonyl and a C₁₃ ketone.

Addition of one mole of P(C₂H₅)₃ formed a crystalline complex which was identical with the compound obtained from cyclododecatriene-centro-nickel and P(C₂H₅)₃.

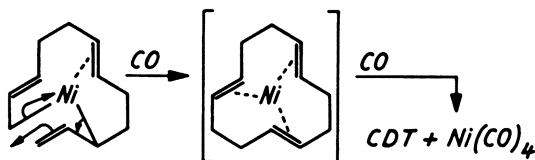
How can these results be interpreted? To clear up this question, the following mechanism for the structure of this intermediate complex has been proposed:



Formula II shows one trans-double bond which is shared with the nickel atom. Furthermore, there are six carbon atoms which are in the state of an *sp*²-hybridization. Each C atom shares one π -electron with the nickel. (The complex shows the correct molecular weight for NiC₁₂H₁₈, and there is no absorption in the infrared spectrum characteristic of double bonds.) This formulation has some relationship to structures which have been recently proposed by different authors (2, 4) for various allylic groups bonded to transition metal carbonyls.

Formulas I and III represent two alternate structures with σ bonds between the carbon and nickel, which allow the above-mentioned reactions to be explained in a classical manner:

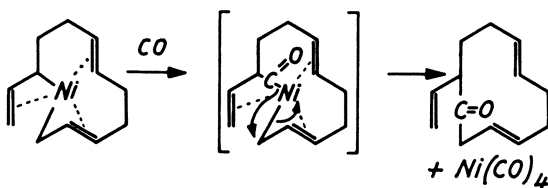
Reaction with carbon monoxide at room temperature effects an electron migration resulting in ring closure. Then cyclododecatriene is displaced by more CO molecules:



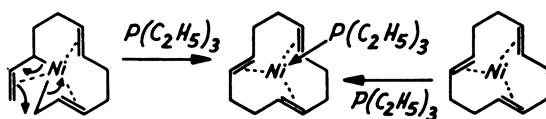
Hydrogenation prevents ring formation because hydrogen atoms become bonded to both ends of the chain; *n*-dodecane is obtained as the hydrogenation product.

Heat-initiated electron migration leads to ring closure. This step is similar to the first step of the CO reaction. The following decomposition gives cyclo-dodecatriene, which forms cyclododecane when hydrogenated.

In the course of the CO reaction at -60°C ., one CO molecule will be introduced between one of the Ni-C bonds formulated in the alternative structures, and electron migration results in formation of the ketone:



Finally, the addition of one molecule of $\text{P}(\text{C}_2\text{H}_5)_3$ induces an electron migration with formation of cyclododecatriene. No displacement occurs and the product obtained is identical to that prepared from the cyclododecatriene-centro-nickel complex itself:



Summary

A definite intermediate in the trimerization reaction, which gives very detailed information about the reaction mechanism has been isolated. In addition, a very simple method for the synthesis of 1,5-cyclo-octadiene in yields of 95% has been developed. This process seems to have some technical interest, because 1,5-cyclo-octadiene is a very valuable starting material for producing suberic acid and caprolactam.

Literature Cited

- (1) Burks, R. E. Sekul, A. A. (to Cities Service Research and Development Co.), U. S. Patent 2,972,640 (April 27, 1959).
- (2) Dehm, H. C., Chien, J. C. W., *J. Am. Chem. Soc.* **82**, 4429-30 (1960).
- (3) Greenwood, N. N., Morris, J. H., *J. Chem. Soc.*, **1960**, 2922-7.
- (4) Heck, R. F., Breslow, D. S., *J. Am. Chem. Soc.* **83**, 1097-102 (1961).
- (5) Reed, H. W. B., *J. Chem. Soc.* **1954**, 1931-41.
- (6) Sekul, A. A., Sellers, H. G. (to Cities Service Research and Development Co.), U. S. Patent 2,964,575 (April 2, 1959).
- (7) Wilke, G., *J. Polymer Sci.* **38**, 45-50 (1959).
- (8) Ziegler, K., Gellert, H. G., Holzkamp, E., Wilke, G., *Brennstoff-Chem.* **35**, 321-5 (1954).
- (9) Ziegler, K., Martin, H., *Makromol. Chem.* **18/19**, 186-94 (1956).

- (10) Ziegler, K., Sauer, H., Bruns, L., Froitzheim-Kühlhorn, H., Schneider, J., *Liebigs Ann. Chem.* **589**, 122-56 (1954).
- (11) Ziegler, K., Wilms, H., *Ibid.*, **567**, 1-43 (1950).

RECEIVED October 9, 1961.

Production of C₁₂-C₁₈ Alpha-Olefins by Polymerization of Ethylene on Triethylaluminum

HARRY TECKLENBURG and ADRIAAN KESSLER

Research and Development Department, Exploratory Development Division, The Procter & Gamble Co., Cincinnati, Ohio

C₁₂-C₁₈ olefins are prepared by a modified Ziegler α -olefin process based on ethylene and triethylaluminum. The process consists of five steps: buildup, displacement, separation, alkylation, and recycle. The major chemical and economic problems encountered are wide molecular weight distribution of the products and incomplete recovery of triethylaluminum. Catalysts consisting of alkylaluminums and colloidal nickel are needed for the alkylation-displacement steps; however, the amount of nickel has to be very low because in the other process steps, nickel favors side reactions. The yield of α -olefins in the C₁₂-C₁₈ range is increased by using coordination compounds of triethylaluminum with a Lewis base followed by azeotropic distillation. In the Chlorex process, (bis- α -chloroethyl) ether is used because of easy availability and low cost.

The pioneering work of Karl Ziegler on aluminum-carbon bond chemistry has resulted in several important industrial processes. One of these involves polymerization of ethylene with triethylaluminum and titanium chloride to produce high density polyethylene. Another process results in high molecular weight normal alcohols via the addition of ethylene to triethylaluminum followed by oxidation and hydrolysis (7, 8). A plant using this process is expected to be on stream in the near future.

In his many publications, Ziegler has pointed out that a variety of other useful materials may be produced through the ethylene-triethylaluminum reactions. One of these routes deals with the production of high molecular weight n - α -olefins (4, 5, 9, 10).

Ziegler's proposed α -olefin process consists of two chemical reactions. In the first, ethylene is added in a controlled manner to triethylaluminum to produce high (C₄ to C₂₂) molecular weight alkylaluminums (Figure 1). This reaction has been extensively studied. The reaction proceeds smoothly at moderate

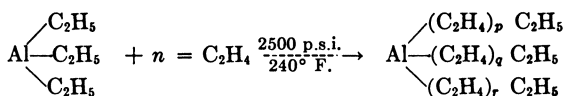


Figure 1. Buildup reaction

conditions, 2500 p.s.i. and 240° F. A small amount of α -olefin is produced through a thermal cracking side reaction. Ethylene addition to aluminum proceeds in a statistically random manner. Consequently, the resultant alkylaluminums cover a wide molecular weight range as described by the Poisson distribution.

In the second reaction, ethylene is reacted with the alkylaluminums to form n - α -olefins and to regenerate triethylaluminum (Figure 2). Although the reaction can be conducted without a catalyst by operating at high temperatures (3, 6), the reaction is normally carried out at lower temperatures in the presence of a nickel, cobalt, or platinum catalyst. Reaction conditions are moderate, 2500 p.s.i. and 200° F. when less than 0.01% of nickel catalyst is used. The catalyst is formed in situ by the addition of a nickel salt. A small amount of alkylaluminum will react with the nickel salt, reducing it to colloidal nickel.

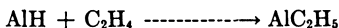
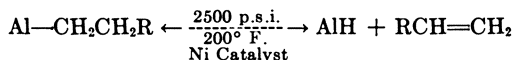


Figure 2. Displacement reaction

The net, over-all reaction of the Ziegler α -olefin process is the addition of ethylene to alkylaluminums to form n - α -olefins and to regenerate triethylaluminum.

Economic evaluation indicates two areas as being vital to any industrial process. The first of these involves the wide molecular weight distribution of the product. Considerable economic value would accrue, if the molecular weight distribution were narrowed to approach that of coconut oil (Figure 3.) Such a narrow distribution demands recycle of the low-molecular-weight olefins so that their molecular weight may be increased to the desired weight range by further addition of ethylene.

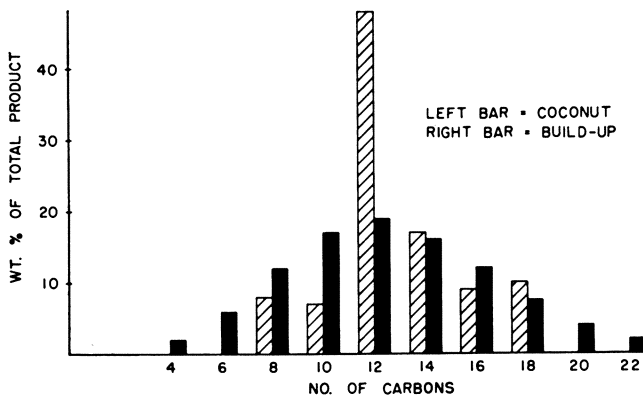


Figure 3. Chain length distributions of coconut oil vs. ethylene buildup

The second area of importance involves the complete and economic recovery of triethylaluminum. If this is accomplished, the triethylaluminum can be recycled and therefore will enter the net process essentially as a catalyst.

A complicating feature in any α -olefin process where C_{12} and C_{14} olefins must be separated from triethylaluminum (TEA) is the difficulty encountered in effecting this separation. Because of the small volatility differences among dodecene, tetradecene, and TEA, good separations will require efficient, multiplate columns. With such equipment, high still pot temperatures will be encountered, even at very low overhead pressures. Under such conditions, backreaction of TEA with the dodecene and tetradecene occurs rapidly and excessive olefin and TEA loss will result.

This article covers the authors' investigations into the two critical areas previously mentioned and includes considerable discussion on means of circumventing the prevailing difficulties.

α -Olefin-Triethylaluminum Reactions

Alkylation Reaction. In the second reaction of the Ziegler α -olefin process, ethylene is added to alkylaluminums in the presence of nickel catalyst to form n - α -olefins and triethylaluminum (Figure 2). In the presence of nickel, alkylaluminums seem to exist in a state of dynamic equilibrium between the alkylaluminum on one hand and α -olefin and aluminum hydride on the other (9). In displacement, the equilibrium is forced to the olefin-triethylaluminum side by introducing ethylene into the system. The reverse reaction can be accomplished by adding α -olefins to the system and by removing ethylene as it is formed. The final molecular weight distribution of the alkylaluminums formed will be the same as that of the olefin fed to the system. This reverse reaction—formation of alkylaluminums from triethylaluminum and olefins—might be called alkylation.

This basic displacement-alkylation exchange is catalyzed very effectively by nickel. Present studies have been restricted to the use of various nickel compounds and it has been concluded that colloidal, metallic nickel is the most active form. In practice, addition of some easily reduced nickel salt—i.e., nickel formate—to the alkylaluminum mixture results in efficient reduction to colloidal nickel.

The major side reaction accompanying the alkylation reaction is isomerization of the α -olefins to internal olefins. The internal olefins formed as a result of isomerization are unreactive toward triethylaluminum and represent a loss to the process. It is therefore important to minimize the extent of double bond shifting.

Isomerization results from the simultaneous contact of triethylaluminum, nickel, and α -olefins and is strongly dependent on both temperature and catalyst level. Low temperature operation is necessary at the expense of increasing the required reaction time (Table I).

Table I. Effect of Alkylation Temperature on Isomerization

Temp., °F.	(Raney nickel catalyst)		
	Alkylation Completeness, %	Unreacted Olefin Isomerized, %	Reaction Time, Hr.
141	47	16	0.15
75	79	8	1.50

The catalyst level should be set as low as possible. Decreasing catalyst concen-

**American Chemical Society
Library**

tration is also accompanied by a decrease in reaction rate (Table II). Obviously, an over-all balance must be struck involving temperature and catalyst level on one hand, and the allowable loss of product as internal olefin on the other.

Table II. Effect of Catalyst Level on Isomerization

(Raney nickel catalyst at 77° F.)

<i>Nickel Level, P.P.M.</i>	<i>Reaction Time, Hr.</i>	<i>Alkylation Completeness, %</i>	<i>Unreacted Olefin Isomerized, %</i>
10,000	1	82	36
5,000	1	83	14
2,000	1.3	78	4
1,000	1.8	79	4

In addition to the factors just discussed, isomerization seems to be appreciably affected by the ratio of triethylaluminum to olefin. Since the alkylation reaction is relatively slow at the temperature and catalyst levels necessary for minimizing isomerization, mixing of the entire olefin and triethylaluminum streams will give a system relatively high in free triethylaluminum during the initial stages of the reaction. Significantly, more isomerization will result under these conditions than if the triethylaluminum is added over a period of 0.5 hour or more, so that the free TEA level at any given time is kept low (Table III).

Table III. Effect of Alkylaluminum Level on Isomerization

(Raney nickel catalyst)

<i>Time to Add TEA to Olefin</i>	<i>Alkylation Completeness, %</i>	<i>Unreacted Olefin Isomerized, %</i>
57 minutes	73	9
20 seconds	71	20

A favorable factor tending to limit isomerization is that in any practical olefin process, only the lower molecular weight olefins, C₁₀ and below, will be recycled for alkylation. As long as a reasonable recovery of the triethylaluminum can be achieved, there will be more TEA available than required for stoichiometric addition of all the recycled light olefins. This, of course means that it will not be necessary to push for complete alkylation of the recycled TEA. Since it can be shown that isomerization increases rapidly as alkylation is pushed past aluminum-dialkylethyl toward complete alkylation, the advantage of a partial alkylation is obvious (Figure 4).

One of the vexing problems in developing an integrated α -olefin process is the necessity of using colloidal nickel in the displacement and alkylation steps, while in the rest of the process, buildup and olefin-TEA separation, the presence of nickel is very undesirable. The effect of nickel in these operations is to cause premature displacement during buildup, premature alkylation (TEA loss) during separation, and branched and internal olefin formation during both steps.

The colloidal nickel catalyst cannot be removed by conventional filtration techniques nor have effective means of deactivation by poisoning been found. Ziegler claims that addition of colloidal iron will poison the nickel catalyst. The use of iron and other potential nickel poisons has been studied in some detail. Salts of Cd, Cu, Cr, Fe, Hg, Se, V, and Zn along with phenylacetylene and sulfur dichloride have been tested as nickel deactivators. Iron, cadmium, and copper salts seemed effective in limiting alkylation between olefins and triethylaluminum

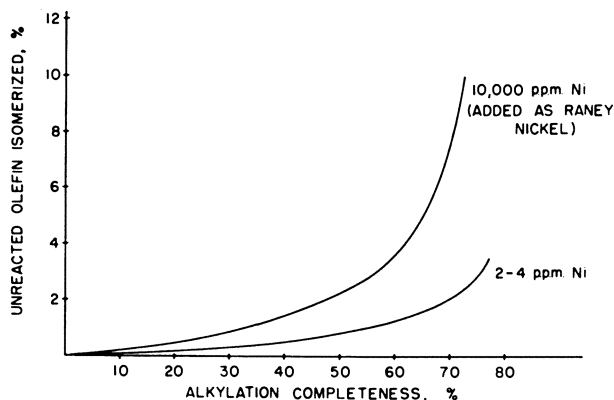


Figure 4. Effect of alkylation completeness on isomerization

during the separation phase of the process with cadmium being perhaps more effective and freer from undesirable side reactions. However, none of these materials were effective nickel deactivators at the conditions necessary for buildup.

Only a compromise solution to the nickel dilemma has been found. A combination of an extremely low catalyst level and a fairly high reaction temperature will allow one to conduct the alkylation reaction—as well as subsequent reaction steps of the α -olefin process scheme—with a minimum amount of side reactions. The use of such small amounts of catalyst necessitates fairly long alkylation reaction times (Table IV).

Table IV. Recommended Alkylation Conditions

(Nickel formate catalyst)

Feed	Temp., °F.	Catalyst, P.P.M. Ni on TEA Basis	Time, Hr.	Internal Olefin, %	
				50% completion	70% completion
C ₆ -C ₁₀ olefins excess	140- 180	2-4	4-5	1	2

Displacement Reaction. Much of what has been said about the alkylation reaction is also valid for the displacement reaction. Here also it is of importance to keep the nickel level as low as possible, not only to prevent isomerization and branching during displacement, but especially to circumvent trouble during the subsequent separation of TEA from olefins.

The displacement reaction is followed by a separation step. This step is necessary in order to remove the high molecular weight olefins (C₁₈ to C₂₀) and the nickel catalyst from the recirculation stream. Were the separation step to be omitted, the high molecular weight olefin fraction and the nickel catalyst would—in a recycle process—quickly build up to an unacceptable high level. Thus, separation must be viewed as an integral part of the preceding displacement reaction and the displacement should be conducted in such a manner that side reactions during separation are minimized.

Contrary to the alkylation reaction, it is necessary to push displacement to the highest possible completeness. Any alkylaluminum that has not been converted to TEA and olefins will wind up in the bottoms of the evaporator and con-

stitute a loss of TEA as well as ethylene. It is not surprising, therefore, to find that higher nickel levels are required for the displacement reaction than for the alkylation reaction (Figure 5).

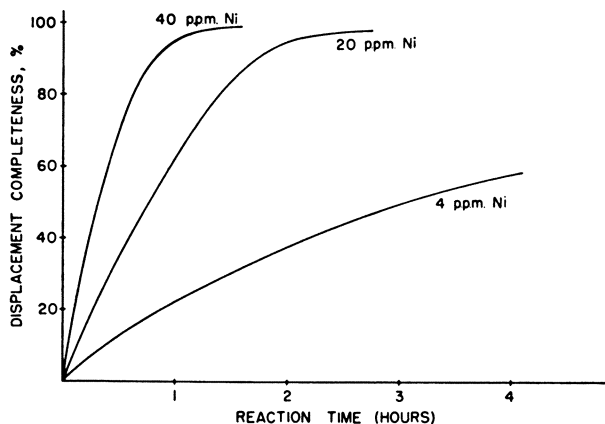


Figure 5. Effect of catalyst level on rate of displacement

At least 20 p.p.m. of nickel (TEA basis) are required in order to obtain 97 to 99% displacement within 2 hours (200° F., 2000 p.s.i. of ethylene). After completion of the reaction, when the ethylene pressure is released, a displacement reaction product containing traces of nickel catalyst tends to revert to alkylaluminum. This reaction takes place slowly at room temperature and atmospheric pressure, but the rate accelerates at the conditions required for TEA-olefin separation. It is no surprise, then, that even after only a few seconds' contact a significant amount of back-alkylation will take place.

A number of displacement mixtures have been processed in a small-scale, wiped-film evaporator. The residence time of the liquid phase in this apparatus is approximately 15 seconds. Notwithstanding this short residence time, it was found that at least 10% of the TEA present in the feed back-alkylates and stays in the bottoms as alkylaluminum. Although it appears reasonable to expect that somewhat better results can be obtained when working with an easier to control, larger scale evaporator, it is unlikely that the TEA loss at this stage can ever be reduced below a 5 to 10% level.

With the three main reaction steps of the process—buildup, displacement, and alkylation—shown to be feasible, the next step in this investigation was to explore the feasibility of performing the necessary separations between TEA and olefins and also to arrange the various reaction steps to provide a complete α -olefin process with TEA recycle.

Separation of Triethylaluminum from Product α -Olefin

A large number of methods for the separation of triethylaluminum and the product n - α -olefins have been investigated. Room or low temperature separations based on solvent extraction, absorption, or crystallization have been uniformly unsuccessful. Therefore it seemed that the only hope for success lay in devising some scheme employing volatility differences in order to effect a separation, or partial separation, of triethylaluminum from the product α -olefin.

Evaporative Process. Two methods of conducting the separation and recycle process have been investigated. According to the first method, the process is arranged in such a manner that only evaporators (agitated, wetted-wall type) are needed for the various separation steps.

The process is based on the previous observation that in the absence of ethylene, olefins alkylate TEA in proportion to the concentration of each individual olefin present in the alkylation mixture. Thus, the distribution of alkyl groups of the alkylated TEA will be equal to the olefin chain length distribution fed to the alkylator.

By maintaining a heavy recycle of low molecular weight olefins through the alkylation reactor, a ratio of 6 parts of C_6 to C_{10} olefins to one part of C_{12} and higher olefins can be maintained in the reactor. Accordingly, one will obtain alkylaluminums containing six C_6 to C_{10} alkyl groups for one alkyl group in the C_{12} to C_{18} range (Figure 6).

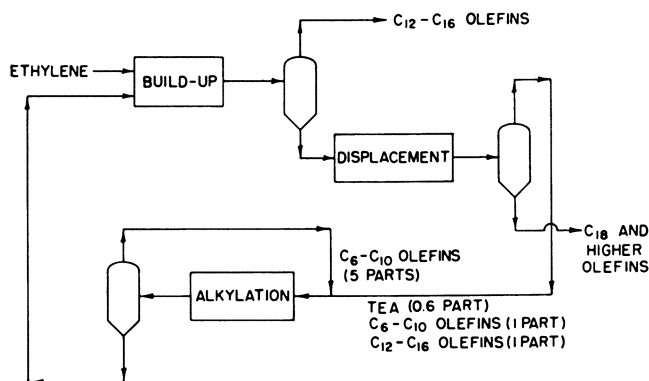


Figure 6. Evaporative α -olefin process

The product from the alkylator is then recycled to the buildup reactor. The built-up alkyls will contain the product olefins which can now be separated from the alkylaluminums, since their volatility relative to the alkyls is high. This part of the process has been suggested by Ziegler and is feasible (10).

An advantage of the process is that virtually all of the olefins can be removed from the TEA recycle stream in only two separation steps. A serious disadvantage, however, is the huge volume of material recirculating through the alkylator. This means that large pieces of equipment will be needed and a sizable utility load can be expected. Also, because of the large quantities of olefins present, the amounts of internal C_6 to C_{10} olefins formed during alkylation will be rather high: 5 to 6% on the basis of the C_{12} to C_{18} olefin product stream. These internal olefins will tend to build up in the recycle stream, since they are not reactive with TEA, so a portion of the recycle must be continuously bled off.

A problem still to be considered is the effect of the transfer of traces of nickel from the alkylation reactor to the buildup reactor.

The presence of nickel during the buildup reaction tends to cause displacement rather than to promote buildup. This has to be avoided as far as possible, since it leads to formation of vinylidene-type, branched olefins. Also, the olefins formed by displacement during the buildup step possess a relatively flat chain

length distribution curve. Thus, one might wind up with producing more C_8 to C_{10} α -olefins than can be taken care of in the alkylation reactor. These side reactions can be kept to a minimum by conducting the alkylation reaction with the minimum amount of nickel catalyst (4 p.p.m. on TEA basis). Buildup of C_8 to C_{10} alkylaluminums alkylated at optimum conditions resulted in the formation of 10 to 15% olefins. This compares well with 5 to 10% olefin formation during buildup in a completely nickel-free system.

The olefin product distribution has been calculated by assuming an aluminum buildup according to the Poisson distribution function. For these calculations, it was assumed that the alkylation reaction is conducted to 58% completeness and that two ethylene groups per pass are added to the alkylaluminums during buildup.

Calculations showed that 73% of the olefin product stream can be placed in the desired C_{12} to C_{18} chain length range. This is a considerable improvement over the 58% attained with a simple recycle process without the alkylation reaction.

Chlorex Process. An even higher percentage of α -olefins can be placed in the C_{12} to C_{18} chain length range, when following a second method of carrying out the α -olefin process. This method is based on the ability of TEA to form coordination compounds with a Lewis base (1,2).

Compounds such as ethers, tertiary amines, or dialkyl sulfides have been considered. A detailed study was made of the reaction between TEA and ethers to find an ether which would facilitate TEA-olefin fractionation, while leaving TEA still sufficiently reactive for use in subsequent reaction steps.

The strength of the complexes formed with ethers depends on the electron-releasing capacity and the steric configuration of the particular ether used (Table V). Initially, it was planned to deactivate TEA by reaction with a strong complex

Table V. TEA-Ether Complexes

Strong complexes	}	No buildup possible at 250° F., 2500 p.s.i.
Straight-chain ethers Dibenzyl ether		
Intermediate complexes	}	Buildup rate 30-50% of regular rate
Dimethoxybenzene		
Methoxybenzene (anisole)		
Ethoxybenzene (phenethole) Phenylbenzyl ether Chlorex[(bis- β -chloroethyl) ether]		
Weak complexes	}	Buildup rate about 75% of regular rate
Diphenyl ether		

former such as dibenzyl ether, in order to break this complex again after completing the necessary TEA-olefin separations, and thus to be able to regenerate TEA for use in subsequent reaction steps. It was found, however, that the complexes—once formed—cannot be broken again. When destructive distillation at temperatures of 500° to 600° F. was attempted, TEA decomposed before the complex could be broken.

The next best approach was to use ethers of intermediate complexing ability. TEA coordination compounds formed with such ethers are still able to add ethylene and can be built up to alkylaluminums at reduced rates. As a fortuitous feature, it was found that after buildup to C_{10} or higher alkylaluminums, the bond strength of the complex is sufficiently reduced that the ether can be removed by a simple, evaporation step.

In the group of ethers of intermediate complexing ability, Chlorex [(bis- α -chloroethyl) ether] is preferred because of easy availability and low cost. Presence of electron negative chlorine atoms in the Chlorex molecule reduces the electron-releasing capacity of the oxygen atom and in turn reduces the bond strength with TEA.

Addition of Chlorex has the following main effects on TEA-olefin fractionation:

Side reactions during fractionation are suppressed.

A TEA-Chlorex azeotrope, boiling at a 32° F. higher temperature than uncomplexed TEA, is formed.

A ternary, TEA-Chlorex-tetradecene azeotrope is formed. This azeotrope boils at a lower temperature than the binary azeotrope.

The main side reaction encountered during vacuum fractionation at elevated temperatures, is back-reaction of TEA with α -olefin to form alkylaluminums. This reaction takes place even in the absence of nickel catalyst. As shown, the presence of Chlorex (at a 1 to 1 TEA to Chlorex ratio) cuts alkylation in half (Figure 7).

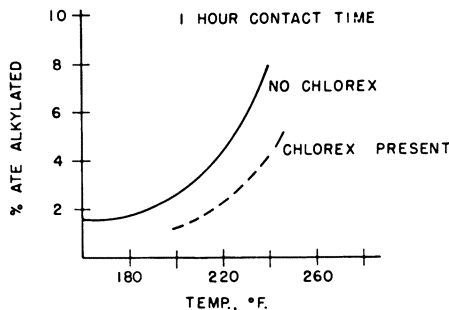


Figure 7. Thermal alkylation of triethylaluminum during distillation to diethylalkylaluminum

The TEA-Chlorex azeotrope consists of approximately 1 part of TEA and 1 part of Chlorex. The presence of Chlorex increases the relative volatility between dodecene and TEA from 1.4 to 11.0 as measured in a Colburn equilibrium still. Separation of dodecene from TEA thus becomes a relatively simple matter. Most of the dodecene can be removed with little TEA contamination in a column with five to ten theoretical plates operating at a reflux ratio of 1 to 1.

The ternary, tetradecene-TEA-Chlorex azeotrope consists of approximately 2 parts of tetradecene, 1 part of TEA, and 1 part of Chlorex. The boiling point of this azeotrope is several degrees below the boiling point of the binary azeotrope. An essentially complete separation between the ternary and binary azeotropes has been achieved in a column of approximately five theoretical plates at a reflux ratio of 1 to 1.

Thus, given a stream containing TEA, Chlorex, and C_{12} to C_{14} olefins, the dodecene, tetradecene, and a portion of the TEA feed can be removed overhead from the remainder of the TEA. When producing detergent-range olefins, the TEA-olefin stream is of such a composition that 60 to 70% of the TEA recycle will remain in the still pot after removal of tetradecene as a ternary azeotrope. This means that sufficient TEA, freed of dodecene and tetradecene, will be available for use in the alkylation reaction. A recycle process for the production of

α -olefins with Chlorex as separation aid can now be worked out. The resulting process is rather complicated with a large number of evaporation and distillation steps. A simplified version is shown (Figure 8).

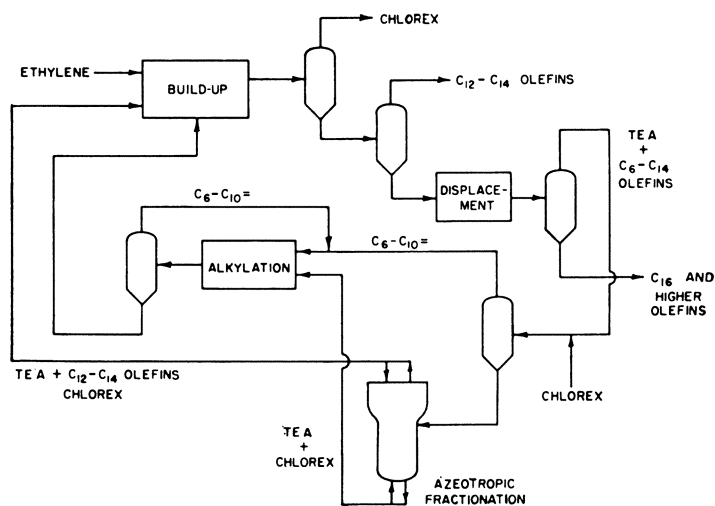


Figure 8. Chlorex α -olefin process

The major steps in the process are buildup, displacement, separation, and alkylation. A convenient starting point in analyzing the system is the effluent from the displacement reactor. The stream at this point consists primarily of triethylaluminum, ethylene, α -olefins from C_6 to C_{18} and above, and minor quantities of the nickel displacement catalyst.

Ethylene is rather easily recovered because of its high volatility and this step is not shown. TEA and the C_6 to C_{14} olefins are then taken off overhead, leaving the C_{16+} olefins, alkylaluminums resulting from back-alkylation, and the nickel catalyst in the bottoms stream. Wiped film evaporators are used here—high rectification efficiency is not required—since such equipment subjects the product to a minimum of time at high temperature. C_{16} , C_{18} , and any other olefins of value are recovered from the bottoms stream as desired.

Chlorex is added to the overhead stream, and since the complexing reaction is practically instantaneous, the resulting mixture can be fed without delay into another evaporator. The overheads stream from this separation is essentially C_6 to C_{10} olefins. Since the bottoms stream has previously been freed of nickel catalyst, it can be successfully distilled as long as reasonable temperature limits are met. The distillation overheads are composed of C_{12} olefin, the C_{14} olefin-TEA-Chlorex ternary azeotrope, and some of the TEA-Chlorex complex. This stream is sent to the buildup reactor. The still bottoms contain most of the TEA, freed of C_{12} and C_{14} olefins, and they can therefore be used to alkylate the C_6 to C_{10} stream. An excess of the C_6 to C_{10} cut is maintained as recycle to aid in alkylation. The alkylated stream is fed into the buildup reactor at about the halfway point. Actually, it would probably be best to alkylate the C_6 to C_8 olefins separately from the decene. This would allow splitting the recycle streams

so that most of the ethylene will be added to the recycle TEA and least to the decene.

Once the triethylaluminum is built up to long chain alkyls, the strength of the alkylaluminum-Chlorex complex is weakened so that Chlorex can easily be recovered after buildup. The principal product consisting of C_{12} and C_{14} olefins is also taken off at this point and the remaining alkylaluminums are then ready for displacement in the next operation cycle.

A calculation of the product distribution theoretically feasible with the process just outlined shows that 84 to 85% of the olefin product stream can be placed in desired C_{12} to C_{18} chain length range.

For this calculation, it was assumed that the alkylation reaction was conducted to 75% completeness and that in the buildup reactor 4.5 ethylene groups are added per pass to the recirculated TEA, 2.5 ethylene groups to the C_6 to C_8 alkylaluminums, and 1.5 ethylene groups to the C_{10} alkylaluminums. A good comparison between the various methods of producing α -olefins can be made by plotting the chain length distribution of the olefin product streams. This graph clearly indicates the advantage of the Chlorex process (Figure 9).

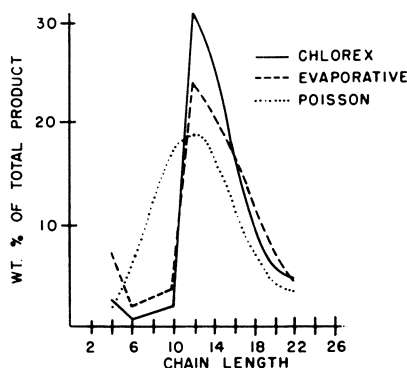


Figure 9. α -Olefins chain length distribution

In the evaporative process, considerably higher amounts of low molecular weight olefins are formed—especially butene—at the cost of reducing the amounts of dodecene and tetradecene produced.

Conclusion

Both of the processes discussed offer significant improvements over the α -olefin process suggested by Ziegler. The starting point for both is a reduction of the nickel catalyst in the displacement and alkylation steps to low enough levels that the rest of the processes can be operated without poisoning or destroying the catalyst.

One process makes no attempt to separate product olefins from TEA after displacement, but employs a heavy recycle of C_6 to C_{10} olefins in alkylation to obtain a selective alkylation of these olefins with the free TEA in the displacement stream before recycle through buildup.

The other process capitalizes on complex formation between TEA and β, β' -dichloroethyl ether to allow separation of sufficient free TEA from the displace-

ment stream to allow direct alkylation of the lower molecular weight (C_8 to C_{10}) olefins.

Both processes are complicated by carry-over of nickel into the separation and buildup steps. Significant simplification of both processes would be possible, if a satisfactory means of inactivating the catalyst could be found.

Literature Cited

- (1) Bonitz, E., *Ber.* **88**, 742 (1955).
- (2) Geiseler, G., Knothe, W., *Ibid.*, **91**, 2446 (1958).
- (3) Skinner, W. A., Bishop, E., Cambour, P., Fugua, S., Lim, P., *Ind. Eng. Chem.* **52**, 695 (1960).
- (4) Ziegler, K., *Angew. Chem.* **64**, 323 (1952).
- (5) *Ibid.*, **68**, 721 (1956).
- (6) *Ibid.*, **72**, 829 (1960).
- (7) Ziegler, K., Ger. Patent **1,014,088** (July 21, 1960).
- (8) Ziegler, K., U. S. Patent **2,699,457** (Jan. 11, 1955).
- (9) Ziegler, K., Gellert, H. G., Holzkamp, E., Wilke, G., Duck, E., Kroll, W. R., *Liebigs Ann. Chem.* **629**, 172 (1960).
- (10) Ziegler, K., Wilke, G., Holzkamp, E. (to K. Ziegler), U. S. Patent **2,781,410** (Feb. 12, 1957).

RECEIVED September 6, 1961.

Degradation of Polymers

ROBERT SIMHA

Department of Chemistry, University of Southern California, Los Angeles, Calif.

In the main chain breakdown of a polymer by pyrolysis, two competing processes are decisive: a random scission caused by intermolecular radical attack and a depropagation of macroradicals. In terms of these, the observed correlations between monomer yields, rates of volatilization, and decrease of average molecular weight can be interpreted. The relative importance of the two mechanisms for a specific polymer is a function of its structure and this accounts for the wide qualitative and quantitative differences between different systems. For a given structure, the initial average molecular weight, the distribution of chain lengths, branching and impurities or structural inhomogeneities in the chain have important kinetic consequences. The role of these factors presents important experimental and theoretical problems which have been investigated conclusively only in part. Another problem is a quantitative or qualitative analysis of the radicals present in a pyrolyzing polymer.

Kinetic studies of free radical mechanisms or heat stability tests of new polymers have evolved from the large amount of experimental work, during the past 15 years, on the rates of volatilization of polymers (9, 11, 22). Concurrently, general theories on the degradation process were developed (18, 22) and their quantitative conclusions were compared with experimental results. The limited experimental data and the complexity of the equations involved have restricted the comparisons for the most part to special cases which could be treated analytically.

In this article, we summarize the basic kinetic observations and principles involved in pyrolytic degradations and present some selected and partially solved problems on reactions based on chain breakdown of vinyl-type polymers.

Basic Observations

After a polymerization has been initiated, the important step is the propagation of active centers, the rate of which equals $k_p MR$, where M and R represent

monomer and (in a free radical process) radical concentrations, respectively. This latter rate increases with increasing temperature. At the same time, however, k_2R , the rate of the reverse process—namely, the depropagation or evolution of monomer from a radical—also increases. We have the following relation between the corresponding activation energies

$$E_p + \Delta H = E_2 \quad (1)$$

where ΔH is the thermodynamic heat of polymerization. Hence, the depropagation increases more rapidly with temperature. Finally, at the so-called ceiling temperature, T_c , the two rates become equal (5). T_c is a function of monomer concentration and is conventionally referred to one mole per liter or 1 at. for a gaseous monomer. The evaluation of ceiling temperatures has been discussed in detail by Dainton and Ivin (5) who have tabulated values for a series of vinyl polymers. It is of interest to compare these temperatures with another set of temperatures, characteristic of the degradation process. They involve an arbitrary choice of a reference rate of decomposition. Table I shows decomposition temperatures T_d (28), referred to a rate of volatilization of 1% per minute in vacuum. The latter varies with the degree of conversion to volatiles, either decreasing monotonically or reaching a maximum. The reference rates used in the construction of Table I are the largest ones throughout. There are considerable uncertainties in the magnitudes of the T_c 's, augmented by the fact that the reference states vary for different polymer-monomer systems. Nevertheless, for most polymers shown, T_d is considerably larger than T_c —as expected—but in polyethylene, both are about equal. For polytetrafluoroethylene, on the other hand, T_d is lower by about 150° C. which implies a relatively high rate of decomposition. This cannot be associated with a low value for the activation energy E_2 in Equation 1, since ΔH is about 40 kcal. per mole (15), considerably higher than for hydrogenated polymers. Hence, the radical concentration must be high. This, in turn, would indicate a high rate of initiation and/or low probability of termination which may be a chemical or simply a physical effect, arising from a diffusion controlled and, therefore, reduced termination rate.

Table I. Decomposition Temperatures, T_d , for a Series of Polymers, Referred to 1%/Minute (28)

<i>Polymer</i>	<i>T_d °C.</i>
Tetrafluoroethylene	510
Ethylene	400
Propylene	380
Styrene	360
Methyl methacrylate	330
Methacrylonitrile	>200
Isobutylene	340
α -Methylstyrene	290
Formaldehyde	>100

The T_d 's in Table I imply wide variations in rates, but not necessarily in mechanism, which could possibly be simple monomer depropagation. That this is not so, in all cases, is concluded at once from an inspection of the volatile decomposition products. Table II (18) summarizes the mass spectrometric yields of monomer, obtained by Madorsky and his colleagues at the National Bureau of Standards. Briefly, we note the high yields of monomer in the α -substituted and fluorinated vinyls. Elimination of the α -substituents or the fluorine atoms reduces considerably the monomer yield. This is illustrated by a comparison of poly-

(methyl methacrylate) with poly(methyl acrylate), poly(α -methylstyrene) with polystyrene, and polytetrafluoroethylene with polytrifluoroethylene. Thus, we observe a wide spectrum of monomer yields ranging from practically zero in polyethylene to almost 100% in α -substituted polymers and Teflon.

Table II. Monomer Yields

Polymer	Formula	Weight %	Polymer	Formula	Weight %
Methyl methacrylate	$\begin{array}{c} \text{CH}_3 \\ \\ -\text{CH}_2-\text{C}- \\ \\ \text{CH}_3\text{OCO} \end{array}$	>95	β -Deuterostyrene	$\begin{array}{c} \text{H} \\ \\ -\text{CHDC}- \\ \\ \text{C}_6\text{H}_5 \end{array}$	42
Methyl acrylate	$\begin{array}{c} \text{H} \\ \\ -\text{CH}_2-\text{C}- \\ \\ \text{CH}_3\text{OCO} \end{array}$	2	Isobutylene	$\begin{array}{c} \text{CH}_3 \\ \\ -\text{CH}_2-\text{C}- \\ \\ \text{CH}_3 \end{array}$	≈ 20
α -Methylstyrene	$\begin{array}{c} \text{CH}_3 \\ \\ -\text{CH}_2-\text{C}- \\ \\ \text{C}_6\text{H}_5 \end{array}$	>95	Propylene	$\begin{array}{c} \text{H} \\ \\ -\text{CH}_2-\text{C}- \\ \\ \text{CH}_3 \end{array}$	2
α -Deuterostyrene	$\begin{array}{c} \text{D} \\ \\ -\text{CH}_2-\text{C}- \\ \\ \text{C}_6\text{H}_5 \end{array}$	70	Ethylene	$-\text{CH}_2-\text{CH}_2-$	0.025
m -Methylstyrene	$\begin{array}{c} \text{H} \\ \\ -\text{CH}_2-\text{C}- \\ \\ \text{C}_6\text{H}_4-\text{CH}_3 \end{array}$	52	Vinylcyclohexane	$\begin{array}{c} \text{H} \\ \\ -\text{CH}_2-\text{C}- \\ \\ \text{C}_6\text{H}_{11} \end{array}$	~ 0.1
Styrene	$\begin{array}{c} \text{H} \\ \\ -\text{CH}_2-\text{C}- \\ \\ \text{C}_6\text{H}_5 \end{array}$	42	Tetrafluoroethylene	$-\text{CF}_2-\text{CF}_2-$	>95
			Trifluorostyrene	$\begin{array}{c} \text{F} \\ \\ -\text{CF}_2-\text{C}- \\ \\ \text{C}_6\text{H}_5 \end{array}$	75
			Trifluorochloroethylene	$-\text{CF}_2\text{CFCl}-$	28
			Trifluoroethylene	$-\text{CF}_2\text{CFH}-$	<1
			Vinylidene fluoride	$-\text{CH}_2\text{CF}_2-$	<1
			Vinyl fluoride	$-\text{CH}_2\text{CHF}-$	<1

A similar spectrum emerges when we study the rates of decrease of molecular weight and hence physical properties and the rates of volatilization, both as a function of the weight fraction volatilized. The following general correlation holds (18):

High monomer yield \rightarrow Low rate of decrease of molecular weight \rightarrow High initial rate of volatilization.

The series poly(methyl methacrylate), polystyrene, and polyethylene is considered as an example. When 50% of the polymer has been volatilized, the degree of polymerization of the first polymer may change by ca. 20%—it is really a function of the initial molecular weight as shown below. In polyethylene, on

the other hand, we have reached chain lengths in the lubricating range, at this stage, even if the initial molecular weight is of the order of millions. In polystyrene, the decrease at a comparable extent of decomposition is intermediate—namely, by a factor of about 10. The decrease in the ratio $DP/DP(0)$ of the instantaneous and initial degrees of polymerization is a sensitive function of the latter in the α -substituted systems. This has been observed first in poly(methyl methacrylate) (10) and is illustrated for poly(α -methylstyrene) in Figure 1. Regardless of the scatter, the higher fraction is reduced more rapidly. Rates as a function of conversion are convenient to measure and have been obtained for a large number of polymers. We shall only note that in the systems with high monomer yields, the rates are initially large and decrease monotonically as the reaction proceeds, whereas in other polymers, such as polystyrene and linear polymethylene, a maximum occurs between 25 and 40% conversion. Significant exceptions to this correlation between rates and monomer yields are discussed later.

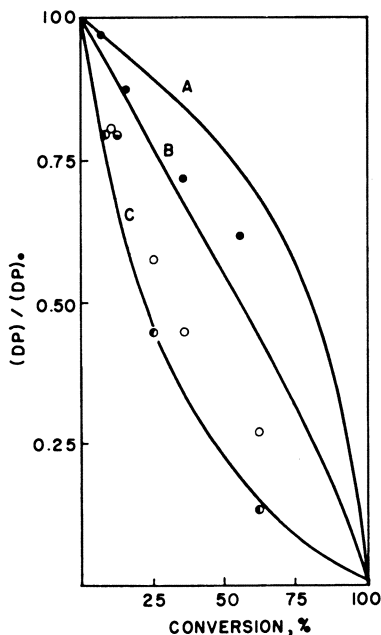


Figure 1. Effect of initial molecular weight on relative molecular weight decrease for poly(α -methylstyrene)

● 11×10^6 ○ 6×10^6 ● 1×10^6

A, B, and C represent theoretical curves for qualitative comparison only
From Simha, R., and Wall, L. A., *J. Chem. Phys.* 29, 894 (1958), Figure 9

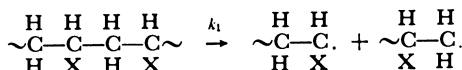
COURTESY *The Journal of Chemical Physics*

Basic Theory

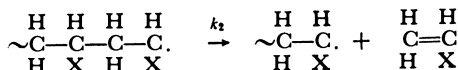
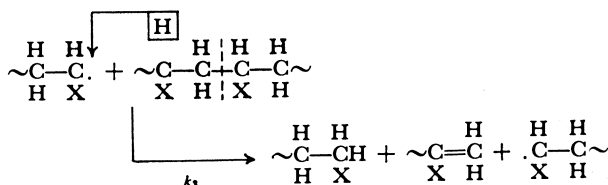
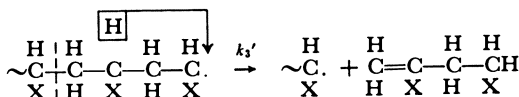
Some years ago Simha, Wall, and Blatz (24, 25) first developed a theory which accomplished two things. It established a unified point of view for the interpretation and correlation of the phenomena just summarized and it yielded

quantitative expressions for the rates and molecular weights of a degrading system as solutions of a set of difference-differential equations. Clearly, the free radical-induced degradation will proceed through a series of elementary reactions of the general type discussed in relation to the pyrolysis of low molecular weight compounds. Now, we are concerned with the total amount of volatiles, rather than their detailed composition (except for the monomer fraction), and with the molecular weight and the molecular weight distribution of the residue. It appears, then, that we can avoid a detailed consideration of the possible elementary reactions in our formulation of the kinetics. The mathematical difficulties would be considerable, even if these elementary processes were adequately known. Therefore, we introduced in our theory (25) a minimum number of reactions which are necessary to account for the "spectrum" observed. The reactions follow:

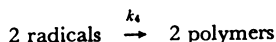
Initiation



Propagation

Transfer
(intermolecular)Transfer
(intramolecular)

Termination (disproportionation)



The depropagation reaction produces monomer, and the competing transfer and termination processes yield units in the decomposing radicals which ultimately result in nonmonomeric volatiles. In general, we have two important routes to pyrolysis, one through unzipping of polymer radicals, the other by means of random scission, resulting from a random attack of radicals on polymer molecules. The preponderance of one or another mode of breakdown depends on steric factors and the presence of labile groups.

Steric factors. It follows from Equation 1 and the known values of E_p and ΔH that E_2 is smaller by about 5 kcal. per mole for poly(methyl methacrylate) than for polystyrene. This is caused by the difference in ΔH which reflects steric effects. At 600° K., it means a factor of about 60 in the rates of depropagation, assuming the entropies of activation to be equal.

Availability of labile groups for abstraction (as in polymethylene). Moreover, ΔH for polymethylene is larger by about 10 kcal. per mole than for poly(methyl

methacrylate) and random scission is favored on two counts, as compared with the latter polymer, poly(α -methylstyrene) or even polystyrene. The above two factors are not entirely independent, however. The absence of α -substitution results both in a large ΔH and availability of a site for radical attack. Teflon, on the other hand, considering the monomer yield, degrades by unzipping. This is opposed by the high heat of polymerization, about 40 kcal. per mole (15), and is favored by the absence of labile groups. An additional factor, contributing to large average zip lengths, is a diffusion-controlled termination of radicals which is to be expected, particularly, in such a polymer. It appears, then, that the thermal stability of Teflon, in vacuum at least, may be ascribed to the absence of labile groups for radical attack and the extremely high E_2 as a consequence of the extremely high ΔH .

We will not present here the equations which follow from the above set of reactions, nor their analytical or numerical solutions (25, 26). These solutions provide the total rate of volatilization and the molecular weight distribution of the degrading polymer as a function of a dimensionless time parameter, the initial characteristics of the polymer, and two kinetic parameters—namely, the ratios:

$$\begin{aligned} 1/\epsilon - 1 &= \frac{\text{propagation}}{\text{transfer} + \text{termination}} = \text{number average zip length} & (3) \\ \sigma &= \frac{\text{transfer}}{\text{initiation}} = \text{transfer ratio} \end{aligned}$$

When the zip length is numerically large, of the order of a polymer chain length, the initial molecular-weight will determine whether a chain will be volatilized through one single zip, on the average, or will require repeated initiation followed by unzipping. This explains the results in Figure 1. The theory accounts for the correlation between monomer yields, molecular weight decrease, and rate in terms of the two parameters, Equation 3. When random scission is the dominant step, a maximum rate results, since volatiles are obtained from scissions near the chain ends and their number reaches a maximum. The gradual transition from the condition of a monotonically decreasing rate to a maximum one, as the zip length is reduced and the transfer ratio increases, has been demonstrated by high speed computations (26). When random scission is important, a third parameter must be considered which accounts for the competition between the rates of degradation and evaporation of relatively small molecules (24). In this manner, we estimated from kinetics and the average molecular weight of the volatiles that chain lengths of about 70 carbons lead to evaporation during the degradation of polymethylene. This agrees reasonably with what we would expect from the vapor pressures of *n*-alkanes at temperatures near 400° C.

The integration of the kinetic difference-differential equations results in independent expressions for the rate, average DP , and molecular weight distribution in a degrading polymer (25, 26). On the other hand, and mathematically more simple, we may search for intermediate solutions which interrelate two directly observable quantities—namely, the rate and the instantaneous number average DP . Physically, it is clear that relations must exist between the instantaneous values of the molar concentration of polymer, the rate of change of this concentration, and the rate of production of volatiles. Gordon (7) first derived such an expression for a special case of the scheme, Equation 2. The general expressions were derived by Simha (21). We have to distinguish two cases depending upon whether initiation of radicals in Equation 2 occurs at the chain ends or at random along the chain. A decision can be made, in some instances, from the dependence

of the initial rate on molecular weight. In methyl methacrylate, for example, the initiation starts at the chain ends (10), but then continues at random (3).

If initiation proceeds only at the chain ends and $\sigma = 0$, the result is (7, 21):

$$dC/dt[1 + 2(1/\epsilon - 1)/\bar{P}] + 2(1/\epsilon - 1)(1 - C)/\bar{P}^2 d\bar{P}/dt = 4k_1(1/\epsilon - 1)(1 - C)/\bar{P} \quad (4a)$$

where \bar{P} is the number average DP of the residue and C the weight fraction of polymer volatilized. If initiation is random and transfer exists, the result is a good approximation (21):

$$dC/dt \left[1 + \frac{2}{\bar{P}}(1/\epsilon - 2) \right] + 2(1/\epsilon - 2)(1 - C)/\bar{P}^2 d\bar{P}/dt = 2k_1[1/\epsilon + \sigma - (3/\epsilon - 1)/\bar{P} + (\sigma/2)(3/\epsilon - 7)/\bar{P}](1 - C) \quad (4b)$$

Two special cases are of interest—namely, $\epsilon \rightarrow 0$ (very long zip) in Equation 4a, and $\epsilon \rightarrow 1$ (random scission) in Equation 4b. The first result is:

$$dC/dt = (2k_1 - d\bar{P}/dt \cdot 1/\bar{P})(1 - C)$$

As long as the molecular weight changes slowly enough, the reaction is of first order and the over-all rate is determined by the rate of initiation. In the second case, Equation 4b yields:

$$dC/dt(1 - 2/\bar{P}) - 2(1 - C)/\bar{P}^2 d\bar{P}/dt = 2k_1(1 + \sigma)(1 - 2/\bar{P})(1 - C)$$

This expresses the fact that the rate of breaking bonds is proportional to the number of bonds. The effective rate constant for this process is $2k_1(1 + \sigma)$.

Equations 4a,b provide means for evaluating the kinetic parameters by combined measurements of the rate and the number average molecular weight. Conversely, if the kinetic parameters have been determined, for example, by measurements of the initial rate as a function of molecular weight, the molecular weight change may be estimated from the more readily measured rate of volatilization. It must be noted in this connection that the coefficients ϵ and σ are only approximately constant and independent of C , since they are both functions of the radical concentration R . For the case corresponding to Equation 4a we find (21, 26):

$$k_4R^2 = k_4R^2(t = 0) \cdot (\bar{P}_0/\bar{P})(1 - C) \quad 1/\epsilon - 1 = k_2/(k_4R) \quad (5a)$$

whereas in Equation 4b we have

$$k_4R^2 = k_4R^2(t = 0)(1 - C) \quad 1/\epsilon - 1 = k_2/[k_4R(1 + \sigma/2)] \quad \sigma = k_3R/k_1 \quad (5b)$$

The designation " $t = 0$ " refers to the initially established steady state concentration of radicals. We note that in Equation 5a, the variations of C and \bar{P} operate in opposite directions. Up to conversions of 20%, ϵ and σ may safely be regarded as constants. Equations 4a,b may be used in the differential or integrated forms (21), to yield expressions for \bar{P} in terms of the observed rate,

$$K = (1 - C)^{-1} dC/dt$$

both for constant and variable ϵ and σ . Gordon (7) has applied Equation 4a to the pyrolysis data on polystyrene by neglecting the second and third terms on the left hand side of this equation. It is not obvious that this is permissible and results, moreover, in an initial rate proportional to $\bar{P}_0^{-1/2}$ which remains to be observed. However, it is difficult to measure, in this polymer, the true initial rate and any molecular weight effect may be wiped out within a very short time interval (see below).

When the rates can be extrapolated accurately to $C \rightarrow 0$, as in polymers of methyl methacrylate or α -methylstyrene, estimates of the parameters can be obtained. The consistency of these estimates can then be tested by the application of Equations 4a,b.

The discussion of the essential features in the experimental and theoretical approaches to the free radical degradation of polymers is thus completed. We introduce the next section with a summary table which is subdivided according to the two extremes of degradation: unzipping and random scission. The first part of Table III describes the influence of basic structure and the second deals with secondary factors for a given structure. When a polymer is processed at elevated temperatures, volatilization and deterioration of physical properties during short time intervals are a matter of concern; hence initial rates are important.

Table III. Influence of Various Factors on Degradation

<i>Factors</i>	<i>Unzipping</i>	<i>Random Scission</i>
Basic chemical structure	α -Substitution, nonlabile groups for transfer (Methyl methacrylate, α -methylstyrene, tetrafluoroethylene)	No substitution, labile groups, active radicals (Methyl acrylate, ethylene, incomplete fluorination with removal of side groups)
Loss of volatiles	Rapid initially (monomer)	Slow initially (nonmonomer)
Loss of physical properties (molecular weight)	Slow	Rapid
<i>Secondary Factors</i>		
Method of preparation; incorporation of catalyst fragments, double bond formation	Affects locus of initiation and thus magnitude and molecular weight dependence of rate (methyl methacrylate)	
Initial molecular weight, M		
Random initiation	Initial rate $\propto M$	$\propto M^{-1}$, but rapidly $\rightarrow M^0$
Chain end initiation	Initial rate $\propto M^0$	
Increase in initial molecular weight	Molecular weight decrease more rapid	No effect
Initial molecular weight distribution	Unchanged	Narrows, if $M_w/M_n > 2$ Broadens, if $M_w/M_n < 2$
Branching		Enhances rate; initially chain end effect, then "weak" branch points

Effect of Polymer Average Molecular Weight, Molecular Weight Distribution, and Branching

The dependence of the initial rate on the number average molecular weight is readily seen from the following: If the ratio of average zip to chain lengths is large compared with unity, the rate of production of monomer units is proportional to the product of the chain length and the number of initiating sites. The latter are either chain ends or all bonds in the polymer backbone. In random scission, however, the number of chain ends is initially the determining factor for the rate of formation of volatiles, but this effect of molecular weight is very rapidly obliterated by the formation of new chain ends. Subsequently, and as long as the initial chain length is chosen so as to be large compared with L , the critical length for vaporization, the rate is independent of molecular weight. If k is the effective rate constant determined by initiation and transfer, we have (26):

$$dC/dt = k(2C)^{1/2}L[1 - (2/3)(2C)^{1/2} + (2/9)C + 0(C^2)] \quad (6)$$

for $(L/\bar{F}_0)^2 \ll 2C \ll 1/2$. Thus, we observe practically at the start a half-order rate.

The transition between the two regions of molecular weight dependence is well demonstrated by poly(α -methylstyrene) (26). Figure 2 shows the dependence of the initial rate on the initial chain length or twice the DP of a series of fractions. The variation is linear for small N , indicating that initiation occurs at random. A plateau is approached at a molecular weight of about 6×10^5 . Since the zip length is large, the state of random scission is never approached in this polymer and the existence of a plateau is not related to Equation 6. It arises because the initial rate becomes proportional to the average zip length, which is independent of molecular weight [see Equation 2c, in (26)] in random initiation. The full lines in Figure 2 are computed from the theory (26) and result in a value of 1300 monomer units for the average zip length in the bulk degradation of poly(α -methylstyrene). More recently, depolymerization in solutions of Decalin and diphenyl ether was studied (8). The dependence of the rate on molecular weights as well as the observed first order of the reaction agree with the theoretical conclusions. In contrast to Figure 2, however, even for a molecular weight of 6.5×10^5 , no departures from a simple proportionality are found. We conclude that the average zip length is at least five times as large than in bulk degradation, although the temperature was 40°C . lower. It is appropriate to point out here that an apparent first order rate in C is not a sufficient criterion for a zip length many times longer than the chain length. This is indicated by our high speed computations (26). Curves A, B, and C [Figure 1 in (26)] are all linear up to at least 25% conversion, although the zip length varies by about a factor of 10. Even when zip and chain lengths are almost equal, curve D, the departures are not

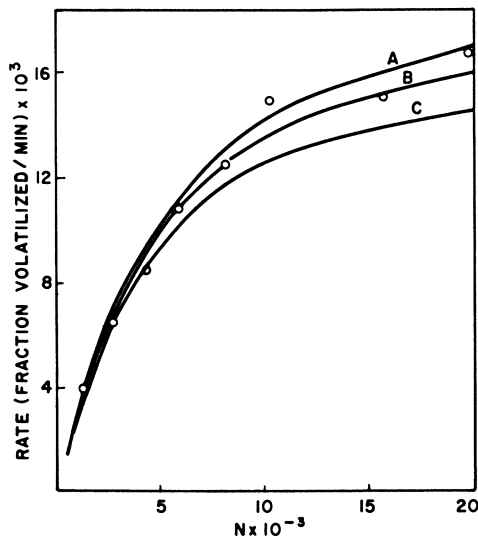


Figure 2. Effect of initial molecular weight on initial rate of degradation for poly(α -methylstyrene)

N is twice the DP

Full lines correspond to theory with zip length of $1300 \pm 10\%$

From Simha, R., and Wall, L. A., *J. Chem. Phys.* **29**, 894 (1958), Figure 10

COURTESY *The Journal of Chemical Physics*

pronounced. Similarly, a proportionality of the rate to the initial molecular weight for random initiation (or independence in end initiation) persists even when the ratio of the two lengths is only 2 [see curves A, B, C (Figure 3) in (26)], while even when it approaches unity, the departure from linearity is only 33% (26).

The complete expressions for the initial rates as functions of molecular weight have been given earlier (20, 23, 26). It will suffice to recall the result for terminal initiation in the transition region of molecular weights corresponding to the flat portion of Figure 2 and long zip length. The initial rate decreases as the inverse square root of the initial molecular weight. The physical property requirements, such as brittleness and ease of fabrication, usually dictate the choice of a molecular weight range. In the case of a typical polymer such as poly(α -methylstyrene), a compromise between these requirements and a choice of low molecular weights, suggested by the rates of degradation, may be necessary. For an end-initiated polymer, however, high molecular weights would be favorable to minimize degradation.

The initial molecular weight is important for the rate of decrease of the relative chain length in unzipping as well as random scission polymers. For the latter, the molecular weight ratio is:

$$\bar{P}/\bar{P}_0 = [1 + (2C)^{1/2}]/[1 + (2C)^{1/2}\bar{P}_0/L] \quad C \ll 1/4 \quad (7)$$

which indicates a sharper decrease for the larger \bar{P}_0 . In an unzipping system, a qualitatively similar effect is observed, although for different reasons. As the initial molecular weight increases relative to the zip length, the molecular weight starts to decrease more rapidly, because on the average, macroradicals are terminated at least once before volatilization is possible (Figure 1). Slowly varying molecular weights during the degradation of poly(methyl methacrylate) have been demonstrated much earlier (10).

Most of the experimental work has so far been carried out with moderately fractionated samples or with whole polymer without examination of the resulting changes in molecular weight distribution. Similarly, in the full use of the theory the emphasis has been on kinetic features. Our general considerations and equations are, of course, not affected by the presence of polydispersity. Recently, it has been recognized that much can be learned from studies on the changes in polydispersity taking place during the reaction. Experimental research along these lines has been considerably facilitated by the development of comparatively rapid column fractionation techniques. Furthermore, now it is possible to polymerize monomers to controlled and high degrees of homogeneity. "Living" polymers were used in the work on polymers of α -methylstyrene at the National Research Council of Canada (4, 8).

As long as the zip length is so large that the number average molecular weight of the residue remains practically constant, the distribution will also not change. This will be true, regardless of the details of the initial distribution, provided no appreciable fraction of chain lengths comparable to the zip length is present. What happens when this condition is not obeyed, as for example, in a polymer of methyl methacrylate or α -methylstyrene of large average molecular weights? There is one distribution which plays a special role—namely, the exponential distribution which may be written in the form

$$Q_k = 1/\bar{P} \cdot (1 - 1/\bar{P})^{k-1} \quad 1 \leq k \leq \infty \quad (8)$$

where Q_k is the fraction of k -mers. This distribution is rigorously realized in a polycondensation polymer. For low conversions, an addition polymer in which

termination takes place exclusively by disproportionation, also follows approximately Equation 8. Provided the kinetics, Equation 2, are valid, or slightly modified to include termination by radical combination, this distribution is maintained upon degradation (1). For example, the ratio of weight to number average DP remains equal to 2. Moreover, in the special case of terminal initiation and no chain transfer, it can be shown (7, 21) that the center of the distribution, Equation 8, is not even displaced, regardless of the zip length. This would also hold for an unbounded, so-called box distribution, $Q_k = \text{constant}$, for $k \leq \infty$, but this is hardly a realistic representation of polymer distributions. This result is to be contrasted with the behavior observed for a fractionated polymer degrading by an identical mechanism, where constancy is approached only for long zips. It may be understood as a compensatory interaction between the distributions of chain and zip lengths which, in this special case, are both of the exponential type. Initially there are fewer large chains, but they have a better chance of at least partial survival than the more numerous short ones which are more likely to be completely volatilized before completion of the reaction (7, 21).

Poly(methyl methacrylate) is the only polymer so far which approximates the kinetic requirements for the existence of this phenomenon; however, it has not been demonstrated experimentally, presumably because Equation 8 was not obeyed. Again, the polymerization kinetics for this system should favor the validity of Equation 8.

Provided then that Equation 2 is an adequate description of the degradation mechanism, an initial distribution will broaden or narrow on pyrolysis, if it is narrower or wider than the exponential one. The magnitude of this effect has so far been computed only in two special cases. A homogeneous polymer preparation which unzips rapidly, gives a broad, symmetrical band when plotted on a weight basis. The band is centered around one half the original DP , when about 10% of the material has been volatilized (25). With increasing conversion, the distribution shifts and becomes asymmetrical, decreasing more slowly in the range of large molecular weights.

Solutions of the rate equations are missing here for moderate zip lengths and at such intermediate conversions, that the broad band becomes experimentally accessible by fractionation techniques. This appears to have been the problem in the investigation of poly(α -methylstyrene) in solution (8), discussed previously. The average molecular weight decreases by 6%, when $C = 10\%$, but no change in the distribution could be detected. This is what we would expect from the theoretical result (25, 26). In the degradation of the solid polymer (4), where the average zip length is considerably shorter, a significant broadening of an originally narrow (anionic polymer) distribution and a shift of the peaks at 10 and 20% conversion could be observed.

A study of the pyrolysis of polypropylene between 250° and 295° C. (6) provides an example of the opposite extreme; namely, a random scission. In this instance, the equations for a homogeneous polymer (14) can be readily extended to include the effect of polydispersity. In order to obtain significant amounts of high polymer, extremely low conversions, less than 0.3%, were used. This corresponds to less than 10^{-3} for α , the fraction of bonds broken. Figure 3 shows the change in distribution. The original polymer is very broadly distributed, with a weight to number average ratio of 9, which decreases to 3 and 2, respectively, for the curves exhibited. The agreement between experimental distributions, as obtained by column fractionation and the theoretical expressions, based on the assumption of random scission, is very good, indeed.

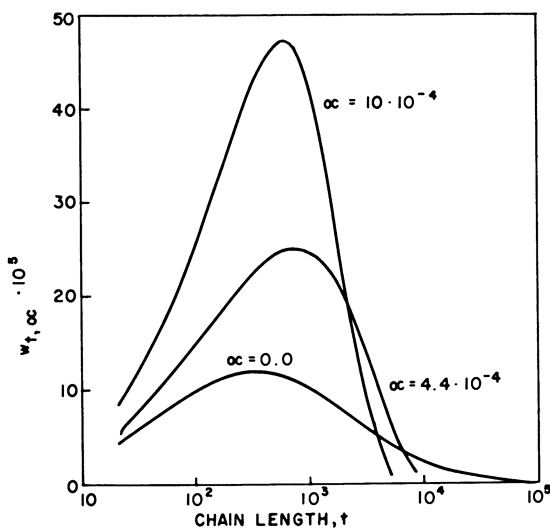


Figure 3. Molecular weight distribution (weight fraction) of polypropylene at initial and two subsequent stages of degradation

Parameter α is the fraction of bonds broken (6)

From Davis, T. E., *et al.*, *J. Polymer Sci.*, in press

COURTESY *The Journal of Polymer Science*

These results provide additional confirmation for the mechanism of pyrolysis of simple polyolefins. The absence of monomer in the volatile products, the maxima in the rate curves, and the sharp decrease in the intrinsic viscosity for linear polymethylene (29) and polypropylene (2, 6, 13, 30) all point to an essentially random scission, due to pronounced intermolecular chain transfer, Equation 2. However, deviations appear when α , the fraction of bonds broken, or, what amounts to the same, the number average DP is examined as a function of time. For small α , the former relation should be one of simple proportionality and linearity in $1/\bar{P}$. Instead, for both polypropylene (6) and polymethylene [see Figure 5, in (29)] curvature appears, indicating a reduction of the scission rate after an initial period of rapid degradation. For polypropylene this has been interpreted as a breaking of "weak" and "normal" bonds. Between 250° and 280° C., one weak link per 2.4×10^4 is found (6). At 295° C., the existence of more than two types of bonds would have to be postulated.

In polymethylene, between 380° and 400° C., the deviations from randomness are largest at the lowest temperature, as indicated by Figure 5 in (29). The information available for this system is insufficient, but we can estimate roughly one weak link per 1400 between 390° and 400° C. with a ratio of 5 for the rate constants in a linear polymethylene prepared from diazomethane. These numbers are not unreasonable in terms of trace impurities in the atmosphere containing oxygen, or residues and structural inhomogeneities present initially in the chain. The former hypothesis might be tested by subjecting carefully purified polymers to degradation in controlled atmospheres containing predetermined small amounts of oxygen. At relatively low temperatures—i.e. below 300° C.—the effect of

hydroperoxides in the chain in initiating decomposition and lowering the activation energy for polypropylene from about 60 to 65 to 30 to 40 kcal. per mole has been demonstrated (17).

It should be noted that the weak link mechanism does not offer the only possible explanation for departures from random scission in linear polyolefins or from predictions of our kinetic theory, in general. In the case at hand, the effective rate constant for bond breaking is $k_1 + k_3R \approx k_3R$. It follows from Equation 5b that the rate is reduced by a factor $(1 - C)^{1/2}$. This effect, however, is negligible, because C hardly exceeds 10% in the experiments discussed. The radical concentration R will also be reduced, if the termination reaction in Equation 2 is diffusion controlled. Provided the rate of disproportionation is related to the macroscopic viscosity of the medium, this change in R will be most pronounced in random scission-type polymers in general, and at the beginning and high temperatures in particular, when the average molecular weight decreases most rapidly. The effect should be accentuated by large initial chain lengths, Equation 7. At the present time, no experimental or theoretical decision between these alternative explanations is possible.

The effect of (short chain) branches can be conveniently studied in polyolefins. High pressure polyethylene is known to contain variable amounts of such branches. Here also, the observed monomer yield, practically zero, is in accord with a predominance of chain transfer and, if intermolecular, should result in random scission. A comparison of branched and linear polyethylene has been carried out some time ago (12, 29). More recently, it has been extended to copolymers prepared from a series of diazoalkanes with varying chain length and composition (30). Figure 4, derived in part from data in (27), shows a typical experimental result for a linear and branched system. Whereas the former shows the maximum rate predicted by theory, the branched polymer yields a monotonic rate, at least beyond 10% conversion, found otherwise only in unzipping polymers. In a linear system, this signifies pronounced intramolecular transfer. Here, however, we have to examine the effect of the branches, which provide an increased number of chain ends for volatilization. Moreover, the tertiary C-H bonds act as sites for enhanced free radical attack and hence scission, Equation 2. The theory for branched chains degrading by random scission with effective rate constants k_I for secondary and k_{II} for tertiary linkages has been developed by Simha (19). We may expect an increase in the rate of pyrolysis on both counts. Indeed, the initial rate is (19, 29):

$$\lim (1/k_I)dC/dt = L(L - 1)/\bar{P} + (b/2\bar{P})s(s - 1) + (bs/\bar{P})k_{II}/k_I \quad (9)$$

where b is the number of branches per chain and $s < L$ the length of a branch. The expressions for finite conversions are lengthy and will not be reproduced here. C and the rate dC/dt depend on two quantities besides s . These are the ratio k_{II}/k_I and the ratio Lb/\bar{P} between L and the average distance between two branch points. Figure 5 shows some typical results (19). The numerical values selected for the parameters are typical of low branch densities (less than 1%). Moreover, Lb/\bar{P} varies from 0.8 to 1.6. For higher values resulting from a choice of $L = 70$, our equations are only approximately valid. The results shown may be understood from the following: If all bonds are ruptured at an identical rate, the initial rate dC/dt ($C < 0.1\%$) is enhanced by the presence of branches, because of the large number of chain ends. This effect is very soon overcompensated and the rate comparatively reduced, since linear molecules are split into smaller fragments

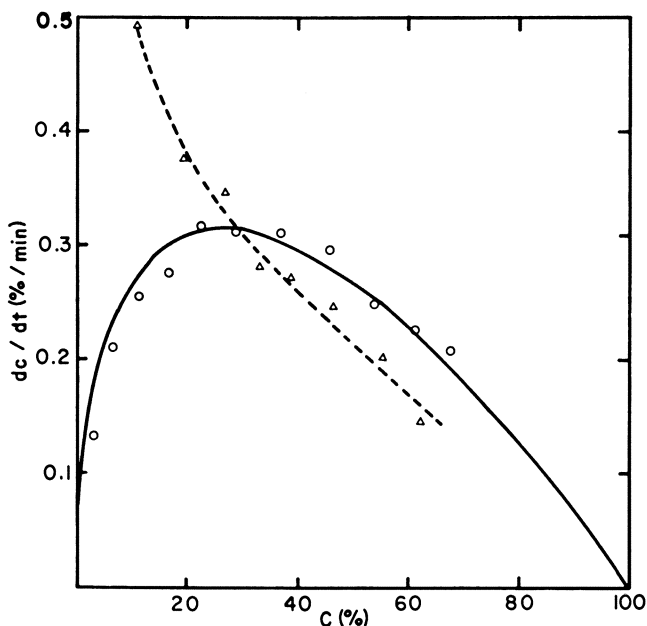


Figure 4. Rates of pyrolysis of linear and branched polyethylene at 400° C. as a function of the degree of volatilization

○ Experimental for linear polymer, molecular weight ca. 5×10^4
 Solid line. Theoretical, random scission; $L = 72$
 Dashed line and Δ. Experimental for branched polymer, DYNF; molecular weight > 9100, 3.7 CH₃ per 100 CH₂ (16, 27)
 Vertical scale is to be multiplied by 2

(increased number of chain ends) than the branched species, where the backbone has statistically a better chance of survival. The short branches, on the other hand, do not contribute sufficiently to the total weight C of volatiles. Thus, an acceleration in the decomposition rate at finite conversions is entirely due to an increase in the rate of abstraction on tertiary C—H linkages and possibly a similar increase in the subsequent rate of decomposition of the C—C bond, Equation 2. For differences in the rates of the former process, expected from the kinetics of low molecular weight hydrocarbons, the increase in the rates of the branched polymers would be measurable. However, for such values, the position of the maxima in the rate curves remains practically unchanged, Figure 5. The maximum is displaced to C 's smaller than 26%, the value for a linear chain, as the ratios k_{II}/k_I and Lb/\bar{P} increase sufficiently. Our numerical evaluation of the theoretical results (19) so far permits us only to state that for the values of Lb/\bar{P} indicated, the maximum is displaced to 18 and 13% as k_{II}/k_I assumes values of 50 and 100, respectively. Now for the branched sample in Figure 4, the characteristic ratio of lengths equals $L \times 3.7/100$ and may therefore be as high as 2.6. The ratio k_{II}/k_I required for comparable shifts will be less. In the copolymers studied (30), only the starting ratio of monomers is known. This ratio, rather than the branch density, is also higher than in our numerical examples.

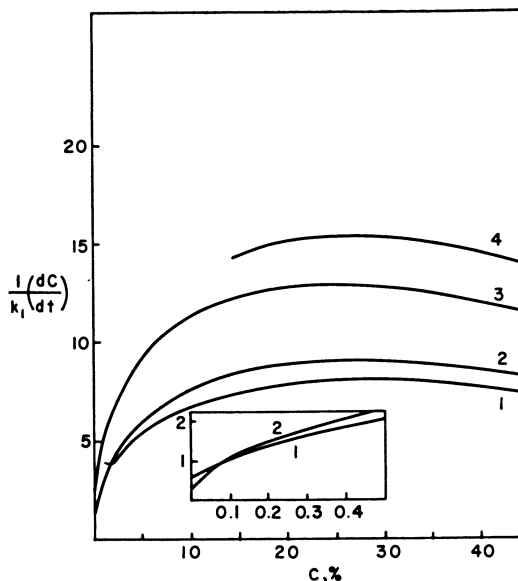


Figure 5. Theoretical rates of volatilization of linear and branched polymers of the random scission type as a function of conversion and for varying degrees of branching and ratios of rate constants

$$\bar{P} = 2500, s = 4$$

1. $L = 25, k_{II} = k_I, b = \bar{P}/30$

2. As in 1 with $b = 0$

3. As in 1 with $k_{II} = 10k_I$

4. As in 1 with $L = 49$

Inset. Initial portion of curves 1 and 2

From Simha, R., *J. Chem. Phys.* **24**, 796 (1956),
Figure 2

COURTESY *The Journal of Chemical Physics*

We have to contend here with the problem of characterization, in the case of copolymers, and a lack of numerical evaluation of the theory for samples of high branch density. Nevertheless, it appears safe to conclude from the theory that large ratios of the rate constants would be required to account for the observations in branched polyolefins, although these should be carried to lower conversions, say 10%. If an intramolecular abstraction through radicals formed in the pendant branches is possible at the expense of intermolecular attack (19, 27), it will effectively weaken the bonds near branch points and provide a physical basis for large ratios k_{II}/k_I . Such a mechanism has consequences for the rate of decrease of molecular weight which have not been explored so far. The rates increase with the degree of branching. For a series of polyethylenes, ranging from 3.7 to 8.7 CH_3 per 100 CH_2 (16), the rate at 40% volatilization changes by a factor of 3 (27).

A particular aspect, ordinarily one of the first to be explored in a free radical process, has hardly received attention. It is a qualitative proof of the existence and quantitative analysis of the types of radicals present in the system. There are obvious difficulties in a pyrolyzing polymer, but they, we expect, will be overcome. In this manner, it may even become possible to provide estimates of the rate constants in Equation 2.

Acknowledgment

The author thanks T. E. Davis for use of his manuscript prior to publication.

Literature Cited

- (1) Boyd, R. M., *J. Chem. Phys.* **31**, 321 (1959).
- (2) Bresler, S. E., Osminskaya, A. T., Popov, A. G., *Resins, Rubbers, Plastics* **14**, 703 (1960).
- (3) Brockhaus, A. Jenckel, E., *Makromol. Chem.* **19**, 262 (1956).
- (4) Cowie, J. M. G., Bywater, S., *J. Polymer Sci.* **54**, 221 (1961).
- (5) Dainton, F. S., Ivin, K. J., *Quart. Revs. (London)* **12**, 61 (1958).
- (6) Davis, Th. E., Tobias, R. L., Peterli, E. B., *J. Polymer Sci.*, in press.
- (7) Gordon, M., *Trans. Faraday Soc.* **53**, 1662 (1957).
- (8) Grant, D. H., Vance, E., Bywater, S., *Ibid.*, **56**, 1697 (1960).
- (9) Grassie, N., "Chemistry of Vinyl Polymer Degradation Processes," Butterworth, London, 1956.
- (10) Grassie, N., Melville, H. W., *Discussions Faraday Soc.* **2**, 378 (1947).
- (11) Jellinek, H. H. G., "The Degradation of Vinyl Polymers," Academic Press, New York, 1955.
- (12) Madorsky, S. L., *J. Polymer Sci.* **9**, 133 (1952).
- (13) Madorsky, S. L., Straus, S., *J. Research Natl. Bur. Standards* **53**, 361 (1954).
- (14) Montroll, E. W., Simha, R., *J. Chem. Phys.* **8**, 721 (1940).
- (15) Patrick, R., *Advances in Fluorine Chem.* **2**, 1 (1961).
- (16) Rugg, F. M., Smith, J. J., Wartman, L. H., *J. Polymer Sci.* **11**, 1 (1953).
- (17) Schooten, J. v., Wijga, P. W. O., *Soc. Chem. Ind. Monograph No. 13*, 432 (1961).
- (18) Simha, R., *Collection Czechoslov. Chem. Commun.* **22**, 250 (1957).
- (19) Simha, R., *J. Chem. Phys.* **24**, 796 (1956).
- (20) Simha, R., *J. Polymer Sci.* **9**, 465 (1952).
- (21) Simha, R., *Trans. Faraday Soc.* **54**, 1345 (1958).
- (22) Simha, R., Wall, L. A., "Catalysis," Vol. 6, P. H. Emmet, ed., Reinhold, New York, 1958.
- (23) Simha, R., Wall, L. A., *J. Phys. Chem.* **56**, 707 (1952).
- (24) Simha, R., Wall, L. A., *J. Polymer Sci.* **6**, 39 (1951).
- (25) Simha, R., Wall, L. A., Blatz, P. J., *Ibid.*, **5**, 615 (1950).
- (26) Simha, R., Wall, L. A., Bram, J., *J. Chem. Phys.* **29**, 894 (1958).
- (27) Wall, L. A., *Soc. Chem. Ind. Monograph No. 13*, 146 (1961).
- (28) Wall, L. A., *SPE Journal* **16**, (No. 8) 1 (1960).
- (29) Wall, L. A., Madorsky, S. L., Brown, D. W., Straus, S., Simha, R., *J. Am. Chem. Soc.* **76**, 3430 (1954).
- (30) Wall, L. A., Straus, S., *J. Polymer Sci.* **44**, 313 (1960).

RECEIVED September 6, 1961.

Prepolymer Technology for Cross-Linked Plastics

STUART H. RIDER and EDGAR E. HARDY

Research Department, Plastics Division, Monsanto Chemical Co., Springfield, Mass.

Three-dimensional polymers can be made by cross-linking low molecular weight prepolymers. The structure of these new macromolecules can be carefully designed and controlled through choice and synthesis of the component fragments as well as through control of cross linking. In this new and important area of plastics technology a new term "structoset" designates cross-linked, irreversible high polymers prepared from structurally well-defined, nonrandom prepolymer segments by chemical reaction during the application process. Prepolymers are classified according to structural parameters into three groups: random, structo-terminal, and structopendant. Cross linking is carried out by heat or amines, anhydrides, aldehydes, isocyanates, peroxides, and vinyl monomers. Molecular structure-physical properties correlations and end uses of the structosets are also discussed.

Cross-linked plastics, because of their retention of physical properties at elevated temperatures, chemical resistance, low creep, and versatility of application are being used in increasing amounts as materials of engineering. Of the 5.5 billion pounds of plastics sold in 1960, 1.8 billion or 32% were cross-linked plastics (19). While some of the older members of this family, such as phenolic molding powder, show little or no growth, the newer materials such as polyesters, epoxy resins, and polyurethanes are growing very rapidly.

Much of the success of these newer systems has been due to a unique prepolymer technology. It is this concept of prepolymer processing which has allowed the development of many new applications and the design of structural plastics with well-defined and highly desirable properties.

Prepolymer technology can logically be divided into three phases.

Prepolymer Preparation. A well-defined, low molecular weight polymer is synthesized. This prepolymer must be stable, have the base structure desired in the finished product, and cure in the desired manner.

Process Rheology. Since the polymerization reaction is completed during the fabrication step, the initial rate of viscosity increase and the gel point, must

be designed so that the fabricator's process will be economical and efficient.

Physical Properties. The product, at completion of the reaction, must have the physical properties to do the job required. These physical properties, as will be shown later, are dependent upon the structure of the prepolymer.

Thus, prepolymer processing contrasts sharply with thermoplastic processing. Thermoplastics are polymerized to completion during the plastics' manufacture. The fabricator applies heat and pressure by means of extrusion, injection molding, or calendering to produce the finished article.

The prepolymer concept, per se, is not new. In fact, the oldest synthetic polymer—Baekeland's phenolic resin—was made through an intermediate, soluble prepolymer. The major success of the newer systems is due to the use of well-defined prepolymer units and more versatile cross-linking mechanisms. The older thermoset plastics were randomly built up from their base monomers and therefore control of their growth and structure was difficult and limited.

It is important to differentiate between the older random thermosets and these newer systems. Since control and design of structure are the key to modern prepolymer technology, we would like to introduce the new designation "structo-set" polymers for those cross-linked plastics which are obtained from well-defined, nonrandom prepolymer units.

In order to obtain a clearer understanding of prepolymer technology, the theory of gelation is first discussed. A classification of prepolymers is then introduced and finally the available quantitative data on structure-property relationships are reviewed. References cited are usually to the most complete and general source and not necessarily to the original publication.

Theory of Gelation

Carothers (17) recognized very early that if monomers with more than two reactive sites were polymerized, gelation resulted. He proposed a simple formula to relate the average functionality (f , number of reactive sites) to the degree of reaction (P_c) at which gelation could be expected.

$$P_c = \frac{2}{f}$$

Carothers suggested that an average functionality be used, when more than one species were present. He cited as an example, the simple system of glycerol and phthalic anhydride—two moles of glycerol and three of phthalic anhydride—five moles all together containing twelve reactive sites (glycerol is trifunctional and phthalic anhydride is bifunctional). Average functionality, f , of the system then becomes $\frac{12}{5}$ or 2.4 and the critical degree of reaction at which gelation takes place should be approximately 83%.

Flory (9) treated gelation on a statistical basis and developed general equations for gelation and molecular weight distribution. Using the assumptions of equal reactivity of all functional groups and that intramolecular condensation is small, the concept of a branching coefficient, α , was introduced. The branching coefficient is defined as the probability that a given functional group of a branch unit leads to another branched unit. The multifunctional monomer or prepolymer is considered as a branching unit. The chain is defined as the portion of the molecule between branching units. For trifunctional monomers reacting with difunctional monomers, if $\alpha < 1/2$, the chance is greater than even that the chain

will end in an unreacted group. If $\alpha > 1/2$ the probability is that each chain results in two new chains, thus leading to an infinitely large network. Gelation occurs when $\alpha (f - 1)$ exceeds unity. The critical value of α is

$$\alpha_c = \frac{1}{(f - 1)}$$

The use of an average value of f is also suggested when a variety of multifunctional components are present.

Equations have been developed relating α to the extent of reaction, P . In general, the observed results of α_c are slightly higher than those calculated indicating that some of the reactive sites are lost in intramolecular connections. Flory cites the case of pentaerythritol ($f = 4$) and adipic acid. For this case, $\alpha = P^2$ and $\alpha_c = 1/3$ with $P_c = 0.577$. The experimental result was $P_c = 0.63$.

In a more complicated discussion, Flory goes on to develop the molecular weight distributions prior to and beyond the gel point. The sol fraction after the gel point decreases until $\alpha = 1$, when only very small amounts of monomer should be left.

The rheological behavior of a random prepolymer is shown in Figure 1. The initial viscosity is very low. This allows for the penetration, mixing, and wetting of pigments or fillers that are necessary with these systems. As the critical degree of reaction is approached, the viscosity increases very rapidly and gelation takes place without a large incremental change in degree of reaction.

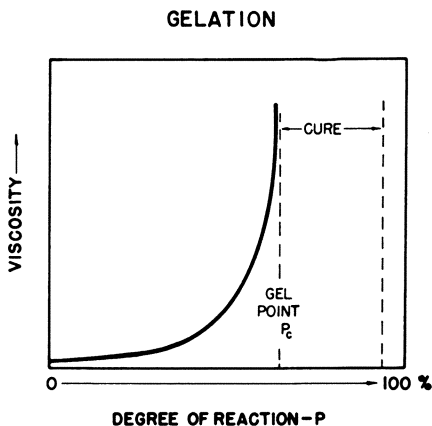


Figure 1. Rheological behavior of a random prepolymer during processing

This sudden gel formation is usually interpreted as the formation of a small per cent of infinite space network. The formation and control of the gel phase are vital in the processing of random thermosets and structosets. For example, too rapid gelation can cause poor bond strength in laminated and bonded structures. Too slow gelation could cause the collapse of a foam. The amount of reaction required for gelation can be controlled by the functionality of prepolymer units, f_{pp} .

When considering the gelation of structosets, the molecular weight of the prepolymer segments is relatively high and the functionality of the prepolymers can be very high as compared to the functionality of the cross linker, f_c , which often is only 2 or 3.

If we consider an ethylene glycol-maleic anhydride prepolymer of a degree of polymerization of 10, f_{pp} would be 10, while the cross linker may have an f_c of only 2. A limited amount of work has been done, such as the recent work by Gordon (11,12), who studied the gelation of a polyethylene fumarate polyester cross-linked with methyl methacrylate and found that this system conformed to gelation theory. It is interesting to note that gelation theory confirms the important finding that gelation takes place at very low degrees of reaction when prepolymers of large functionality are used.

Flory has also extended his approach to cover cross-linked linear polymers and concluded that, for large prepolymer molecules, a ratio of one cross link per two prepolymer molecules is sufficient for gelation. An extensive review of this subject has been published by Lilley (15).

Of particular importance is the understanding that in these systems, reaction is not complete at the gel point. Additional cross links are introduced into the polymer system during the curing stage, which is essentially the stage between the gel point and the completion of the reaction. Measurement and fundamental study of this curing phase have been difficult because the products are no longer soluble. Best results to date have been obtained by measuring the effect of cure time and temperature in relation to certain key physical properties. Swelling measurements in strong solvents are a powerful tool at low degrees of cross linking.

Prepolymer Classification

Before going into the structure-property relationships, a clearer understanding can be obtained by a closer look at the prepolymer itself and the important parameters in its structure.

Early prepolymers of the random type are classified by Baekeland (18) whose nomenclature has been widely accepted for thermosetting resins.

A stage: the polymer is soluble and fusible, $P < P_c$.

B stage: the polymer is insoluble in common solvents, but is still fusible, $P > P_c$.

C stage: the polymer is highly cross-linked and does not soften on heating.

With the advent of the structosets, relationship between the density of cross linking, the average molecular weight between cross links, and the character of the segments becomes more controllable; so the following classification is proposed (Figure 2).

Random Prepolymers. These prepolymers are built up from polyfunctional monomers reacting statistically according to the theories of Flory. Reaction is stopped at a desired prepolymer molecular weight, usually by cooling. Final polymerization is achieved by heating; therefore the term thermoset is used for them.

The degree of reaction of these prepolymers must be less than the critical degree of reaction, P_c , in order to remain at the Baekeland A stage. The concept of prepolymer functionality, f_{pp} , is not significant in this case, as the reaction is only temporarily held back at a degree of reaction $P < P_c$.

Prepolymers for structosets fall into two major groups.

Structoterminal Prepolymers. The reactive sites are located at the end of a major polymer chain. Maximum control of the length and type of chain in finished structoset polymers is obtained with this type of prepolymer.

These prepolymers are characterized by low prepolymer functionality, f_{pp} ,

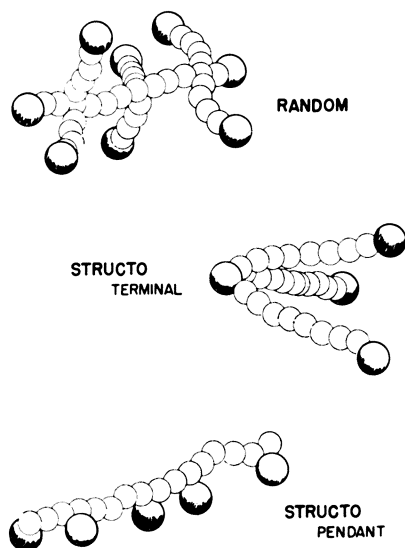


Figure 2. Classification of prepolymers

usually from 2 to 4 and a high average molecular weight between cross links, M_c . They are usually synthesized by condensation reactions as typified by polyesters and polyethers for urethane elastomers. These systems were first recognized for their many potential uses and studied extensively by Bayer and coworkers in Germany (2).

Structopendant Prepolymers. The reactive or functional groups are distributed along the prepolymer chain. Examples are the epoxies, unsaturated polyesters, and the thermoset acrylics.

Structopendant prepolymers generally have relatively high functionality, f_{pp} , and a low molecular weight between cross links, M_c . A maleic anhydride-ethylene glycol polyester with a molecular weight of 1600 would have an f_{pp} of 11, and a backbone M_c of 116, if fully cross-linked.

These prepolymers are often synthesized from monomers having two types of functionality, under conditions allowing one type of functionality to react, while leaving the other unchanged. Cross linking may then be carried out through the second type of functionality.

Important Prepolymer Systems

Polyether Prepolymers. These prepolymers are widely used in urethane chemistry (Figure 3) in this country and have reached major commercial significance in the last five years (14). Monomers most commonly employed are ethylene and propylene oxide. The prepolymers usually employed are structo-terminal chains having hydroxyl functional end groups. Molecular weights range from 500 to 4000 with the lower molecular weight materials being used for more rigid and the higher molecular weight materials for more flexible end products. By variation in chain lengths and type of chain, a great variety of final properties are possible by cross linking these prepolymers with diisocyanates or triisocyanates. An interesting structoterminal prepolymer is often formed by lengthening the

polyether prepolymers with an appropriate number of moles of diisocyanate. The materials obtained are still true prepolymers of low viscosity and good processability. However, even the so-called "one-shot" polyurethane system uses polyether prepolymers as the raw material.

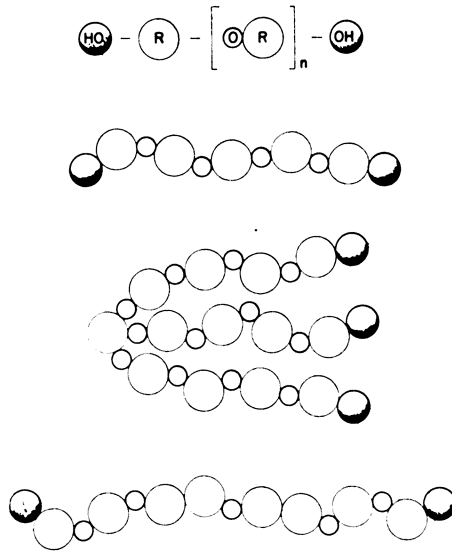


Figure 3. Schematic representation of polyether prepolymers

Epoxy Prepolymers. These prepolymers are commonly formed from Bisphenol A and epichlorhydrin (Figure 4). A variety of other materials are also employed, but to a lesser extent. The lowest member of the series might well be considered structoterminal, while all the others must be considered as structopendant prepolymers. Molecular weights range from a few hundred to about 4000 for commonly used industrial epoxy prepolymers. Most common cross-linking agents are amines and anhydrides; however, epoxies may also be combined with a variety of other polymer systems (25).

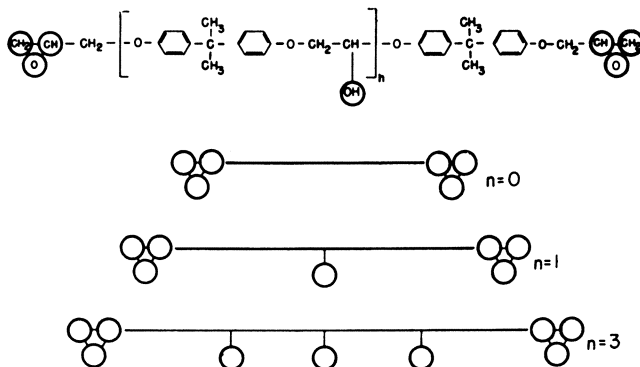


Figure 4. Schematic representation of epoxy prepolymers

Polyester Prepolymers. Commercially important polyester prepolymers are of three major types (Figure 5). Structoterminal polyester prepolymers are used extensively in polyurethane chemistry and are structurally very similar to the structoterminal polyethers employed for the same purposes. Monomers used are dibasic acids and polyols such as adipic acid and ethylene glycol. Usually, an excess of glycol is used to obtain terminal hydroxyl groups. Molecular weights of the most commonly employed prepolymers range from a few hundred to 3000. Cross-linking agents or chain extenders are di- and triisocyanates.

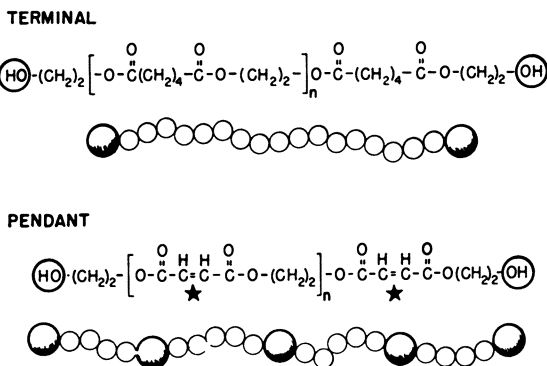


Figure 5. Schematic representation of polyester prepolymers

Unsaturated polyester prepolymers, on the other hand, are of the structopendant type. While they have also usually terminal hydroxyl groups, cross linking is carried out primarily through the structopendant double bond. Monomers employed are unsaturated anhydrides (maleic anhydride) and polyols as illustrated by the prepolymer from maleic anhydride and ethylene glycol. Molecular weights of the prepolymers are in the same ranges of a few hundred to 4000. Cross linking is usually done through vinyl compounds such as styrene.

One major use of polyesters, the alkyd coating resins, is based on random prepolymers reacted with unsaturated fatty acids. Gelation phenomena have been studied extensively and the gelation theories of Carothers, Flory, and Stockmayer were developed with polyester random prepolymers. Only recently, Gordon (11, 12) has extended the gelation theory to the structopendant polyester system cross-linked by vinyl monomers.

Phenolics. These plastics allow the preparation of both random prepolymers, such as Baekeland's A stage and true structopendant prepolymers, commonly known under the term novolaks (Figure 6). Novolaks permit one to take advantage of the newer prepolymer technology. Monomers are phenol, cresols, and formaldehyde. Molecular weights of the novolaks are between 300 and 700. Novolaks are obtained through careful selection of reaction conditions and catalysis of the phenol-formaldehyde reaction. Molecular weight, as well as the ratio of 2,2'- and 2,4'-links, can be controlled. These structural factors, studied extensively by Wood (28), have an effect on the physical properties of the cured polymer network.

Cross-linking systems employed are hexamethylenetetramine or paraformaldehyde. The OH function can also be used by reaction with epichlorohydrin to form epoxy novolaks.

lular weight prepolymers are often used in coating systems in combination with other prepolymers and cross-linking agents (6).

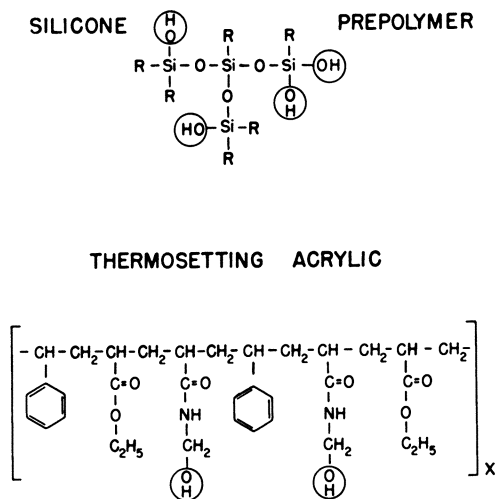


Figure 8. Schematic structure of silicone and thermoset acrylic prepolymers (4)

The thermoset acrylics (20) of major importance in the coating industry, in recent years, have been developed primarily by Canadian Industry Ltd. and by Pittsburgh Plate Glass Co. in this country (4). Raw materials are acrylamide, acrylic acid, acrylates, and styrene. Cross-linking agents are amino and epoxy resins. The materials are also self-cross-linking. They are usually sold as solutions in paint solvents.

These are examples of the building blocks employed in the preparation of structoset polymers. Variations of these building blocks, as well as of the way in which they are put together, allow development of a great variety of useful properties from these systems.

Structure-Property Relationship for Cured Prepolymers. Types of cross-linked polymers illustrating the basic parameters involved in such systems are shown in Figure 9. Amorphous linear polymers such as polystyrene exhibit no cross linking, but their chain segments are frozen in place and at room temperature, the polymer is in a glassy state, hard and rigid. Elastic rubber exhibits a relatively low degree of cross linking and the segments between cross links are free to move rather than be in the glassy state. The random thermoset polymers usually have a high degree of cross linking with a wide distribution of molecular species. The structoset polymers have a more uniform, ordered structure with well-defined segments. The structure of these polymers can be varied from elastomeric to heat-resistant.

The amount of basic study of property-structure relationships seems to vary inversely with the degree of cross linking. Thermoplastics have been studied intensively by solution and x-ray techniques. Elastomers have been explored using swelling techniques in strong solvents which yield valuable data on the chain length between cross links. Studies on highly cross-linked systems have been limited mostly to measurements of how physical properties vary with the state of cure.

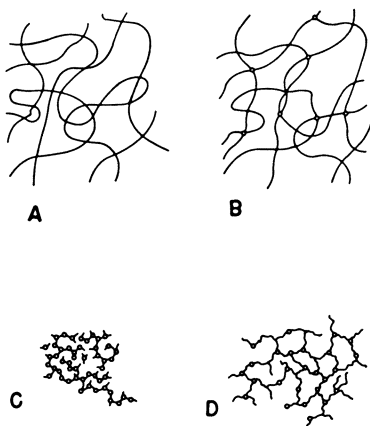


Figure 9. Schematic representation of types of cross-linked polymers

- A. Amorphous linear polymer
- B. Cross-linked polymer, rubber
- C. Random thermosetting polymer
- D. Ordered structoset polymer

In further discussion of cross-linked systems, the following structural factors are of importance.

\bar{M}_c , using the suggestion of Flory, is defined as the average molecular weight of the portion of the molecule or chain between two branch points.

Z_c is the effective number of carbon to carbon bonds between two branch points. The nature of the chain strongly affects properties.

ρ is density of cross linking. Although presented in different ways in the literature, the suggestion of Fox and Loshaek (10) is used here. Density of cross linking is expressed as moles of cross linker per gram of cross-linked polymer. If the cross linker is long in relation to the chain, then the effective number of carbon to carbon bonds in the cross linker becomes important and a term Z_x for the cross linker may be considered.

T_g , glass transition temperature, is the temperature at which a polymer has an abrupt change in volume expansion coefficient and heat capacity. As the temperature is raised through the T_g range, the polymer changes from a relatively hard, brittle, glassy material to a softer, more rubbery substance (3).

Before proceeding to the more quantitative aspects, a qualitative discussion is given with frequent reference to Figure 10.

In the case of thermoplastics, most properties change with molecular weight up to a limiting value and thereon are little affected by further molecular weight increases. In the structosets, molecular weight consideration is of primary concern during processing and curing. Final polymer structure is an infinite network, so the term molecular weight loses its importance and \bar{M}_c becomes critical.

We have previously stressed that network formation rapidly increases viscosity and causes gelation. Cross linking after that point increases the apparent glass transition temperature. Figure 11 illustrates the effect of degree of cross linking on the dynamic modulus of a thermoplastic and a cross-linked polymer. The point at which modulus drops off rapidly is approximately the glass transition temperature.

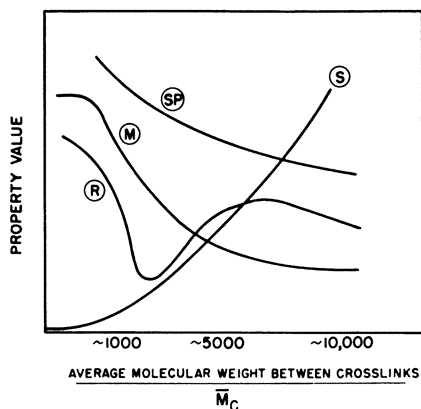


Figure 10. Qualitative relationship of physical properties to chain length between branch points

- SP. Softening point
 S. Solvent swelling
 M. Modulus of elasticity
 R. Resilience, rate of recovery from deformation

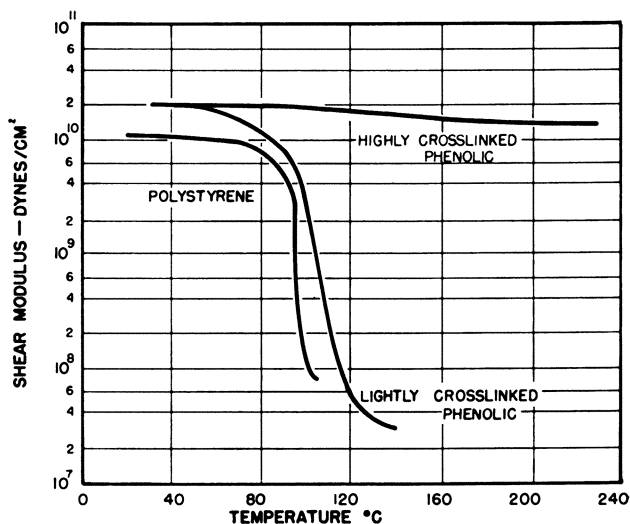


Figure 11. Dynamic mechanical properties of polymers

From Drumm, M. F., Dodge, C. W. H., and Nielsen, L. E.,
Ind. Eng. Chem. 48, 76 (1956)

COURTESY *Industrial and Engineering Chemistry*

Other important bonding points can be obtained through chain entanglement and through the occurrence of crystalline regions, as well as through secondary chemical bonds resulting from hydrogen bonding.

Crystallization in structosets, as well as in thermoplastics, is promoted by linearity, close and regular fit of polymer chains, strong intermolecular forces, and stiff units in the chain which restrict rotation. Crystallization may well be regarded

as another form of cross linking and has a similar effect. The key difference is that crystalline forces are disrupted reversibly by heat as contrasted with stable, true chemical cross linking. Secondary chemical bonds usually play a more limited role in structosets, while side chains and cross links tend to separate the groups which might induce hydrogen bonding.

The ease of rotation of chain segments has a great influence on the properties of a polymer structure. As previously discussed, this is a function of polymer structure and temperature. The glass transition temperature of a polymer is that temperature at which backbone segments begin to rotate. An ideal noncrystalline polymer is a glass below the transition temperature and a non-Newtonian viscous liquid at temperatures above T_g . Thus, normally, plastics have T_g values above the use temperature, while elastomers have T_g values below the use temperature.

In the structosets, the glass transition temperature is particularly affected by cross linking, which has a major effect on the ease of rotation.

For thermosetting polymers (Figure 10), structosets as well as elastomers, key properties such as the glass transition temperature and softening point increase as the chain length between cross links becomes shorter. As would be expected, solvent swelling decreases as cross linking increases.

The effect on modulus of elasticity and resilience of reducing average chain length between cross links is dependent on whether the T_g of the chain segments is above or below the temperature at which the test is being conducted. Figure 10 illustrates the case in which the T_g is below the test temperature and the uncross-linked polymer is a viscous liquid. As \bar{M}_c is reduced by cross linking, the modulus of elasticity increases until a plateau is reached. Further cross linking does not appreciably raise the modulus of elasticity.

The effect on resilience (approximate rate of recovery from deformation) of reducing \bar{M}_c is more complex. At relatively low degrees of cross linking, the system exhibits rubbery elasticity. As \bar{M}_c decreases due to further cross linking, T_g increases and as it approaches the test temperature, a point of maximum damping is achieved. Here the resilience is at a minimum. Further decrease in \bar{M}_c increases resiliency until the sample become an elastic solid.

In the second case, in which the T_g of the chain segment is above the test temperature, the uncross-linked polymer is a brittle solid. Cross linking does not appreciably increase the modulus of elasticity or resiliency, but has a very strong influence (discussed later) on the temperature dependence of these properties.

Quantitative relationship of chemical structure to physical properties in network polymers has received considerably less attention and study than in the case of thermoplastics. However, in recent years, progress has been made towards elucidation of the quantitative relationships between structure and properties. We have chosen to illustrate the quantitative effect of structural factors on physical properties in four representative areas: glass transition temperature, modulus of elasticity, mechanical damping, solvent resistance.

Glass Transition Temperature. The formation of a three-dimensional network in a polymer does not eliminate the so-called glass transition temperature, but it does raise the temperature at which it occurs. Cross linking reduces the mobility of the segments, but does not prevent the thermal motion of flexible segments. Of particular interest is the work of Fox and Loshaek (10) who have studied the relationship of the physical structure of network polymers to the glass transition temperature.

Their work points out that the change in glass transition of a cross-linked polymer is due to the combined effects of cross linking $(\Delta T_g)_\rho$ and the structure of the cross-linking molecules $(\Delta T_g)_c$.

$$(\Delta T_g) = (\Delta T_g)_c + (\Delta T_g)_\rho$$

They have been able to show that these two effects may be separated and that the change in the glass transition temperature is equal to a constant times the density of cross linking ρ , at moderate degrees of cross linking.

$$(\Delta T_g)_\rho = K\rho$$

They studied, therefore, a cross-linking styrene-divinylbenzene copolymer system (Figure 12). The structural similarity between styrene and divinylbenzene was assumed to make the compositional factor in the equation negligible. It is evident that their data fit the equation. This relationship is less valid at high degrees of cross linking because of a decreasing efficiency of cross linking.

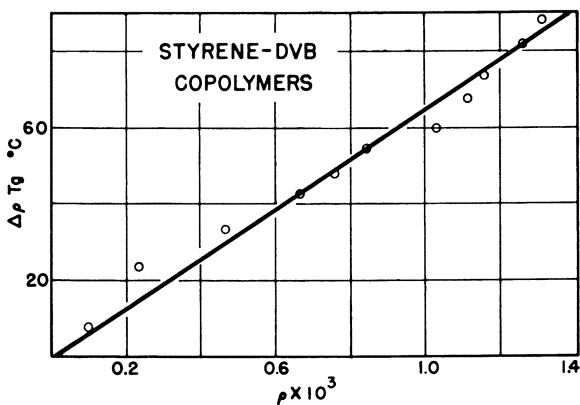


Figure 12. The increase in the glass temperature of polystyrene with increasing concentration of moles per gram of divinylbenzene

From Fox, T. G., and Loshaek, S., *J. Polymer Sci.* 15, 371 (1955)

COURTESY *Journal of Polymer Science*

If, however, a very different cross-linking agent such as the highly flexible decamethylene glycol dimethacrylate is used, the contribution to the lowering of the glass transition temperature made by the flexible cross linker may outweigh the cross-linking effect (Figure 13). Loshaek (16) has shown that the copolymerization theory may be used to determine the glass transition of the base polymer, and, with this correction, the relationship between glass transition temperature and density of cross links holds also in these systems.

Polymers with an extremely high degree of cross linking, such as phenolics, do not show a measurable glass transition temperature up to 200° C.

Modulus of Elasticity. Drumm (7) and Nielsen (21) have shown that the room temperature modulus of elasticity of highly cross-linked polymers is not markedly affected by cross linking (Figure 14). As the degree of cross linking increases, the temperature sensitivity of the modulus of elasticity decreases greatly. The phenolic cross-linked structure is highly rigid and tightly cross-linked, which

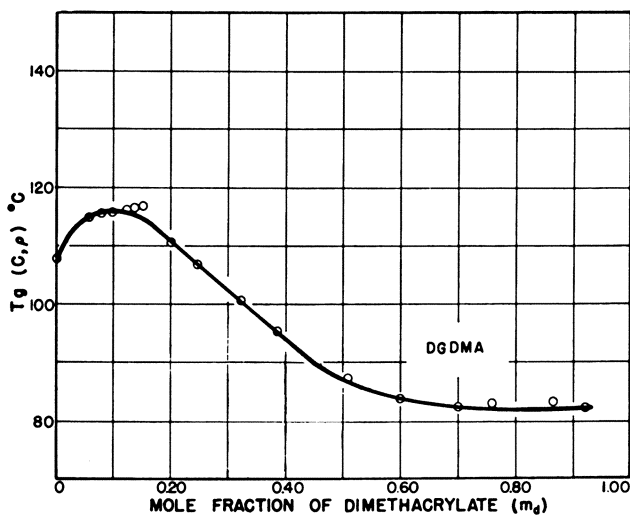


Figure 13. Glass temperature plotted vs. m_d for copolymers of methyl methacrylate and decamethylene dimethacrylate

From Loshak, S., *J. Polymer Sci.* 15, 391 (1955)

COURTESY *Journal of Polymer Science*

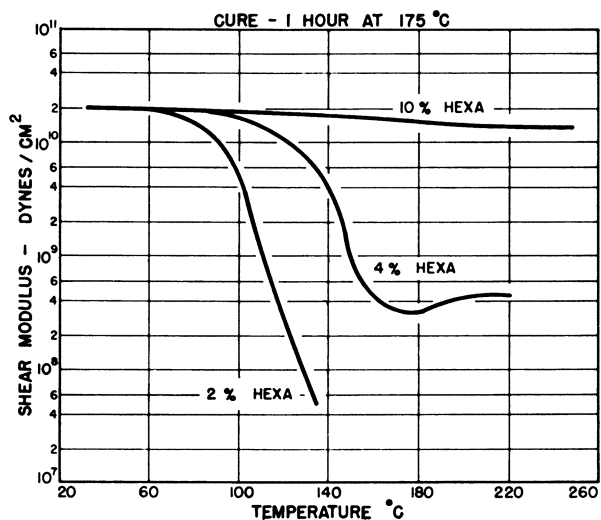


Figure 14. Dynamic properties of a phenol-formaldehyde novolak cross-linked with various amounts of hexamethylenetetramine by heating for one hour at 175° C.

From Drumm, M. F., Dodge, C. W. H., and Nielsen, L. E., *Ind. Eng. Chem.* 48, 76 (1956)

COURTESY *Industrial and Engineering Chemistry*

accounts for its ability to withstand temperature of 500° F. for prolonged periods and the temperature of rocket exhaust gases for short periods.

In the less highly cross-linked systems, the effect of the structure of the segments becomes extremely important.

Thus, in three selected polyurethane systems, the longer the hydrocarbon chain in the segments, the lower the temperature of relaxation (Figure 15).

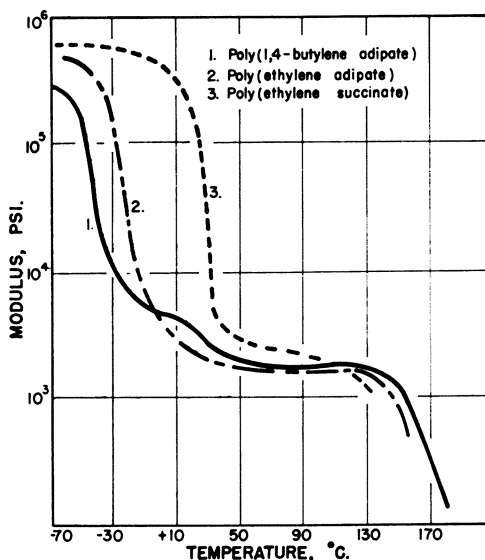


Figure 15. Effect of polyester on Clash-Berg torsional modulus of polyester urethane elastomers

From Saunders, J. H., *Rubber Chem. and Technol.* 33, 1259 (1960)

COURTESY *Rubber Chemistry and Technology*

Mechanical Damping. The dynamic mechanical properties of viscoelastic materials as used to reduce and control vibrations is a field of ever increasing interest. Ungar and Hatch (26) have recently surveyed the field and have suggested that polymer designers have many tools at their disposal to select, and synthesize polymers with the desired viscoelastic characteristics. The logarithm of the decay of vibration in a dynamic mechanical test is an index of the damping of the viscoelastic material. Cross linking generally decreases the peak in the damping curve, while at the same time markedly broadening it. Figure 16 illustrates the effect of increased cross linking on the damping peak of a phenolic resin. When cross linking becomes so great that chain segment mobility is not permitted, the damping peak is eliminated.

Certain structosets of low chain segments T_g are good viscoelastic damping materials. Figure 17 shows the damping curve of a urethane structoset specifically designed to exhibit a broad damping range.

Another practical example of the study of damping in ordered structosets and thermosets is in the manufacture of punching-grade, phenolic electrical laminates. These materials punch well, if they are in the region of high damping, while they are very brittle and fracture, if in the region of low damping.

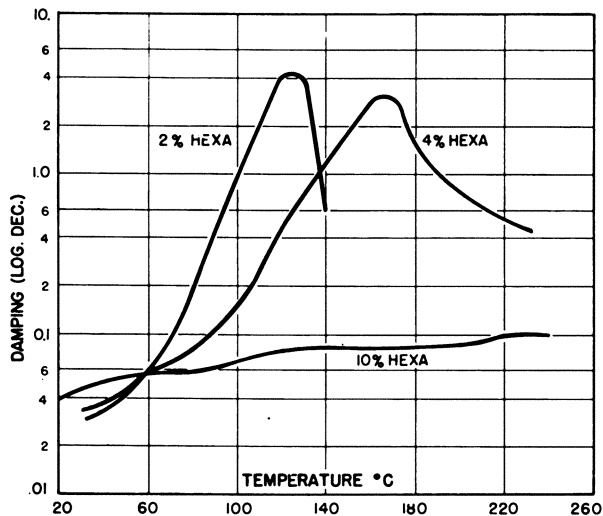


Figure 16. Dynamic properties of a phenol-formaldehyde novolak cross-linked with various amounts of hexamethylenetetramine by heating for one hour at 175° C.

From Drumm, M. F., Dodge, C. W. H., and Nielsen, L. E., *Ind. Eng. Chem.* 48, 76 (1956)

COURTESY Industrial and Engineering Chemistry

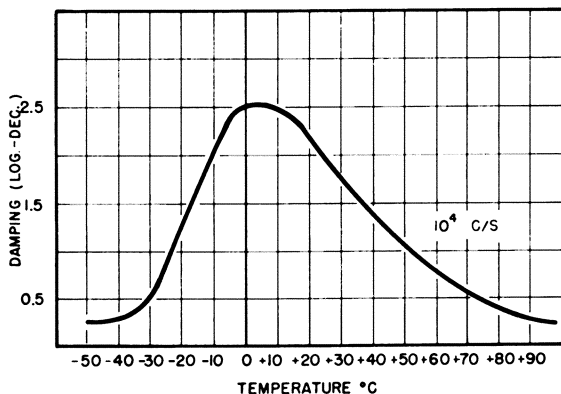


Figure 17. Mechanical damping of urethane elastomer (8)

Solvent Resistance. One of the outstanding characteristics of the polymer networks is their solvent resistance. Increases in cross linking density make it more and more difficult for solvent molecules to penetrate the polymer structure and to swell the network. Also, as cross linking increases, the ratio of sol to gel as previously discussed, decreases. The effect of increasing amounts of cross linker on the swelling index and per cent soluble of a cross-linked phenolic novolak (structopendant) is given in Figure 18. Thus, with increased cross linking, swelling rapidly decreases to become almost negligible. At low cross linking,

extractables are as high as 30%. They rapidly decrease as gel content approaches 100% with essentially no extractables at high cross link density.

The correlation of average molecular weight between branch points with the swelling of a urethane elastomer is shown in Figure 19. As the chain length between cross links increases, or cross linking decreases, swelling is increased, since the solvent molecule can penetrate more readily the three-dimensional polymer.

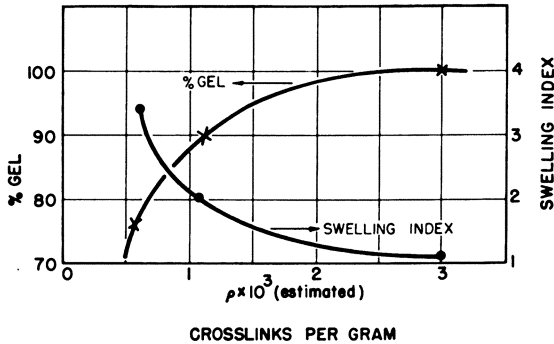


Figure 18. The effect of strong solvents on cross-linked phenolics

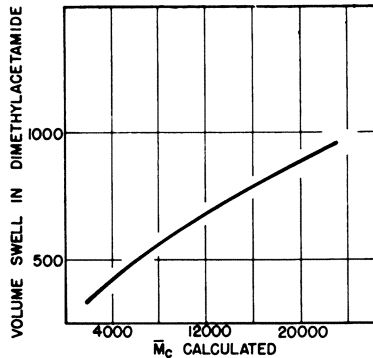


Figure 19. Effect of \bar{M}_c on swelling of a polyester urethane elastomer

From Saunders, J. H., *Rubber Chem. and Technol.* 33, 1259 (1960)

COURTESY *Rubber Chemistry and Technology*

No discussion of the structoset polymers is complete without some highlights relating to their present and future industrial applications. Major utility of these systems is derived from the fact that they are usually low in viscosity, readily soluble, and easy to handle during application. In contrast to the older thermosets, heat is not a specific requirement for the development of high molecular weight. Frequently, the structosets are converted to the final cross-linked polymer and attain ultimate properties in situ.

The rapid growth of structoset urethanes in foams is due to a combination of

the ability to incorporate into the polymer rigid or elastic properties at will, to use relatively inexpensive polyester and polyether prepolymers, to cure rapidly on the foam machine, and to form foams in situ. Low curing temperatures allow ordered structosets to perform a vital function as binders in solid rocket propellants.

The excellent properties which can be designed into the final molecule, as well as low application temperatures, make epoxies extremely useful in many electrical applications. Structoset coatings, based on a great variety of prepolymers, are widely used because one is able to tailor coatings for a variety of end uses and to obtain satisfactory properties combined with good economics.

In conclusion, we have shown some of the key correlations between structure and properties of the structosets and hope that this presentation will not only further the understanding and use of these materials, but will also stimulate additional fundamental research.

Acknowledgment

The authors wish to thank the Monsanto Chemical Co. for permission to publish this paper and L. E. Nielsen and C. A. Magarian for their helpful discussion and criticism.

Literature Cited

- (1) Applegath, D. D., *Offic. Dig. Federation Paint & Varnish Production Clubs* **33**, 137 (1961).
- (2) Bayer, O., Müller, E., *Angew. Chem.* **72**, 934 (1960).
- (3) Billmeyer, F. W., "Textbook of Polymer Chemistry," p. 40, Interscience, New York, 1957.
- (4) Christenson, R. M., Hart, D. P., *Offic. Dig. Federation Paint & Varnish Production Clubs* **33**, 684 (1961).
- (5) Clark, H., Adams, R. G., *Modern Plastics* **37**, 132 (1960).
- (6) Dow Corning Corp., Midland, Mich., Technical Literature, Nos. 7-100 and 7-903.
- (7) Drumm, M. F., Dodge, C. W. H., Nielsen, L. E., *Ind. Eng. Chem.* **48**, 76 (1956).
- (8) Farbenfabriken Bayer A.G., Leverkusen, Germany, "Vulkollan as an Elastic Construction Material," p. 18, 1960.
- (9) Flory, P. J., "Principles of Polymer Chemistry," p. 348, Cornell Univ. Press, Ithaca, N. Y., 1953.
- (10) Fox, T. G., Loshaek, S., *J. Polymer Sci.* **15**, 371 (1955).
- (11) Gordon, M., *J. Chem. Phys.* **22**, 610 (1954).
- (12) Gordon, M., Grieverson, B., McMillan, I. D., *J. Polymer Sci.* **18**, 497 (1955).
- (13) Greenspan, F. P., Johnston, C., Reich, M., *Modern Plastics* **37**, 142 (1959).
- (14) Heiss, H. L., Saunders, J. H., Morris, M. R., Davis, B. R., Hardy, E. E., *Ind. Eng. Chem.* **46**, 1498 (1954).
- (15) Lilley, H. S., *Paint Technol.* **22**, 441 (1958).
- (16) Loshaek, S., *J. Polymer Sci.* **15**, 391 (1955).
- (17) Mark, H., Whitby, G. S., eds., "Collected Papers of W. H. Carothers on High Polymeric Substances," Interscience, New York, 1940.
- (18) Martin, R. W., "Chemistry of Phenolic Resins," Wiley, New York, 1956.
- (19) *Modern Plastics* **38**, 82 (1961).
- (20) Murdock, J. D., Segall, G. H., *Offic. Dig. Federation Paint & Varnish Production Clubs* **33**, 709 (1961).
- (21) Nielsen, L. E., *SPE Journal* **16**, 525 (1960).
- (22) Petropoulos, J. C., Frazier, C., Cadwell, L. E., *Offic. Dig. Federation Paint & Varnish Production Clubs* **33**, 719 (1961).
- (23) Rochow, E. G., "Chemistry of the Silicones," 2nd ed., Wiley, New York, 1951.
- (24) Saunders, J. H., *Rubber Chem. and Technol.* **33**, 1259 (1960).
- (25) Skeist, I., "Epoxy Resins," Reinhold, New York, 1959.
- (26) Ungar, E. E., Hatch, D. K., *Prod. Eng.* **32**, 44 (1961).
- (27) Vogel, H. A., Bittle, H. G., *Offic. Dig. Federation Paint & Varnish Production Clubs* **33**, 699 (1961).
- (28) Wood, E. N., *SPE Tech. Papers* **5**, No. 40-1 (Jan. 1959).

RECEIVED September 6, 1961.

Low-Temperature Polycondensation Processes

P. W. MORGAN

*Pioneering Research Division, Textile Fibers Department,
E. I. du Pont de Nemours and Co., Inc., Wilmington, Del.*

Polycondensation at room temperature between two or more fast-reacting intermediates is becoming widely used because of its convenience and speed. The interfacial polycondensation system, in particular, which employs two immiscible liquids, is applicable to a wide variety of chemical structures: amides, urethanes, esters, sulfonates, sulfonamides, and ureas. Many products can be made at low temperature which could not be formed by melt methods because of their infusibility or thermal instability. The low temperature procedures are subject to the effect of many variables, but these are readily controlled and acceptable conditions for use with new polymers or intermediates can usually be found. The processes are readily scaled up in simple batch equipment or continuous reactors. Special areas of application are the direct formation of fibers from the reactants and polycondensation on fiber substrates.

Many condensation polymers are formed by the interaction of bifunctional intermediates with the elimination of a small by-product molecule at each point of combination. A well-known example is the commercial preparation of 6-6 nylon. For this preparation, a diamine and a diacid are combined to form a polymeric salt, which then is subjected to heat and later to heat and vacuum; water is eliminated and a linear polyamide is formed.

The preparation of nylon in this way requires high temperature, special pressure and vacuum equipment, and a lengthy reaction period. The use of such processes is limited almost wholly to the preparation of polymers which are fusible and thermally stable.

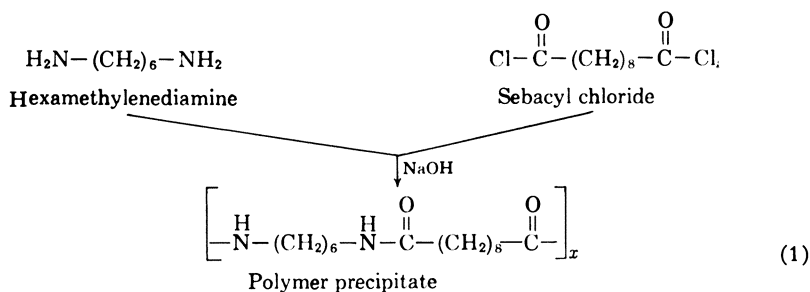
There have come into prominence in the past few years fast, low-temperature processes for the preparation of condensation polymers (12, 22).

The chemistry of these processes is old and simple—in fact, the application of this chemistry to polymer-making is not new. Much work on polyurethanes was done, 20 years ago, by Farbwerke Hoechst A.-G. in Germany. Out of this work

came Perlon U, made by the reaction of diisocyanates and glycols (6, 17). Both earlier and later references (12) to other polymers may be found, but many of these polymers did not possess high molecular weight.

Neither a historical review nor a complete story of this field of polymer making is presented here. Rather, this is a series of views of the chemistry and procedures, from which one may obtain some idea of the potential as well as of the limitations of the methods. The discussion includes only reactions which yield essentially linear polymers, bypassing polyurethane foams and phenol-formaldehyde condensates.

Equation 1 shows the reaction for the preparation of 6-10 polyamide. The 6-10 notation stands for the number of chain carbon atoms in the two intermediates, the diamine structure being designated first. In place of diacids, which terminate in OH groups, one uses diacid chlorides which are extremely reactive toward amines even at room temperature or below. Hydrogen chloride is the by-product rather than water, which is eliminated in the conventional high-temperature process. The average polymer size, indicated by the subscript in Equation 1, may be 25 to 100 repeat units. This is equal to the molecular weights obtained by melt processes.



Range of Chemical Structures and Polymer Properties

By varying the structures between the functional groups, many polyamides can be made. By changing the functional groups, other classes of polymers are obtained. The principal limitations result from too great a reduction in reactivity of the intermediates or the production of intermediates or polymers with insufficient stability for effective use. Table I shows some of the possible polymer classes.

The change from one chemical class to another, as in Table I, will produce changes in polymer properties such as solubility and melting point. The same type of change within a polymer class can be produced by varying the structures connecting the functional groups. Low-temperature polycondensation procedures are especially applicable to the formation of polymers with wide property differences, as indicated in Table II.

Polycondensation Procedures

The majority of the reactions listed in Table I are best carried out by use of two immiscible liquid phases, one of which is preferably water. The water phase contains the diamine or diol and any added alkali. The other phase consists of the diacid halide and an organic liquid, such as carbon tetrachloride, dichloro-

Table I. Chemical Classes of Polymers from Low-Temperature Polycondensation Processes

	<i>Linking Structure in Polymer</i>	<i>Reacting Groups in Intermediates</i>
Amide (7, 14)	$\begin{array}{c} \text{O} \\ \parallel \\ -\text{N}-\text{C}- \end{array}$	$\begin{array}{c} \text{O} \\ \parallel \\ -\text{N}-\text{H} + \text{Cl}-\text{C}- \end{array}$
Urea (20)	$\begin{array}{c} \text{O} \\ \parallel \\ -\text{N}-\text{C}-\text{N}- \end{array}$	$\begin{array}{c} \text{O} \\ \parallel \\ -\text{N}-\text{H} + \text{Cl}-\text{C}-\text{Cl} \end{array}$
Urethane (27)	$\begin{array}{c} \text{O} \\ \parallel \\ -\text{N}-\text{C}-\text{O}- \end{array}$	$\begin{array}{c} \text{O} \\ \parallel \\ -\text{N}-\text{H} + \text{Cl}-\text{C}-\text{O}- \end{array}$
Sulfonamide (18)	$\begin{array}{c} \text{H} \quad \text{O} \\ \quad \parallel \\ -\text{N}-\text{S}- \\ \parallel \\ \text{O} \end{array}$	$\begin{array}{c} \text{H} \quad \text{O} \\ \quad \parallel \\ -\text{N}-\text{H} + \text{Cl}-\text{S}- \\ \parallel \\ \text{O} \end{array}$
Phosphonamide (5)	$\begin{array}{c} \text{H} \quad \text{O} \quad \text{H} \\ \quad \parallel \quad \\ -\text{N}-\text{P}-\text{N}- \\ \\ \text{R} \end{array}$	$\begin{array}{c} \text{H} \quad \text{O} \\ \quad \parallel \\ -\text{N}-\text{H} + \text{Cl}-\text{P}-\text{Cl} \\ \\ \text{R} \end{array}$
Ester (3)	$\begin{array}{c} \text{O} \\ \parallel \\ -\text{O}-\text{C}- \end{array}$	$\begin{array}{c} \text{O} \\ \parallel \\ -\text{O}-\text{H} + \text{Cl}-\text{C}- \end{array}$
Carbonate (16)	$\begin{array}{c} \text{O} \\ \parallel \\ -\text{O}-\text{C}-\text{O}- \end{array}$	$\begin{array}{c} \text{O} \\ \parallel \\ -\text{O}-\text{H} + \text{Cl}-\text{C}-\text{Cl} \end{array}$
Sulfonate (4)	$\begin{array}{c} \text{O} \\ \parallel \\ -\text{O}-\text{S}- \\ \parallel \\ \text{O} \end{array}$	$\begin{array}{c} \text{O} \\ \parallel \\ -\text{O}-\text{H} + \text{Cl}-\text{S}- \\ \parallel \\ \text{O} \end{array}$

methane, xylene, or hexane. The polymerization takes place at or near the liquid interface and therefore the process has been named interfacial polycondensation.

The following outline shows the simplicity of the procedure:

A few of the polycondensation reactions may be performed in a single liquid phase. Examples of this are the reaction of diisocyanates with diols (8) or diamines (7) and the formation of polycarbonates from bisphenols and phosgene in a solvent with pyridine as the acid acceptor (15, 22).

Low-temperature polycondensation reactions are best carried out with high-speed stirring (1, 14), although there are examples of successful reactions performed with only moderate stirring. Home blenders are excellent reaction vessels. The processes may be scaled up easily by use of large cans or drums and overhead stirrers. Polymerization may be carried out continuously in T-tubes or other devices. Figure 1 illustrates a glass laboratory apparatus for continuous polymerization.

Table II. Variation in Physical Properties and Order in Polymers from Low-Temperature Polycondensation Processes

<i>Property or Structural Characteristic</i>	<i>Example</i>	
Soluble and fusible	$-\text{N} \begin{array}{c} \diagup \\ \diagdown \end{array} \text{N} - \overset{\text{O}}{\parallel} \text{C} - (\text{CH}_2)_8 - \overset{\text{O}}{\parallel} \text{C} -$	(14)
Thermally unstable	$-\text{N} \begin{array}{c} \diagup \\ \diagdown \end{array} \text{N} - \overset{\text{O}}{\parallel} \text{C} - \text{O} - \text{CH}_2 - \text{CH}_2 - \text{O} - \overset{\text{O}}{\parallel} \text{C} -$	(21)
Infusible, but soluble	$-\text{N} \begin{array}{c} \diagup \\ \diagdown \end{array} \text{N} - \overset{\text{O}}{\parallel} \text{C} - \text{C}_6\text{H}_4 - \text{C}_6\text{H}_4 - \overset{\text{O}}{\parallel} \text{C} -$	(7)
Insoluble, network	$ \begin{array}{c} \text{H} \qquad \qquad \qquad \text{H} \quad \text{O} \qquad \qquad \qquad \text{O} \\ \qquad \qquad \qquad \quad \parallel \qquad \qquad \qquad \parallel \\ -\text{N} - (\text{CH}_2)_3 - \text{N} - (\text{CH}_2)_3 - \text{N} - \text{C} - (\text{CH}_2)_8 - \text{C} - \\ \qquad \qquad \qquad \qquad \qquad \qquad \qquad \qquad \qquad \qquad \qquad \qquad \parallel \\ \qquad \qquad \qquad \qquad \qquad \qquad \text{C} - (\text{CH}_2)_8 - \text{C} - \\ \qquad \qquad \qquad \qquad \qquad \qquad \parallel \qquad \qquad \qquad \parallel \\ \qquad \qquad \qquad \qquad \qquad \qquad \text{O} \qquad \qquad \qquad \text{O} \end{array} $	(10)
Ordered and block structures		(9)

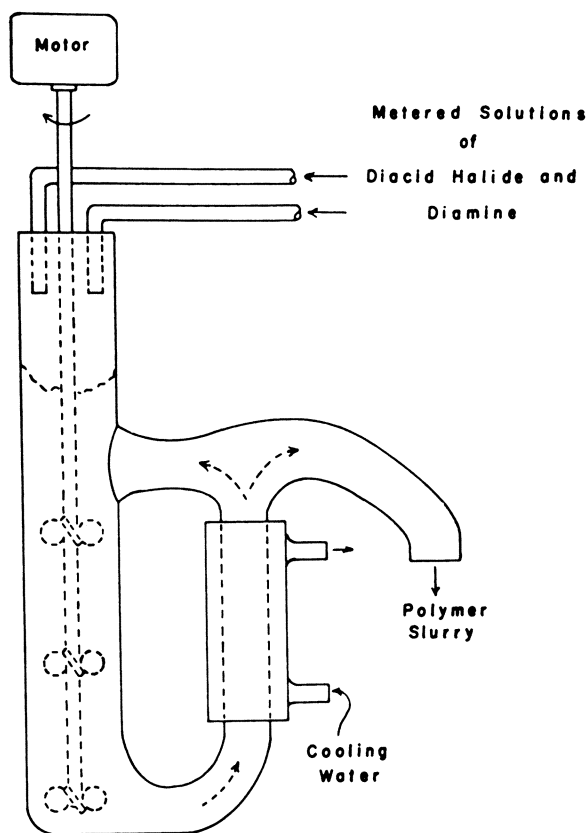
**Figure 1. Continuous polymerizer**

Table III. Stirred Interfacial Polycondensation Process Steps*Polycondensation reaction*

1. Make up reactant solutions
2. Mix vigorously, 1 to 5 minutes

Polymer isolation

1. Polymer precipitates naturally or add a nonsolvent
2. *a.* Filter or centrifuge polymer precipitate
b. Alternatively, steam off low-boiling solvents
3. Wash
4. Dry

Use

1. Isolate polymer solution directly and cast or spin
2. Redissolve polymer and spin, cast or coat
3. Compact powder and mold or extrude

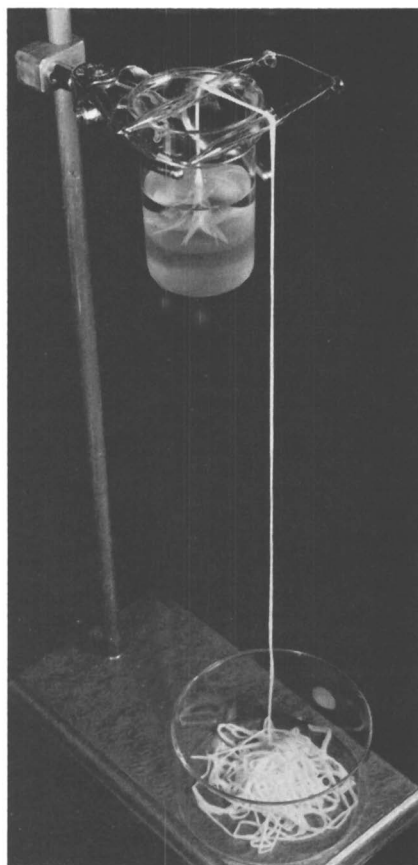


Figure 2. Continuous formation of 6-10 polyamide in an unstirred interfacial polycondensation system

If the complementary phases for an interfacial polycondensation are brought together without stirring, and if the organic liquid is a nonsolvent for the polymer, a thin film of polymer forms at once at the interface. Under the right conditions, this film is tough and has high molecular weight. When the film is grasped and

pulled from the area of the interface, more polymer forms at once and a collapsed sheet or tube of polymer may be withdrawn continuously (Figures 2 and 3). This type of polymerization has been used as a lecture demonstration (13). Since the omission of stirring decreases the number of variables, the method has also been used to study the polymerization mechanism.

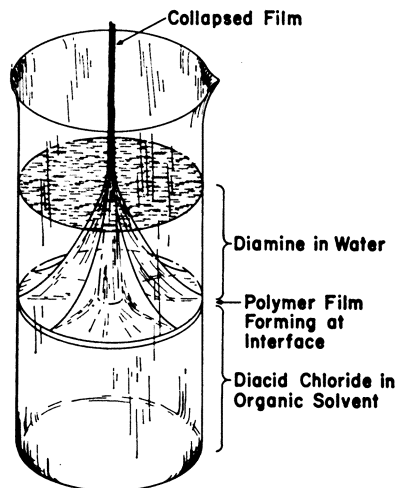


Figure 3. Diagram of film formation in unstirred interfacial polycondensation system

The yield of polymer by this process is only 25 to 50% because much unreacted material is carried away upon the film, whereas the yields from stirred procedures are usually between 75 and 100%.

Variables Affecting Interfacial Polycondensation Reactions

Polymers may often be made successfully in a nonsystematic manner. However, higher quality polymers and higher yields are obtained by attention to the effects of some of the many process variables. Several of the more important ones are listed in Table IV.

Table IV. Important Variables in Interfacial Polycondensation Procedures

1. Chemical reaction rate
2. Precipitation rate of the polymer (including its degree of swelling or solubility)
3. Purity of materials
4. Hydrolysis of the acid halide
5. Stirring rate
6. Phase volume ratio and concentration of the intermediates

Stirring rate and reactant concentration are considered briefly.

Figure 4 presents several plots relating the inherent viscosity of the polymer (which is a measure of molecular weight) to the concentration of sebacyl chloride in the preparation of 6-10 polyamide. The diamine concentration was held constant for each plot. This is a polymerization system from which the polymer precipitates very rapidly. For the unstirred preparations (A) and those with a

medium stirring rate (B), the peaks in inherent viscosity occur at about the same acid chloride concentration. With high-speed stirring, the highest viscosity occurs at a higher acid chloride concentration.

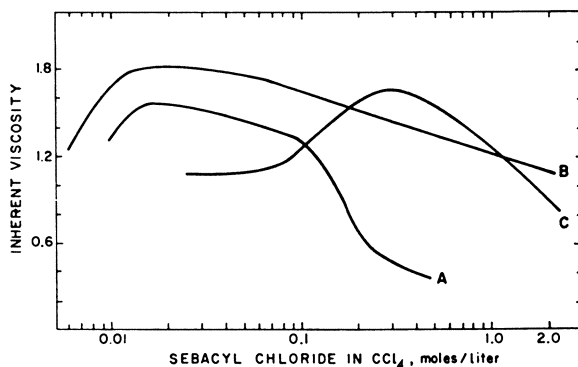


Figure 4. Polyamide 6-10, product solution viscosity vs. reactant concentrations in polymerization reactions

- A. Without stirring
 B. With stirring, medium speed, total liquid volume, 600 ml.
 C. Full speed with total liquid volume, 300 ml.
 In all cases, diamine concentration is 0.10M

The peaks presumably result from the attainment of conditions under which the quantities of the two reactants reaching the polymerization site in the organic solvent are most nearly equivalent. As the quantity of reactants in the system as a whole is increased, stirrability decreases and this accounts for part of the decline in quality toward the right of the plots for the stirred reaction mixtures.

The peaks in inherent viscosity represent more than the conditions under which polymers with the highest molecular weights may be made. At such a peak point, the numbers of amine and carboxyl end groups per unit weight are most nearly equivalent, the molecular weight distribution is nearest to that characteristic of a polyamide made by the melt method, and the yield of polymer is highest in the stirred system (14).

The preceding discussion applies to a polyamide which precipitates. Figure 5 shows that for poly(sebacyl piperazine) (first structure, Table II), which remains dissolved in the organic solvent, there are likewise coincident peaks in the plots of inherent viscosity and yield vs. the concentration of acid chloride.

Some Practical Applications

In addition to the use of low-temperature polycondensation reactions as a research tool leading to new polymers, several other applications have been described.

The unstirred, interfacial polycondensation procedure has been used to produce fibers with dimensions useful for textiles. This was accomplished by use of very small interfaces or by extruding a solution of one reactant into a bath of the dissolved complementary reactant (10). Under some conditions the fibers may be ribbon-like as a result of the collapse of the initial tubular structure (11).

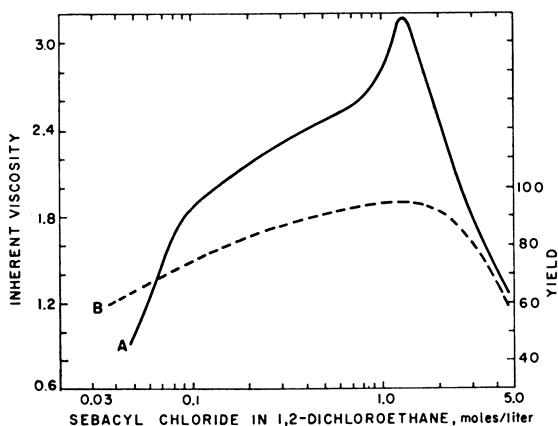


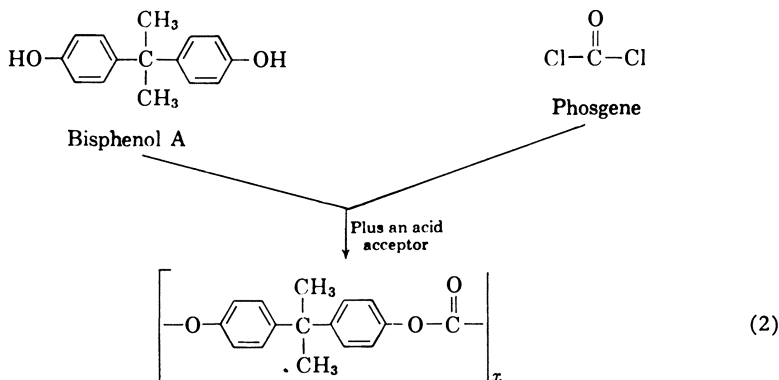
Figure 5. Polyamide Pip-10, stirred polymerization reactions with the polymer in metastable solution

A. Product solution viscosity vs. reactant concentration
 B. Yield vs. reactant concentration

Conditions. Diamine concentration 0.1M, full speed stirring, total liquid volume, 400 ml.

Whitfield, Miller, and Wasley (19) have described a shrink-proofing treatment for wool which employs interfacial polycondensation. The fabric is first wet out with a dilute aqueous solution of hexamethylenediamine, the excess liquid is squeezed out, then the fabric passes through a dilute solution of sebacyl chloride in a water-immiscible organic solvent. Polycondensation takes place here with the formation of a thin film of polyamide about the fibers. The excess liquid is pressed out and the fabric is washed and dried. The gain in fabric weight is only a few per cent and it is said that there is no stiffening or marked change in physical properties. Yet the wool can now be put through ordinary laundry cycles and drying treatments without shrinkage.

Polycarbonates from bisphenols (Equation 2) have reached commercial importance. They may be made by several methods, including both low- and high-temperature procedures (16). A recently constructed plant for the preparation of the polycarbonate from Bisphenol A [2,2-bis(4-hydroxyphenyl)propane] is reported to use phosgene in a low-temperature process (2). The reaction is carried out in a single solvent for the reactants and polymeric product. Pyridine is used as the acceptor for by-product hydrogen chloride.



The solution of polymer and pyridine salt is washed with water to remove the salt, the aqueous wash liquors are decanted, and the polymer is isolated by use of a precipitating liquid or nonsolvent.

The polymer is then collected, washed, dried, pelletized, and passed on for extrusion or other forming steps. Pyridine and solvents are recovered in additional operations. Chohey gives a detailed process diagram (2).

Conclusion

Low-temperature polycondensation processes provide polymer chemists with a broadly applicable and fast laboratory tool, with which rapid surveys of a large number of polymer structures are possible. Semiscale preparations are easy and even plant-scale operations are feasible. Already one such operation has been started. On a large scale, solvent recovery and waste disposal present some economic problems.

The next five years will bring forth many more publications on new research in this field and further practical applications will be emerging.

Literature Cited

- (1) Beaman, R. G., Morgan, P. W., Koller, C. R., Wittbecker, E. L., Magat, E. E., *J. Polymer Sci.* **40**, 329 (1959).
- (2) Chohey, N. P., *Chem. Eng.* **67**, No. 23, 174 (1960).
- (3) Conix, A., *Ind. Eng. Chem.* **51**, 147 (1959).
- (4) Conix, A., Laridon, U., *Angew. Chem.* **72**, 116 (1960).
- (5) Harris, D. M., Jenkins, R. L., Nielsen, M. L., *J. Polymer Sci.* **35**, 540 (1959).
- (6) Hill, R., "Fibres from Synthetic Polymers," Elsevier, New York, 1953.
- (7) Katz, M. (to E. I. du Pont de Nemours and Co.), U.S. Patent **2,888,438** (May 26, 1959).
- (8) Lyman, D. J., *J. Polymer Sci.* **45**, 49 (1960).
- (9) Lyman, D. J., Jung, S. L., *Ibid.*, **40**, 407 (1959).
- (10) Magat, E. E., Strachan, D. R. (to E. I. du Pont de Nemours and Co.), U.S. Patent **2,708,617** (May 17, 1955).
- (11) *Ibid.*, **2,798,283** (July 9, 1957).
- (12) Morgan, P. W., *S.P.E. Journal* **15**, 485 (1959).
- (13) Morgan, P. W., Kwolek, S. L., *J. Chem. Educ.* **36**, 182, 530 (1959).
- (14) Morgan, P. W., Kwolek, S. L., *J. Polymer Sci.*, in press.
- (15) Schnell, H., *Ind. Eng. Chem.* **51**, 157 (1959).
- (16) Schnell, H., *Plastics Inst. (London) Trans.* **20**, No. 75, 143 (1960).
- (17) Smith, L. H., "Synthetic Fiber Developments in Germany," pp. 491-2, 700-10, Textile Research Institute, New York, 1946.
- (18) Sundet, S. A., Murphey, W. A., Speck, S. B., *J. Polymer Sci.* **40**, 389 (1959).
- (19) Whitfield, R. E., Miller, L. A., Wasley, W. L., *Textile Research J.* **31**, No. 8, 704 (1961).
- (20) Wittbecker, E. L. (to E. I. du Pont de Nemours and Co.), U.S. Patent **2,816,879** (Dec. 17, 1957).
- (21) Wittbecker, E. L., Katz, M., *J. Polymer Sci.* **40**, 367 (1959).
- (22) Wittbecker, E. L., Morgan, P. W., *Ibid.*, **40**, 289 (1959); and papers following.

RECEIVED September 6, 1961.

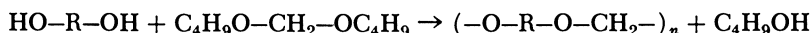
Process for Preparing High-Molecular-Weight Polyformals of Alicyclic Diols

W. J. JACKSON, Jr., and J. R. CALDWELL

Research Laboratories, Tennessee Eastman Co., Division of Eastman Kodak Co., Kingsport, Tenn.

Low-melting polyformals were made by Carothers by heating aliphatic diols and dibutyl formal in the presence of acidic catalysts. When attempts were made to prepare polyformals of alicyclic diols by this method, low-molecular-weight, colored polymers were obtained. A new process was therefore developed for preparing these polyformals. In this process, a diol and paraformaldehyde are heated in a hydrocarbon solvent in the presence of an acidic catalyst, and water is azeotropically removed. Depending upon the type of diol, the polymer is built up to a high molecular weight in this solution or in the solid phase. This process is superior to the conventional dibutyl formal method in that polymers with high molecular weights and substantially no color can be obtained. The process, developed for preparing polyformals of alicyclic diols, should also be applicable to various other types of diols.

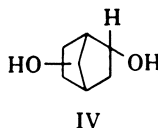
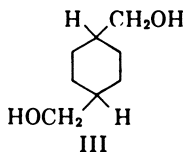
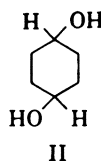
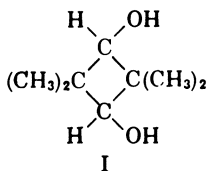
Polyformals were first prepared by Carothers (3, 6) by heating aliphatic diols and dibutyl formal in the presence of acidic catalysts:



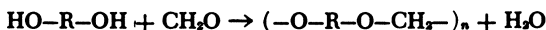
After the butyl alcohol was removed, the polymers were built up by heating the melt under reduced pressure. Since these polyformals of aliphatic diols had very low melting points (below 75° C.), their utility was limited. Apparently, no higher melting points have been reported for polyformals. In attempts to obtain higher-melting polyformals, the following alicyclic diols were used: *cis*-, *trans*-, and 1 to 1 *cis*-/*trans*- mixture of 2,2,4,4-tetramethyl-1,3-cyclobutanediol (I); *trans*-1,4-cyclohexanediol (II); *trans*-1,4-cyclohexanedimethanol (III); and 2,5- or 2,6-norbornanediol (IV).

Polyformals of high molecular weight were not obtained from these diols by interchange with dibutyl formal. Carothers reported that a polyformal can be

made with 1,4-cyclohexanediol by this method, but did not describe the polymer (3). Since no other method for preparing polyformals was described in the literature, a new process was developed. A diol, paraformaldehyde, and an acidic



catalyst are heated in a water-immiscible solvent, and water is removed as an azeotrope with the solvent (2). Some of the polymers prepared by this process could be built up in solution. Others attained high molecular weights when the particles were heated under reduced pressure at temperatures below their melting points. The reaction may be represented as follows:



This polymerization method was also applied to 1,10-decanediol, one of the aliphatic diols used by Carothers.

Experimental

Materials. **2,2,4,4-TETRAMETHYL-1,3-CYCLOBUTANEDIOL.** The diol was a commercial product (Tennessee Eastman Co.). Unless otherwise indicated, the diol consisted of a *cis*-/*trans*- mixture with about a 1 to 1 isomer ratio. The *cis*- isomer was obtained from the isomer mixture by transforming the *trans*- isomer into an unsaturated aldehyde with aqueous sulfuric acid (4). The *trans*-diol was obtained by preparing the diformate of the isomer mixture, separating the *trans*- derivative from the *cis*- derivative by recrystallization, and converting the *trans*-diformate to the diol by methanolysis (5).

***trans*-1,4-CYCLOHEXANEDIMETHANOL.** The diol was obtained from the *cis*-/*trans*- mixture by crystallization. The isomer mixture was a commercial product (Tennessee Eastman Co.).

***trans*-1,4-CYCLOHEXANEDIOL.** The diol was obtained by isomerization of a *cis*-/*trans*- mixture of the diol with an equimolar amount of sodium in refluxing diethylene glycol diethyl ether by a modification of the procedure of Batzer and Fritz (1).

2,5- or 2,6-NORBORNANEDIOL. The compound was prepared by adding acetic acid across the double bond of the cyclopentadiene-vinyl acetate Diels-Alder adduct and then converting this diacetate to the diol, which was an isomeric mixture.

1,10-DECANEDIOL. The diol (Eastman-grade) was purified by recrystallization.

PARA-FORMALDEHYDE. The aldehyde (Baker and Adamson reagent grade, Allied Chemical Corp.) was, according to the manufacturer, of at least 95% purity. A sample was checked and found to be 96% pure, calculated as formaldehyde.

SOLVENTS. The solvents were commercial grades, except benzene (Baker and Adamson reagent grade). The other solvents were distilled before use.

CATALYSTS. The catalysts were commercial products.

DIBUTYL FORMAL. The compound was prepared by refluxing a mixture containing 5.0 moles of formaldehyde, 11 moles of butyl alcohol, 25 grams of *p*-toluenesulfonic acid, and 500 ml. of benzene. The water which was formed during the reaction was collected in a Dean-Stark trap attached to a Vigreux column. This required about 4 hours. The solution was then cooled, washed with sodium bicarbonate solution, dried with sodium sulfate, and distilled. The product, a colorless liquid, boiled at 55° C., 6 mm. of Hg, n_D^{20} 1.4061. The yield was about 80%.

Dibutyl Formal Method. A procedure similar to that of Carothers (3, 6) was used in preparing polyformals from diols and dibutyl formal. Usually, 0.10 mole of dibutyl formal, 0.105 mole of the cyclic diol, and a catalytic amount of an acidic compound were heated in a metal bath at the boiling point of dibutyl formal (180° C.). If no butyl alcohol distilled over in about 0.5 hour, more catalyst was added. When insufficient butyl alcohol was obtained after about 2 hours, more catalyst was added. When an appreciable amount of the alcohol had been collected, the bath temperature was increased to 200° C. for about 1 hour. The pressure was then reduced to 0.5 mm. of Hg, while the prepolymer was stirred. If buildup of polymer did not take place in 1 to 2 hours (indicated by an increase in viscosity of the melt), the bath temperature was increased to 250° C.

The polyformals which were obtained in this manner from the alicyclic diols were highly colored, and their inherent viscosities were below 0.4 (determined using 60/40 phenol-tetrachloroethane mixture as solvent). Catalysts which were used were ferric chloride, methanedisulfonic acid, camphorsulfonic acid, antimony trifluoride, and titanium tetrafluoride. Polymers were not obtained with the latter two.

Paraformaldehyde Method. 2,2,4,4-TETRAMETHYL-1,3-CYCLOBUTANEDIOL. A 2-liter, three-necked flask was fitted with a glass stirrer, thermometer, and Dean-Stark trap which was filled with distilled cyclohexane and attached to a water-cooled condenser. In the flask were placed 216 grams (1.5 moles) of 2,2,4,4-tetramethyl-1,3-cyclobutanediol (1 to 1 cis-/trans- mixture), 52.2 grams (1.65 moles, if 95% pure) of paraformaldehyde, 1200 ml. of distilled cyclohexane, and 0.20 gram of methanedisulfonic acid in a 10 to 25% aqueous solution. (The catalyst solution had been treated with Darco G-60 to remove all color.) While this mixture was stirred at 60° C., the paraformaldehyde depolymerized to formaldehyde, which reacted with the diol. Complete reaction of these two components was indicated when they had gone into solution. This required about 1 hour.

The temperature of the mixture was then raised to 70° C. While this temperature was maintained with an automatic controller, the pressure was reduced until the cyclohexane was refluxing rapidly. This was accomplished by connecting the top of the reflux condenser through a dry ice trap to a vacuum line. The pressure was adjusted with a valve which bled air into the system between the condenser and trap. The reflux was fairly rapid in order to remove the water at a reasonable rate. Normally, about 5 hours was required to remove all of the water. In addition to the water which was in the catalyst solution, about 31 ml. of water collected in the Dean-Stark trap. (Apparently the aqueous layer contained some products from the excess formaldehyde, because the theoretical amount was 27 ml.) During the later stages of the reaction, some black material collected on the wall of the flask.

One-half hour after no more water was obtained in the Dean-Stark trap, the hot solution was decanted from the black residue and filtered through a fluted filter. The solution was kept hot during the filtration step to prevent the separation of prepolymer. The cyclohexane was then distilled, while the solution was heated under reduced pressure (water aspirator) on the steam bath. The residue consisted of white particles and powder with an inherent viscosity of 0.1 to 0.2. (All inherent viscosities were determined using 60 to 40 phenol-tetrachloroethane mixture as solvent.) The yield was virtually quantitative.

Analysis. Calculated for $C_9H_{16}O_2$: C, 69.3%; H, 10.3%. Found: C, 68.7%; H, 10.3%.

After the above prepolymer was ground to pass a 20-mesh screen, it was heated under a pressure of 0.1 mm. of Hg for 1 hour, while the temperature was

raised from 160° to 260° C. The temperature was then held at 260° C. for 1 hour. The polymer was obtained as white particles with inherent viscosities of 1.2 to 1.3.

Analysis. Calculated for $C_9H_{16}O_2$: C, 69.3%; H, 10.3%. Found: C, 69.2%; H, 10.2%.

Polyformals of the individual *cis*- and *trans*- isomers of the diol were similarly prepared.

The thermal stability of the polyformal of the *cis*-/*trans*-diol mixture was increased by treatment with an amine. A mixture of 2 grams of polyformal, 0.02 gram of tributylamine, and 10 ml. of methanol was stirred for 0.5 hour. When the polymer was heated in a film press at 300° C. for 4 minutes, the inherent viscosity decreased from 1.21 to 0.99. The inherent viscosity decreased to 0.81 when the polymer had not been stabilized.

The polymer could also be stabilized by treatment with acetic anhydride and sodium acetate. A mixture of 20 grams of the polyformal (20- to 40-mesh particles), 100 ml. of acetic anhydride, and 0.2 gram of sodium acetate was stirred for 3 hours at 130° C. The polymer was then collected and washed by stirring it with acetone, methanol, and water several times. When the polymer was heated in a film press at 300° C. for 4 minutes, the inherent viscosity decreased from 0.96 to 0.85.

The melting ranges and solubilities of the tetramethylcyclobutanediol polyformals are given in Table I.

trans-1,4-CYCLOHEXANEDIOL. A mixture of 11.6 grams (0.10 mole) of *trans*-1,4-cyclohexanediol, 3.3 grams (0.105 mole, if 95% pure) of paraformaldehyde, 0.05 gram of *p*-toluenesulfonic acid, and 40 ml. of benzene was stirred at 60° C. for 1 hour. The solution was then refluxed for 2 hours, and the water which formed was collected in a Dean-Stark trap filled with benzene. More paraformaldehyde (0.15 gram) was added, and the mixture was stirred at 60° C. for 0.5 hour before refluxing for 1 hour. Another 0.15 gram of paraformaldehyde was added, and the simmering and refluxing procedures were repeated. (These extra additions of paraformaldehyde were probably not necessary in this procedure, since solid-phase buildup was used, and only two experiments were carried out with this diol.) The benzene was then removed under reduced pressure, while the mixture was heated on the steam bath.

After the white, crystalline residue was ground to pass a 40-mesh screen, it was heated under a pressure of 0.1 mm. of Hg for 1.5 hours, while the temperature was raised from 150° to 193° C. The temperature was then held at 193° C. for 2 hours. The polymer, a white powder, had an inherent viscosity of 0.53. Its melting point and solubilities are given in Table I. The elemental analysis was not obtained.

trans-1,4-CYCLOHEXANEDIMETHANOL. A mixture of 28.8 grams (0.20 mole) of *trans*-1,4-cyclohexanedimethanol, 6.3 grams (0.20 mole, if 95% pure) of paraformaldehyde, 0.10 gram of *p*-toluenesulfonic acid, and 40 ml. of benzene was stirred at 60° C. for 1 hour. During this time the diol and paraformaldehyde went into solution. While this mixture was refluxed for 1.5 hours, 3.5 ml. of water collected in a Dean-Stark trap which was filled with benzene and attached to the flask. Additional paraformaldehyde (0.3 gram) was added, and the mixture was stirred at 60° C. for 0.5 hour and then refluxed for 1 hour. Since the mixture was very viscous, more benzene was added. Paraformaldehyde (0.3 gram) was added twice more, and the heating and refluxing procedures were repeated. It was also necessary to add more benzene because the solution again became very viscous. The catalyst in the polymer solution was neutralized by adding a few drops of ammonium hydroxide (and some ethanol to aid miscibility). The solvent was removed from a portion of the solution by heating on the steam bath under reduced pressure. The polymer had an inherent viscosity of 0.57.

Analysis. Calculated for $C_9H_{16}O_2$: C, 69.3%; H, 10.3%. Found: C, 68.6%; H, 10.4%.

The remainder of the benzene solution was poured into methanol with stirring. The white powder obtained had an inherent viscosity of 0.67. Its melting point and solubilities are given in Table I.

Analysis. Calculated for $C_9H_{16}O_2$: C, 69.3%; H, 10.3%. Found: C, 68.6%; H, 10.4%.

Perchloric acid was used as the catalyst in a procedure similar to that with *p*-

Table I. Physical Properties of polyformals of Alicyclic Diols

Diol	Melting Range, °C. ^{a,b}	Solubility ^c	
		Chloro- form	Hot toluene
1/1 <i>cis</i> -/ <i>trans</i> -2,2,4,4-tetramethyl-1,3-cyclobutanediol	283-291	Sol.	Sol.
<i>cis</i> -2,2,4,4-Tetramethyl-1,3-cyclobutanediol	284-289	Swollen	Swollen
<i>trans</i> -2,2,4,4-Tetramethyl-1,3-cyclobutanediol	275-280	Insol.	Insol.
<i>trans</i> -1,4-Cyclohexanediol	206-210	Insol.	Insol.
<i>trans</i> -1,4-Cyclohexanedimethanol	83-86	Sol.	Sol.
2,5- or 2,6-Norbornanediol	83-98	Sol.	Sol.

^a The lower figure of each range was the temperature at which the polymer began to soften. The higher figure was the temperature at which the polymer began to flow.

^b Melting ranges of tetramethylcyclobutanediol polyformals were determined under nitrogen in sealed capillaries. In air, these polymers melted at about 200° to 210° C. Melting ranges of the other polymers were determined in air with polarized light. They melted at approximately the same temperatures under nitrogen.

^c All of the polyformals were soluble in hot tetrachloroethane and insoluble in methanol, ethyl acetate, and naphtha.

toluenesulfonic acid. The components of the reaction mixture were 43.2 grams (0.30 mole) of *trans*-1,4-cyclohexanedimethanol, 11.3 grams (0.36 mole, if 95% pure) of paraformaldehyde, 120 ml. of benzene, and 1 drop (0.05 gram) of 60% perchloric acid. Two 0.3-gram portions of paraformaldehyde were added with a 1-hour stirring period at 60° C. and a 1-hour refluxing period after each addition. The catalyst was neutralized as before and the benzene was removed. The polymer had an inherent viscosity of 0.88.

2,5- OR 2,6-NORBORNANEDIOL. This polymer was prepared by a procedure similar to that for cyclohexanedimethanol using *p*-toluenesulfonic acid as catalyst. After concentration of a portion of the benzene solution, a polymer with an inherent viscosity of 0.28 was obtained. When the benzene solution was poured into methanol, a semisolid product was obtained. After being dried, the product, a clear, brittle resin, had an inherent viscosity of 0.49. Its melting range and solubilities are given in Table I.

Analysis. Calculated for C₈H₁₂O₂: C, 68.6%; H, 8.6%. Found: C, 68.5%; H, 8.6%.

1,10-DECANEDIOL. The polymer obtained from this diol was prepared similarly to that from cyclohexanedimethanol, but twice as much *p*-toluenesulfonic acid was used as catalyst and a 20% excess of paraformaldehyde was present at the beginning of the reaction. After concentration of a portion of the benzene solution, a polymer was obtained with an inherent viscosity of 0.87. When the catalyst was not neutralized before concentration, the polymer was degraded and an inherent viscosity of only 0.27 was obtained.

Discussion

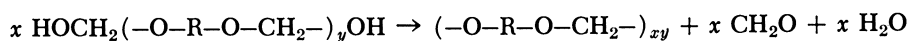
Description of Process. This process is superior to the conventional dibutyl formal method in that polyformals can be obtained with high molecular weights and substantially no color. A mixture of a diol, paraformaldehyde, acidic catalyst, and hydrocarbon solvent is stirred at 60° C. for about 1 hour. During this time, the paraformaldehyde depolymerizes and reacts with the diol. When complete solution is attained, the mixture is refluxed and the water formed in the reaction is azeotropically removed. When the prepolymer is to be built up in solution, two or three additional increments of paraformaldehyde are added and the reaction is continued. The viscosity of the solution increases as the molecular weight of the polymer increases. When the prepolymer is to be built up by the solid-phase method, the solvent is removed and the prepolymer isolated.

Prepolymers from the tetramethylcyclobutanediol isomers and from cyclohexanediol were built up by the solid-phase method—that is, the 20- to 40-mesh

particles were heated under reduced pressure at temperatures somewhat below their melting points. The polyformals of cyclohexanedimethanol, norbornanediol, and decanediol melted too low to be built up by this method, but were effectively built up in solution. Very low molecular weights were obtained when the prepolymers were built up in the melt phase under reduced pressure.

The solid-phase method of building up polyformals is applicable only to high-melting polymers. The required melting point is not known, but the polyformal of *trans*-1,4-cyclohexanediol melted at 206°–10° C. and that of the *cis*-/*trans*-mixture of 2,2,4,4-tetramethyl-1,3-cyclobutanediol melted appreciably higher. The solution method did not appear to be applicable to building up the polyformals of these two diols, since inherent viscosities below 0.4 were obtained. The solution method may be most applicable to primary diols, such as cyclohexanedimethanol and decanediol, which gave polyformals with inherent viscosities of 0.9.

Elemental analyses of the polyformals agreed with or were reasonably close to the calculated values; therefore, the polymers contained substantially no poly-(methylene oxide) in the chains. Since excess formaldehyde was used in preparing the prepolymers, presumably their chains were terminated with hydroxymethyl groups. Both water and formaldehyde must then be eliminated during the buildup of polymers:



Reaction Variables. An excess of paraformaldehyde was necessary (15 to 35 mole % excess was used) when the prepolymers were built up in solution. An excess evidently was not necessary when the prepolymers were built up in the solid phase. In experiments with tetramethylcyclobutanediol, a polymer with an inherent viscosity of 1.2 was obtained when the diol was present in 5 mole % excess, but the polymer was brown. When the paraformaldehyde was in excess, the amount was not critical, but it was necessary to use a minimum of about 10 mole % excess in order to obtain white polymers. Polyformals with inherent viscosities of 0.5 or greater were obtained when the molar excess of paraformaldehyde ranged from 2 to 40%. The highest inherent viscosities (above 1.0) were obtained when the excess was about 10 mole %. When trioxane was used as the formaldehyde source instead of paraformaldehyde, reaction did not take place (no water was obtained).

Benzene was a satisfactory solvent for preparing the polyformals of all the diols, except tetramethylcyclobutanediol. The polyformal of this diol could be readily obtained when benzene was used, but, unlike the polyformals of the other diols, this one was somewhat brown. The color was due to a benzene-soluble impurity which was formed during the reaction. When the prepolymer was built up, this color was greatly intensified and speckled polymer particles were obtained. A more satisfactory solvent was one in which the dark impurities were insoluble. They could then be removed by filtration before concentration of the prepolymer solution. Hexane gave good results, but the purity of the hexane appeared to be critical. (Brown- and tan-speckled polymer particles were often obtained after the solid-phase buildup, unless the hexane had been treated with oleum.) Cyclohexane gave white polymers with high inherent viscosities after buildup if the maximum reaction temperature during prepolymer formation was limited to 70° C. This was accomplished by carrying out the reaction under slightly reduced pressure. (Colored polymers were obtained if the prepolymer preparation was carried out in cyclohexane at its normal boiling point of 80° C.)

Effective catalysts for preparing the polyformals were *p*-toluenesulfonic acid, camphorsulfonic acid, methanedisulfonic acid, and perchloric acid. Various other acidic compounds were evaluated as catalysts with tetramethylcyclobutanediol. In these experiments, 0.5 to 1.0 gram of acidic compound per mole of tetramethylcyclobutanediol was normally added. If insufficient water was obtained, more catalyst was added. If the prepolymer was obtained but an appreciable amount of brown color was present, less catalyst was then used. Compounds which did not catalyze the reaction (no water obtained) were phosphoric acid, zinc chloride, trifluoroacetic acid, and heptafluorobutyric acid. Incomplete reactions (insufficient water) took place with concentrated hydrochloric acid, concentrated nitric acid, zinc fluoroborate, or Amberlite IRC-50 ion exchange resin as catalyst. A prepolymer was obtained when boron trifluoride etherate was used, but buildup did not take place in the solid phase (catalyst probably too volatile). Brown or speckled-brown polymers (after solid-phase buildup) were obtained with catalysts containing sulfonic acid groups (benzenesulfonic, dodecylbenzenesulfonic, sulfacetic, methanetrisulfonic, sulfuric, *p*-toluenesulfonic, camphorsulfonic, and methanedisulfonic acids). To obtain white polymers from tetramethylcyclobutanediol it was necessary to treat the solvent and prepolymer reaction mixture as previously described. (White polyformals were obtained from the other diols without this treatment.)

In these experiments with tetramethylcyclobutanediol, it was found that methanedisulfonic acid gave higher polyformals than the other catalysts. Inherent viscosities up to 1.7 were obtained, whereas values of only 0.8 to 0.9 resulted with camphorsulfonic acid or *p*-toluenesulfonic acid and 0.7 when perchloric acid was used. It was necessary to use 0.002 to 0.005 equivalent of camphorsulfonic acid or toluenesulfonic acid per mole of diol in order to obtain the polyformal, but 0.001 equivalent of perchloric acid or 0.001 to 0.002 equivalent (0.0005 to 0.001 mole) of methanedisulfonic acid was sufficient to catalyze the polymerization in the various solvents. When appreciably less catalyst was used, the polymers did not build up, and when appreciably more was used, brown polymers were obtained.

Titration indicated that almost all of the methanedisulfonic acid catalyst (or its reaction products) was present in the black material which was deposited on the flask walls during the latter stages of the tetramethylcyclobutanediol prepolymer preparation when hexane was the solvent. Since the catalyst is very soluble in water and insoluble in hydrocarbons, it evidently came out of solution with some decomposition products when no water remained in the system. An analysis of the prepolymer indicated that only 0.002% sulfur (1% of the original catalyst) was present. After solid-phase buildup, less than 0.001% sulfur was found in the polymer.

Thermal Stabilization of Polyformals. Polyformals, built up in solution, were neutralized with a little ammonium hydroxide when they were to be isolated by concentration under reduced pressure on the steam bath. This prevented breakdown of the polymer because of the acidic catalyst. The degradation was particularly bad with polyformals obtained from primary diols (cyclohexanedimethanol and decanediol). In one experiment, the polyformal of decanediol was obtained with an inherent viscosity of 0.9 when the catalyst had been neutralized and 0.3 when it had not been neutralized. Breakdown under these conditions was not observed with the prepolymer of tetramethylcyclobutanediol.

Degradation of the polyformal of tetramethylcyclobutanediol occurred when the polymer powder was heated in a film press at 300° C. The decrease in in-

herent viscosity was 33% (1.2 to 0.81) when the polymer was heated for 4 minutes. When the polymer was stabilized by stirring the particles in methanol with 1 weight % of tributylamine, the reduction in inherent viscosity was 18% under these conditions. Appreciably less stabilization was obtained with ammonia, trimethylamine, or pyridine. Presumably, this stabilization is due to neutralization of the acidic catalyst.

Acetylation of the polymer end groups by heating with acetic anhydride and sodium acetate was also effective in stabilizing the polymer. After this treatment, the decrease in inherent viscosity was only 11% under the above conditions.

Physical Properties of Polyformals. The polyformals of the alicyclic diols had higher melting points than any previously reported for polyformals. Those of the tetramethylcyclobutanediol polymers were unusually high, about 280° to 290° C. under nitrogen (Table I). Surprisingly, these polymers softened at about 200° to 210° C. in air. Since this lower melting range was due to air oxidation of the polymers, it was possible to protect them by the addition of conventional antioxidants. The other polyformals had substantially the same melting points under nitrogen as in air.

All of the polymers were soluble in hot tetrachloroethane, but, unexpectedly, the polyformal of the tetramethylcyclobutanediol isomer mixture was also soluble in chloroform and in hot toluene.

Since formals are readily hydrolyzed by dilute acids, polyformals would be expected to be unstable to acids. The tetramethylcyclobutanediol polyformal, however, was unusually resistant to acid hydrolysis. A 1-mil film did not begin to disintegrate in 10% hydrochloric acid at 100° C. until after 4 hours. The resistance of this polymer to alkaline hydrolysis was outstanding. A film did not begin to disintegrate when immersed in 10% sodium hydroxide solution at 100° C. for 7 days.

Acknowledgment

Thanks are due R. Gilkey and K. P. Perry for their contributions to this work.

Literature Cited

- (1) Batzer, H., Fritz, G., *Makromol. Chem.* **14**, 211 (1954).
- (2) Caldwell, J. R., Jackson, W. J., Jr. (to Eastman Kodak Co.), U. S. Patent **2,968,646** (Jan. 17, 1961).
- (3) Carothers, W. H. (to E. I. du Pont de Nemours & Co.), *Ibid.*, **2,071,252** (Feb. 16, 1937).
- (4) Hasek, R. H., Clark, R. D., Chaudet, J. H., *J. Org. Chem.* **26**, 3130 (1961).
- (5) Hasek, R. H., Elam, E. U., Martin, J. C., Nations, R. G., *Ibid.*, **26**, 700 (1961).
- (6) Hill, J. W., Carothers, W. H., *J. Am. Chem. Soc.* **57**, 925 (1935).

RECEIVED September 6, 1961.

Nucleophilic Polymerization of Heterocycles

ALFRED KREUTZBERGER

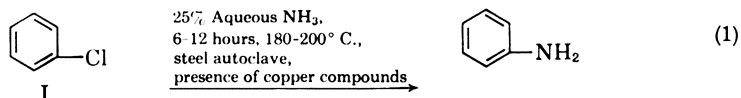
Scientific Laboratory, Ford Motor Co., Dearborn, Mich.

Investigations aimed at employing the unique properties of heterocycles to incorporate such rings into polymeric chains are reported. The most prominent characteristic of an aromatic heterocycle of the pyridine type is the tendency of the hetero atom to withdraw π -electron density from the ring. Particularly, the C atoms adjacent to the hetero atom become thereby positively charged and thus represent the sites of attack by nucleophilic agents. The principle of nucleophilic polymerization of heterocycles is applied in the use of bifunctional nucleophiles.

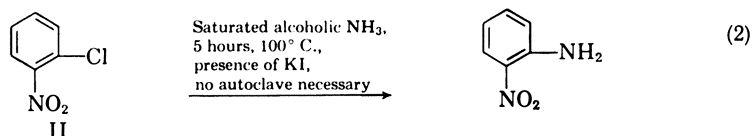
Aromatic heterocyclic rings show a great many similarities in behavior to carbocyclic compounds. Particularly marked is the pronounced stability of nuclei of both systems during many chemical reactions. In addition to these similarities, the presence of hetero atoms entails certain behavior differences typical of heterocyclic systems. While the chemistry of aromatic carbocyclic systems with regard to formation of polymers is fairly well established, relatively little is known about the suitability of heterocyclic rings for polymer formation. Thus, it has been the purpose of these investigations to evaluate typical heterocyclic behavior with respect to the possibilities of incorporating heterocyclic rings directly into polymeric chains. Excluded from these considerations have been such heterocyclic systems in which substituents attached to the ring are instrumental in polymer formation. Examples of this type are resin formation from melamine which is based essentially on the chemistry of aromatic amino groups, or the synthesis of fibers from vinylpyridines typifying the chemistry of ethylenic double bonds. In contrast to these examples, the present discussion is restricted to the heterocyclic ring as such.

Depending on the nature of the attack on an aromatic nucleus, reagents are classified as electrophilic, nucleophilic, or radical. The fact that most chemists associate the term "aromatic substitution" with nitration, sulfonation, or azo coupling of the benzene ring demonstrates the predominance of the electrophilic substitution type in the carbocyclic series. However, the presence of a hetero atom in the ring changes the electron distribution in such a manner that nucleophilic substitutions gain more importance. That this situation is identical with the effect exercised by certain substituents attached to a carbocyclic system can

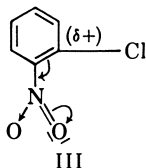
be demonstrated by a comparison of two concrete cases. The chlorine atom in chlorobenzene (I), under ordinary conditions, cannot be replaced by the amino group when ammonia is used as a typical nucleophilic agent. Not until very rigid conditions are applied will this reaction proceed (1), (Equation 1).



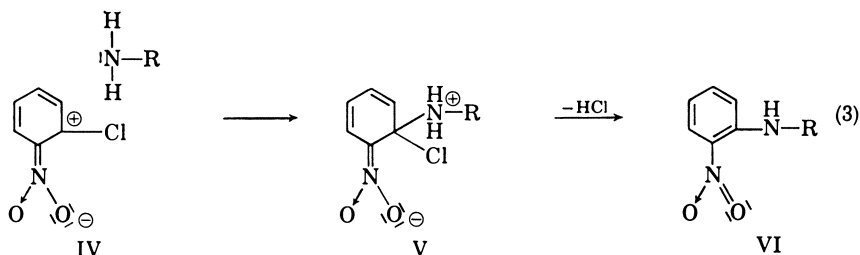
The chlorine atom in I, however, can be activated by the introduction of a nitro group into the same ring, thereby considerably facilitating the substitution of Cl in II by NH_2 (22) (Equation 2).



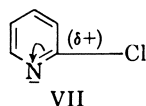
In the light of modern electronic theory, the nitro group in II has made the molecule accessible to nucleophilic attack due to its negative resonance effect (-R effect). It thus withdraws π -electron density from the ring so as to impart alternate charges on the conjugated system. Ortho and para positions thereby become amenable to attack by nucleophilic agents. This situation is represented by structure III with respect to the ortho position.



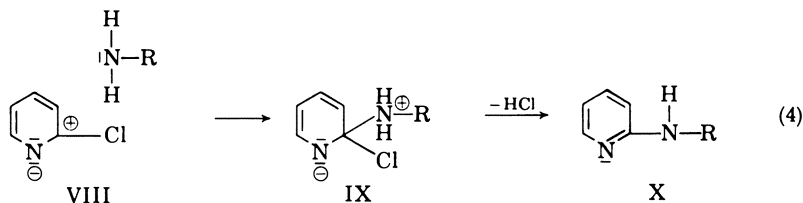
The indicated electronic shift would result in a species (IV) containing a positively charged ortho position which would now accept the unshared pair of electrons from the attacking nucleophilic agent, the amine, to form the transition state (V). The latter finally eliminates one mole of hydrogen chloride with formation of the end product (VI) (Equation 3).



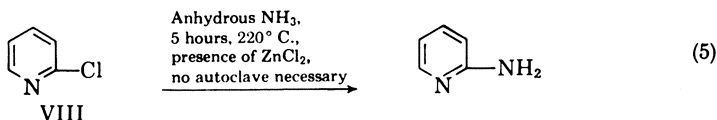
There exists a striking analogy in the behavior of carbocyclic nitro compounds and aromatic heterocycles and it has therefore been concluded that the hetero atom—e.g., nitrogen in pyridine—effects a similar electron displacement as does the nitro group in nitrobenzene. In the heterocyclic series, the structure parallel to *o*-chloronitrobenzene (III) would be that of 2-chloropyridine (VII).



That pyridine species with decreased electron densities at positions adjacent to the nitrogen atom make significant contributions to the resonance hybrid even in the ground state has been shown by dipole measurements (12, 14). Interaction with a nucleophilic agent is consequently expected to follow a mechanism analogous to that involving *o*-chloronitrobenzene (Equation 4).



The hetero ring atom in 2-chloropyridine (VII) thus facilitates the reaction with ammonia in a manner similar to that of the nitro group in *o*-chloronitrobenzene (II) (6) (Equation 5).

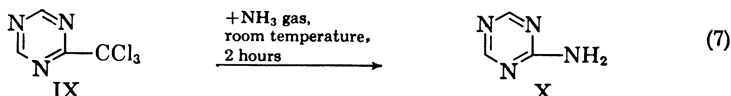
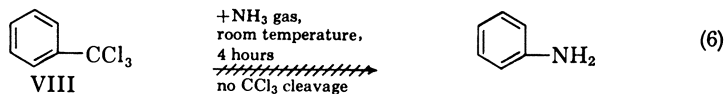


In principle, the activating power of a hetero atom equals approximately that of a nitro group (13). An increase of hetero atoms in one and the same ring is expected to facilitate nucleophilic substitution even more.

Replacement of VII by a 2,6-dihalopyridine and of NH_3 by a bifunctional nucleophilic agent in Equation 5 represents the basis for a general nucleophilic polymerization process. It is obvious, however, that hydrogen halide as a by-product is disadvantageous in polymer formation because of its potential tendency to cleave bonds again. The nucleophilic substitution mechanism provides a bypass to this situation. As can be seen from Equations 3 and 4, chlorine leaves the transition states (V and IX), respectively, as an anion. Thus, the problem would be to attach to the ring a suitable anion other than chlorine which, upon leaving the ring, would combine with a proton to form an inert entity.

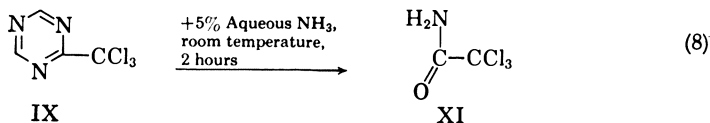
The trichloromethyl group appears to meet these requirements. This group is known to leave as an anion (2) in nucleophilic substitution reactions involving compounds of the type of chloral, trichloroacetic acid, and trichloroacetone, and subsequently to combine with a proton to form chloroform.

Two fundamental experiments demonstrate clearly the activation of the CCl_3 group by the hetero ring atom. While there is no reaction when ammonia is

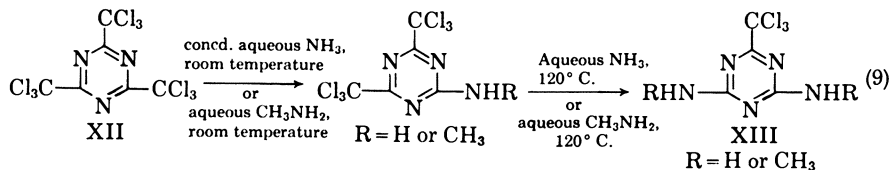


passed into α,α,α -trichlorotoluene at room temperature (Equation 6), facile nucleophilic attack occurs on 2-trichloromethyl-*s*-triazine under the same conditions (Equation 7).

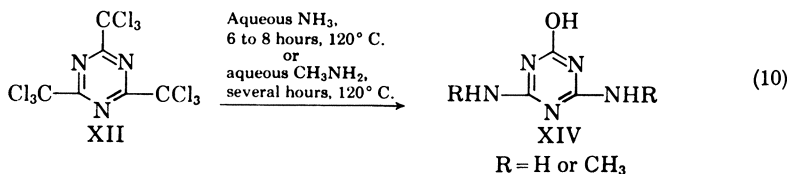
2-Trichloromethyl-*s*-triazine (IX) also appeared to be a suitable model compound for substitution studies with aqueous ammonia. However, the surprising result was obtained that IX undergoes ring cleavage rather than substitution. Concentrated as well as dilute aqueous ammonia cleaves the ring in IX at room temperature to form trichloroacetamide (Equation 8). Even water alone brings about this ring cleavage, but the reaction time in this case is about 1 week.



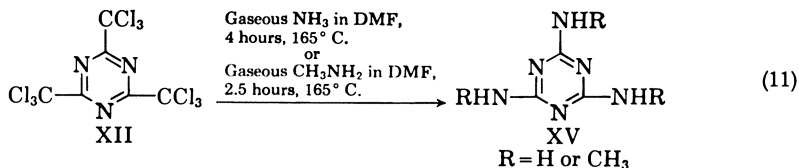
This tendency to ring cleavage seems to be limited to the un- and mono-substituted *s*-triazine ring, for trisubstituted *s*-triazine derivatives are stable under the same conditions. Moreover, they are amenable to nucleophilic attack by aqueous amines, when carrying suitable substituents—e.g., the trichloromethyl group. The first two substituents in 2,4,6-tris(trichloromethyl)-*s*-triazine (XII) may thus be replaced rather easily by the NH_2 and NHCH_3 groups through the action of aqueous ammonia or aqueous methylamine, respectively (Equation 9) (20).



However, the attempt to replace the last CCl_3 group in XII by the same reaction resulted in displacement by an OH group (Equation 10).

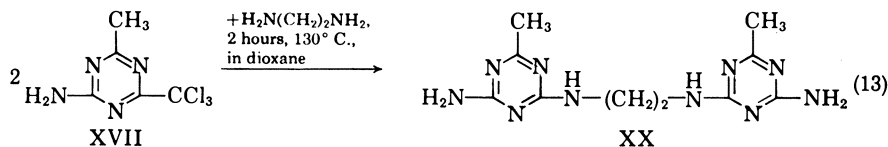
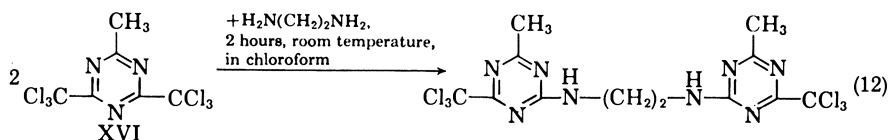


This reaction clearly shows the competition between two nucleophiles, amine and water. Furthermore, it suggests that under certain conditions other suitable OH-containing nucleophilic agents may attack the ring at the CCl_3 -bonded site. On the other hand, it is to be concluded that substitution by NHR of the last CCl_3 group on the ring can be accomplished only in OH-free media. This idea has been verified by the use of solvents like chloroform, dioxane, acetonitrile, and *N,N*-dimethylformamide (DMF) (Equation 11) (10).



Subsequent fundamental studies have, for the time being, been directed toward the development of a nucleophilic polymerization process leading to linear polymers. A nonfunctional group was used as one of the three substituents on the *s*-triazine ring. Thus, 2-methyl- and 2-phenyl-4,6-bis(trichloromethyl)-*s*-triazine (XVI) followed exactly the previously established reaction paths. Reaction with aqueous ammonia under rather mild conditions replaced only one of the two trichloromethyl groups by NH₂ producing the corresponding 2-amino-4-trichloromethyl-*s*-triazines (XVII). Under more stringent conditions, the last CCl₃ group was replaced by OH, to form the 2-hydroxy-4-amino-*s*-triazines (XVIII), however, and only gaseous ammonia under anhydrous conditions replaced all CCl₃ groups by amino groups, forming thereby the 2,4-diamino-*s*-triazines (XIX) (10). Compound XVI could not be induced to react with oxygen nucleophiles other than water—e.g., methanol under pressure or phenol at 100° C.

The new procedure of replacing all trichloromethyl groups attached to the heterocyclic ring by the amino group may now be employed to incorporate the rings into chains by choosing the proper diamines as the nucleophilic agent. Ethylenediamine may serve to connect two triazine rings with one another, Equations 12 and 13.



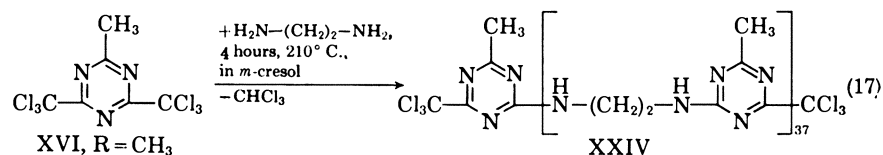
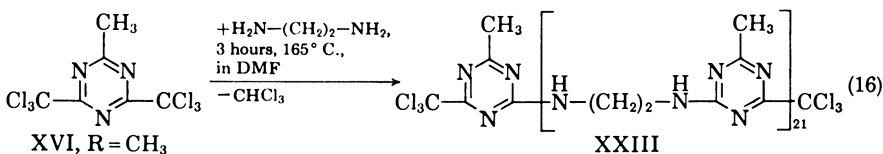
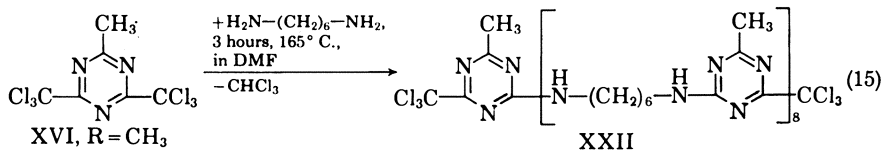
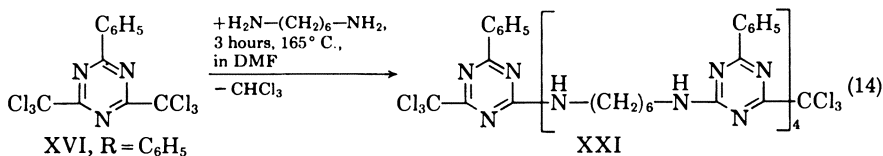
Equation 12 at the same time demonstrates the principle of linking many heterocyclic rings into a linear chain by nucleophilic replacement of trichloromethyl groups. Its adaptation to a higher reaction temperature and somewhat longer reaction time leads thus to a new nucleophilic polymerization process of heterocycles. In this case, the molar ratio between XVI and the diamine should be adjusted as closely as possible to 1:1. The molecular weights of the polymers obtained were determined by measurements of specific viscosity. A comparison of the latter with the analytically found chlorine values revealed that the polymer chains were terminated by trichloromethyl groups.

The first factor found to determine chain length was the nonfunctional substituent attached to the *s*-triazine ring. Under the same experimental conditions, XVI carrying the bulkier phenyl group led to the polymer (XXI) of molecular weight 1500 (Equation 14), while XVI, (R = CH₃) yielded polymer XXII having a molecular weight of 2000 (Equation 15).

Furthermore, the chain length proved to be dependent on the type of diamine used. Again, under the same conditions as shown in Equation 15, replacement of 1,6-hexanediamine by ethylenediamine yielded polymer XXIII with a molecular weight of 3500 (Equation 16).

Chain length dependence on the solvent used and concurrently on reaction temperature was demonstrated in an experiment involving the same components as given in Equation 16, but using *m*-cresol in place of *N,N*-dimethylformamide.

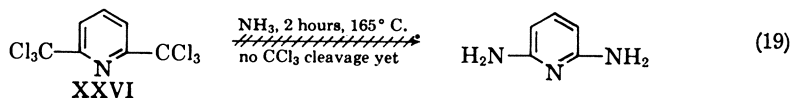
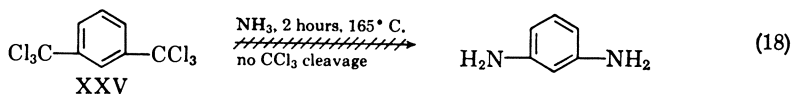
Polymer XXIV thus obtained exhibited an average molecular weight of 6000 (Equation 17).

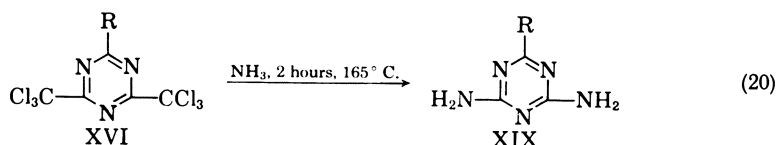


The new polymer type is adaptable to the fabrication of fibers and the melt spinning technique can successfully be employed.

A very favorable factor in this nucleophilic polymerization process is the inertness of the leaving component, chloroform. Polymer isolation is facilitated by insolubility in most common organic solvents so that addition—e.g., of acetone or petroleum ether—to the reaction mixture precipitates the polymer formed.

By another series of reactions, it may once more be demonstrated that it is the hetero atom which, by virtue of the -R effect, withdraws π -electron density from the adjacent C atoms and thereby makes the latter amenable to attack by nucleophilic agents—e.g., amines. Thus, ammonia is incapable of displacing the CCl_3 group in $\alpha,\alpha,\alpha,\alpha',\alpha',\alpha'$ -hexachloro-*m*-xylene (XXV) (Equation 18). In 2,6-bis(trichloromethyl)pyridine (XXVI) the -R effect of the N atom is not yet strong enough to make the neighboring C atoms accessible to nucleophilic attack (Equation 19). The combined activating power of three N atoms in one ring as in 2,4-bis(trichloromethyl)-*s*-triazines (XVI) finally is sufficient to impart enough positive charge to ring C atoms, thereby making them the preferential sites for attack by nucleophilic agents (Equation 20).





It must be borne in mind, of course, that substitutions are generally kinetically controlled processes in which the activation energy plays an important role. Provided, however, that the energy requirement for proceeding from the initial to the transition states is favorable, various bifunctional nucleophiles should be capable of entering a nucleophilic polymerization reaction as outlined above.

Experimental

Effect of Ammonia. α,α,α -TRICHLOROTOLUENE (VIII). A dry stream of gaseous ammonia was passed for 4 hours into 19.6 grams of VIII (0.1 mole) at room temperature. Within 5 minutes, the originally colorless, transparent liquid became slightly turbid, but no heat evolution was noticeable. The introduction of ammonia was discontinued and the reaction contents were subjected to vacuum distillation. The entire reaction yielded only one component which was identified as unchanged VIII. Of the two boiling points, b.p.₂₃ 110.7° C. (18) and b.p.₂₅ 105° C. (19), cited in the literature, the one found in this distillation agrees with the latter. The experimental refractive index, n_D^{20} was 1.5573 and is consistent with the literature value (5).

2-TRICHLOROMETHYL-*s*-TRIAZINE (IX). Based on the structure elucidation of *s*-triazine and the unique ring cleavage of this heterocycle by nucleophiles (8, 11), IX has recently become available by use of the appropriate amidine (16).

Dry, gaseous ammonia was introduced into 5.9 grams of IX (0.03 mole) diluted with 20 ml. of dimethylformamide. Within 0.5 hour, white crystals started to precipitate and the reaction mixture gradually became warm. When, after 2 hours, the reaction was complete, the solids were filtered under vacuum. Recrystallization from water gave white, sturdy needles melting at 227–28° C. (corr.). They were identified as 2-amino-*s*-triazine (X) by mixed melting point with an authentic specimen (4). A total yield of 2.3 grams (82.2%) of X was obtained, including the amount obtained by work-up of the dimethylformamide filtrate.

Analysis. Calculated for $\text{C}_3\text{H}_4\text{N}_4$: C, 37.50%; H, 4.19%; N, 58.31%. Found: C, 37.32%; H, 3.98%; N, 58.50%.

Ring Cleavage of 2-Trichloromethyl-*s*-triazine (IX). An amount of 30 ml. of 5% aqueous ammonia was added to 4.0 grams of IX (0.02 mole) at room temperature. The two immiscible layers soon penetrated each other and became translucent, and white, heavy needles started to crystallize. The reaction seemed complete within 2 hours. The crystalline solids were collected on a Büchner funnel and dried; the yield was 2.1 grams or 64.3%. By recrystallization from water, colorless prisms were obtained. Their melting point of 141° C. (corr.) remained unchanged when mixed with authentic trichloroacetamide (XI) (23).

Analysis. Calculated for $\text{C}_3\text{H}_2\text{Cl}_3\text{NO}$: C, 14.79%; H, 1.24%; Cl, 65.49%; N, 8.63%. Found: C, 14.70%; H, 1.29%; Cl, 65.54%; N, 8.80%.

Complete Replacement of CCl_3 by NH_2 . 2,4,6-TRIS-(TRICHLOROMETHYL)-*s*-TRIAZINE (XII). A solution containing 8.7 grams of XII (0.02 mole) in 25 ml. of DMF was maintained for 4 hours at a temperature of 165° C., during which time a dry stream of ammonia was introduced. Upon cooling, a tan solid precipitated which was filtered under vacuum and dried. It could be recrystallized from water and proved to be identical in every respect, with melamine (XV, R = H) (17). Conclusive proof was obtained by mixed melting point of the picrate (21). The amount of 1.2 grams of XV (R = H) corresponds to a yield of 48%.

2-METHYL-4,6-BIS-(TRICHLOROMETHYL)-*s*-TRIAZINE (XVI, R = CH_3). While a solution containing 9.9 grams of XVI (R = CH_3) (0.03 mole) in 25 ml. of DMF was heated for 2 hours at 160° to 165° C., a stream of dry, gaseous ammonia was introduced. During cooling of the solution, a beige solid precipitated which was

filtered under vacuum and dried. By recrystallization from water with the aid of activated charcoal, 1.9 grams (51%) of glittering scales were obtained. Their melting point of 278–79° C. (corr.) was undepressed when mixed with an authentic sample of 2-methyl-4,6-diamino-*s*-triazine (XIX) (15).

Attempted Use of Methanol as Nucleophile. An autoclave was charged with a solution of 6.6 grams (0.02 mole) of 2-methyl-4,6-bis(trichloromethyl)-*s*-triazine (XVI, R = CH₃) in 15 ml. of DMF and 10 ml. of methanol and heated for 3 hours at 110° C. under autogenous pressure. After cooling, the reaction contents were subjected to vacuum distillation. The solid remainder, when recrystallized from methanol, melted at 96° C. A mixed melting point with an authentic sample (3) proved this material to be unaltered starting material (XVI, R = CH₃); recovery was quantitative.

Nucleophilic Linking of Two Heterocyclic Rings. Ethylenediamine (2.4 grams, 0.04 mole) was added to a solution containing 9.1 grams of 2-amino-4-methyl-6-trichloromethyl-*s*-triazine (XVII) in 15 ml. of dioxane. This reaction mixture was boiled for 2 hours at 130° C., during which time a yellowish solid gradually deposited. The latter, after cooling, was filtered under vacuum and dried. Because it was insoluble in all common organic solvents, the solid was purified by boiling out with acetone to free it from any starting material. The analysis identified the remaining solid as *N,N'*-bis(2-amino-4-methyl-6-triazinyl)-ethylenediamine (XX); m.p. 328° to 330° C. (corr.); the yield was 2.4 grams (42%).

Nucleophilic Polymerization of *s*-Triazines. 2-PHENYL-4,6-BIS(TRICHLOROMETHYL)-*s*-TRIAZINE (XVI, R = C₆H₅). The transparent, yellowish solution containing 7.8 grams (0.02 mole) of XVI (R = C₆H₅) and 2.3 grams (0.02 mole) of 1,6-hexanediamine in 30 ml. of *N,N*-dimethylformamide was heated for 3 hours at 165° C. During this heating period, the solution changed to a brownish viscous liquid which, after cooling, was stripped of solvent under vacuum. Repeated trituration with water of the somewhat sticky residue furnished the polymer in the form of a tan, granular material weighing, after drying, 4.9 grams (83.5% yield). The product had a melting point of 115–16° C. (corr.) and a molecular weight of 1500. The elemental analysis indicated structure XXI for this polymer.

Analysis. Calculated for C₇₁H₈₁Cl₆N₂₃: C, 58.04%; H, 5.56%; Cl, 14.48%; N, 21.92%. Found: C, 57.80%; H, 5.46%; Cl, 14.73%; N, 21.61%.

2-Methyl-4,6-bis(trichloromethyl)-*s*-triazine (XVI, R = CH₃). With 1,6-Hexanediamine. A mixture consisting of 9.9 grams (0.03 mole) of (XVI, R = CH₃), 3.5 grams of 1,6-hexanediamine (0.03 mole), and 25 ml. of DMF was heated for 3 hours at 165° C., during which time the polymeric condensation product precipitated gradually. The reaction mixture was cooled, diluted with acetone, boiled for a short time, and filtered. The solid was insoluble in lower boiling solvents like carbon tetrachloride and acetone, but soluble in higher boiling solvents like nitrobenzene. Purification was accomplished best by successive extractions with boiling acetone, ethanol, and carbon tetrachloride, when a yellow powder was obtained, m.p. 200–01° C. (corr.). Elemental analysis along with the average molecular weight of 2000 identified this material as (XXII). The weight of 2.5 grams corresponds to a yield of 37%.

With Ethylenediamine. In 25 parts by weight of *N,N*-dimethylformamide were dissolved 10 parts by weight of XVI (R = CH₃) and 2 parts by weight of ethylenediamine. The solution was heated for 3 hours at reflux temperature, thereby precipitating a yellowish brown mass. Acetone was added to the cooled suspension, and the solid product was filtered under vacuum and then boiled successively with acetone and ethanol. The yellowish powder amounted to 3.5 grams (73% yield), m.p. about 250° C. Based on elemental analysis and molecular weight determination which gave a value of 3500, the polymer has been assigned structure XXIII.

***m*-Cresol as Solvent.** To a solution containing 9.9 grams (0.03 mole) of 2-methyl-4,6-bis(trichloromethyl)-*s*-triazine (XVI, R = CH₃) in 25 grams of *m*-cresol was added 1.8 grams (0.03 mole) of ethylenediamine and the reaction mixture was heated for 4 hours at 210° C. After cooling, the reaction content was stripped of solvents. The crude, brown residue could best be purified by successive extractions with acetone and ether. A slightly yellow powder was obtained which was insoluble in all common organic solvents; m.p. about 370° C. (corr.);

average molecular weight, 6000. The elemental analysis agreed with structure XXIV. The yield was 3.0 grams (64%).

Stability of 2,6-Bis(trichloromethyl)pyridine (XXVI) toward Nucleophilic Substitution. The colorless solution containing 6.2 grams (0.02 mole) of XXVI in 25 ml. of DMF was heated for 2 hours at 165° C., during which time gaseous ammonia was passed in. When, after cooling, the reaction mixture was stripped of solvent under vacuum, a white, crystalline solid remained. Recrystallized from a methanol-water mixture, the substance had a melting point of 86–87° C. which was not depressed when mixed with an authentic sample (XXVI) (7, 9). The recovery of XXVI was quantitative.

Literature Cited

- (1) Aktien-Gesellschaft für Anilin-Fabrikation, Berlin, Ger. Patent **204, 951** (1908).
- (2) Arndt, F., Eistert, B., *Ber.* **68**, 196 (1935).
- (3) Dachlauer, K. (to I. G. Farbenindustrie A.-G.), Ger. Patent **682, 391** (1939).
- (4) Diels, O., *Ber.* **32**, 696 (1899).
- (5) Dummer, E., *Z. anorg. Chem.* **109**, 37 (1919).
- (6) Fischer, O., *Ber.* **32**, 1297 (1899).
- (7) Graf, R., Zettl, F., *J. prakt. Chem.* [2] **147**, 197 (1936).
- (8) Grundmann, C., Kreuzberger, A., *J. Am. Chem. Soc.* **76**, 632, 5646 (1954).
- (9) Koenigs, W., Happe, C., *Ber.* **36**, 2907 (1903).
- (10) Kreuzberger, A., *J. Am. Chem. Soc.* **79**, 2629 (1957).
- (11) Kreuzberger, A., Grundmann, C., *J. Org. Chem.* **26**, 1121 (1961).
- (12) Leis, D. G., Curran, B. C., *J. Am. Chem. Soc.* **67**, 79 (1945).
- (13) Mangini, A., Frengnelli, B., *Gazz. chim. ital.* **69**, 86 (1939).
- (14) Middleton, B. A., Partington, J. R., *Nature* **141**, 516 (1938).
- (15) Nencki, M., *Ber.* **7**, 776 (1874).
- (16) Schaefer, F. C., Peters, G. A., *J. Am. Chem. Soc.* **81**, 1470 (1959).
- (17) Smolin, E. M., Rapoport, L., "s-Triazine and Derivatives," Vol. 13 in "Chemistry of Heterocyclic Compounds," pp. 309–10, Interscience, New York, 1959.
- (18) Swarts, F., *Bull. soc. chim. Belges* **31**, 375 (1922).
- (19) Timmermans, J., *Ibid.*, **27**, 334 (1913).
- (20) Weddige, A., *J. prakt. Chem.* [2] **33**, 81 (1886).
- (21) Werner, A., *J. Chem. Soc.* **107**, 721 (1915).
- (22) Wohl, A., *Ber.* **39**, 1951 (1906).
- (23) Zincke, T., Kegel, O., *Ibid.*, **23**, 241 (1890).

RECEIVED September 6, 1961.

Polymerization of Acrylamide in Aqueous Solution by a Continuous Process

T. J. SUEN, A. M. SCHILLER, and W. N. RUSSELL

Stamford Laboratories, American Cyanamid Co., Stamford, Conn.

A laboratory scale, continuous process for the polymerization of acrylamide in aqueous solution is described. The reaction conditions can be held constant within narrow limits and the effect of small changes in individual variables, such as temperature, initiator concentration, and chain transfer agent concentration, can be quantitatively ascertained. Some experimental results are presented showing the effect of these factors on the molecular weight of the polymer. The data are examined vis-à-vis some theoretically derived equations.

Vinyl polymerization as a rule is sensitive to a number of reaction variables, notably temperature, initiator concentration, monomer concentration, and concentration of additives or impurities of high activity in chain transfer or inhibition. In detailed studies of a vinyl polymerization reaction, especially in the case of development of a practical process suitable for production, it is often desirable to isolate the several variables involved and ascertain the effect of each. This is difficult with the conventional batch polymerization technique, because the temperature variations due to the highly exothermic nature of vinyl polymerization frequently overshadow the effect of other variables. In a continuous polymerization process, on the other hand, the reaction can be carried out under very closely controlled conditions. The effect of an individual variable can be established accurately. In addition, compared to a batch process, a continuous process normally gives a much greater throughput per unit volume of reactor capacity and usually requires less labor.

During the authors' investigation of acrylamide polymerization in aqueous solutions, a laboratory scale continuous process, with reactors of 2- or 3-liter capacity, was developed. It offered simple and flexible operation, and close control of conditions. This article describes the technique adopted and some experimental results showing the effect of individual variables on the molecular weight of the polymer formed. A theoretical treatment of the continuous polymerization process has been made recently by Jenkins (4). The empirical data obtained in the present work are examined with the aid of theoretical relationships.

Equipment and Procedure

The arrangement of the apparatus is shown in Figure 1. The monomer feed solution containing the chain transfer agent and the initiator feed solution were pumped from the reservoirs by a duplex Zenith pump through the inlet tubes into the reactor. Through another entrance into each of the inlet tubes, nitrogen gas was passed into the reactor for the purpose of providing an inert atmosphere and preventing the backflow of the reaction product into the inlet tube. The rate of flow of nitrogen was determined by counting the gas bubbles per minute in the bubblers which were inserted between the inlet tubes and the nitrogen cylinder. The polymerization product was collected, by gravity flow from the outlet tube, in the product receiver.

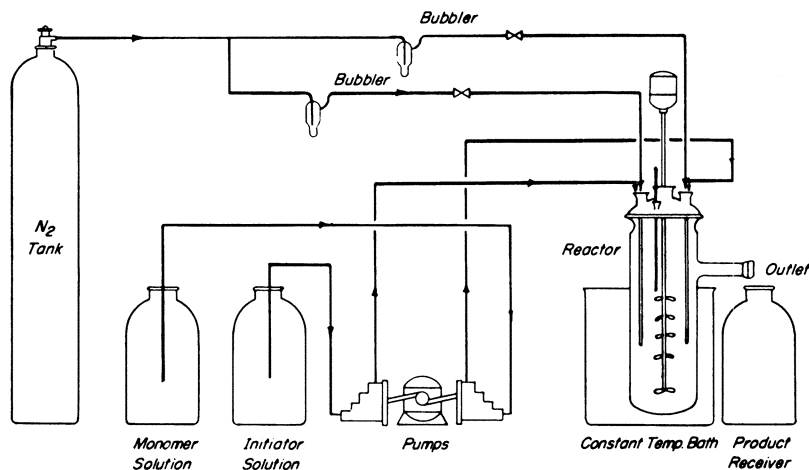


Figure 1. Arrangement of apparatus

The all-glass reactor consisted of two detachable parts. The upper part was equipped with four necks for fitting the two inlet tubes, a thermometer, and a powerful multiple-blade stirrer. The lower part of the reactor was immersed in a constant temperature bath, equipped with both heaters and cooling coils. The temperature bath was controlled by a J-tube type thermostat sensitive to $\pm 0.1^\circ \text{C}$.

The reactor is of very simple design. It contains no intricate parts. As long as the mixing is adequate, scaling up the operation presents no problem. It was found that the geometry of the reactor is of no consequence, provided good mixing can be achieved. In the present investigation, four reactors of different dimensions were used (Table I). No noticeable differences in performance were observed. Indentations on the surface, however, should be eliminated, as they provide dead space where formation of solid polymer gels tends to occur.

Table I. Dimensions of Reactors Used

Reactor No.	Depth below Outlet Tube, Cm.	Inside Diameter, Cm.	Approx. Working Capacity, Liters
1	14.0	14.3	2.2
2	36.0	10.5	3.0
3	16.5	15.2	2.7
4	28.9	12.1	3.0

As the pumps were of identical dimensions and were mounted on the same variable-speed drive, monomer and initiator solutions were introduced into the

reactor at the same volume rate. Table II shows the compositions of a pair of typical feed solutions.

Table II. Typical Feed Solutions

Monomer Solution	Parts by Weight
Acrylamide	100
2-Propanol	0.50
Water	403.2
Total	503.7
<i>Initiator Solution</i>	
$K_2S_2O_8$	0.08
Water	496.2
Total	496.3

In the present work, potassium persulfate was used as the initiator and 2-propanol as the chain transfer agent. Their concentrations in the feed [I] and [S], respectively, as shown in Figures 3 to 8, are expressed in per cent of the total weight of the sum of the two solutions. In Figure 9, however, concentrations are expressed in moles per liter.

The pumping rate was adjusted according to the desired residence time, R , which is defined as the working capacity of the reactor divided by the total volume rate of flow through the reactor. For instance, if the reactor has a capacity of 3 liters, a rate of 1.5 liters per hour for each of the two solutions corresponds to a residence time of 1 hour.

To start a run, the reactor was first filled with a previously prepared polyacrylamide solution more or less of the same description as the product desired. Nitrogen gas was turned on and the contents of the reactor were heated to the desired temperature. The two feed solutions were then pumped into the reactor. The temperature of the reactor contents would drop by 5° to 10° C. as the cold

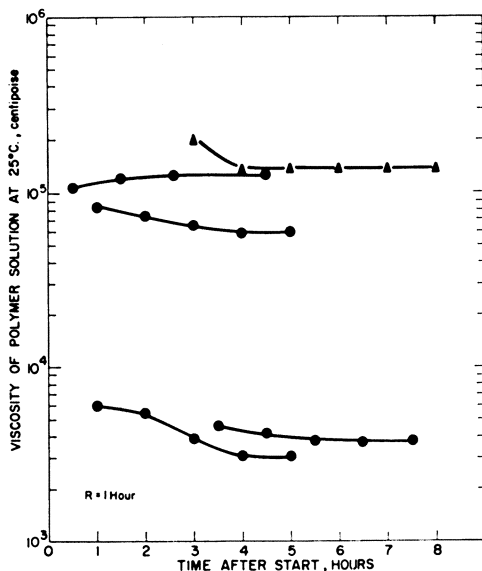


Figure 2. Viscosity readings of several representative runs

solutions were first introduced. Once the polymerization was initiated, the temperature began to rise steadily and gradually leveled off. The reaction temperature could be accurately maintained with $\pm 0.2^\circ$ C. during the steady state. Because of the cold feed, the temperature of the bath was usually 5° to 15° C. above the reaction temperature.

Samples of the polymerization product were collected at regular intervals

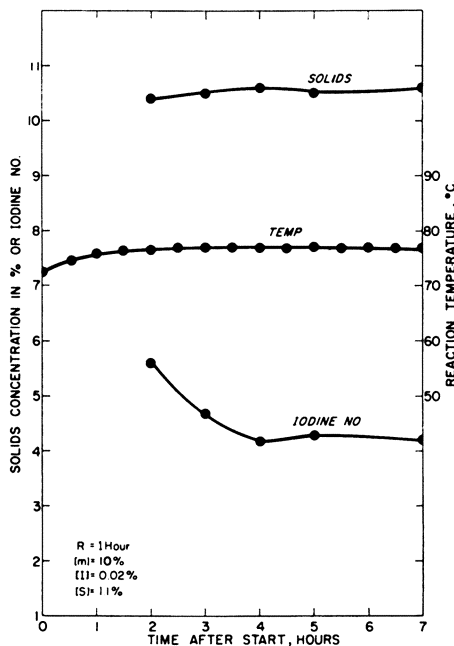


Figure 3. Solids concentration, iodine number, and reaction temperature readings of a representative experiment

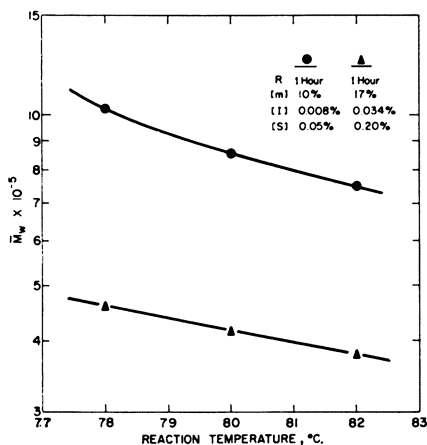


Figure 4. Effect of reaction temperature on molecular weight of polymer

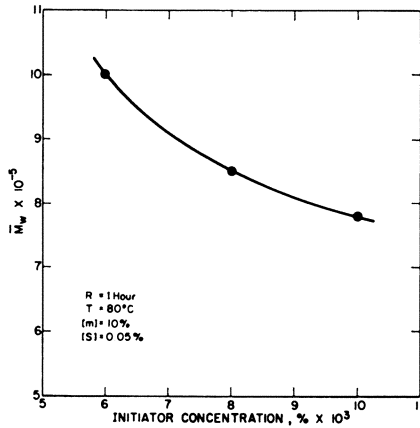


Figure 5. Effect of initiator concentration on molecular weight of polymer

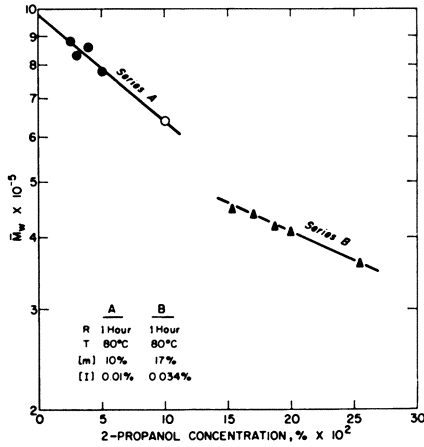


Figure 6. Effect of 2-propanol concentration on molecular weight of polymer

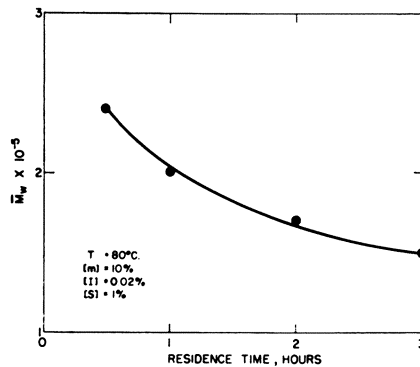


Figure 7. Effect of residence time on molecular weight of polymer

and analyzed for solids and residual monomer concentrations, $[M]$. The latter was determined by a bromate-bromide titration, essentially the same procedure as that described by Lucas and Pressman (6), except that mercuric sulfate was omitted. The viscosity of the polymer solutions, as prepared, was determined with a Brookfield viscometer. Weight average molecular weight values, M_w , were obtained from viscosity measurements through known relationships (1).

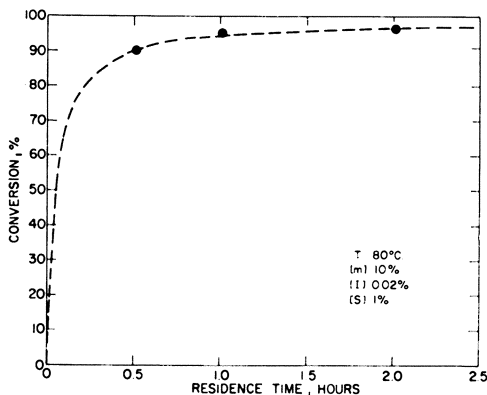


Figure 8. Effect of residence time on conversion

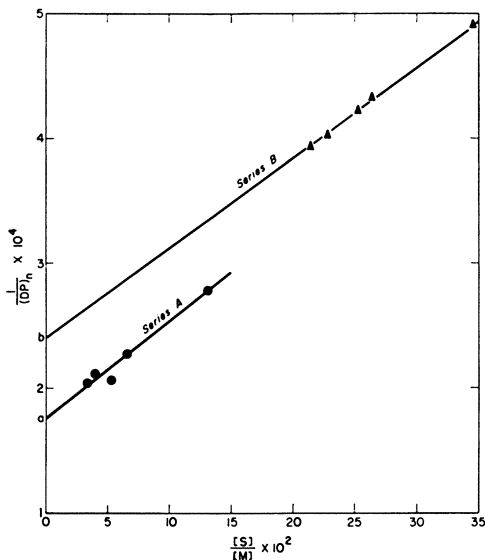


Figure 9. Determination of the chain transfer activity of 2-propanol

Results and Discussion

The Prestationary Period. In carrying out a chemical reaction by a continuous process it takes a considerable time before the steady state is reached. The minimum length of time required for a run to reach the steady state must be ascertained. After the start of continuous flow through the reactor, the material

originally present in the reactor will be gradually depleted. A true steady state cannot prevail until the original material is reduced to a negligible level. Assuming constancy of operating conditions and perfect mixing in the reactor, it can be easily calculated (3) that the fraction of the original material, F , remaining in the reactor after time, t , is governed by the equation:

$$F = E^{-t/R} \quad (1)$$

where R is the residence time. Numerical values of F after 1, 2, 3, and 4 multiples of residence time are 0.37, 0.13, 0.049, and 0.018, respectively. In other words, after 3 to 4 R , the quantity of the original material left amounts only to a few per cent, and this length of time may be taken as the prestationary period. Figure 2 shows the viscosity readings for several runs at different concentrations. They level off after about $4R$. Figure 3 shows the temperature readings, solids contents, and iodine numbers vs. time. These also indicate that the steady state is approached at $4R$.

The calculated, prestationary period as shown above is somewhat longer than that calculated by Jenkins (4). In these derivations, he takes the fictitious case that the reaction vessel is filled with the feed mixture which is then instantaneously raised to the reaction temperature at the same moment as flow is commenced at the specified rate. This, of course, is impossible to achieve in actual practice.

Effect of Molecular Weight. In the present work, the major objective was to examine quantitatively the influence of some of the individual operating variables on the molecular weight of the polymer formed. Some representative results are shown in Figures 4 to 7. The molecular weight, \bar{M}_w , is very sensitive to the reaction temperature, T , initiator concentration, $[I]$, 2-propanol concentration, $[S]$, and residence time, R .

The variations in T , $[I]$, and $[S]$ (Figures 4 to 6) are small, but the changes in molecular weight are distinctive and unmistakable. Particularly noticeable is the fact that a 2° C. difference in temperature induces a significant increase or decrease in molecular weight. In usual batch polymerizations, it is not easy to control the temperature within this range, especially during the early stage. The usefulness of a continuous process in offering very close control of the reaction conditions and hence the uniformity of the product is thus clearly demonstrated.

Conversion. Under the experimental conditions employed, the conversion is fairly insensitive to the residence time (Figure 8). Jenkins (4) has derived the following equations relating the fractional conversion, Y , to the residence time, R :

$$Y = 1 - \frac{[M]}{[m]} \quad (2)$$

$$\frac{[m]}{[M]} = 1 + \sqrt{\frac{KR^2}{kR + 1}} \quad (3)$$

where $[M]$ is the monomer concentration in the product or in the reactor, $[m]$ the monomer concentration in the feed, k the unimolecular rate constant for the decomposition of the initiator, and K a constant under a given set of reaction conditions. The curve shown in Figure 8 is calculated according to Equations 2 and 3, with $k = 5.5 \times 10^{-3}$ minute $^{-1}$, based on Kolthoff and Miller (5), and K evaluated from one of the experimental points.

Chain Transfer Activity of 2-Propanol. The presence of 2-propanol reduced the molecular weight of polyacrylamide very effectively (Figure 6). An estimate of the chain transfer activity of 2-propanol can be obtained by replotting the data according to the following equation (2)

$$\frac{1}{DP_n} = \left(\frac{1}{DP_n} \right)_0 + C_s \frac{S}{[M]} \quad (4)$$

where DP_n is the number average degree of polymerization, C_s is the chain transfer constant, and subscript 0 refers to conditions without the chain transfer agent. Jenkins (4) derived a more elaborate equation involving chain transfer. That equation can be simplified to Equation 4, if $C_s \left(\frac{[m]}{[M]} - 1 \right)$ is much smaller than 1. This condition exists in the present case. As two series of experiments were performed, the chain transfer activity of 2-propanol in both cases can thus be compared. The degree of discrepancy may also serve as a check on the reliability of the data.

In calculating DP_n , a ratio of $\bar{M}_w/\bar{M}_n = 2.5$ was assumed (7). Although the monomer concentrations, $[m]$, in the feed solutions used in these two series of experiments were different, the average monomer concentrations, $[M]$, in the products (and hence presumably in the reactor) turned out to be practically the same because of different degrees of conversion. In both cases $[M] = 0.13$ mole per liter. As shown in Figure 9, the two lines are nearly parallel. From the upper curve, $C_s = 7.2 \times 10^{-4}$; from the lower curve, $C_s = 7.8 \times 10^{-4}$ (both values for 80° C.). The agreement is gratifying.

The numerical value of C_s depends on the $[M]$, which was difficult to determine with high accuracy because of possible residual polymerization after the product left the reactor. A more reliable determination, by R. R. Aloia of these laboratories, of C_s for 2-propanol in the polymerization of acrylamide at 50° C. by the conventional method gave a value of 1.9×10^{-3} .

In Figure 9, let a and b be the intercepts of the two lines on the vertical axis. The ratio b/a gives an estimate of the ratio of molecular weights of the two polymers that would have been obtained in the absence of the chain transfer agent. If the very small chain transfer activity of the monomer is neglected, $\frac{1}{DP_n}$ should be proportional to $[X]/[M]$ where $[X]$ is the concentration of radicals in the reactor. Jenkins (4) has shown that where k_p is the propagation rate constant

$$[X] = \frac{[m] - [M]}{k_p[M]R}$$

In the cases under consideration, $[m]_A = 1.45$ moles per liter, $[m]_B = 2.52$ moles per liter, $[M]_A = [M]_B = 0.13$ mole per liter, and $R_A = R_B = 1$ hour. Therefore

$$b/a = ([m]_B - [M]_B)/([m]_A - [M]_A) = 1.8$$

The value of b/a read from Figure 9 is $2.4/1.7 = 1.4$.

Literature Cited

- (1) American Cyanamid Co., "Polyacrylamide," New Product Bull. **34** (1955).
- (2) Flory, P. J., "Principles of Polymer Chemistry," p. 141, Cornell Univ. Press, Ithaca, N. Y., 1953.
- (3) Hitchcock, F. L., Robinson, C. S., "Differential Equations in Applied Chemistry," pp. 14-16, Wiley, New York, 1923.
- (4) Jenkins, A. D., *Polymer* **1**, 79-89 (1960).
- (5) Kolthoff, I. M., Miller, I. K., *J. Am. Chem. Soc.* **73**, 3057 (1951).
- (6) Lucas, H. J., Pressman, D., *Ind., Eng. Chem., Anal. Ed.* **10**, 140-2 (1938).
- (7) Suen, T. J., Rossler, D. F., *J. Appl. Polymer Sci.* **3**, 126 (1960).

RECEIVED September 9, 1961.

Continuous Recycle Copolymerization. Design for Effective Heat Exchange and for Handling Inert Diluents

R. L. ZIMMERMAN, J. S. BEST, P. N. HALL, and A. W. HANSON

The Dow Chemical Co., Midland, Mich.

Continuous recycle copolymerization is a method of producing copolymers of predictable and homogeneous composition by partial polymerization, devolatilization, and direct recycle of recovered monomers. Operation of the polymerization reactor at higher than about 30% polymer solids requires heat exchange from a viscous mass that is in laminar flow with poor heat transfer to the wall of the vessel. By continuous removal of a portion of the partial polymer solution from the reactor, mixing with the incoming monomers, and cooling in a side arm heat exchanger before returning to the reactor, the heat exchange efficiency can be improved and operation at higher per cent solids is facilitated. Excessive buildup in the monomer recycle of inert ingredients from the feed can be prevented by fractional distillation. Continuous solution polymerization can be accomplished by adding solvent to the reactor-devolatilizer-recycle system and feeding only monomers.

By the method of continuous recycle copolymerization, a monomeric mixture can be polymerized to yield a copolymer of the same composition as the monomer feed mixture—regardless of disproportionate monomer reactivities—because the system automatically adjusts the monomer mixture composition in the reaction zone in order to reach a steady state. The copolymer thus obtained showed a very good composition homogeneity, and the conditions and reasons leading to it were discussed (3) along with two aspects of continuous recycle polymerization: attainment of the steady state conditions and maintenance of a close material balance.

Of particular interest to the process engineer is the problem of heat exchange in polymer reactions where the heat of polymerization must be dealt with and viscous fluids are encountered which have poor heat exchange characteristics. This article offers a unique design (2) for heat exchange in recycle copolymerization and in addition delves further into the practical outcome of feedback in the recycle of inert ingredients including added solvents.

As illustrated in the flow diagram (Figure 1), monomeric constituents are pumped into a reactor fitted with a side arm heat exchanger which may be either heated or cooled. The effluent monomer-polymer solution from the reactor is split into two main streams, one of which is recirculated back through the heat exchanger and the other is forwarded to the devolatilizer. Recovered monomer is condensed and returned through the side arm heat exchanger to the polymerizer, while the product polymer is extruded.

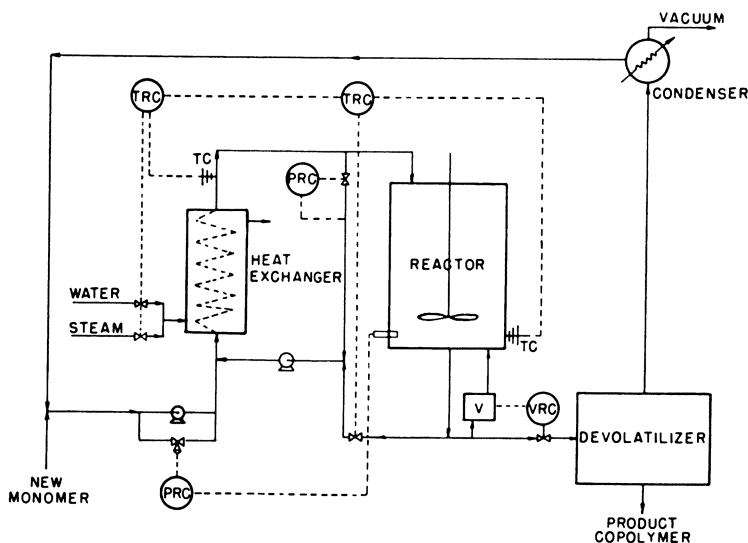


Figure 1. Flow diagram

PRC = pressure recorder controller
 TRC = temperature recorder controller
 TC = thermocouple
 V = viscometer
 VRC = viscosity recorder controller

Heat Exchange

The heat exchanger has a recirculation bypass to ensure that the monomer-polymer sirup from the reactor and the incoming monomer are homogeneously mixed. The side arm heat exchange system provides an inventory of cooled material which can be quickly injected into the reactor to produce rapid cooling of the reactor contents.

Although the vinyl polymerization reaction itself is exothermic, the over-all heat effect at the side arm heat exchanger may be endothermic, adiabatic, or exothermic depending on the percentage of polymer (herein referred to as "per cent solids") in the reactor. This can be shown by considering the heat balance in the reactor (Figure 2) with the heat of polymerization balanced by the cooling effect of incoming material.

$$P\Delta H_p = (P + R + G)(T_2 - T_1)C_p \quad (1)$$

P , R , and G represent flow rates in pounds per hour, ΔH_p is the heat of polymerization, C_p the heat capacity of monomer and polymer, T_2 the reactor temperature, and T_1 the temperature of material entering the reactor.

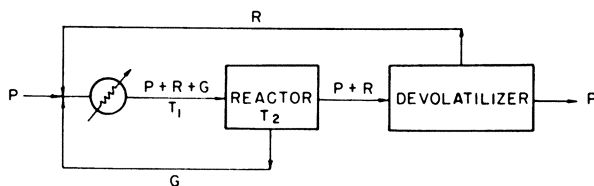


Figure 2. Material flow per hour

P = polymer product rate and monomer feed rate
 R = monomer recycle rate
 G = monomer-polymer recycle rate
 T_1 = side arm heat exchange temperature
 T_2 = reactor temperature

In one hour, a total of $P + R$ pounds of monomer-polymer is displaced from the reactor. The devolatilizer separates solid material, P pounds, from monomer, R pounds. Therefore, the average fraction of polymer solids, f , in the reactor is given by the relation,

$$f = \frac{P}{P + R} \quad (2)$$

For the case where no monomer-polymer is recycled to the side arm exchanger, $G = 0$, and Equation 1 may be written

$$f\Delta H_p = (T_2 - T_1)C_p \quad (3)$$

This relationship is shown (Figure 3) for the homopolymerization of styrene, where $\Delta H_p = 300$ B.t.u. per pound and $C_p = 0.5$ B.t.u. per °F. per pound. The data show that the monomer entering the heat exchanger (Figure 2) will have to be heated or cooled depending on f and T_2 . With the monomer entering the exchanger at room temperature (taken as 30° C.), endothermic operation is involved when $T_1 > 30^\circ$ C., exothermic when $T_1 < 30^\circ$ C., and adiabatic when $T_1 = 30^\circ$ C. For a typical reactor temperature of 130° C., the monomer must be

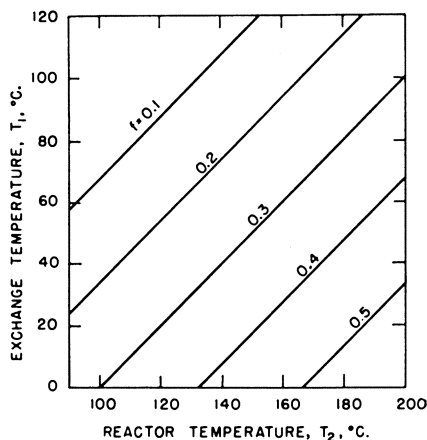


Figure 3. Polymerization of styrene with no monomer-polymer recycle according to Equation 3

cooled below 30° C. when the polymer solids fraction is higher than about 30%, but the exchanger has limited low temperature capabilities, unless refrigeration is provided. If, however, monomer-polymer is recycled through the side arm exchanger, greater cooling capacity is available in the stream $P + R + G$ (Figure 2) and exothermic operation at higher per cent solids is possible. In order to show the effect of this recycle, it is convenient to express the flow as the recycle ratio, N , defined by

$$N = \frac{G}{P + R} \quad (4)$$

The recycle ratio, therefore, relates the flow G to the flow $P + R$. Equation 1 may then be written

$$f\Delta H_p = (1 + N)(T_2 - T_1)C_p \quad (5)$$

A plot of N vs. T_2 for $T_1 = 30^\circ \text{C}$., $\Delta H_p = 300$, and $C_p = 0.5$ is shown in Figure 4. The recycle ratio increases for higher values of f and for lower values of T_2 . Figure 5 shows that for a given fraction of solids, higher exchange temperature, T_1 , required higher recycle ratios.

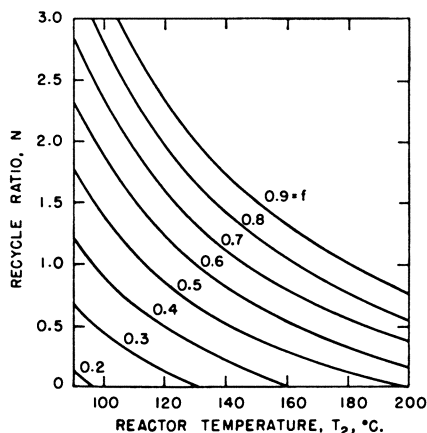


Figure 4. Styrene polymerized at high per cent solids by recycling monomer-polymer through the side arm exchanger

Exchange temperature, $T_1 = 30^\circ \text{C}$.

In order to gain some insight into actual rather than relative flow rates, it is necessary to know the polymerization rate. Let r represent the fractional rate of polymerization expressed as the fraction of the reactor capacity converted to polymer per hour.

$$P = rC \quad (6)$$

Further, let g represent the fraction of the reactor capacity which is recycled to the side arm exchanger,

$$G = gC \quad (7)$$

and h the fraction of the reactor capacity which is forwarded to the devolatilizer.

$$P + R = hC \quad (8)$$

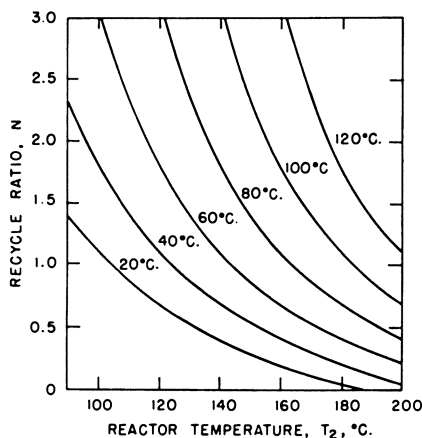


Figure 5. High exchange temperatures require relatively more recycle of monomer-polymer to the exchanger

Fractional solids, $f = 0.5$
 Temperatures on the curves are exchange temperatures

From Equations 2, 4, 6, and 7

$$g = \frac{rN}{f} \quad (9)$$

and

$$h = \frac{r}{f} \quad (10)$$

For $f = 0.5$, Table I gives experimental values of r vs. T_2 for styrene.

Table I. Rate of Polymerization at 50% Solids

Reactor Temperature, T_2 , °C.	Rate, % of Reactor Capacity/Hour, $r \times 100$
90	0.8
100	1.6
120	6.0
140	20
160	60
180	160

Figure 6 shows the flow of material forward to the devolatilizer, and recycle to the side arm exchanger as required to maintain a heat balance. For the given conditions, the recycle rate of monomer-polymer goes through a maximum, and is quite low at both very low or very high temperatures. There is also a crossover at $T_2 = 115^\circ \text{C}$. where G and $P + R$ are equal.

It is perhaps worth noting that the monomer recycle vapor condenser is also a heat exchanger for the reactor. In the above discussion, the recycled monomer was considered to be at 30°C . For this condition the condenser removes not only the heat put in by the devolatilizer, but cools the monomer considerably below the reactor temperature.

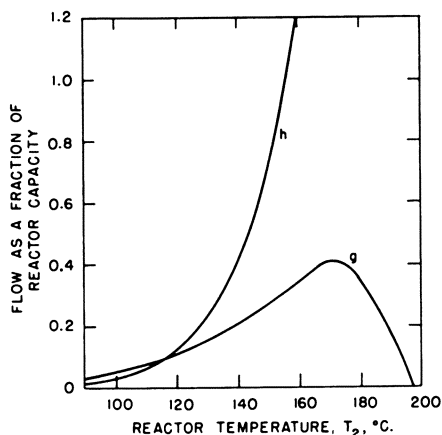


Figure 6. Actual flow of monomer-polymer forward to the devolatilizer, h, and recycled, g, to the exchanger

Fractional solids, $f = 0.5$
Exchange Temperature, $T_1 = 30^\circ \text{C}$.

Operational Control

Control of the reactor in the manner shown in Figure 1 makes it possible to maintain accurately a specified temperature and per cent solids in the reactor, even when operating on the verge of a runaway polymerization. The reactor temperature controller adjusts the rate of monomer-polymer circulated through the heat exchanger, so that if a rise in temperature occurs more monomer-polymer goes to the exchanger and is replaced by cooler fluid. The same controller, in addition, can reset the temperature controller on the heat exchange medium and thus increase the capacity of the exchanger to handle an even greater heat load as would be encountered in a runaway case.

Assuming a perfect material balance with no extraneous losses, the input of new monomer should match the output of polymeric product. To accomplish this and maintain essentially constant polymer solids in the reactor, the solids content should be measured and used to control the displacement of monomer-polymer solution with monomer. A satisfactory method is to use a torque tube viscometer (1) in a side stream of monomer-polymer and use a viscosity recorder-controller to control a valve forwarding monomer-polymer to the devolatilizer. Reactor pressure is used to control monomer input, replacing the monomer-polymer solution forwarded to the devolatilizer.

Viscosity and Mixing

From a practical standpoint, the most significant operating problems involve the fluid viscosity of polymer solutions and the mixing of viscous and nonviscous streams. Figure 7 illustrates the wide range of viscosities encountered in polystyrene-styrene solutions (4). These data are given in terms of temperature, per cent solids, and the temperature at which the polymer was made—i.e., in effect, the molecular weight. For normal pumping and mixing, a viscosity of less than about

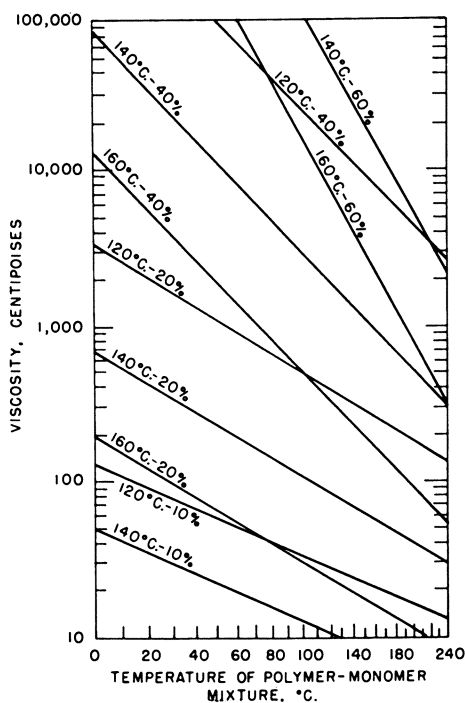


Figure 7. Absolute viscosity of polystyrene solutions in isopropylbenzene

Polymers were prepared at the indicated temperature and dissolved at the corresponding per cent solids

5000 centipoises is desired. Therefore, in reactor and heat exchanger, the temperature-solids-molecular weight relationships must be such that fluid streams are maintained.

Uniform copolymer composition as well as efficient liquid-liquid heat exchange requires rapid mixing of viscous and nonviscous streams. Reynolds numbers in the range of 5 to 15 were calculated for typical monomer-polymer solutions being handled, which means that laminar flow with little or no turbulence is involved. One way to provide mixing is to pass the fluid through a pump. Mixing efficiency was tested in a pipe fabricated into a loop encompassing a positive displacement gear-type pump. The ratio of loop circumference to the pipe's inner diameter was 15:1. The loop was filled with a solution of polystyrene in styrene having an absolute viscosity of 1700 centipoises. At 215 r.p.m. pump speed, calculation showed that on the average the solution made 141 passes per hour or one pass per 25.5 seconds at a velocity of 0.384 foot per second. Monomer entered in the downstream side of the pump and monomer-polymer was displaced at the upstream side of the pump. A blue dye (Alizarin blue) was prepared as a 1% solution in styrene and approximately 100 ml. of the solution was injected at the inlet. Injection required about two seconds. Samples of the polymer sirup were taken at the outlet every second for 24 seconds, then every minute. Results are plotted in Figure 8. The dye appeared first at the outlet in 10 seconds or approximately one half the time calculated for one pass. In laminar flow, the

advanced parabolic front in the center of the pipe travels twice as fast as the average of the whole cross section. In 30 seconds, or in a little more than the time for one average pass, the mixing was nearly complete. At 107 r.p.m., the mixing time was about 60 seconds.

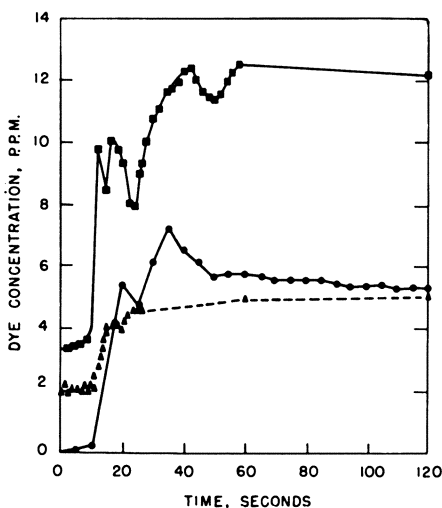


Figure 8. *Mixing of dye in monomer-polymer circulated through a gear pump*

▲ 215 r.p.m.
● ■ 107 r.p.m.

Heat Transfer Efficiency

Advantages in heat transfer efficiency are gained by using the instant heat exchange systems (Figure 1). One of the well-known effects of laminar flow of viscous masses is the poor transfer of heat to a surface. Therefore, the reactor walls represent relatively undesirable surfaces for heat exchange. For typical high molecular weight polymers, fluid viscosity is affected more by the per cent solids than by temperature (Figure 7). In the side arm exchanger, recycled monomer-polymer is diluted by monomer which usually results in a fluid of much lower viscosity in spite of the fact that the exchange temperature is lower than the reactor temperature. In addition, it is practical to have a greater surface to volume ratio in the exchanger than in the reactor.

Efficient heat transfer is also obtained in the monomer recycle condenser where viscosity is no problem.

Buildup of Inerts

Direct feedback of recovered monomer in recycle copolymerization may lead to buildup of inert materials that can affect the polymerization reaction. This point is illustrated in the copolymerization of styrene and α -methylstyrene. A 22-day experiment was conducted in which the feed was a mixture of 25% α -methylstyrene and 75% styrene and polymerization was effected at 125° C. The monomer contained about 0.5% of inerts, consisting primarily of ethylbenzene

and cumene. Polymer solids in the reactor were maintained in the range of 35 to 40% and the volatile content of the copolymer produced was less than 0.5%. In four days (Table II), the polymerization rate had dropped and mass spectrometric analysis indicated a buildup of inerts. A small portion of the recycle monomer stream was then continuously removed by fractional distillation. This resulted in rate and molecular weight increases and kept the inerts from building up excessively.

Table II. Continuous Recycle Copolymerization of Styrene and α -Methylstyrene

Days	Relative Output Rate	Polymer Viscosity, ^a Centipoises	Monomer Recycle		
			Fractionated, wt. %	Inerts, wt. %	MS, ^b wt. %
1	0.95	12.4	0	0.8	27.0
4	0.71	11.0	0	1.3	33.4
11	0.77	11.9	1.8	2.6	34.5
18	0.73	12.3	3.0	3.2	34.8
24	0.89	14.1	6.0	3.6	30.5

^a Solution, 10% in toluene.

^b MS = α -methylstyrene.

For this copolymer system, reactivity ratios were calculated in an earlier article (3): $r_1 = 1.25 \pm 0.05$ and $r_2 \pm 0.1$. Figure 9 is a plot of the data in weight per cent. On the 18th day of the experiment, when the α -methylstyrene concentration in the recycle was 36% (based on monomers), the polymer should have contained 27%; 28% was found by infrared analysis.

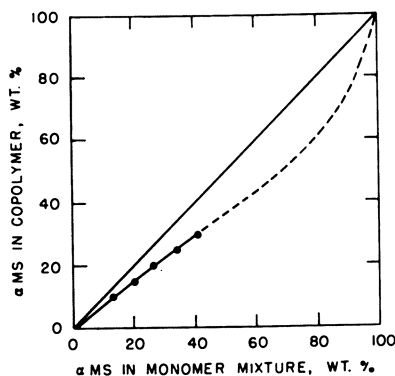


Figure 9. Copolymer composition for styrene (M_1) and α -methylstyrene (M_2)

Added Solvents

In some cases it is desirable to conduct a copolymerization in the presence of a solvent. Table III illustrates the effect of solvent concentration on the copolymerization of styrene and acrylonitrile. Higher concentrations of solvent produced a pronounced lowering of the rate without changing the molecular weight as measured by the solution viscosity of the copolymer.

Table III. Styrene and Acrylonitrile Copolymerized in Methyl Ethyl Ketone

Solvent, %	Relative Output Rate	Polymer	
		Viscosity, ^a centipoises	Volatile, %
3.8	1.0	42.2	1.6
9.3	0.51	36.1	1.3
12.8	0.35	41.8	0.9

^a Solution, 10% in methyl ethyl ketone.

For these experiments, a portion of the solvent was introduced slowly into the recycle vapor line. Samples were taken after the solvent had distributed itself throughout the polymerizer, devolatilizer, and recycle equipment. No solvent was added to the feed monomer, although for long periods of operation a small amount of solvent would normally be required in the feed to make up for solvent lost through the extruder as part of the volatile in the copolymer product and also, possibly, lost through the condenser into the vacuum system.

Acknowledgment

The authors thank their numerous associates in the work upon which this article is based and in particular, N. W. Howell, D. E. Moore, and W. E. O'Connor.

Literature Cited

- (1) Barstow, O. E. (to Dow Chemical Co.), U.S. Patent 2,817,231 (Dec. 24, 1957).
- (2) Hanson, A. W., Best, J. S. (to Dow Chemical Co.), *ibid.*, 2,989,517 (June 20, 1961).
- (3) Hanson, A. W., Zimmerman, R. L., *Ind. Eng. Chem.* 49, 1803 (1957).
- (4) Wiley, R. M., Dow Chemical Co., Midland, Mich., unpublished data.

RECEIVED September 6, 1961.

Devolatilization of Viscous Polymer Systems

GEORGE A. LATINEN

Plastics Division, Monsanto Chemical Co., Springfield, Mass.

The removal of residual volatile components from polymers is an operation of some importance in the plastics industry. A generalized, although somewhat idealized, model for continuous, wiped-film devolatilization of viscous polymer melts is presented which relates devolatilization capability to important geometry, operating, and fluid property variables. The applicability and limitations of the model are analyzed experimentally. The data support many aspects of the theory, but also reveal certain deficiencies in the model which should be considered in designing for maximum efficiency.

Depending on the particular manufacturing process, a polymer may sometimes contain volatile residues such as moisture, unpolymerized monomer, solvents, or other impurities. These volatile components frequently have to be removed, or reduced to very low levels, before the polymer can be satisfactorily processed into high quality finished products. This so-called "devolatilization" is usually accomplished during the final extrusion step by passing the hot polymer melt in wiped-film fashion through a partially filled, highly evacuated section of the extruder (Figure 1). In this devolatilization zone, the volatile components diffuse to the polymer-vapor interface, evaporate into the vapor space, and are removed from the system through a vent opening which connects to an external vacuum supply.

In addition to its devolatilizing capability, the design of an efficient devolatilizing screw section capable of handling highly viscous polymer melts at high flow rates involves a number of other practical considerations, such as frictional heat generation, forwarding capacity, fillage, etc. The latter are treated in detail by Bernhardt (2). This article deals exclusively with the devolatilization step, but does not attempt to examine the virtues of specific designs. It does attempt to relate, in a general way, the devolatilizing capability of any screw design which embodies a wiped-film principle in terms of the pertinent system variables which are either known or can be estimated or measured for a given geometry.

The mathematical development which follows does not suffer from lack of simplifying assumptions. Although the removal of a volatile component from a homogeneous, viscous polymer melt in a wiped-film type flow system seems rela-

tively simple, there are a number of uncertainties involved. How well does the cross-sectional mixing action transfer volatile components into the regions where the surface films are being regenerated? What effect does the viscoelastic nature of the melt have on surface film roughness? Can axial dispersion be characterized in terms of an axial eddy diffusivity, which impiles a random mixing process. gradient transport, etc.? Simplifications will be made in developing the mathematical model, but experimental data will also be presented to test the general validity of the model and some of the more important assumptions which are made. Devolatilization of styrene monomer from polystyrene melts was selected, since it represents a typical polymer system and an accurate test for residual monomer was available.

All the development data presented here are restricted to volatile contents of approximately 1% by weight or less. This represents a range of wide industrial importance. Within this range, also, various fluid properties such as film surface characteristics, molecular diffusivity, etc., would be expected to be relatively constant and independent of residual monomer level, thereby simplifying the system considerably.

Theory

A typical two-stage devolatilizing screw (2), shown schematically in Figure 1, is used for illustrative purposes. The interphase mass transfer step is taken up first, and then the over-all flow equation.

Consider the cross-sectional view shown in Figure 1, *B*, and for ease of illustration assume that the barrel is rotating with a linear velocity πDN with respect to the stationary screw. Depletion of a volatile component from the polymer phase takes place by molecular diffusion through the immediate surface layers of the wall film, *abc* (formed by the clearance between the screw land and barrel wall), and the nip film, *dc*, followed by evaporation from their respective interfaces into the vapor space and out of the system. The wall film is continually regenerated by the "wiping" action of the screw land, and the nip film by the circulatory fluid motion in the advancing helical nip. The following three important assumptions are made:

1. The material in the nip at any axial position has a uniform volatile concentration, *C*—i.e., the nip mixing is sufficiently intense to wipe out bulk cross-sectional concentration gradients which normally tend to develop through the combined action of surface depletion and the seemingly inevitable tendency for the flow to channel through the core of the advancing helical nip.

2. The polymer film mass transfer resistance is controlling and the interfacial and vapor phase resistances are zero, or at least negligible by comparison. The surface concentration of a volatile component, therefore, will be the equilibrium value, *C**, as determined by its partial pressure in the vapor space at the prevailing melt temperature.

3. The molecular diffusivity is independent of concentration and may be treated as a constant at the average melt temperature in the devolatilizing zone.

The wall film, *abc*, is considered first. It is continually deposited on the cylinder wall at point *a* with a uniform initial concentration, *C*, equal to that of the nip (assumption 1). The surface concentration immediately drops to the equilibrium value, *C** (assumption 2). The initial shear gradient in the film at point *a* quickly disappears and the surface layers will rotate with the barrel until absorbed and mixed by the nip at point *c*. It can be shown that over the range of

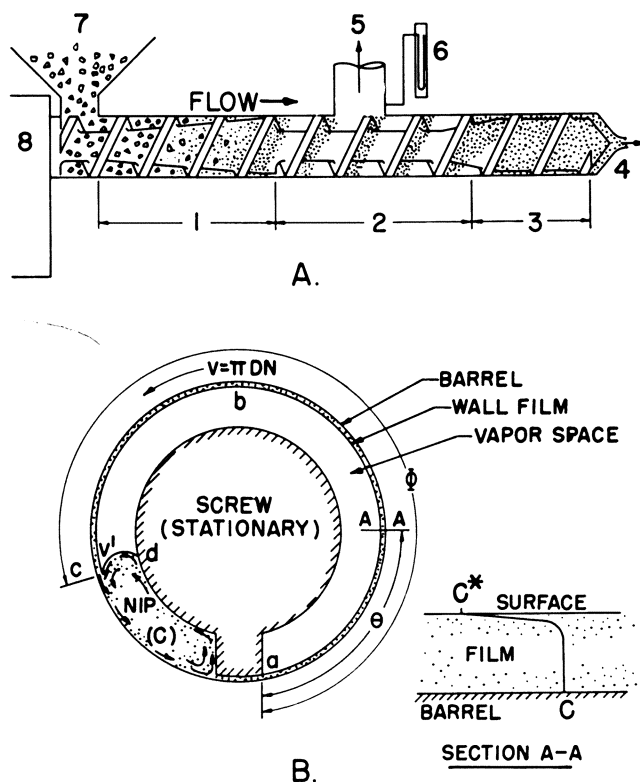


Figure 1. Typical two-stage devolatilizing extruder

A. Schematic diagram

- | | |
|------------------------------|-----------------------------|
| 1. Plasticating zone | 5. Vent to vacuum system |
| 2. Devolatilizing zone | 6. Mercury manometer |
| 3. Pressure development zone | 7. Feed hopper |
| 4. Die | 8. Gear reduction and drive |

B. Cross-sectional view

typical extruder rotational speeds, the surface exposure time, θ , per pass is so short that the concentration gradients which result from diffusion through the surface layers penetrate but a very short distance, less than 0.001 inch, below the surface. Since the total film thickness is usually several times this value, the diffusion is identical to that from the face of a semi-infinite slab initially at a uniform concentration, C , into a reservoir maintained at a lower constant concentration, C^* . At time θ after the deposition of the film, the instantaneous film coefficient $(k_m)_\theta$ may be related to the corresponding surface gradient, which in turn may be expressed in terms of the molecular diffusivity (assumed constant) and exposure time (3):

$$(k_m)_\theta(C - C^*) = D_m \left(\frac{\partial C}{\partial y} \right)_\theta = D_m \frac{(C - C^*)}{(\pi D_m \theta)^{1/2}} \quad (1)$$

Integrating Equation 1 over the total surface exposure time θ (= distance $abc/\pi DN$) gives the effective film coefficient, \bar{k}_m , for that particular film:

$$\bar{k}_m = \frac{1}{\theta} \int_0^\theta (k_m)_\theta d\theta = 2 \left(\frac{D_m}{\pi \theta} \right)^{1/2} \quad (2)$$

The same treatment applies to the regenerated nip surface film, dc . The velocity gradient would be zero at the surface, except perhaps when elastic forces predominate. The surface exposure time may be approximated by $\Theta = \text{distance } dc/\pi DN \sin\phi$, where ϕ is the screw helix angle measured from the cross-sectional plane.

Each surface film of area S (per unit length of devolatilizer) has a specific exposure time, or regeneration rate, and hence is associated with a specific \bar{k}_m , Equation 2. For any number, 1,2,3,... n separate films, therefore, the effective product of the diffusion film coefficient and surface area is given by the summation:

$$\bar{k}_m S = \sum_{n=1}^n 2S_n \left(\frac{D_m}{\pi\Theta_n} \right)^{1/2} \quad (3)$$

where the S 's and Θ 's are the individual surface film areas (per unit length of devolatilizer) and their respective surface exposure times.

For a given geometry, it seems reasonable to assume that the surface areas, S_n , would be proportional to barrel diameter D , and that the surface regeneration rates, $1/\Theta_n$, would be proportional to the rotational speed, N :

$$S_n = a_n \pi D, \quad (1/\Theta_n) = b_n N; \quad n = 1, 2, 3, \dots, n \quad (4)$$

Substituting into Equation 3 yields the final equation:

$$\begin{aligned} \bar{k}_m S &= 2D(\pi D_m N)^{1/2} [a_1 b_1^{1/2} + a_2 b_2^{1/2} + \dots + a_n b_n^{1/2}] \\ &= 2\beta D(\pi D_m N)^{1/2} \end{aligned}$$

$$\text{where} \quad \beta = \sum_{n=1}^n a_n b_n^{1/2} \quad (5)$$

β may be defined as "geometry efficiency" and, other conditions remaining equal, gives a relative comparison of the devolatilizing capability of different screw geometries. For a perfectly smooth, cylindrical wall film which is regenerated once per revolution by a hypothetical blade of zero land width and zero nip volume $\beta = 1$. For the geometry pictured in Figure 1 (18° helix angle), β is estimated at 1.2, again assuming mirror-smooth film surfaces. It is possible, however, that the rubbery, viscoelastic nature of many polymer melts may result in rough film surfaces of specific areas greater than unity and hence larger β values than would be predicted from geometry when based on smooth films. Nucleation and vaporization below the film surface would also increase specific surface area, but this is not very likely to occur in the low volatile concentration range of around 1% or less.

The Flow Equation. Consider a differential cross-sectional slice, dx , at distance x from the feed end of the devolatilizer. A volatile component material balance across this slice will include net inputs due to mean axial flow and axial dispersion (the latter arising from the nip mixing action), and depletion through the regenerated surface films. In addition to the three assumptions made above, it is assumed that uniform conditions prevail throughout the length—i.e., constant u , ρ , S , w , D_m , etc.—and that the effect of axial dispersion may be characterized by a constant axial eddy diffusivity, E . The steady-state material balance for a volatile component across dx reduces to:

$$EA \left(\frac{d^2C}{dx^2} \right) - uA \left(\frac{dC}{dx} \right) - \bar{k}_m S(C - C^*) = 0 \quad (6)$$

(axial eddy diffusion)
(mean flow)
(depletion)

where A = total cross-sectional melt area, u = mean linear axial melt velocity, C = concentration of diffusing component at x , C^* = the equilibrium value, and $\overline{k_m S}$ = effective value of the product of diffusional film coefficients and their surface areas (Equations 2 to 5).

Let $X = x/L$ and $A = w/u\rho$, where L = axial length of devolatilizing section, w = mass throughput rate, and ρ = melt density. After substituting into Equation 6 and rearranging, one obtains:

$$\left(\frac{d^2C}{dX^2}\right) - \left(\frac{uL}{E}\right)\left(\frac{dC}{dX}\right) - \left(\frac{uL}{E}\right)\left(\frac{\overline{k_m S L \rho}}{w}\right)(C - C^*) = 0 \quad (7)$$

The dimensionless group (uL/E) is the familiar, axial Peclet number for mass transfer which characterizes the effect of axial dispersion, or so-called "back-mixing," in flow systems. Strictly speaking, its use implies a completely random mixing process and a spectrum of mixing scales extending down to molecular dimensions. Its significance has been discussed at length in the literature (4, 7, 8, 10) (see also Results). The dimensionless group $(\overline{k_m S L \rho}/w)$ is one form of the so-called extraction number which takes into account the other variables pertinent to the devolatilization step.

Material balances at the ends, assuming that the ends behave as perfect diffusion barriers (reasonable), provide the two necessary boundary conditions (12)

$$\left(\frac{dC}{dX}\right)_{x=0} = -\left(\frac{uL}{E}\right)(C_i - C_{z=0}); \quad \left(\frac{dC}{dX}\right)_{x=1} = 0 \quad (8)$$

The Correlating Equation. Equation 7, together with the boundary conditions of Equation 8, is readily solved to give the final equation in terms of the desired outlet-to-inlet extractable volatiles concentration ratio:

$$\frac{C_0 - C^*}{C_i - C^*} = \frac{(a^2 + 4b)^{1/2} e^{m_1}}{(b/a)[e^{(a^2 + 4b)^{1/2}} - 1] - [m_2 - m_1 e^{(a^2 + 4b)^{1/2}}]} \quad (9)$$

where $a = uL/E$, $b = (uL/E)(\overline{k_m S L \rho}/w)$
 $m_1 = [a + (a^2 + 4b)^{1/2}]/2$
 $m_2 = [a - (a^2 + 4b)^{1/2}]/2$

Equation 9 is plotted in Figure 2 for several values of the axial dispersion number, E/uL ,—i.e., the reciprocal of the above-mentioned axial Peclet number. E/uL approaches zero as piston-type or plug flow is approached, and approaches infinity as a completely mixed condition is approached. It is seen that axial dispersion has an increasingly detrimental effect on devolatilization as the extraction number, N_{ext} , increases. The applicability of Equation 9 and the validity of some of the assumptions contained therein will be tested experimentally in the section on Results.

Experimental

A typical devolatilizing extruder 2.5 inches in diameter, capable of being fitted with interchangeable devolatilizing screw sections, was used. It is shown schematically in Figure 1. At the feed end, a plasticating section supplies a homogeneous, hot polymer melt of initial volatile content C_i to the devolatilizing zone. At the other end, a pressure-developing section removes the hot, devolatilized melt of volatile content C_0 , and develops sufficient pressure to force the material through appropriate screen-packs and dies. In the experimental setup, a valve was used before the die to control backpressure and hence the effective length of the devolatilizing zone. The average melt temperature in the devolatilizing zone was measured by probing the melt with a fast response

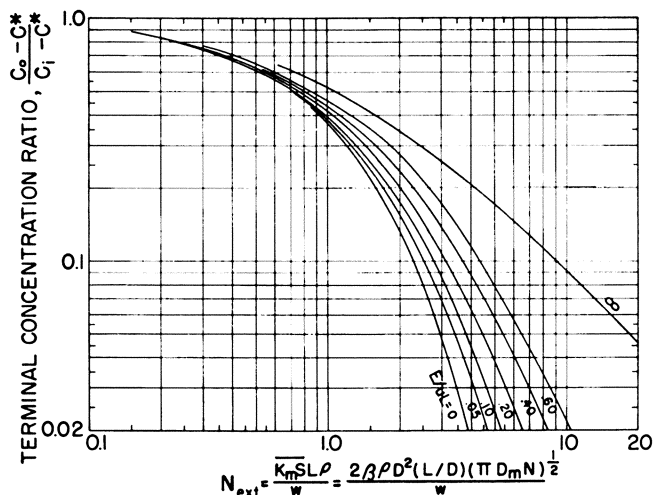


Figure 2. Wiped-film devolatilizer correlation, Equations 5 and 9

Major assumption: perfect cross-sectional nip mixing

thermocouple through the vent opening immediately after each run, after momentarily stopping the screw. The pressure in the vapor space surrounding the screw was measured by means of a mercury manometer located close to the vent opening.

Polystyrene feeds containing styrene monomer in varying amounts up to 0.8% by weight were used in evaluating devolatilization performance. Styrene monomer was selected as the volatile component, since an accurate analytical test (based on ultraviolet absorption by the styrene double bond) for its presence, even in very small amounts, was available. Changes in styrene concentration resulting from thermal polymerization or depolymerization during passage through the extruder were negligibly small over the range of temperature and residence times involved.

Two plasticating feed screws were used, one of which provided approximately 45% greater throughput at equal rotational speeds. This served to decouple to some extent the approximately linear relationship between the independent variables throughput rate and rotational speed. Melt temperature in the devolatilizing zone was varied by varying the plasticating section barrel temperatures. The devolatilizing zone barrel temperature was adjusted to approximately the melt temperature in that zone for each run.

Range of Experimental Variables. Two devolatilizing screw sections were used: a typical 18° helix screw (constant pitch—constant root diameter) (Figure 1) designated screw A, and a special (classified) devolatilizing screw designated screw B. Most of the experimental work was done with the latter, using a 4¹/₄ length-to-diameter ratio.

Screw A	$D = 2.5$ inches	$L/D = 4$ (approx.)
Screw B	$D = 2.5$ inches	$L/D = 4^{1/4}$ and 10
Rotational speed, N	60 to 244 r.p.m.	
Throughput, w	53 to 215 pounds per hour	
Average melt temp., T	404° to 482° F.	
Vacuum	5 to 20 mm. Hg (absolute)	
Feed monomer, C_i	Up to 0.8 weight % of styrene in polystyrene	

Results

The terminal concentrations, C_i and C_0 , were determined analytically, and the equilibrium values, C^* , were calculated from the following equation (1, 5) at the prevailing melt temperature and monomer vent pressure:

$$\ln \frac{P}{P_0} = \ln \phi_0 + \phi_p + \gamma \phi_p^2 \quad (10)$$

where P and P_0 = vapor pressure of solution and solvent, respectively; ϕ_0 and ϕ_p = volume fraction of solvent and polymer, respectively, at the prevailing temperature; and γ = a parameter measuring solvent affinity for polymer. For many commonly encountered polymer solutions where the solvent is nonpolar in character, $\gamma = 0.4$. The curves (Figure 5) for the styrene-polystyrene system are calculated from Equation 10. It is seen that relatively high temperatures and vacuum are necessary to obtain low equilibrium values.

The axial dispersion number, E/uL , was estimated for the $4^{1/4}$ L/D screw B geometry using a small, visual flow model which provided tracer pulse injection into the feed stream and direct discharge. The test fluid was a high-viscosity polystyrene solution and the tracer material was a highly colored sample of this same test fluid. Values of approximately 0.2 were estimated from the outflow tracer dispersion curves (6) at fillages comparable to those observed in the extruder. The cross-sectional mixing appeared to be good, with little evidence of channeling, and it was assumed that for this screw geometry, at least, E/uL satisfactorily characterizes the effect of axial dispersion. For different L/D ratios, the following relationship was assumed a priori:

$$E/uL \propto \frac{(\text{intensity} \times \text{scale})_{\text{mixing}}}{uL} \propto \frac{(ND)D}{(ND)L} \propto 1/\left(\frac{L}{D}\right) \\ \text{i.e., } E/uL = \frac{0.2 \times 4^{1/4}}{(L/D)} = 0.85/\left(\frac{L}{D}\right) \quad (11)$$

Comparison of Devolatilization Data with Figure 2. Referring to Figure 2, it is seen that once β is estimated from the screw geometry, which can be done if smooth surface films are assumed, every term in the extraction number, N_{ext} , presumably is known for a given set of operating conditions. The axial dispersion number, E/uL , is given by Equation 11, and hence it should be possible to calculate the exit monomer concentration, C_0 , and compare it with the measured value. Unfortunately, reliable molecular diffusivity data for styrene in polystyrene at high temperatures were not found. Therefore, the molecular diffusivity, D_m , was treated as the unknown, and several values were calculated at low and high temperatures (but otherwise under nearly identical conditions) from Figure 3 and the measured C_i and C_0 values. These values are plotted (Figure 2) in terms of the usual $\log D_m$ vs. $1/T$ coordinates. The calculated activation energy of 9.0 kcal. per gram-mole seems reasonable for a diffusion process and agrees well with the data of Newitt and Weale (9) on diffusion of small molecules through polystyrene. If this is the true value for styrene, the temperature effect on devolatilization is wholly determined by its effect on D_m . The absolute D_m values, however, should be closer to the nitrogen and ethylene curves, if the latter may be assumed to be correct. An explanation for these apparently high values is that the actual regenerated film surfaces in the devolatilizer are not mirror-smooth as assumed. Therefore, the calculated β value based on unit specific area would be low, requiring a higher D_m to compensate. Extrapolated data on diffusion of styrene in polystyrene by Vsurkov and Ryskin (11) are also shown, but

were considered unreliable in view of the extensive extrapolation from 300° F. and below, and also because the activation energy of 44 kcal. seems unreasonably high.

Figure 4 shows all the experimental C_0 data for the short screws and the corresponding values calculated from Figure 2. Molecular diffusivities at the various temperatures were taken from Figure 3, and the equilibrium values from Figure 5. The scatter is not too bad, and indicates that the model fairly well predicts the effect of rotational speed, throughput rate, and molecular diffusivity on devolatilization performance. The data also indicate that the geometry efficiency, β (which were different for the two screws) has some merit, and provides a convenient means for comparing the relative efficiency of different screw designs.

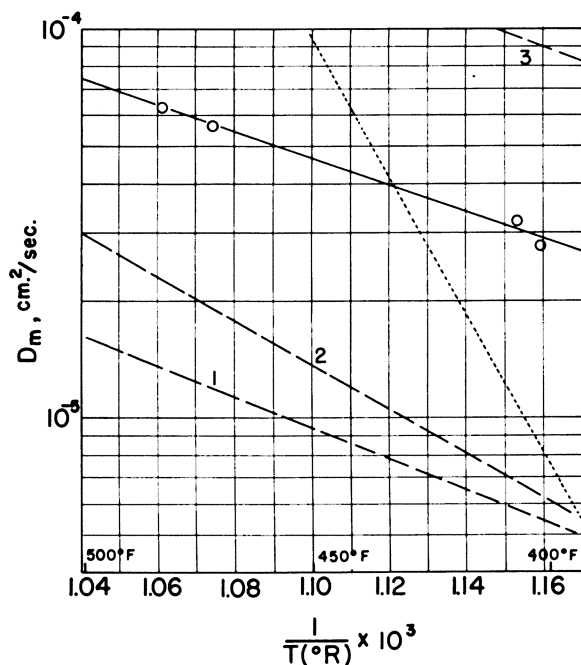


Figure 3. Molecular diffusivity of small molecules in polystyrene melts

Solid curve. Calculated values for styrene from devolatilization data (this study) with 4-1/4 L/D screw B devolatilizing section

Activation energy = 9 kcal. per gram-mole

Dashed curves. Data of Newitt and Weale (9)

1. Nitrogen, activation energy = 10.1 kcal. per gram-mole

2. Ethylene, activation energy = -

3. Hydrogen, activation energy = 9.6 kcal. per gram-mole

Dotted curve. Data of Vsurkov and Ryskin (11)

Styrene, activation energy = 44 kcal. per gram-mole (?)

Effect of L/D (a Check on Assumption 1)

In the derivation of Figure 2, the assumption of complete cross-sectional nip mixing is admittedly a questionable one in view of the typically high viscosities of these polymer melts and lack of turbulence in flow. Complete nip

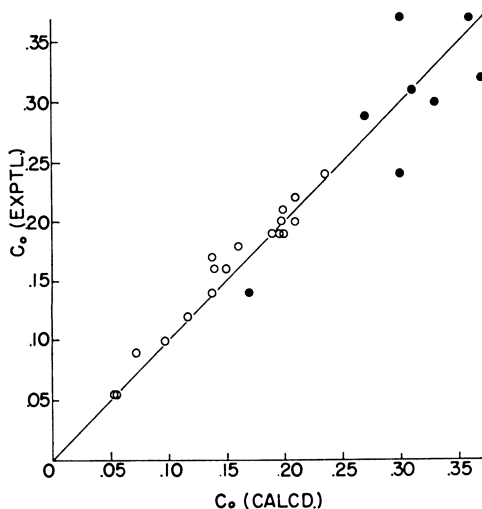


Figure 4. Comparison of experimental data with calculated values from Figure 2 by using $E/ul = 0.2$ and molecular diffusivities from Figure 3

O Screw B section, 4-1/4 L/D

● Screw A section, 4 L/D (approx.); system styrene-polystyrene

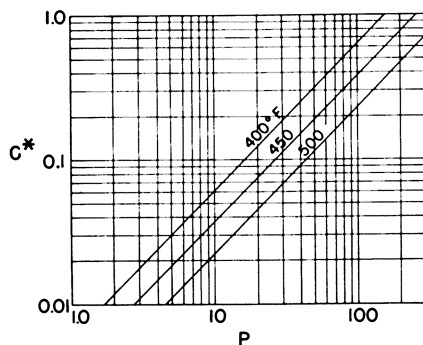


Figure 5. Equilibrium of styrene monomer in polystyrene, Equation 10

P. Partial pressure, styrene monomer in vapor space, mm. Hg absolute

C*. Equilibrium concentration, styrene in polystyrene, weight per cent

mixing implies that the surface films at any axial position are regenerated with a uniform initial concentration equal to the bulk concentration at that point. This situation provides the maximum available driving force for diffusion from the surface layers and is the case, of course, at the inlet where the material enters with a uniform concentration. This will not be the case further down the barrel, however, if the rate of monomer transfer through the bulk material due to cross-sectional mixing is insufficient to replenish the monomer which is continually

depleted from the surface layers. Under these conditions, therefore, a long screw would appear to be less efficient than a short screw when compared on the basis of Figure 2.

To check this assumption, devolatilization data were obtained using a relatively long (10 L/D) screw B section. The effective L/D was then calculated by using Figures 2, 3, and 5. Values of approximately 10 would be expected, if the assumption of complete nip mixing were correct. Instead, the following calculated values were obtained:

L/D , calculated	7.6	7.1	7.9	7.1	7.2	7.6	Av. = 7.4
Revolutions per minute	120	120	120	210	120	120	
T , °F.	424	427	427	441	449	458	

This is a sizable discrepancy and definitely indicates a need for an additional cross-sectional bulk transport term in the original differential material balance, Equation 6. An approximate, but much simpler, way to take into account lack of cross-sectional mixing would be to multiply the extraction number, N_{ext} (Figure 2) by an exponential correction term, ε , of the form:

$$\varepsilon = e^{-B(L/D)} \quad (12)$$

$$(N_{ext})_{corr.} = e^{-B(L/D)} \left[\frac{2\beta\rho D^2(L/D)(\pi D_m N)^{1/2}}{w} \right] \quad (13)$$

As L/D approaches zero, ε approaches unity, as expected. As L/D increases, ε decreases, but with a continually decreasing rate. This is also as one would expect, since the effect of the initial boundary condition becomes less important as L/D gets large.

Applying Equation 12 to the experimental data for screw B yields:

$$\frac{\varepsilon(4^{1/4}L/D)}{\varepsilon(10L/D)} = e^{5.75B} = \frac{10}{7.4} = 1.35 \quad \therefore B = 0.052$$

from which:

$$\varepsilon(4^{1/4}L/D) = 0.80 \text{ and } \varepsilon(10L/D) = 0.59$$

It is estimated, therefore, that the $4^{1/4} L/D$ and $10 L/D$ screw B sections are only 80 and 59% as efficient, respectively, as they would have been if the cross-sectional nip mixing had been perfect.

Conclusions

In some respects, the viscous flow behavior of polymer melts simplifies the problem of characterizing vacuum devolatilization. The effective wiped-film mass transfer coefficient reduces to a very simple form of the penetration model, expressible in terms of molecular diffusivity and surface regeneration rate. In other respects, the problem is more complex. The data indicate that the effective diffusional surface areas of the regenerated films are greater than would be predicted from geometry, assuming mirror-smooth surfaces. It is reasonable to expect that the surface film characteristics will depend on the viscoelastic nature of the melt and, therefore, should be affected by such variables as shear, surface regeneration rates, etc. The data also indicate that rapid cross-sectional mixing is not easily

achieved with these viscous materials, which can substantially reduce devolatilizing efficiency. At the high throughput rates characteristic of modern extruder practice, the problem of attaining rapid cross-sectional mixing with a minimum of channeling is probably one of the major considerations in designing efficient devolatilizing screws. The resulting axial dispersion, on the other hand, has been found to be satisfactorily low in melt-conveying screws and is a relatively minor consideration by comparison.

More devolatilization data with several polymer systems plus accurate molecular diffusivity and equilibrium data are needed in order to characterize this unit operation more precisely. This article represents but a preliminary study of some of the more important variables involved.

Acknowledgment

The authors thank the Monsanto Chemical Co. for permission to publish this article and R. P. Bishop and R. W. Jones for contributions to it.

Nomenclature

- A = cross-sectional area of polymer phase, L^2
 B = empirical constant, Equation 12,
 C = volatile concentration at distance x , or X , M/L^3
 C_i = inlet volatile concentration (initial volatile concentration in melt at extraction zone) M/L^3
 C_0 = outlet volatile concentration (volatile concentration in melt after devolatilizing) M/L^3
 C^* = equilibrium volatile concentration (Figure 5), M/L^3
 D = diameter of devolatilizer, L
 D_m = molecular diffusivity of volatile component, L^2/θ
 E = axial eddy diffusivity, L^2/θ
 ε = empirical correction term, Equation 12,
 L = length of devolatilizing section, L
 N = rotational speed of screw, $1/\theta$
 P = partial pressure, volatile component in vapor phase, mm. Hg
 P_0 = vapor pressure of pure volatile component, mm. Hg
 S = surface area of a regenerated surface film per unit length of devolatilizer, L^2/L
 T = average melt temperature, T
 X = fractional axial distance from devolatilizer feed end,
 a, b = proportionality constants, Equation 4,
 \bar{k}_m = instantaneous diffusional film coefficient at surface exposure time, θ , L/θ
 \bar{k}_m = average diffusional film coefficient over total exposure time Θ , L/θ
 $\bar{k}_m S$ = effective product of \bar{k}_m and S for a multiplicity of films, Equation 3, L^2/θ
 u = mean axial linear melt velocity, L/θ
 w = mass throughput rate, M/θ
 x = axial distance from devolatilizer feed end, L
 y = distance coordinate normal to film surface, L
 α = proportional to,
 β = geometry efficiency, Equation 4, 5,
 γ = parameter which measures solvent affinity for polymer, is 0.4 for many common nonpolar solvents, Equation 10,
 ρ = melt density, M/L^3
 θ = arbitrary exposure time of a surface element, θ
 Θ = total exposure time of a surface element, θ
 ϕ = screw helix angle measured from cross-sectional plane, degrees
 ϕ_0 = volume fraction, volatile component in polymer phase,
 ϕ_p = volume fraction, polymer in polymer phase,

Literature Cited

- (1) Amos, J. L., Roach, A. F., *Ind. Eng. Chem.* **47**, 2442 (1955).
- (2) Bernhardt, E. C., "Processing of Thermoplastic Materials," Reinhold, New York, 1959.
- (3) Carslaw, H. S., Jaeger, J. D., "Conduction of Heat in Solids," p. 41, Oxford Univ. Press, London, 1947.
- (4) DeMaria, F., White, R. R., *A.I.Ch.E. Journal* **6**, 473 (1960).
- (5) Hildebrand, J. H., Scott, R. L., "Solubility of Non-Electrolytes," Chap. 20, Reinhold, New York, 1950.
- (6) Latinen, G. A., Stockton, F. D., "Application of the Diffusion Model to Longitudinal Dispersion in Flow Systems," A. I. Ch. E. National Meeting, St. Paul, Minn., September 1959.
- (7) Levenspiel, O., Bischoff, K. B., *Ind. Eng. Chem.* **51**, 1431 (1959).
- (8) Levenspiel, O., Smith, W. K., *Chem. Eng. Sci.* **6**, 227 (1957).
- (9) Newitt, D. M., Weale, K. E., *J. Chem. Soc.* **1948**, 1541.
- (10) Van der Laan, E. Th., *Chem. Eng. Sci.* **7**, 187 (1958).
- (11) Vsurkov, S. N., Ryskin, G. Y., *J. Tech. Physics (U.S.S.R.)* **24**, No. 5, 797-810 (1954).
- (12) Wehner, J. F., Wilhelm, R. H., *Chem. Eng. Sci.* **6**, 89 (1956).

RECEIVED September 29, 1961.

Centrifuges for Linear Polyolefin Dispersions

CHARLES M. AMBLER

The Sharples Corp., Philadelphia, Pa.

Several types of centrifuges are applicable to the resolution of the various systems formed in the production of linear polyolefins. The performance characteristics of four of these that have been successfully used in this service are described in terms of a typical, but nonspecific, process.

Several types of centrifuges are specifically applicable to the various dispersion systems formed in the production of linear polyolefins. Each of these has one or more unique characteristics to meet the requirements for the separation and purification of the polymer from a particular system. This article presents briefly the characteristics of several centrifuges with respect to these systems.

During the past several years, a number of articles have been published on the theory of centrifugation (2), the design of centrifuges (4), and their laboratory and commercial application (3). To summarize these: Commercial centrifuges are applicable to the separation or resolution of multiphase systems. The solid bowl centrifuge or the centrifugal settler may be used when a significant difference in density exists between the phases. The perforated basket centrifuge or the centrifugal filter may be used when the particles of the dispersed phase have sufficient mechanical strength to withstand the compressive forces involved and to leave sufficient void or interstitial space between them for the passage of the continuous phase under the action of centrifugal force.

During these same years the "hunting licences" granted under the Ziegler patents have resulted in a number of systems consisting of polyolefin particles dispersed in a variety of fluids. Hexane, heptane, xylene, methanol, 2-propanol, and water at a variety of temperatures and corresponding pressures are typical and propylene in liquid form at high pressure is a possibility. In each case, the process requirement is the recovery of polymer particles at maximum concentration with elimination of mother liquor and soluble impurities. These latter may be catalyst residue or other ash-forming constituents and in the case of polypropylene, soluble atactic polymer or other side reaction products. These systems almost ideally meet the specifications of those to the resolution of which commercial centrifuges are applicable.

The centrifugal method meets these requirements by giving high unit capacity, sharpness of separation, both with respect to loss of polymer in the liquid phase and dryness of the separated polymer particles; and particularly in the case of the perforated basket centrifuge by good washing efficiency—i.e., maximum elimination of soluble impurities with minimum consumption of washing solvent.

Since the characteristics of the linear polyolefin dispersions that are being studied and produced vary over wide limits, the selection of the proper centrifuge for a specific separation becomes an important consideration. The performance of a given centrifuge and the economics of its use can frequently be improved by a factor of 2 or more by a minor change in reactor conditions without detrimental effect on the product itself. The role of the pilot plant in this connection cannot be overemphasized. In many cases, pilot plant-size centrifuges have been used to monitor reactor conditions and other process operating variables with substantial economies in the final process.

The first two illustrations are of typical pilot plant-size centrifuges. Figure 1 is a continuous, solid bowl centrifuge especially suitable for studying the recovery and concentration of polymer solids from hydrocarbon mother liquor. It is of the standard model that has been widely used for this purpose in the past. A similar size centrifuge is also available for operation under pressures up to 1 atm. gage and higher if required, for continuous operation in a pressurized system.

Figure 2 is a batch perforated basket centrifuge with a capacity of 0.2 cu. foot of solids per charge. It is designed to permit observation of drain rate and terminal volatile content of the recovered solids in centrifugal fields of from 109

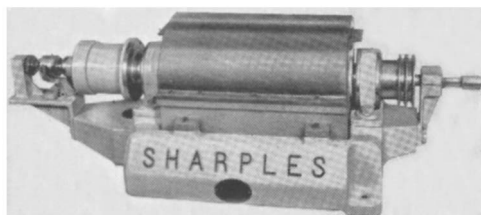


Figure 1. P-600, Super-D-Canter



Figure 2. Mark II, pilot plant centrifuge

to 1744 g at 800 to 3200 r.p.m. For larger scale work, a 20-inch diameter basket suitable for fully automatic operation at pressures up to 1 atm. gage is also available.

Critical data from relatively small samples, of the order of 3 to 5 gallons of feed slurry, can be obtained with both types of centrifuges. The results obtained in terms of capacity *vs.* effluent clarity *vs.* terminal dryness and purity of the recovered solids can be accurately scaled up to the performance of full-sized, commercial centrifuges by means described elsewhere (1). At the same time, both have adequate capacity for processing sufficient product for market evaluation studies.

Much of the work that has been and is being done in the field of polymer chemistry and processing is classified as confidential by many producers. In the remainder of this article, the characteristics and performance of several commercial centrifuges and their applicability to a typical, but nonspecific, multistage polyolefin process (Figure 3) are discussed.

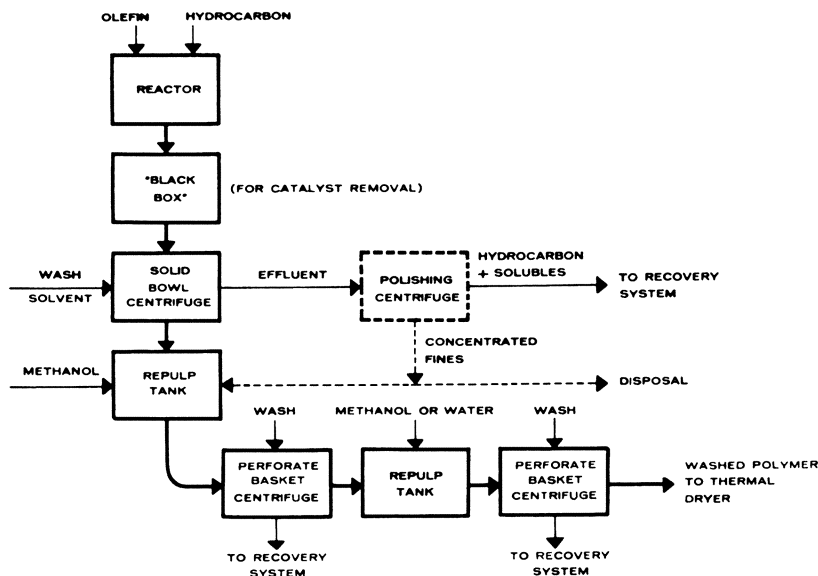


Figure 3. Typical process flow sheet for linear polyolefin production

This process would involve a reactor and a “black box” for total or partial catalyst “killing” and removal. Their workings are only of interest for subsequent stages and only to the extent to which they will govern feed slurry concentration, specific surface area of dispersed polymer particles, content of fines of less than 2 or 3 microns in diameter, and the bulk density of polymer solids. In the subsequent stages of this process, economy and centrifuge performance are favored by high feed slurry concentration, low specific surface area, absence of fines, and high bulk density.

The typical process would yield a slurry of 15 to 18% by weight of polymer solid particles in a hexane dispersion. An operating temperature of at least 80° C. would be required to keep the side products of the reaction—atactic polymer, for example—in solution.

Experience has shown that the perforated basket centrifuge may have poor operating characteristics in this system. In the case of polypropylene, the isotactic polymer particles in contact with hydrocarbon usually have low mechanical strength and under pressure tend to form a nonpermeable cake. In addition, the soft polymer particles tend to coat out on the filter medium and cause it to blind off and become impervious with undesirably high frequency.

Since a substantial difference in density exists, 0.92 gram per cc. for the polymer particles, as compared to less than 0.66 for hexane at the operating temperature, the use of the continuous, solid bowl centrifuge suggests itself. At an operating temperature of 90° C. (required to ensure complete solubility of the atactic polymer with a reasonable allowance for process variables) the vapor pressure of *n*-hexane is 11.3 p.s.i.g., so pressure containment in the centrifuge vessel is required. The continuous centrifuge illustrated in Figures 4 and 5 meets these requirements and is suitable for operation at up to 1 atm. gage and up to 150° C. With minor modifications, it can be made suitable for operation at up to 10 atm. or even higher. When fed a slurry of 15 to 18% weight concentration, it will deliver 2000 to 2500 pounds per hour of dry-basis polymer at 40 ± 10% residual volatile content, depending on the specific surface area of the polymer particles, and with a loss to the effluent of 0.0 to 2.0 grams per liter of polymer depending on the proportion of fines in the feed slurry. By applying a rinse of 1 to 1.5 pounds of pure solvent per pound of polymer to the separated solids in the centrifuge, their retained mother liquor-soluble impurity content will be reduced by a factor of approximately 2.

In this centrifuge, the casing surrounding the rotor as well as the solids' discharge and clarified hydrocarbon discharges are maintained at a system pressure which may be either the vapor pressure of the solvent or inert gas overpressure.

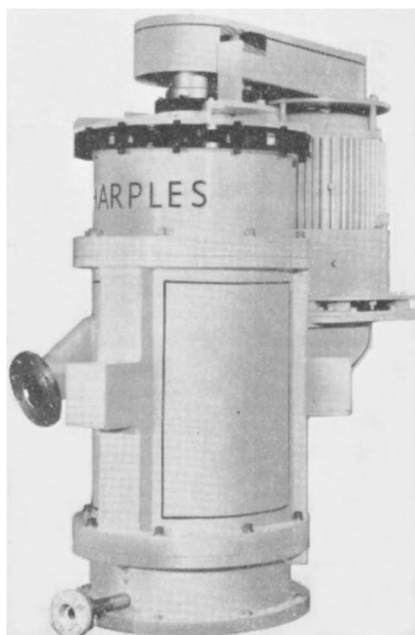


Figure 4. P-4000, Super-D-Canter, solid bowl continuous centrifuge

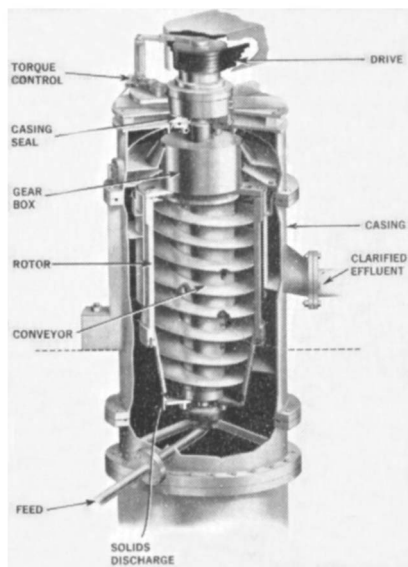


Figure 5. P-4000P, Super-D-Canter section

The feed enters near the center of the rotor. The liquid phase passes upward and overflows at the top of the rotor. As it does so, its solid content is sedimented out to the wall of the rotor by a centrifugal force of over 3000 g. The solids, sedimented against the rotor wall, are conveyed downward by the helical conveyor, carried up out of the liquid layer, and given an opportunity to drain on the smaller diameter beach section before discharging at the bottom to a receiver or conveyor. If displacement of the adhering mother liquor is desired, a rinse of pure solvent can be applied to the solids on the beach.

The system operating pressure is contained by a double-row cooled and lubricated carbon mechanical seal between the casing and rotating shaft in the vapor space at the upper end of the centrifuge assembly.

In this typical process, the recovered polymer solids discharged from the solid bowl centrifuge would be repulped in methanol to complete the killing of the catalyst (if this has not already occurred) and to dissolve ash-forming residues. The methanol also has a physical action on the polymer particles, changing their structure from partially gelatinous to one of relatively high mechanical strength.

Experience has shown that this system is now in satisfactory condition for further separation and purification on perforated basket centrifuges. These, on systems with which they are compatible, have the advantages of more completely separating the solid and liquid phases, recovering the solids at lower residual volatile content, and greatly improved rinsing of the solids for reduction of their mother liquor impurity content, than is possible on the solid bowl type of centrifuge.

A suitable automatic cyclic batch centrifuge for this second stage is shown in Figures 6 and 7. It consists of a perforated rotor or basket that runs continuously at full speed on a horizontal axis. The entire rotating assembly is contained in a casing that may be pressurized to meet system requirements with a

cooled and lubricated double-row mechanical shaft to casing seal. The basket is lined with a wire screen or other filter medium suitable for supporting the solid particles and for permitting passage of the mother liquor under the applied centrifugal force. The operating cycle under fully automatic time control consists of: screen conditioning rinse, feed, cake rinse (one or more applied sequentially), spin to terminal dryness, and unload.

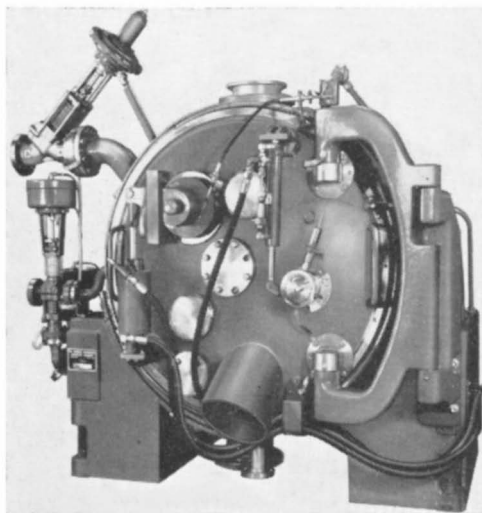


Figure 6. C-41P, Super-D-Hydrator, automatic perforated basket centrifuge

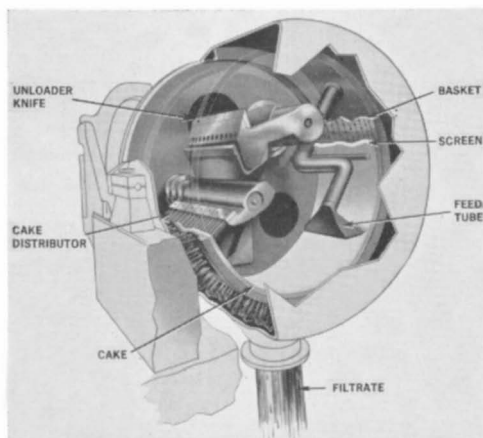


Figure 7. C-41P, Super-D-Hydrator section

The capacity of such a centrifuge varies with the solid concentration of the feed slurry, the drain rate of the mother and rinse liquors through the cake and filter screen, the amount of cake rinse required to attain the desired product purity, the time required to spin to terminal equilibrium volatile content, and the bulk density of polymer in the centrifuge basket. A centrifugal force of 1000 g may be

applied. Since the mother and rinse liquors follow each other sequentially through the casing outlet, they may be separated from each other by operation of a suitable diversion valve in the effluent line.

Various polymer systems show a high degree of variation in drain rate of mother and rinse liquors under centrifugal force. Values have been observed of from 16 pounds per sq. foot of screen area per minute to over 90 pounds with 30 to 50 pounds per sq. foot per minute representing the median range. The centrifuge of Figure 6 has a basket 41 inches in diameter with over 22 inches of effective screen width and a usable solids-holding capacity of over 6 cu. feet. Its capacity will vary from 1400 to over 5000 pounds per hour of dry-basis polymer discharged at between 13 and 40% residual volatile content, depending on the parameters noted above. By rinsing the cake in the basket with approximately 2 pounds of solvent per pound of dry-basis polymer, the soluble impurity content can be reduced by 90 to 95%, in some few cases by as high as 98%, of what it would be if no rinse were applied.

Smaller centrifuges with correspondingly less capacity, but with otherwise similar operating characteristics, are also available.

All of the data required for accurate estimation of capacity and performance can be determined by tests on small batches of polymer dispersion in the centrifuge illustrated in Figure 2.

As shown in the flowsheet (Figure 3), the washed product from the second-stage centrifuge is repulped in an appropriate vehicle preparatory to the final purification stage. This vehicle might be methanol, if a molding grade type of polymer is desired as the end product, water if over-all plant economics dictate a final thermal dryer system suitable for the evaporation of water rather than flammable solvent, or aqueous hydrochloric acid, if the end use of the polymer is for fiber and film production.

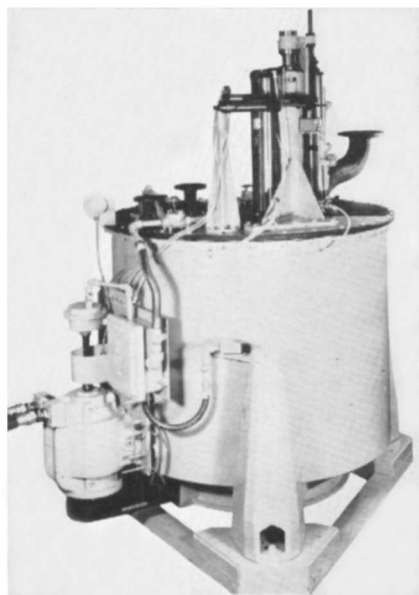


Figure 8. Tornado centrifuge 48×30, rubber covered

For the processing of polymer dispersions in hydrocarbons, equipment constructed of Type 316 stainless steel is generally used. Where the vehicle is an alcohol such as methanol, or water containing traces of metallic chlorides, the use of equipment constructed of Monel or nickel is generally considered more suitable. Both of the centrifuges described above are available with any of these materials as parts in contact with the process material.

For the third stage of the typical process when the vehicle is methanol or water, the same automatic perforated basket centrifuge described under the second stage would be applicable and the capacity and performance would be substantially identical to those reported under second stage operation.

When the vehicle is aqueous hydrochloric acid at pH less than 3, rubber-covered equipment is generally more suitable to withstand the corrosive action. The vertical axis basket centrifuge shown in Figures 8 and 9 lends itself to this

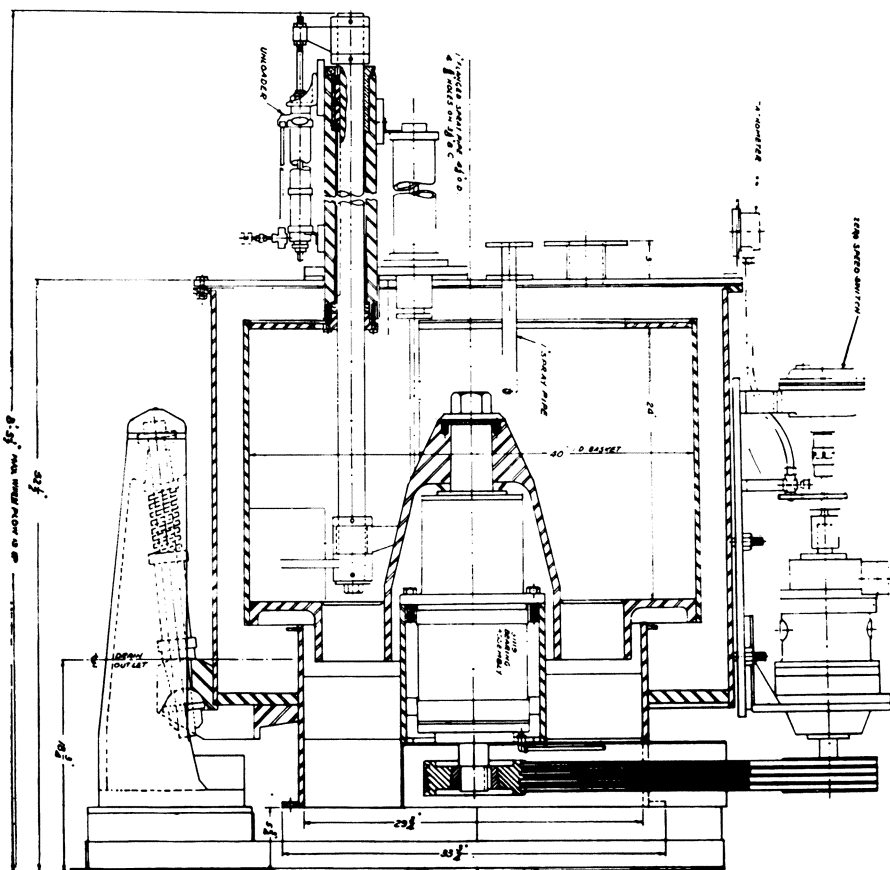


Figure 9. Tornado centrifuge 48x30 section

type of construction. It also is a fully automatic, cyclic batch centrifuge that differs from the horizontal basket centrifuge in that the rotative speed is automatically varied for the successive operations of loading, rinsing, spinning to dryness, and unloading. The model illustrated has a basket 48 inches in diameter by

30 inches deep with a total holding capacity under the lip ring of 16 cu. feet. It will wash and dewater approximately 180 to 360 pounds of polymer (dry-basis) per charge, depending on the bulk density of the polymer, and process up to 6 charges per hour. Its net capacity is therefore in the range of 1000 to 2400 pounds per hour of polymer, dry-basis, discharged usually at $30 \pm 10\%$ residual volatile content. Rinsing efficiency will approximate 90 to 95% displacement of the soluble mother liquor impurities with 2 pounds of rinse per pound of dry-basis polymer.

On slow draining systems with drain rates less than 20 pounds per sq. foot per minute, the larger screen area of the vertical basket centrifuge per unit of cost may make its use economically attractive even on systems where rubber coating is not necessary. It is also available in Monel metal and stainless steel construction.

The flowsheet (Figure 3) also shows that the effluent from the first stage, solid bowl centrifuge may contain up to 2 grams per liter of polymer fines. While the amount of these is usually so small that their recovery is not economical per se, their presence may be undesirable in the solvent recovery system. The automatic desludging type of disk bowl, clarifier centrifuge (Figures 10 and 11) has been found effective in cleaning up or polishing this stream. In operation, the continuous flow of the contaminated liquid is subjected to the clarifying effect of the efficient disk-type centrifuge rotor. The solid particles removed from the fluid are accumulated in the sludge-holding space of the rotor outside the disk stack. At appropriate intervals, a sleeve-type valve forming the perimeter of the rotor is caused to open by the introduction of a hydraulic operating fluid and the accumulated solids are ejected through this opening by a centrifugal force acting on the contents of the bowl. This action can be sufficiently well controlled

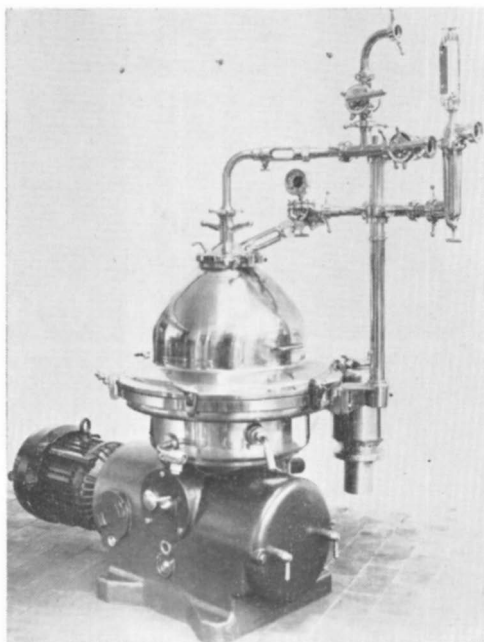


Figure 10. Desludger centrifuge

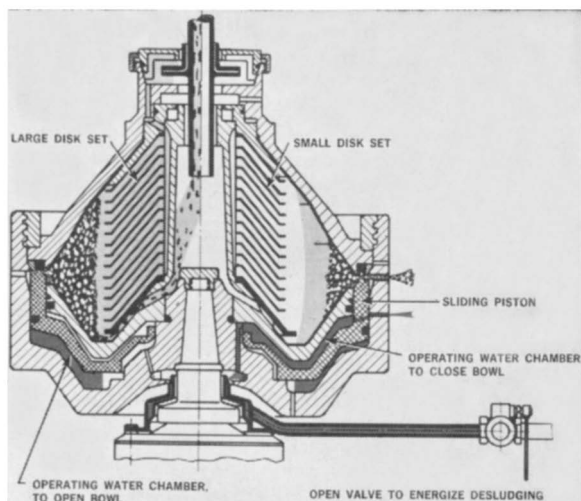


Figure 11. Deslugger centrifuge section

so that only the concentrated solids layer is ejected. This centrifuge is available in two sizes, the smaller with a capacity of 40 to 50 gallons per minute and the larger with a capacity up to 100 gallons per minute. The solids are discharged at a volatile content of approximately 65 to 70% and the clarified liquid will contain practically no solid particles larger than 0.3 micron.

This article has described the typical performance characteristics of several centrifuges that have been successfully applied to the processing of linear polyolefin dispersions. Because of the secrecy surrounding the several processes in use, it has been necessary to give this description in terms of a typical, but non-specific, process that does not reveal the exact operating details of any known process or processor. However, the operating details given are applicable to any polyolefin in purification processes of one or more stages.

Literature Cited

- (1) Ambler, C. M., *J. Biochem. Microbiol. Technol. Eng.* 1, No 2, 185-205 (1959).
- (2) Ambler, C. M., *Ind. Eng. Chem.* 53, 430 (1961).
- (3) Smith, J. C., *Ibid.*, 53, 439 (1961).
- (4) Sullivan, F. E., *Ibid.*, 53, 434 (1961).

RECEIVED September 6, 1961.

Progress in Polymer Syntheses and Applications

HERMAN F. MARK

Polytechnic Institute of Brooklyn, 333 Jay St., Brooklyn 1, N. Y.

New polymers can be prepared from new vinyl monomers specially tailored to contain desired functional groups which also appear in the resulting polymer. Readily available monomers polymerized and copolymerized by new techniques in which one or more parameters are completely novel or partially modified from previously used ones is still another approach to new macromolecules. Copolymerization of ethylene with vinyl-type monomers yields a wide range of plastics, coatings, and adhesives. Homopolymers of aldehydes and epoxides as well as copolymers of these two types of monomers range from rigid, highly crystalline to rubbery. Block and graft copolymerization leads to elastomeric fibers, while solid state polymerization of vinyl compounds has opened up new research vistas. The salient features of these reactions are presented and the relations between polymer structure and properties are considered with the industrial application in view.

There are, in general, two ways to prepare new polymers which have valuable and useful properties. One of them involves the synthesis of a *new monomer*, which embodies by virtue of its chemical nature some interesting and attractive features. If one then polymerizes such a monomer, one finds in the polymer the desired properties resulting from repetition of a large number of monomeric units. In this manner, many new addition polymers have been made from vinyl-type monomers, which had reactive groups such as $-\text{CH}-\text{CH}_2$, $-\text{SH}$, or $-\text{NHCH}_2\text{OH}$. The



resulting polymers displayed the reactivity of these functional groups for such purposes as adhesion, solubility, or cross linking. Also, many high temperature-resistant polycondensation products have been prepared by the use of special aromatic compounds, such as pyromellitic anhydride, naphthalenetetracarboxylic acid, or tetraaminobiphenyl.

Another way to prepare new polymers with valuable properties is to use well-known, readily available, and usually inexpensive monomers, such as ethylene,

propylene, vinyl chloride, acrylonitrile, and others, and to subject them to new polymerization techniques, using novel catalysts, activators, promoters, modifiers or unusual combinations of reaction conditions: temperature, pressure, state of aggregation, rate and type of mixing, high energy radiation, etc. Both approaches have been remarkably successful during the past few years in producing a large number of new and useful polymers in all fields of application and the various articles in this volume have been skillfully assembled to give a vivid picture of the special areas in which significant progress has already been made. The purpose of this concluding article is to add a few more details to this composite picture because certain recent efforts—basically promising—have in some cases already reached the new product or process stages or have given, until now, only scattered and incomplete information on the practical application of the resulting materials.

Copolymerization of Ethylene with Vinyl-Type Monomers

The high pressure polymerization of ethylene can be slightly modified for the copolymerization of ethylene with vinyl- and acrylic-type monomers such as vinyl acetate, vinyl chloride, acrylonitrile, or acrylic esters. Some of these copolymers of ethylene and vinyl acetate or maleic anhydride are already available and have found various applications in plastics, coatings, and adhesives. Copolymers of ethylene and vinyl chloride and of ethylene and acrylonitrile appear particularly interesting because of the low cost of monomers and the properties of the copolymers. Although their synthesis has been disclosed in a number of patents their larger scale production is still in a state of development.

Polymerization of Aldehydes and Epoxides

Formaldehyde and other aldehydes can be polymerized under various conditions to form high molecular weight polymers. Linear polyformaldehyde has been known as Delrin for several years. It is a highly crystalline, rigid polymer and has been used already successfully in molding and extrusion. Polyacetaldehyde has been obtained in an amorphous, atactic form, which is low melting, readily soluble, and rubbery and in two stereoregulated forms (isotactic and syndiotactic) which are crystalline, high melting, and rigid. Copolymers of formaldehyde and acetaldehyde cover the entire range of chemical composition and are rigid and high melting if formaldehyde is in excess and rubbery if there is an excess of acetaldehyde.

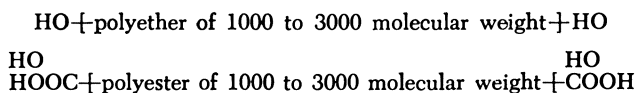
To improve the stability of polyacetals, the end groups have to be protected by etherification with $-\text{CH}_3$ groups or by esterification with acetic or benzoic acids. Copolymers of aldehydes and epoxides have also been prepared; those of formaldehyde and ethylene oxide are especially interesting as high melting, rigid, and slightly soluble plastics. Polymers and copolymers of epoxides have been obtained recently; they have high molecular weight and interesting properties. The rubbery polymers and copolymers of propylene oxide can be cured with sulfur by introducing a side-chain double bond into the linear macromolecule of the polyether backbone chain by means of butadiene monoepoxide or glycidyl methacrylate.

Block and Graft Copolymerization

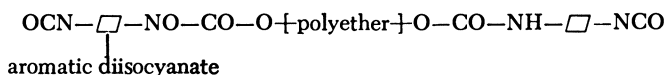
Block copolymerization has given unusual elastomeric fiber formers, which are used to produce the so-called Spandex-type fibers. Blocks of linear, flexible macromolecules of molecular weight between 1000 and 3000 are prepared and hook together by means of their reactive end groups through reaction with bifunctional molecules which introduce into the resulting macromolecules (molecular weight about 20,000) enough stiffness and intermolecular attraction to provide a sufficiently high tensile modulus and tensile strength. Structures of this type can be obtained in different ways, each of which, however, offers certain difficulties. The first step concerns the chemical nature of the primary blocks, which are usually of the polyester or polyether type. It would be very desirable to have hydrocarbon-type primary blocks, but it has not yet been possible to obtain such units with reactive end groups in a satisfactorily controlled bifunctional arrangement. Polyether blocks with hydroxyl end groups are prepared by the atactic polymerization of tetrahydrofuran or propylene oxide, whence they are rubbery enough for a good elastomer, but are somewhat sensitive to light and oxygen which, eventually, cause discoloration and chemical degradation. A hydroxyl group at the end of each chain is easily obtained during polyether formation and is accounted for by the basic reaction mechanism. Rubbery polyester blocks with hydroxyl groups at all chain ends can be prepared by the interaction of adipic or sebacic acids with ethylene or propylene glycols in the presence of an excess of glycol. If one wants carboxyl groups at all chain ends, one works with a corresponding excess of acid, and it is not too difficult to get nearly complete bifunctionality. Polyester blocks are stable towards light and oxygen but evidently are sensitive to hydrolysis. The resilience of polyether blocks is superior to that of polyester blocks, particularly at lower temperatures.

In order to convert the blocks with a molecular weight of about 2000 to linear macromolecules with molecular weights of 20,000 or more, they are first capped with a diisocyanate—normally of the aromatic type—and then expanded with a diamine or dihydroxy compound. Thus, the principal steps in the synthesis of elastic fiber molecules are:

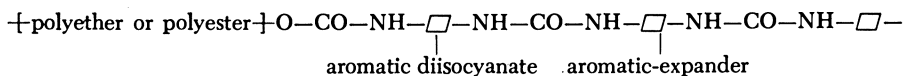
1. Preparation of Primary Blocks.



2. Capping of Blocks.



3. Expansion of Blocks to Macromolecules.



The polyether or polyester blocks provide the necessary rubberiness, whereas the accumulation of relatively stiff links with hydrogen bonding capacity between the elastomeric blocks increases resistance to high temperatures and the action of solvents. It also increases the modulus of elasticity and the ultimate tensile strength of the resulting fibers.

Other types of block copolymers are made for use as adhesives and coatings.

Considerable efforts have been directed, during the last few years, to grafting various vinyl and acrylic monomers on cellulosic fibers or films in order to modify their properties in a predetermined way. It was shown that one can graft large amounts of vinyl-type monomers, such as acrylonitrile or acrylic esters on rayon, cotton, cellophane, paper, and wood, thus modifying the properties of the base material in many respects, and improving, particularly, dimensional stability, water repellency, and resistance to thermal and chemical degradation.

Graft copolymers of hexadiene and styrene on elastomers and polyblends of the resulting materials with polystyrene have paved the way for the technology of high impact strength polystyrenes and other high impact strength resin compositions which incorporate many desirable properties to a higher degree not otherwise possible without resort to the principle of graft copolymerization. To obtain successful grafting without too much homopolymer formation very strict control has to be exerted over the compatibility of the various ingredients, the reactivity of the initiators and activators, and the temperature of the reaction.

Solid State Polymerization

It has long been known that polymerization of nonactivated organic compounds occurs in the solid crystalline state, but the systematic and scientific study of this phenomenon was only begun a few years ago.

The principal conditions for a successful polymerization in the solid crystalline state are:

1. The double bonds must be located within the crystal lattice so that they can react with each other without too much displacement and without appreciable lattice distortions.
2. An initiator of some kind must be introduced into the lattice in sufficient amount to start the growth of chains at a reasonable rate.

Both conditions have been explored during recent years and it was found that some monomers such as formaldehyde, acrylonitrile, and certain acrylic esters and salts polymerize very readily, whereas others do not polymerize at all or only to a very small extent. This difference is explained by the special location of the double bonds within the crystal lattices.

Initiation of polymerization can be obtained by thermal motion of the crystal lattice (for high melting monomers) or preferably by the use of ionizing radiation, either from high energy sources such as β - and γ -rays or by the use of ultraviolet light and even visible light in the presence of sensitizers. It is also possible to distribute in a crystal lattice, at low temperatures, initiating ionic centers, if the monomer is slowly condensed from the vapor phase on a cold plate and single atoms of such materials as lithium, sodium, magnesium, iron, copper, or boron trifluoride, aluminum chloride, and titanium trichloride are added with a molecular beam. If composite systems of this kind are warmed up, rapid polymerization occurs and almost any kind of monomer can be thus converted into a high molecular weight polymer.

RECEIVED March 12, 1962.